Available online at www.sciencedirect.com
ScienceDirect
Ceramics International 38S (2012) S267–S270
CERAMICS INTERNATIONAL
www.elsevier.com/locate/ceramint

Ferroelectric hysteresis behavior and dielectric properties of 1–3 lead zirconate titanate–cement composites

R. Potong [a], R. Rianyoi [a], N. Jaitanong [a], R. Yimnirun [b], A. Chaipanich [a,*]

[a] Department of Physics and Materials Science, Faculty of Science, Chiang Mai University, Chiang Mai 50200, Thailand
[b] School of Physics, Institute of Science, Suranaree University of Technology and Synchrotron Light Research Institute (Public Organization), Nakhon Ratchasima 30000, Thailand

Available online 4 May 2011

Abstract

Lead zirconate titanate (PZT) ceramic was mixed with Portland cement (PC) to form 1–3 connectivity PZT–PC composite using a dice-and-fill technique. Ferroelectric hysteresis behavior and dielectric properties of these composites were investigated using PZT volume content of 60%, 70% and 80%. The results showed that the dielectric constant of the composite materials increased with PZT content and the dielectric constant (ε_r) value is 781 for 80% PZT composite at 1 kHz. The dielectric loss tangent (tan δ) was found to decrease with increasing PZT content and the tan δ value of 80% PZT composite is 0.06. Parallel and series models were also compared to the dielectric measurement results. For the hysteresis measurements, the ferroelectric hysteresis loops can be seen for all composites. The ''instantaneous'' remnant polarization (P_{ir}) was found to increase with increasing PZT content from 3.20 to 4.28 $\mu C/cm^2$ at 90 Hz when PZT volume content used was 60% and 80% respectively.

Keywords: B. Composites; C. Dielectric properties; C. Ferroelectric properties; D. PZT

1. Introduction

Lead zirconate titanate (PZT) is the most popular ferroelectric material, which plays a remarkable role in modern electroceramic industry [1]. Moreover, PZT has high dielectric constant, high electromechanical coupling and high piezoelectric coefficient and has been employed as sensors, actuators and transducers [2–6]. Very recently, there have been developments of piezoelectric materials in order to meet the acoustic matching requirement such as those of piezoelectric-cement based composites for smart concrete structures and civil engineering application [7–16]. The first report work on the use of a 0–3 PZT–white Portland cement composite was by Li et al. [14]. Chaipanich [15] investigated the dielectric and piezoelectric properties of 0–3 PZT–cement composite made from ordinary Portland cement (ASTM type I cement) and PZT. Lam and Chan [16] developed 1–3 piezoelectric ceramic/cement composites with 0.25–0.77 volume fractions of PZT were reported and it was found that the 1–3 composites have good compatibility with civil engineering structure materials while being suitable for high sensitivity. The hysteresis study would thus give an indicative of the remnant polarization and the ferroelectricity behavior of the material. In addition, the dielectric results of the composites with 1–3 connectivity were compared to the parallel, series and cubes models and are presented here in this paper.

In this research, it is therefore interesting to study the ferroelectric hysteresis behavior and dielectric properties of 1–3 connectivity PZT-cement composites.

2. Experimental

Lead zirconate titanate ($Pb(Zr_{0.52}Ti_{0.48})O_3$) powder was initially produced from the two-stage mixed oxide method. Starting precursors were lead oxide (PbO), zirconium oxide (ZrO_2) and titanium dioxide (TiO_2) (Riedel-de Haën, >99% purity). PbO and ZrO_2 were thoroughly mixed and milled in ethanol for 24 h. After that, the mixed powder was stirred, dried and calcined in a closed alumina crucible at 800 °C for 2 h to give $PbZrO_3$. $PbZrO_3$ and TiO_2 powder were then calcined at 900 °C with excess PbO to give the PZT powder. In addition,

* Corresponding author. Tel.: +66 53 943445; fax: +66 53 943445.
E-mail address: arnon@chiangmai.ac.th (A. Chaipanich).

0272-8842/$36.00
doi:10.1016/j.ceramint.2011.04.098

PZT ceramics were then produced by sintering PZT powder at 1200 °C for 2 h. 1–3 Lead zirconate titanate–Portland cement composites of ≈2 mm thick and 12 mm in diameter were fabricated using a dice-and-fill method [16,17]. PZT ceramics of different PZT volume content of 60%, 70% and 80% were used. PZT ceramic disc was cut in one direction (y axial) using a diamond saw (Buehler ISOMET Low speed saw) with a 0.5 mm thick blade. Portland cement (PC) was cast as paste (water/cement = 0.5) on the matrix phase. Thereafter, the samples were placed for curing at 60 °C for five days under a condition of relatively high humidity and cut in second direction (x axial). After filling the second direction of cuts with cement paste, the composites were cured at a temperature of 60 °C and 98% relative humidity for five days before measurements. The dielectric properties of composites were measured using an impedance meter (Hewlett Packard 4194A) at room temperature. The dielectric constant (ε_r) was then calculated from Eq. (1)

$$\varepsilon_r = \frac{Ct}{\varepsilon_0 A} \tag{1}$$

where C is the sample capacitance, t is the thickness, ε_0 is the permittivity of free space constant (8.854×10^{-12} F m^{-1}), and A is the electrode area.

The dielectric constant results were also compared with the composite models as follows:

- parallel model [18]

$$\varepsilon_C = \nu_1\varepsilon_1 + \nu_2\varepsilon_2 \tag{2}$$

- series model [19]

$$\frac{1}{\varepsilon_C} = \frac{\nu_1}{\varepsilon_1} + \frac{\nu_2}{\varepsilon_2} \tag{3}$$

- cubic model [20]

$$\varepsilon_C = \frac{\varepsilon_1 \cdot \varepsilon_2}{(\varepsilon_2 - \varepsilon_1) \cdot \nu_1^{-1/3} + \varepsilon_1 \cdot \nu_1^{-2/3}} + \varepsilon_2 \cdot (1 - \nu_1^{-2/3}) \tag{4}$$

where ε_1 and ε_2 are dielectric constant values of the ceramics phase and the cement phase, respectively, and ν_1 and ν_2 are the volume percentages of the ceramics phase and the cement phase, respectively.

The ferroelectric hyteresis (P–E) loop behaviors of the composites were measured using a computer controlled modified Sawyer–Tower circuit at room temperature.

3. Results and discussion

The dielectric constant (ε_r) of PZT–PC composites is plotted against the PZT content in Fig. 1. The dielectric constant of the composites can be seen to increase with increasing PZT content and the dielectric constant is highest at 781 for 80% PZT composites at 1 kHz. In addition, dielectric loss (tan δ) of composites showing the effect of PZT content can also be seen in Fig. 1. The dielectric loss (tan δ) is found to reduce with

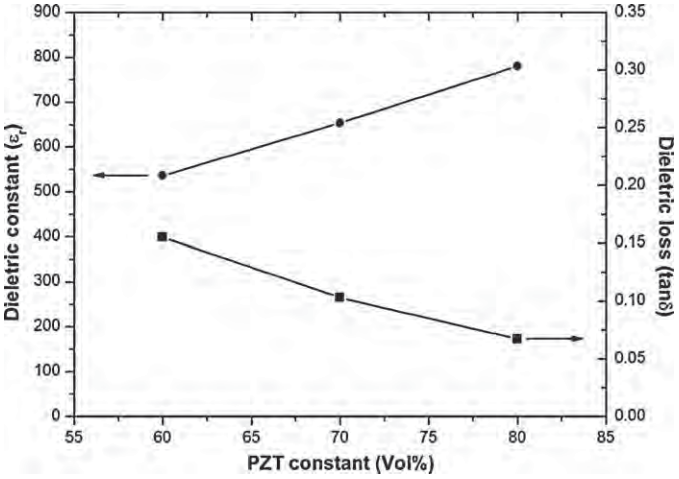

Fig. 1. Dielectric properties results of PZT–Portland cement composites at 1 kHz.

increasing PZT content and the tan δ value of 80% PZT composite is lowest at 0.06 (f = 1 kHz).

Furthermore, the parallel and series models were compared with the results taken from the measurements as shown in Fig. 2. The dielectric results of 1–3 can be seen to fit closest to that of the parallel model and the results are shown to be higher than 0–3 connectivity composites. This is because the 1–3 connectivity is more closely related to the 2–2 parallel models with the complete phase of PZT ceramic in the Y direction. In the case of 0–3 connectivity composites, PZT were randomly distributed particles surrounded by Portland cement matrix and thus the 0–3 composites are more closely related to the series or cube models.

Measured hysteresis loops of the PZT–PC composites are shown in Fig. 3. For comparison, we can define the y-axis intercept at a given applied field as the ''instantaneous'' remnant polarization (P_{ir}) and the x-axis intercept is called the ''instantaneous'' coercive field (E_{ic}) [10]. From Fig. 3, an

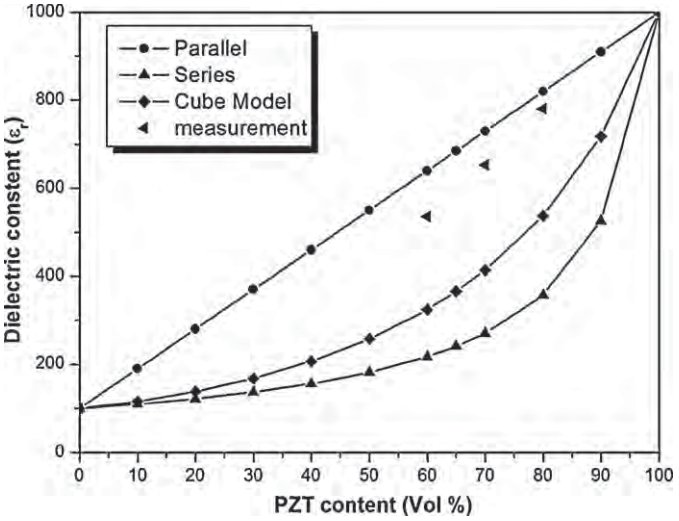

Fig. 2. Comparison of models with the dielectric results of PZT–Portland cement composites.

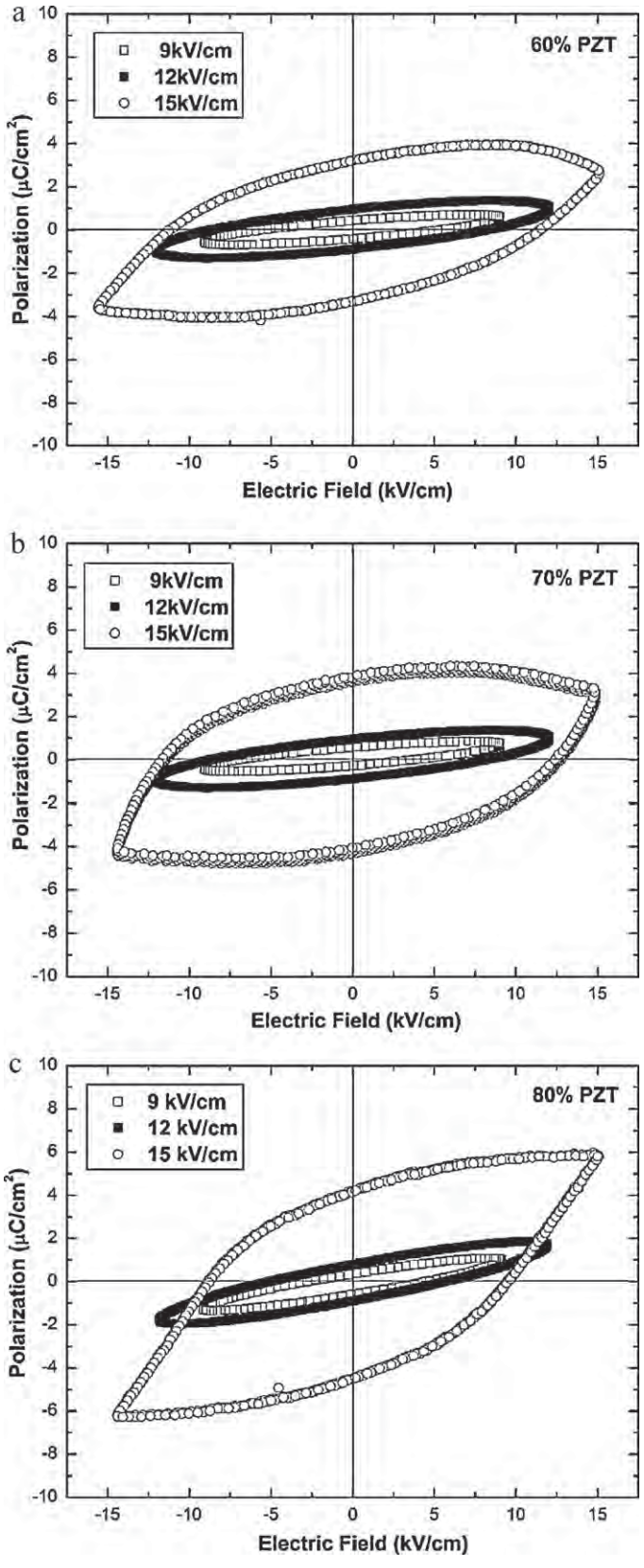

Fig. 3. Effect of external electrical field on the hysteresis loops of the 1–3 connectivity PZT–PC composites at (a) 60% PZT, (b) 70% PZT and (c) 80% PZT.

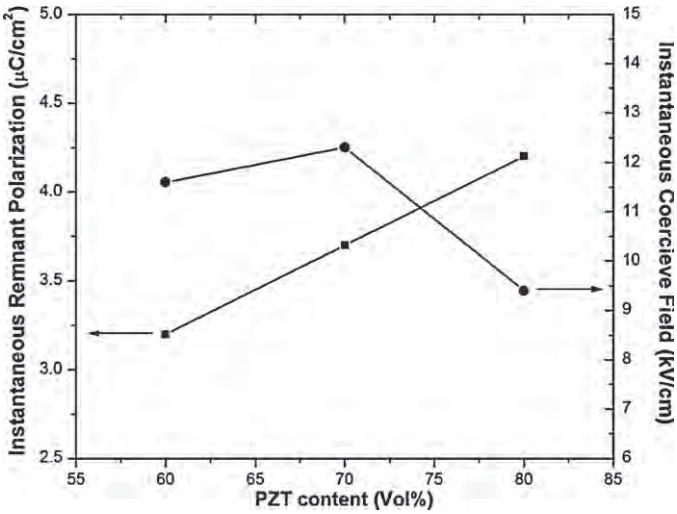

Fig. 4. Effect of PZT contents on instantaneous remnant polarization (P_{ir}) and instantaneous coercive field (E_{ic}) of PZT–Portland cement composites.

increase in the amplitude of the external electrical field make the P–E loops larger and increases its angle to the E axis of inclination [12]. At frequency of 90 Hz, the P_{ir} value can be seen to increase from 0.46 to 3.20 μC/cm^2 (60% PZT), 0.59 to 3.84 μC/cm^2 (70% PZT), and 0.41 to 4.28 μC/cm^2 (80% PZT) when the electric field increases from 9 to 15 kV/cm, respectively. The E_{ic} value can be seen to increase with increasing external electrical field for all composites.

The effect of PZT contents on instantaneous remnant polarization (P_{ir}) and instantaneous coercive field (E_{ic}) of PZT–Portland cement composites is shown in Fig. 4. The P_{ir} value can be seen to increase with increasing PZT content from 3.20 to 4.28 μC/cm^2 at 90 Hz when PZT content increases from 60% to 80%, respectively. On the other hand, the E_{ic} value is 11.60 kV/cm for the composite with 60% PZT and 9.48 kV/cm for the composite with 80% PZT.

However, the loop shape characteristic also changes with PZT content in that the P_{ir} value of 60% PZT is far lower than that of 80% PZT, while the E_{ic} value of 60% PZT is higher than that of 80% PZT. It is due to the fact that a loss from the cement can be seen to be more sensitive at lower PZT volume content and when an external electrical field acts many weak conducting ions such as OH^-, Ca^{2+} and Al^{3+} in the cement matrix begin to migrate besides the polarization of electron, these ions cause higher conducting loss in the composites [10,12,21–23]. Moreover, cement matrix is non piezoelectric and numerous defect in the composite, such as lattice distortion, and phase boundary and pores of cement matrix, which usually cause a leakage current and distortion of hysteresis loops [10,12,21,22].

4. Conclusions

The dielectric and hysteresis properties of 1–3 PZT–Portland cement composites were investigated. The results obtained from the measurements show the dielectric constant of the composites increased with increasing PZT content and that

the dielectric constant was highest at 781 for 80% PZT composites at 1 kHz. The dielectric results of 1–3 were found to fit closest to that of the parallel model and the results are shown to be higher than 0–3 connectivity composites. This is because the 1–3 connectivity is more closely related to the 2–2 parallel models with the complete phase of PZT ceramic in the Y direction. Dielectric loss ($\tan\delta$) was found to reduce with increasing PZT content and the $\tan\delta$ value of 80% PZT composites was lowest at 0.06 for composite at 1 kHz. The ''instantaneous'' remnant polarization (P_{ir}) was found to increase with increasing PZT content. The hysteresis loop can be seen for all composites.

Acknowledgements

The authors would like to express their sincere gratitude to Prof. Tawee Tunkasiri and Dr. Sukum Eitssayeam for their advice and help throughout this research work. The Thailand Research Fund (TRF), Office of the Higher Education Commission (Thailand) and the graduate school of Chiang Mai University are gratefully acknowledged for the financial support of this research.

References

[1] Z. He, J. Ma, R. Zhang, Investigation on the microstructure and ferroelectric properties of porous PZT ceramics, Ceramics International 30 (2004) 1353–1356.
[2] R.E. Newnham, A. Amin, Smart systems: microphones, fish farming, and beyond—smart materials, acting as both sensors and actuators, can mimic biological behavior, Chemtech 29 (1999) 38–47.
[3] K. Uchino, Materials issues in design and performance of piezoelectric actuators: an overview, Acta Materialia 46 (1998) 3745–3753.
[4] R. Ranjan, R. Kumar, B. Behera, R.N.P. Choudhary, Effect of Sm on structural, dielectric and conductivity properties of PZT ceramics, Materials Chemistry and Physics 115 (2009) 473–477.
[5] S.T. Lau, K.W. Kwok, H.L.W. Chan, C.L. Choy, Piezoelectric composite hydrophone array, Sensors and Actuators A: Physical 96 (2002) 14–20.
[6] T. Zeng, X.L. Dong, S.T. Chen, H. Yang, Processing and piezoelectric properties of porous PZT ceramics, Ceramics International 33 (2007) 395–399.
[7] S. Huang, J. Chang, L. Lu, F. Liu, Z. Ye, X. Cheng, Preparation and polarization of 0–3 cement based piezoelectric composites, Materials Research Bulletin 41 (2006) 291–297.
[8] A. Chaipanich, N. Jaitanong, T. Tunkasiri, Fabrication and properties of PZT–ordinary Portland cement composites, Materials Letters 61 (2007) 5206–5208.
[9] A. Chaipanich, N. Jaitanong, Effect of polarization on the microstructure and piezoelectric properties of PZT–cement composites, Advanced Materials Research 55–57 (2008) 381–384.
[10] A. Chaipanich, N. Jaitanong, R. Yimnirun, Ferroelectric hysteresis behavior in 0–3 PZT–cement composites: effects of frequency and electric field, Ferroelectric Letters Section 36 (2009) 59–66.
[11] N. Jaitanong, A. Chaipanich, T. Tunkasiri, Properties 0–3 PZT–Portland cement composites, Ceramics International 34 (2008) 793–795.
[12] N. Jaitanong, R. Rianyoi, R. Potong, R. Yimnirun, A. Chaipanich, Effect of PZT content and particle size on ferroelectric hysteresis behavior of 0–3 lead zirconate titanate–Portland cement composites, Integrated Ferroelectrics 107 (2009) 43–52.
[13] A. Chaipanich, Effect of PZT particle size on dielectric and piezoelectric properties of PZT–cement composites, Current Applied Physics 7 (2007) 574–577.
[14] Z. Li, D. Zhang, K. Wu, Cement-based 0–3 piezoelectric composites, Journal of the American Ceramic Society 85 (2002) 305–313.
[15] A. Chaipanich, Dielectric and piezoelectric properties of PZT–cement composites, Current Applied Physics 7 (2007) 537–539.
[16] K.H. Lam, H.L.W. Chan, Piezoelectric cement-based 1–3 composites, Applied Physics A: Materials Science & Processing 81 (2005) 1451–1454.
[17] H.L.W. Chan, J. Unsworth, Mode coupling in modified lead titanate/polymer 1–3 composites, Journal of Applied Physics 65 (1989) 1754–1758.
[18] S. Mindess, J.F. Young, D. Darwin, Concrete, second ed., Prentice-Hall, Pearson Education, Inc., United States of America, 2003.
[19] D.H. Yoon, J. Zhang, B.I. Lee, Dielectric constant and mixing model of $BaTiO_3$ composite thick films, Materials Research Bulletin 38 (2003) 765–772.
[20] F. Xing, B. Dong, Z. Li, Dielectric, piezoelectric, and elastic properties of cement-based piezoelectric ceramic composites, Journal of the American Ceramic Society 91 (2008) 2886–2891.
[21] C. Xin, S. Huang, C. Jun, L. Zongjin, Piezoelectric, dielectric, and ferroelectric properties of 0–3 ceramic/cement composite, Journal of Applied Physics 101 (2007) 094110.
[22] R. Yimnirun, Change in the dielectric properties of normal and relaxor ferroelectric ceramic composites in BT-PZT and PMN-PZT systems by an uniaxial compressive stress, Ferroelectrics 331 (2006) 9–18.
[23] A. Chaipanich, N. Jaitanong, R. Yimnirun, Effect of compressive stress on the ferroelectric hysteresis behavior in 0–3 PZT-cement composites, Materials Letters 64 (2010) 562–564.

Available online at www.sciencedirect.com
ScienceDirect
Ceramics International 38S (2012) S255–S258
CERAMICS INTERNATIONAL
www.elsevier.com/locate/ceramint

Dielectric and ferroelectric hysteresis properties of 1–3 lead magnesium niobate–lead titanate ceramic/Portland cement composites

A. Chaipanich [a,*], R. Potong [a], R. Rianyoi [a], L. Jareansuk [a], N. Jaitanong [a], R. Yimnirun [b]

[a] Department of Physics and Materials Science, Faculty of Science, Chiang Mai University, Chiang Mai 50200, Thailand
[b] School of Physics, Institute of Science, Suranaree University of Technology and Synchrotron Light Research Institute (Public Organization), Nakhon Ratchasima 30000, Thailand

Available online 4 May 2011

Abstract

In this work, lead magnesium niobate–lead titanate (PMN–PT) ceramic was cut and filled with Portland cement (PC) to produce 1–3 connectivity PMN–PT/PC composites. Dielectric and ferroelectric hysteresis properties of these composites with PMN–PT ceramic volume content of 60% were investigated. Room temperature dielectric constant (ε_r) at 1 kHz of the PMN–PT/PC composite was found to be ≈1500. At higher frequency (20 kHz), the dielectric constant was reduced to the value of ≈1300. Ferroelectric (polarization–electric field) hysteresis loops at 10–90 Hz and varying electric field were measured. The ''instantaneous'' remnant polarization (P_{ir}) at 50 Hz and at the electric field of 7 kV/cm of the PMN–PT/PC composite was found to be ≈10 μC/cm^2. These values of 1–3 composites therefore are promising when compared to previous results of composites at similar conditions.

Keywords: B. Composites; C. Dielectric properties; C. Ferroelectric properties; PMN–PT

1. Introduction

Piezoelectric-cement based composites have been developed in order to meet the acoustic matching of concrete for structural health monitoring application [1,2]. One of the mostly used piezoelectric ceramic materials is lead zirconate titanate (PZT) as it has very high piezoelectric coefficient (d_{33}) and dielectric constant (ε_r) and most of the piezoelectric-cement based composites were produced using PZT as the piezoelectric ceramic in the composite [1,2,7–13] from the previous investigated works [1–18]. Lead magnesium niobate–lead titanate ceramic, $Pb(Mg_{1/3}Nb_{1/2})O_3$–$PbTiO_3$ (PMN–PT) like PZT can be used in the application of smart structures. PMN–PT ceramic has a high dielectric constant (ε_r), high d_{33} value and an ideal curie temperature (T_c) at ≈150 °C compare to PZT at ≈400 °C [19,20]. For cement-based composite produced with piezoelectric materials other than PZT such as PMN–PT very little is known. In this research, PMN–PT/PC composite material was produced in the form of 1–3 connectivity from lead magnesium niobate–lead titanate (PMN–PT) and Portland cement. The dielectric and ferroelectric hysteresis behavior of the composites were then investigated.

2. Experimental

Columbite technique was first used to produce PMN powder. $MgNb_2O_6$ or MN (JCPDS file no. 88-0708) powder was first produced by calcining magnesium carbonate hydroxide pentahydrate $(MgCO_3)_4Mg(OH)_2{\cdot}5(H_2O)$ and Nb_2O_5 at 1150 °C. MN powder was mixed with lead oxide (PbO) in ethanol and milled together in a zirconia ball mill for 24 h, and were calcined at 800 °C to produce PMN powder. Lead titanate ($PbTiO_3$) was produced in a similar manner using mixed oxide method from PbO and TiO_2. XRD of the PMN and PT were determined to ensure their purity [21] before mixing the powder together at molar ratio of 0.67PMN–0.33PT in ethanol and milled together for 30 min (Fig. 1). PMN and PT powder were then pressed into pellets before sintering at 1250 °C for 2 h using a hydraulic press to form disk samples of 15 mm diameter and 2 mm thickness. During calcining and sintering, PbO and

* Corresponding author. Tel.: +66 53 943445; fax: +66 53 943445.
E-mail address: arnon@chiangmai.ac.th (A. Chaipanich).

0272-8842/$36.00
doi:10.1016/j.ceramint.2011.04.095

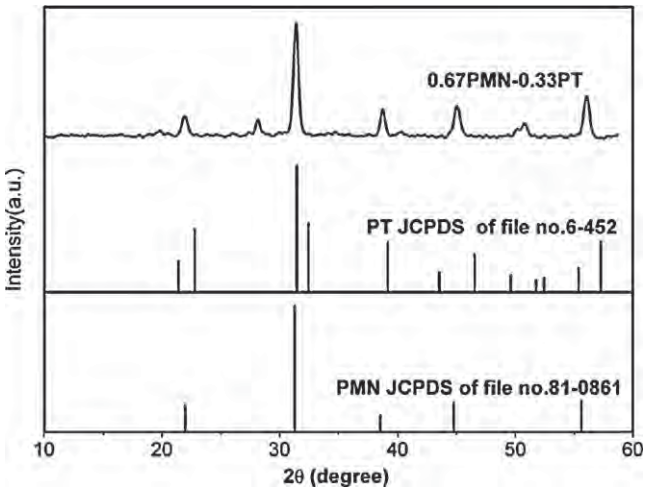

Fig. 1. X-ray diffraction patterns of PMN–PT.

PMN–PT powders were also used as excess powders to cover the sample in order to prevent lead volatilization.

These PMN–PT ceramic were then cut and filled with normal Portland cement (The American Society for Testing and Materials Type I cement) to produce 1–3 connectivity PMN–PT/PC composite using 60% PMN–PT by volume. A schematic diagram of PMN–PT/PC composites with 1–3 connectivity is illustrated in Fig. 2. Thereafter, the composites were placed for curing at 60 °C and 98% relative humidity for 5 days before measurements. An impedance meter (Hewlett Packard 4194A) was used to obtain the capacitance and the dissipation factor (tan δ) of the composites at room temperature and at frequency of 1 kHz. The relative dielectric constant (ε_r) was then calculated from the following equation:

$$\varepsilon_r = \frac{Ct}{\varepsilon_0 A}$$

where C is the sample capacitance, t is the thickness, ε_0 is the permittivity of free space constant (8.854×10^{-12} F m^{-1}), and

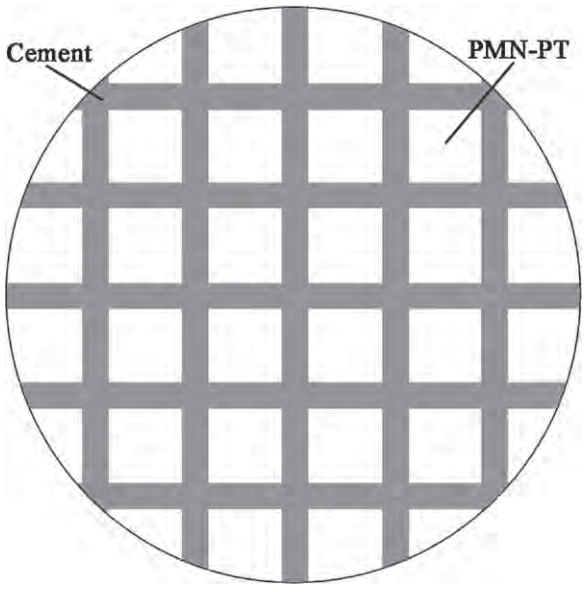

Fig. 2. Schematic diagram of 1–3 PMN–PT/PC composites.

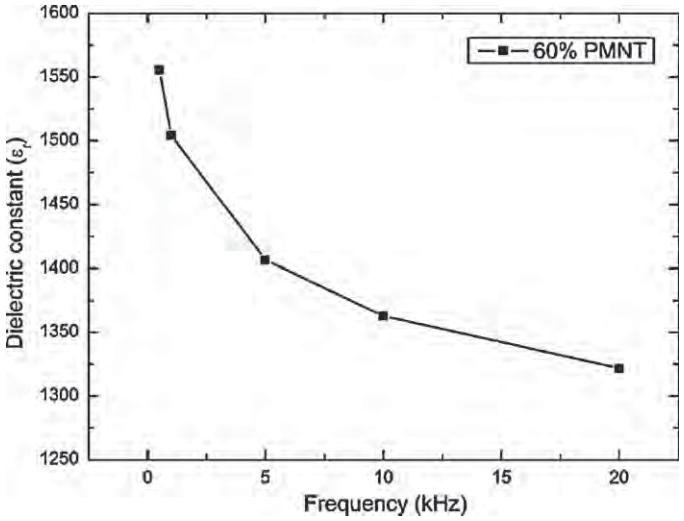

Fig. 3. Dielectric constants of PMN–PT/PC composites as plotted against frequency.

A is the electrode area. The room temperature ferroelectric hysteresis (P–E) loops were characterized using a computer controlled modified Sawyer–Tower circuit. The electric field was applied to a sample by a high-voltage ac amplifier with the input sinusoidal signal with a frequency of 10–90 Hz from a signal generator.

3. Results and discussion

The dielectric constant (ε_r) is shown against the frequency in Fig. 3 where the effect of frequency on the dielectric constant can be seen. The dielectric constant can be seen to decrease with increasing frequency where ε_r is ≈1500 at 1 kHz and ε_r is ≈1300 at 20 kHz. Moreover, when compared to the previous published results of 0–3 PMN–PT/PC composites [2], where ε_r is ≈500–700 for 50–70% PMN–PT, the dielectric constant of these 1–3 PMN–PT/PC composites can be seen to be much greater (almost doubled that of 0–3 composites). The dielectric

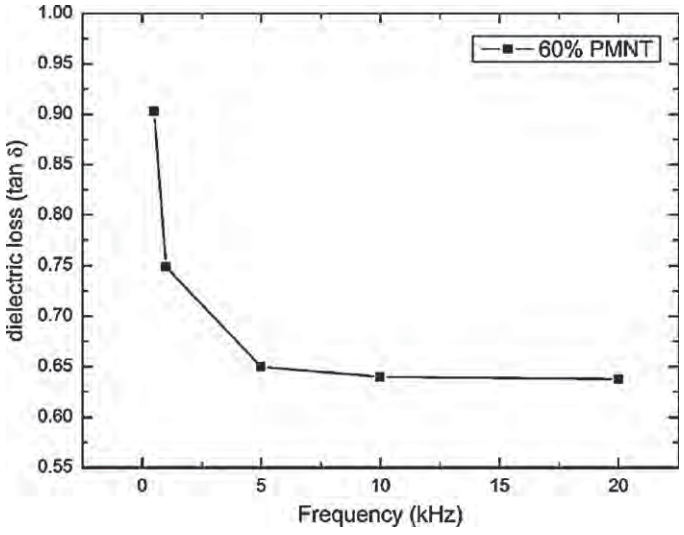

Fig. 4. Dielectric loss of PMN–PT/PC composites as plotted against frequency.

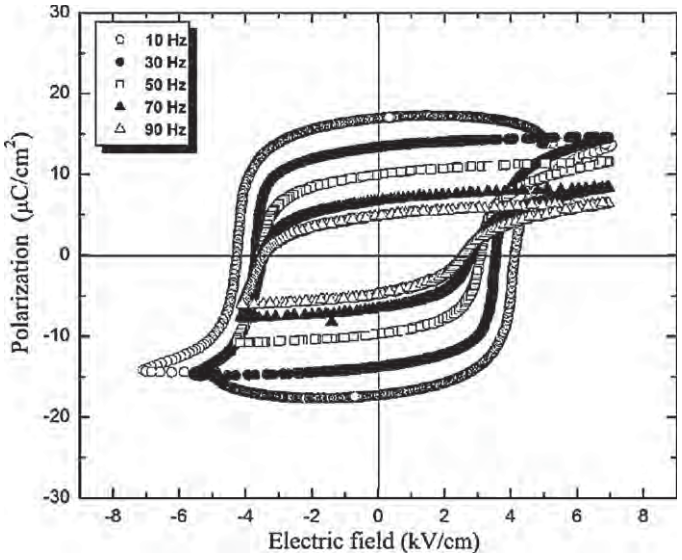

Fig. 5. Ferroelectric polarization–electric field (*P–E*) hysteresis loops of PMN–PT/PC composites at 10–90 Hz.

value therefore becomes closer to that of the pure PMN–PT ceramic where the measured ε_r is ≈2000 at 1 kHz. In addition, the dielectric loss of the composites (Fig. 4) was found to decrease with increasing frequency where the dielectric loss values reduced from 0.9 to 0.65 when the frequency increased from 0.1 to 20 kHz.

Hysteresis loops were plotted at 7 kV/cm and with varying frequency from 10 to 90 Hz (Fig. 5). For comparison, we define the *y*-axis intercept at a given applied field as the ''*instantaneous*'' remnant polarization (P_{ir}), while the *x*-axis intercept as the ''*instantaneous*'' coercive field (E_{ic}). Ferroelectric polarization–electric field (*P–E*) hysteresis loops at 10–90 Hz and varying electric field were observed. Although sharp end characteristic of normal hysteresis loop is seen for these composites, lossy appearance indicated by the increase in the total loop area can also be seen as a consequent of the cement matrix presenting in the 1–3 composites. Therefore, it should be noted here that fully saturated *P–E* loops cannot be achieved for these composites as a result of their highly lossy characteristics due to the presence of the weak conducting ions in the cement matrix [5]. Nonetheless, polarization–electric field (*P–E*) hysteresis loops measurements were still possible. For the ''instantaneous'' remnant polarization (P_{ir}) measured at 50 Hz and at the electric field of 7 kV/cm of the PMN–PT/PC composites was found to be ≈10 μC/cm^2. The effect of the frequency on P_{ir} and E_{ic} of PMN–PT/PC composites can be seen in Fig. 6(a) and (b), respectively. Quite clearly, it can be seen that P_{ir} decreases from 17 to 5 μC/cm^2 as frequency increases from 10 to 90 Hz. The E_{ic} also decreases from 4.2 to 2.5 kV/cm with increasing frequency (10–90 Hz). However, at a particular frequency and electric field used, these values of 1–3 composites are found to be significantly higher than previously published results of 0–3 composites. It is understandable that 1–3 composites essentially contain the piezoelectric ceramic fully aligned in one direction (1 connectivity prism) which allows the ceramic to possess greater dielectric

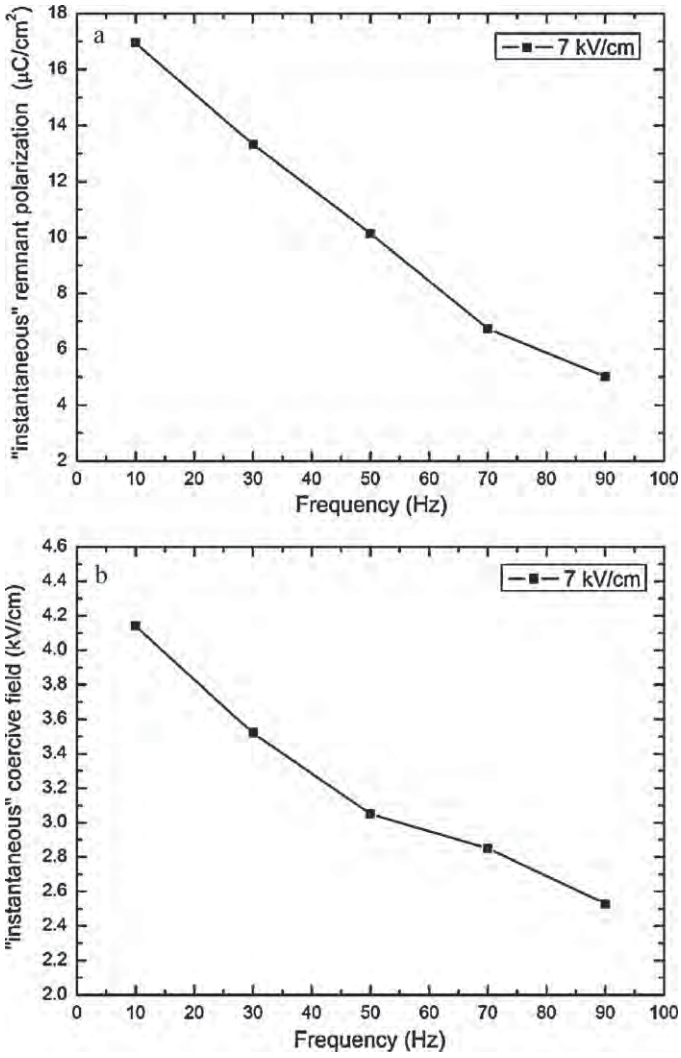

Fig. 6. The effect of the frequency on (a) P_{ir} and (b) E_{ic} of PMN–PT/PC composites.

properties and ferroelectric behavior giving less loss that would otherwise occur in the 0–3 composites. In 0–3 composites, the piezoelectric ceramic existed as random particles surrounded by cement matrix with high loss caused by the conducting ions [5,18,22]. In addition, less contact surface areas between the two materials would improve the properties of 1–3 composites when compared to 0–3 composites having the same volume content of ceramic [11].

4. Conclusions

The dielectric results of 1–3 PMN–PT/PC composites were found to be relatively high (ε_r = 1500 at 1 kHz) and is close to the pure PMN–PT ceramic (ε_r = 2000). Ferroelectric polarization–electric field (*P–E*) hysteresis loops of these composites show lossy appearance indicated by the increase in the total loop area as a consequent cement matrix presenting in the 1–3 composites. However, sharp end characteristics can still be observed. It was found that P_{ir} decreases from 17 to 5 μC/cm^2 as frequency increases from 10 to 90 Hz. E_{ic} value, on the other

hand, decreases from 4.2 to 2.5 kV/cm. At 50 Hz and at the electric field of 7 kV/cm, measured P_{ir} of the PMN–PT/PC composite was found to be ≈10 μC/cm^2. At a similar frequency and electric field used, these values of 1–3 composite are found to be significantly higher than previously published results of 0–3 composites.

Acknowledgements

The authors would like to express their sincere gratitude to staff members at the Electroceramics Research Laboratory for research facilities made possible for this research work. The authors gratefully acknowledge the Thailand Research Fund (TRF), Office of the Higher Education Commission and Chiang Mai University for financial support.

References

[1] S. Huang, J. Chang, R. Xu, F. Liu, L. Lu, Z. Ye, X. Cheng, Piezoelectric properties of 0–3 PZT/sulfoaluminate cement composites, Smart Materials and Structure 13 (2004) 270–274.
[2] Z. Li, D. Zhang, K. Wu, Cement-based 0–3 piezoelectric composites, Journal of the American Ceramic Society 85 (2002) 305–313.
[3] R. Potong, R. Rianyoi, L. Jareansuk, N. Jaitanong, R. Yimnirun, A. Chaipanich, Effect of particle size on the dielectric properties and ferroelectric hysteresis of 0–3 lead magnesium niobate titanate–Portland cement composites, Ferroelectrics 405 (2010) 98–104.
[4] D. Xu, X. Cheng, S. Huang, M. Jiang, Electromechanical properties of 2–2 cement based piezoelectric composite, Current Applied Physics 9 (2009) 816–819.
[5] X. Cheng, S. Huang, J. Chang, Z. Li, Piezoelectric, dielectric, and ferroelectric properties of 0–3 ceramic/cement composite, Journal of Applied Physics 101 (2007) 094110–094116.
[6] C Xin, S. Huang, C. Jun, X. Ronghua, L. Futian, L. Lingchao, Piezoelectric and dielectric properties of piezoelectric ceramic–sulphoaluminate cement composites, Journal of the European Ceramic Society 25 (2005) 3223–3228.
[7] A. Chaipanich, Dielectric and piezoelectric properties of PZT–cement composites, Current Applied Physics 7 (2007) 537–539.
[8] B. Dong, Z. Li, Cement-based piezoelectric ceramic smart composites, Composites Science and Technology 65 (2005) 1363–1371.
[9] N. Jaitanong, A. Chaipanich, T. Tunkasiri, Properties 0–3 PZT–Portland cement composites, Ceramics International 34 (2008) 793–795.
[10] A. Chaipanich, G. Rujijanagul, T. Tunkasiri, Properties of Sr- and Sb-doped PZT–Portland cement composites, Applied Physics A: Materials Science & Processing 94 (2009) 329–337.
[11] A. Chaipanich, Effect of PZT particle size on dielectric and piezoelectric properties of PZT–cement composites, Current Applied Physics 7 (2007) 574–577.
[12] A. Chaipanich, N. Jaitanong, T. Tunkasiri, Fabrication and properties of PZT–ordinary Portland cement composites, Materials Letters 61 (2007) 5206–5208.
[13] N. Jaitanong, H.R. Zeng, G.R. Li, Q.R. Yin, W.C. Vittayakorn, R. Yimnirun, A. Chaipanich, Interfacial morphology and domain configurations in 0–3 PZT–Portland cement composites, Applied Surface Science 256 (2010) 3245–3248.
[14] A. Chaipanich, N. Jaitanong, Effect of PZT particle size on the electromechanical coupling coefficient of 0–3 PZT–cement composites, Ferroelectric Letters Section 36 (2009) 37–44.
[15] A. Chaipanich, N. Jaitanong, R. Yimnirun, Effect of compressive stress on the ferroelectric hysteresis behavior in 0–3 PZT–cement composites, Materials Letters 64 (2010) 562–564.
[16] K.H. Lam, H.L.W. Chan, Piezoelectric cement-based 1–3 composites, Applied Physics A: Materials Science & Processing 81 (2005) 1451–1454.
[17] A. Chaipanich, N. Jaitanong, R. Yimnirun, Effect of carbon addition on the ferroelectric hysteresis properties of lead zirconate–titanate ceramic–cement composites, Ceramics International 37 (2011) 1181–1184.
[18] R. Rianyoi, R. Potong, N. Jaitanong, R. Yimnirun, A. Chaipanich, Fabrication and electrical properties of lead zirconate titanate–cement–epoxy composites, Ferroelectrics 401 (2010) 1–7.
[19] A. Chaipanich, N. Jaitanong, R. Rianyoi, R. Potong, Effect of temperature on the dielectric properties of 0–3 PZT–cement composites, Ferroelectric Letters Section 37 (2010) 76–81.
[20] L. Cao, Y. Xi, Z. Xu, Y. Feng, Research on dielectric and piezoelectric properties of Ta-doped $0.68Pb(Mg_{1/3}Nb_{2/3})O_3$–$0.32PbTiO_3$ ceramics, Ceramics International 30 (2004) 1373–1376.
[21] N. Zhong, X.L. Dong, D.Z. Sun, P.H. Xiang, H. Du, Electrical properties of $Pb(Mg_{1/3}Nb_{2/3})O_3$–$PbTiO_3$ ceramics modified with WO_3, Materials Research Bulletin 39 (2004) 175–184.
[22] V. Tomer, C.A. Randall, G. Polizos, J. Kostelnick, E. Manias, High- and low-field dielectric characteristics of dielectrophoretically aligned ceramic/polymer nanocomposites, Journal of Applied Physics 103 (2008) 034115.

Materials Science and Engineering C 32 (2012) 282–289

Contents lists available at SciVerse ScienceDirect

Materials Science and Engineering C

journal homepage: www.elsevier.com/locate/msec

Optimization of calcium chloride content on bioactivity and mechanical properties of white Portland cement

Pincha Torkittikul, Arnon Chaipanich *

Advanced Cement-Based Materials Research Unit, Department of Physics and Materials Science, Faculty of Science, Chiang Mai University, Chiang Mai 50200, Thailand

ARTICLE INFO

Article history:
Received 12 November 2010
Received in revised form 23 September 2011
Accepted 18 October 2011
Available online 30 October 2011

Keywords:
Cement
Calcium chloride
Bioactivity
Compressive strength
Setting time

ABSTRACT

This research investigates the optimization of calcium chloride content on the bioactivity and mechanical properties of white Portland cement. Calcium chloride was used as an addition of White Portland cement at 0, 1, 2, 3, 4, 5, 6, 7, 8, 9 and 10% by weight. Calcium chloride was dissolved in sterile distilled water and blended with White Portland cement using a water to cement ratio of 0.5. Analysis of the bioactivity and pH of white Portland cement pastes with calcium chloride added at various amounts was carried out in simulated body fluid. Setting time, density, compressive strength and volume of permeable voids were also investigated. The characteristics of cement pastes were examined by X-ray diffractometer and scanning electron microscope linked to an energy-dispersive X-ray analyzer. The result indicated that the addition of calcium chloride could accelerate the hydration of white Portland cement, resulting in a decrease in setting time and an increase in early strength of the pastes. The compressive strength of all cement pastes with added calcium chloride was higher than that of the pure cement paste, and the addition of calcium chloride at 8 wt.% led to achieving the highest strength. Furthermore, white Portland cement pastes both with and without calcium chloride showed well-established bioactivity with respect to the formation of a hydroxyapatite layer on the material within 7 days following immersion in simulated body fluid; white Portland cement paste with added 3%$CaCl_2$ exhibited the best bioactivity.

1. Introduction

Over the past decade, mineral trioxide aggregate (MTA) was developed as a root-end filling material because it is bioactive, biocompatible, and can successfully seal the connection between the root canal system and surrounding tissues [1–6]. According to United States Patent No. 5769638, MTA is essentially a type I ordinary Portland cement with a 4:1 proportion of bismuth oxide added for radiopacity [7]. Due to the low cost and wide availability of Portland cement, many recent studies have focused on the evolution of Portland cement as an alternative to MTA [8–15].

Recently, many studies have compared MTA with white Portland cement (WPC); the findings suggest that WPC has the potential to be used as a less expensive root-end filling material [8–14]. Asgary et al. [10] reported that both MTA and WPC have similar chemical compositions except for bismuth oxide in MTA. Good biocompatibility of MTA and WPC proposed for root-end filling restorations was obtained from the results of Ribeiro et al. [8], which suggests that MTA and WPC have no cytotoxic effects on mouse lymphoma cells and do not induce DNA damage as depicted by the single cell gel (comet) assay. WPC has also been found to have additional advantages. Shahi et al. [15] determined that WPC has better sealing ability than MTA due to bismuth oxide particles would result in the formation of a rough amorphous phase in dentinal walls, and inferior sealing ability [16].

However, the main disadvantage of Portland cement is its long setting time (3 h); this limits its application for use as a dental coronal restorative material because it is easily washed away by saliva before setting [17–18]. Because calcium chloride ($CaCl_2$) is one of the most effective accelerators of hydration and setting in Portland cement paste [19–21], many experiments have been performed to overcome this clinical disadvantage by adding $CaCl_2$ [12, 14, 18, 22–24]. Bortoluzzi et al. [18] reported that the addition of 10% $CaCl_2$ in MTA and WPC provided reductions of 35.5% and 68.5%, respectively, in final setting time. Harrington et al. [25] added 10% and 15% of $CaCl_2$ to WPC and observed a reduction of more than 50% for both initial and final setting times.

In 2002, Abdullah et al. [26] investigated the biocompatibility of accelerated WPC by observing the cytomorphology of SaOS-2 osteosarcoma cells. $CaCl_2$ was used as an accelerator in their investigation in order to reduce setting time. Scanning electron microscopy (SEM) provided evidence that WPC paste with added $CaCl_2$ was nontoxic, and that the addition of $CaCl_2$ as an accelerator had no adverse effect on biocompatibility. This ability is the most exciting aspect of white Portland cement: not only for use as restoration material in dentistry, but also for its potential application in orthopedics.

* Corresponding author. Tel.: +66 5394 3367; fax: +66 5335 7512.
E-mail address: arnon@chiangmai.ac.th (A. Chaipanich).

0928-4931/$ – see front matter © 2011 Elsevier B.V. All rights reserved.
doi:10.1016/j.msec.2011.10.030

In addition, Kokubo et al. [27] developed simulated body fluid (SBF) containing ion concentrations similar to those of human blood plasma. The formation of a hydroxyapatite (HA) layer on the material surface within 4 weeks of exposure to SBF in vitro indicates that the material is bioactive and will form a bond with living tissue.

In spite of the increasing potential clinical applications of WPC with added $CaCl_2$, their bioactivity and dissolution characteristics in SBF have not yet been reported. Accordingly, in this study the optimization of calcium chloride content on the bioactivity of WPC was carried out in SBF in order to determine HA formation. The pH values of the SBF solutions following contact with WPC containing various added amounts of $CaCl_2$ were also measured. In addition, mechanical properties – i.e. setting time, density, compressive strength, and volume of permeable voids – were also investigated.

2. Materials and methods

2.1. Material preparation and characterization

WPC (Siam Cement Ltd., Thailand), $CaCl_2$ (Merck Ltd., Germany) and sterile distilled water (Merck Millipore Ltd., Germany) were used in this investigation. $CaCl_2$ was dried at 120 °C for 12 h and added to WPC at 0 to 10 wt.% (see Table 1). $CaCl_2$ was dissolved in water and was blended with WPC powder using a water to cement ratio of 0.5. In each case of 100 g WPC with X% added $CaCl_2$, X g of $CaCl_2$ was dissolved in 50 g of sterile distilled water, and then blended with 100 g of WPC. Mix proportions are given in Table 1. The mixtures were then cast into rubber molds (10 mm in diameter and 2 mm in height) [28], sealed with plastic wrap and keep at 23 ± 2 °C. After 24 h of setting, the samples were removed from the molds and cured in a water bath at 37 ° C for 7 days. The cured cement pastes were immersed in acetone (100%) to stop hydration, and then air-dried at room temperature. The phase compositions of the pastes were determined by X-ray diffraction using CuKα radiation (Philips PW-3040, The Netherlands). Surface morphology was observed using a low-vacuum scanning electron microscope (JEOL JEM-5910LV, Japan) linked to an energy-dispersive X-ray (EDX) analyzer at the electron microscopy research and service center of Chiang Mai University.

2.2. Setting times

The setting times of WPC pastes containing various amount of $CaCl_2$ were determined using a Vicat needle, according to ASTM C191-99 [29]. The apparatus consisted of a movable rod (300 g, 10 mm in diameter) and a steel needle (1 mm diameter, 50 mm length). $CaCl_2$ was dried at 120 °C for 12 h and added to WPC at 0 to 10 wt.% (see Table 1). First, $CaCl_2$ was dissolved in the amount of water required for normal consistency [30], and then was blended with 650 g of WPC powder (see Table 1). After mixing, the mixture was filled in ring molds and placed on the base plates. Excess paste at the top of each mold was removed. Then a steel needle was plunged into the cement pastes every 10 min to measure the penetration. The initial setting time was determined as the time necessary for achieving a penetration of 25 mm, and the final setting time as the time when the needle could no longer sink into the pastes.

Table 1
Mixture proportion of the cement pastes in this investigation.

Mix	%WPC	%$CaCl_2$	Water to Cement ratio used in Section				
			2.1	2.2	2.3	2.5	2.6
WPC0$CaCl_2$	100	0	0.5	0.257	0.5	0.5	0.5
WPC1$CaCl_2$	100	1	0.5	0.257	0.5	0.5	0.5
WPC2$CaCl_2$	100	2	0.5	0.258	0.5	0.5	0.5
WPC3$CaCl_2$	100	3	0.5	0.259	0.5	0.5	0.5
WPC4$CaCl_2$	100	4	0.5	0.266	0.5	0.5	0.5
WPC5$CaCl_2$	100	5	0.5	0.270	0.5	0.5	0.5
WPC6$CaCl_2$	100	6	0.5	0.280	0.5	0.5	–
WPC7$CaCl_2$	100	7	0.5	0.292	0.5	0.5	0.5
WPC8$CaCl_2$	100	8	0.5	0.304	0.5	0.5	–
WPC9$CaCl_2$	100	9	0.5	0.313	0.5	0.5	–
WPC10$CaCl_2$	100	10	0.5	0.321	0.5	0.5	0.5

2.3. Density

The wet bulk density of WPC containing various amount of $CaCl_2$ was determined according to ASTM C948-81 [31]. $CaCl_2$ was dried at 120 °C for 12 h and added to WPC at 0 to 10 wt.% (see Table 1). $CaCl_2$ was dissolved in water and blended with WPC powder using a constant water to cement ratio of 0.5 (Table 1). The mixtures were cast and set in cubic molds (5 cm × 5 cm × 5 cm) for 24 h, and were cured in a water bath at 37 °C. After 3 and 7 days of curing, the test specimens were removed from the water bath and immediately weighed in water; these masses were recorded as A. Then the surface moisture of specimens was removed with a towel and these saturated surface-dry specimens were weighed in air; the masses were designated as B. The calculation of wet bulk density is as follows, where ρ_w is the density of water [31]:

$$\text{Wet bulk density}\left(\text{g/cm}^3\right) = \frac{B}{B-A} \times \rho_w$$

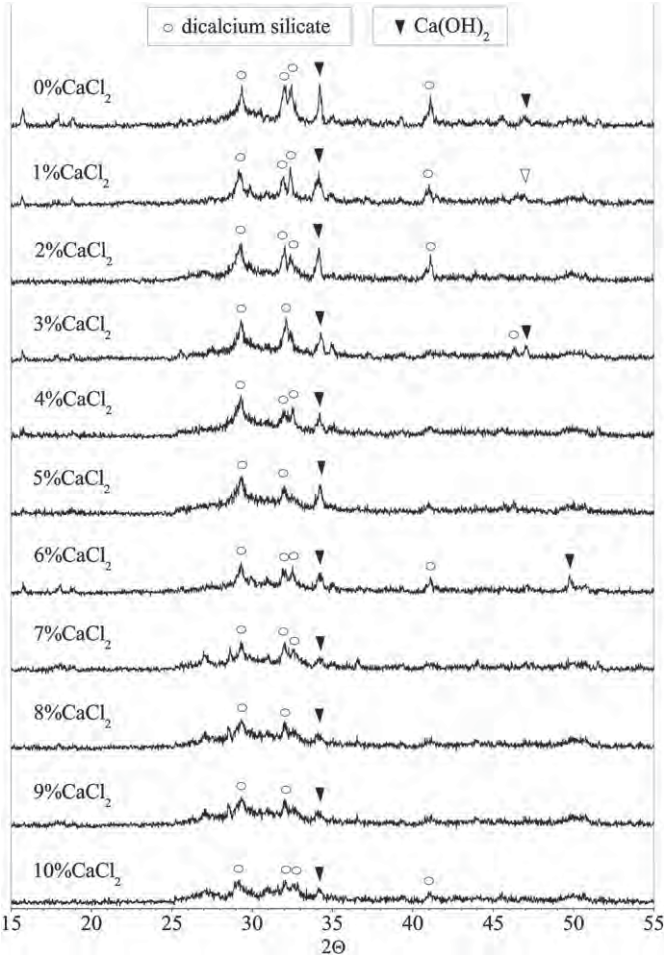

Fig. 1. XRD data for WPC paste with various added amounts of $CaCl_2$ after curing in water bath at 37 °C for 7 days (Pre-immersion).

2.4. Compressive strength

After the specimens had been investigated for wet bulk density, the compressive strength was determined according to ASTM C109-01 [32]. The compressive strength of the pastes was tested at 3 and 7 days of curing in order to determine the effect of $CaCl_2$ at an early age. The specimens were placed on the base plate of the load frame (the smooth sides of specimens were sandwiched between two compression bars) and then were compressed at a loading rate of 0.5 cm^{-1}. The reported results are the averages of three specimens.

2.5. Volume of permeable voids

The volume of permeable voids of WPC pastes containing various amount of $CaCl_2$ was determined according to ASTM C642-97 [33]. $CaCl_2$ was dried at 120 °C for 12 h and added to WPC at 0 to 10 wt.%

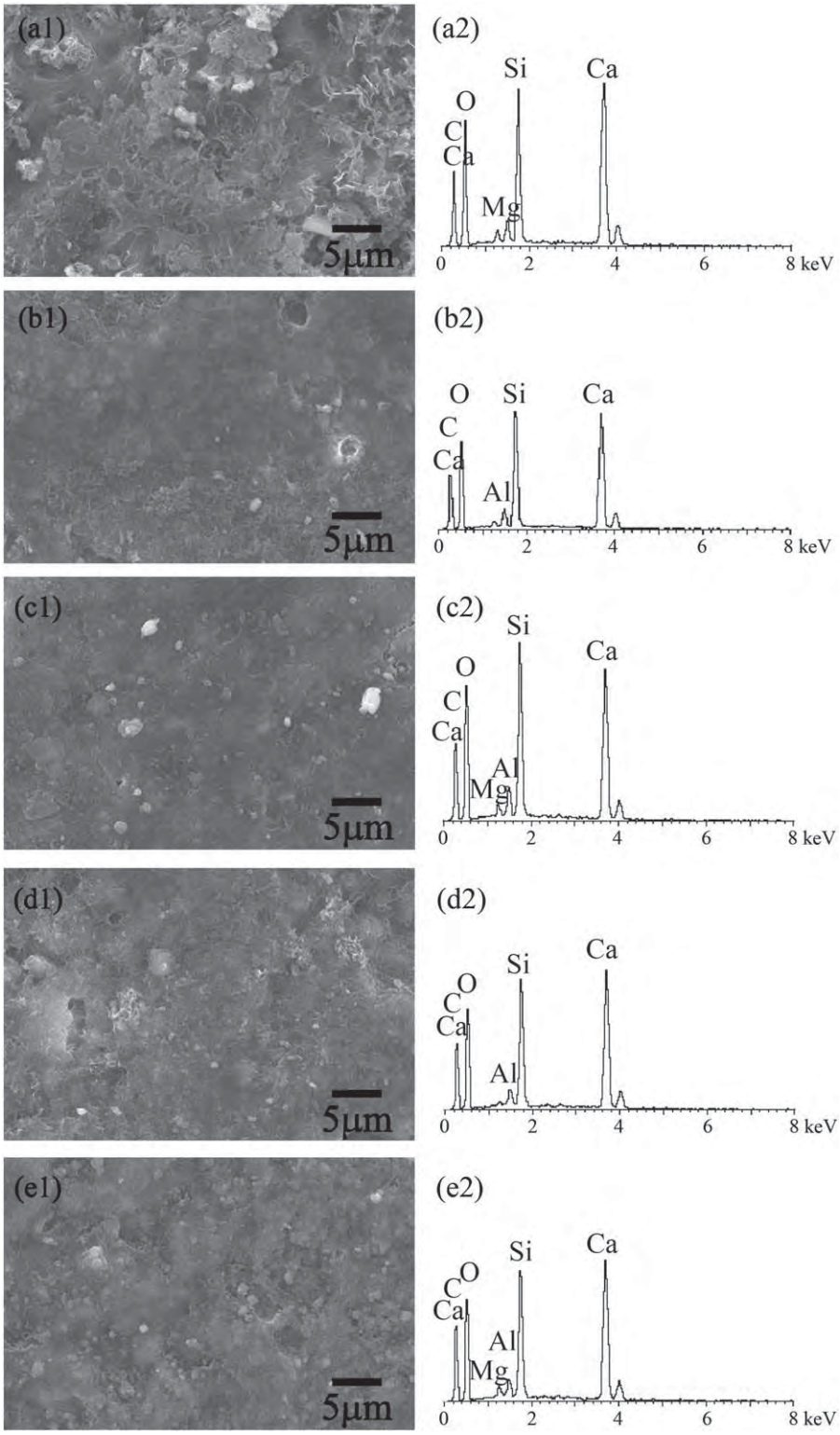

Fig. 2. SEM micrographs and EDX spectra of (a1, a2) WPC0$CaCl_2$, (b1, b2) WPC3$CaCl_2$, (c1, c2) WPC5$CaCl_2$, (d1, d2) WPC7$CaCl_2$ and (e1, e2) WPC10$CaCl_2$ (Pre-immersion).

(see Table 1). The pastes were prepared according to the method described in Section 2.3. After 3 and 7 days of curing in a water bath at 37 °C, the cubic specimens (5 cm × 5 cm × 5 cm) were dried at 100 °C for 48 h and weighed in water; these masses were recorded as C. After drying, the specimens were boiled for 5 h, allowed to cool for 24 h and weighed in water; the specimen mass were recorded as D. Then, the surface moisture of specimens were removed with a towel and weighed in air. These saturated surface-dry mass were designated as E. The masses of C, D and E were then used to determine wet bulk density, with calculations as follows [33]:

$$\text{Volume of permeable voids } (\%) = \frac{E-C}{E-D} \times 100$$

2.6. In vitro bioactivity and dissolution

WPC pastes with 0, 1, 2, 3, 4, 5, 7, 8 and 10% $CaCl_2$ (10 mm in diameter and 2 mm in height) were prepared according to the method described in Section 2.1. The 7-day-cured pastes were immersed in simulated body fluid, SBF solution (pH 7.25) [27], under sessile conditions at 37 °C in hermetically sealed polypropylene containers with a surface area-to-volume ratio of 0.1 cm^{-1} [34]. The pH values of SBF following contact with the pastes were measured at 1, 3 and 7 days using an electrolyte-type pH meter (Sartorius, Germany). After 7 days of immersion, the pastes were removed from the SBF solution, gently rinsed with deionized water and then air-dried at room temperature. The phase compositions and surface morphology of the pastes after immersion in SBF were investigated by X-ray diffraction (using CuKα radiation) and low-vacuum scanning electron microscope linked to EDX analyzer.

3. Results and discussion

3.1. Material characterization

After 7 days of curing in a water bath at 37 °C, the WPC pastes containing 0 to 10% $CaCl_2$ (see Table 1) were characterized by X-ray diffraction (XRD) and scanning electron microscope (SEM) technique. The effect of $CaCl_2$ on cement hydration is shown in Fig. 1. The XRD pattern indicated that the characteristic peaks of calcium hydroxide ($Ca(OH)_2$) decreased with increasing $CaCl_2$ content, because the addition of $CaCl_2$ resulted in higher concentrations of Ca^{2+} and reduced OH^- concentrations during the hydration process [35]. This finding is in agreement with previous studies supporting that $Ca(OH)_2$ formation was significantly reduced with $CaCl_2$ addition [19, 36]. In addition, it is generally accepted that $CaCl_2$ has the ability to accelerate cement hydration. Thus, a reduction in intensity of unreacted dicalcium silicate (C_2S) was observed for WPC containing $CaCl_2$.

SEM micrographs (Fig. 2) of the surface of 7-day-cured WPC pastes containing various amount of $CaCl_2$ demonstrated that no particles are generated on the surface of the samples after cured in a water bath at 37 °C for 7 days. EDX spectra of the pastes confirm the presence of the main elemental constituents of calcium silicate hydrate (C–S–H): calcium (Ca), silicon (Si), aluminum (Al) and oxygen (O).

3.2. Setting time

The effect of $CaCl_2$ on the setting time of WPC pastes is shown in Fig. 3. It can be seen that the initial and final setting times decreased with increasing $CaCl_2$ content. When $CaCl_2$ was added at 0, 1, 2, 3, 4, 5, 6, 7, 8, 9 and 10 wt.%, the initial setting time decreased from 133 min (0% $CaCl_2$) to 61.8, 42.5, 38.4, 34.7, 30, 21.5, 14.4, 11.9, 10 and 8.4 min, respectively; whereas the final setting time decreased from 170 min

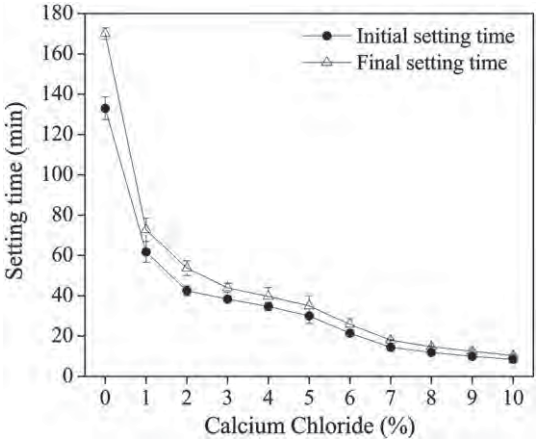

Fig. 3. The effect of $CaCl_2$ on setting time of WPC pastes.

(0% $CaCl_2$) to 72.8, 53.7, 44, 39.7, 35, 25.9, 18, 14.8, 12.5 and 10.4 min, respectively.

The addition of 1, 2, 3, 4, 5, 6, 7, 8, 9 and 10% $CaCl_2$ provided reductions of 53.5%, 68.0%, 71.1%, 73.9%, 77.4%, 83.8%, 89.2%, 91.1%, 92.5% and 93.7% respectively, in the initial setting time of WPC pastes, whereas the final setting time was reduced by 57.2%, 68.4%, 74.1%, 76.6%, 79.4%, 84.8%, 89.4%, 91.3%, 92.6% and 93.9%. Previous effect of $CaCl_2$ on the hydration of Portland cement was reported by Ramachandran et al. [21] that as soon as water comes into contact with Portland cement, the heat of hydration seems to increase with the amount of added $CaCl_2$. The higher amount of heat developed in cement pastes containing greater amounts of $CaCl_2$ is due to the acceleration of hydration of calcium aluminates in the presence of $CaCl_2$ [19]. Thus, it can be inferred that the addition of $CaCl_2$ reduces the setting time of WPC paste due to the acceleration of aluminate phase hydration, which provides rapid setting of the cement pastes.

3.3. Compressive strength

After 3 and 7 days of curing in a water bath at 37 °C, the compressive strength and density of the cubic WPC paste samples (5 cm × 5 cm × 5 cm) containing 0 to 10% $CaCl_2$ were measured (see Table 1). The effect of $CaCl_2$ on compressive strength of the pastes is shown in Fig. 4. It can be seen that all WPC pastes containing $CaCl_2$ demonstrated higher compressive strength than that of pure WPC paste (WPC0$CaCl_2$), because the addition of $CaCl_2$ will results in the acceleration of the C–S–H formation rate which provides strength of

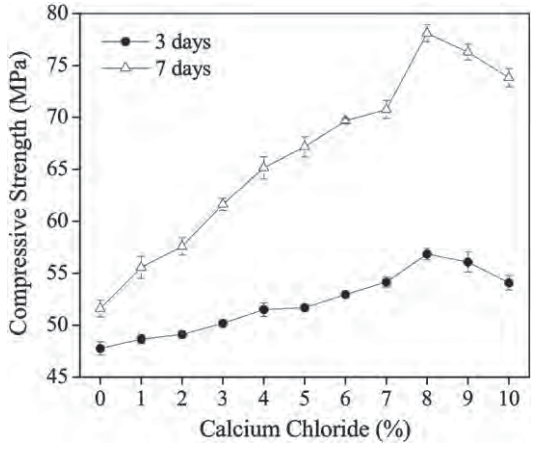

Fig. 4. The effect of $CaCl_2$ on compressive strength of WPC pastes after curing in water bath at 37 °C for 3 and 7 days.

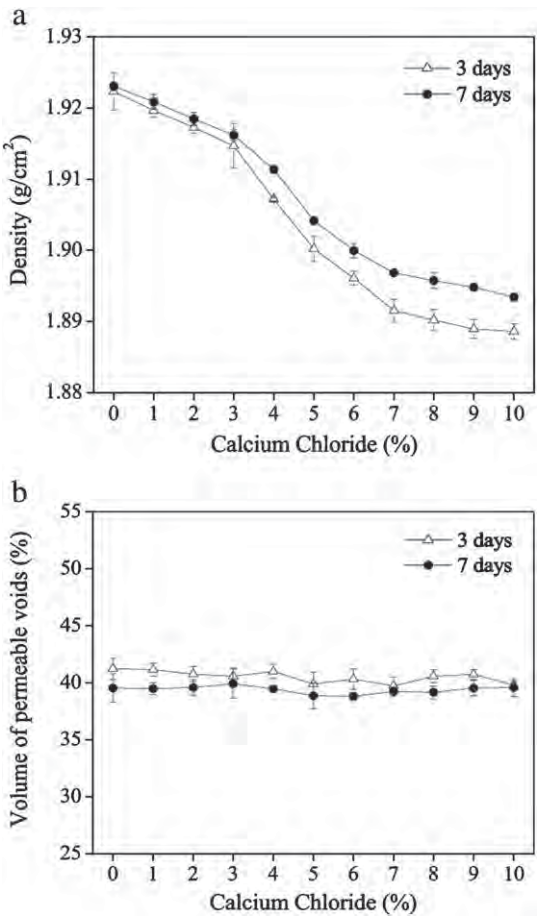

Fig. 5. The effect of $CaCl_2$ on density and volume of permeable voids of WPC pastes after curing in water bath at 37 °C for 3 and 7 days.

the pastes [37]. The compressive strength of WPC pastes at 7 days increased with increasing amounts of $CaCl_2$ up to 8 wt.% (78.1 MPa); this resulted in a 51.4% increase compared to WPC0$CaCl_2$ paste. However, the compressive strength was found to decrease when $CaCl_2$ was added at 9 and 10 wt.%. Therefore, the addition of $CaCl_2$ at 8 wt.% is optimal in order to achieve the highest strength of WPC paste. $CaCl_2$ is also thought to act as a catalyst for the hydration of tricalcium silicate (C_3S), as well as being a catalyst for calcium aluminate giving earlier setting time [19]. Calcium silicates, especially C_3S is known to be mainly responsible for the compressive strength of cement paste

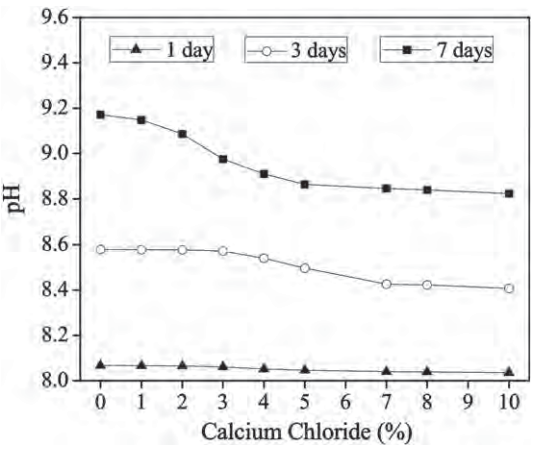

Fig. 6. The effect of $CaCl_2$ on pH of SBF solution after contact with WPC pastes for various times.

at the age tested (3 and 7 days) [19]. It would appear from the results that at 8% $CaCl_2$ is the optimum amount but higher amount would lead to a drop in the strength. This is due to the fact that while adding the $CaCl_2$, there will be less amount of C_3S and it is thought that at greater than 8% the reduction in C_3S become significant. As a consequent the drop in compressive strength is seen.

3.4. Density and permeable voids

After 3 and 7 days of curing in a water bath at 37 °C, the density and porosity of the cubic WPC pastes (5 cm × 5 cm × 5 cm) containing 0 to 10% $CaCl_2$ were measured (see Table 1). The effect of $CaCl_2$ on the density of WPC pastes is shown in Fig. 5(a). The result shows that the density of WPC pastes decreased with increasing $CaCl_2$ content. This can be explained by the fact that the addition of $CaCl_2$ not only increases the rate of formation of C–S–H but also promotes a change of C–S–H morphology, as described by Juenger et al. [37] who used a soft X-ray microscope. The C–S–H formed in WPC pastes containing $CaCl_2$ will have an inhomogeneous structure of low-density and high-density phases, rather than a homogenous dense structure of C–S–H as in WPC0$CaCl_2$ [37].

Furthermore, the lower density of this C–S–H not only decreases the overall density of the cement pastes, but also increases the rate of cement hydration as well. Ions can travel farther through the cement particles and have more space for hydration, thus allowing a greater rate of cement hydration which gives high early strength [37]. This is why the compressive strength of WPC pastes with added $CaCl_2$ was higher than that of WPC0$CaCl_2$ (Fig. 4).

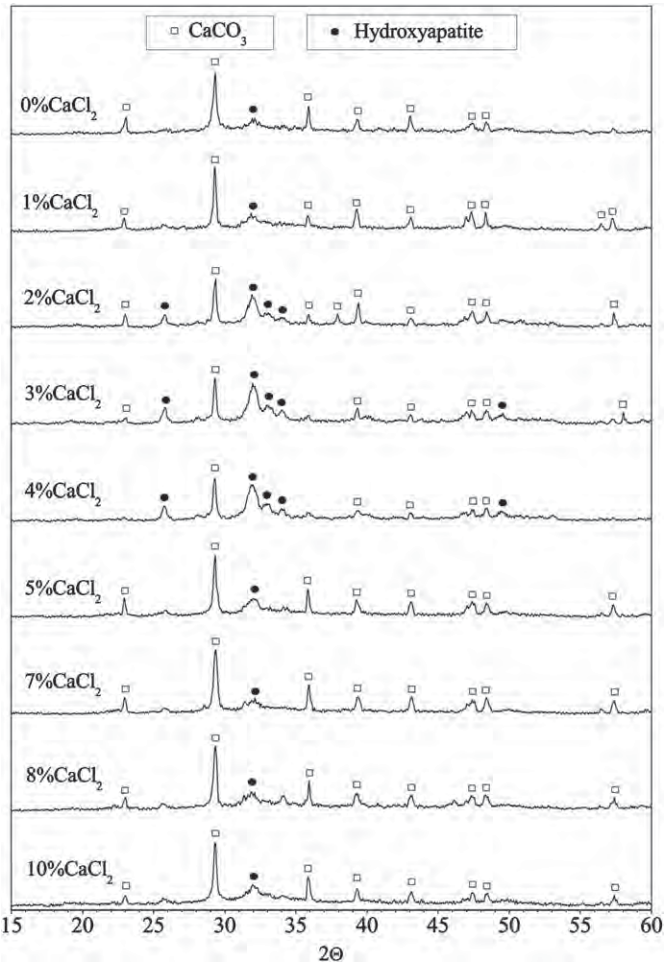

Fig. 7. XRD data for WPC paste with various added amounts of $CaCl_2$ after immersion in SBF solution for 7 days.

The effect of $CaCl_2$ on the volume of permeable voids in cement pastes is shown in Fig. 5(b). It can be seen that this trend is not related to the density results as reported earlier, since the volume of permeable voids in WPC pastes with various amount of $CaCl_2$ were not found to be significantly different from each other. This finding thus confirms the above explanation that the density of WPC pastes with added $CaCl_2$ is lower than that of WPC0$CaCl_2$ due to the less dense structure of C–S–H phase formation. Therefore, the acceleration of the C–S–H formation rate by adding $CaCl_2$ could be considered to be a main factor leading to achieving higher compressive strength (Fig. 4).

3.5. pH measurement

After 7 days of curing in a water bath at 37 °C, WPC pastes containing 0, 1, 2, 3, 4, 5, 7, 8 and 10% $CaCl_2$ were immersed in SBF solution. The effect of $CaCl_2$ on the pH of SBF solution after immersion of cement pastes at various times is shown in Fig. 6. The results indicate that the pH value of SBF solution decreased with an increase of $CaCl_2$ content. The decrease in pH of SBF solution after contact with cement pastes containing $CaCl_2$ in this study corresponds well with the results of Wang et al. [35] who have found that the pH of Ca_3SiO_5 pastes with added $CaCl_2$ is significantly lower than that of pure Ca_3SiO_5 paste.

3.6. In vitro bioactivity

After 7 days of curing in a water bath at 37 °C, WPC pastes containing 0, 1, 2, 3, 4, 5, 7, 8 and 10% $CaCl_2$ were placed in contact with SBF solution (surface area to volume ratio of 0.1 cm^{-1}) in order to investigate the bioactivity of the pastes. The effect of $CaCl_2$ on the formation of HA is shown in Figs. 7–9.

XRD patterns of WPC pastes containing various amount of $CaCl_2$ after immersion in SBF solution for 7 days are shown in Fig. 7. The characteristic peaks of $Ca(OH)_2$ and C_2S were not be detected whereas the main peak of HA and calcium carbonate ($CaCO_3$) were found at $2\theta = 32°$ and 29.6° respectively. This finding can be explained that when the pastes are placed in contact with SBF, $Ca(OH)_2$ will react with SBF and transform to $CaCO_3$. The Ca^{2+} ions leached from the cement matrix will enhance the supersaturation of SBF which can promote the HA layer precipitation cover the surface of the pastes, as can be seen, both characteristic peaks (HA and $CaCO_3$) became the main constituent of the XRD patterns [28, 39].

Moreover, the characteristic peaks of HA were found in all WPC pastes and these finding agree with those reported by previous studies indicating that WPC paste showed good bioactivity with HA formation after immersion in SBF [38–39]. The intensity of the HA peaks of WPC2$CaCl_2$, WPC3$CaCl_2$ and WPC4$CaCl_2$ pastes were obviously higher than that of WPC0$CaCl_2$ paste, while the HA peaks of WPC5$CaCl_2$, WPC7$CaCl_2$, WPC8$CaCl_2$ and WPC10$CaCl_2$ were not

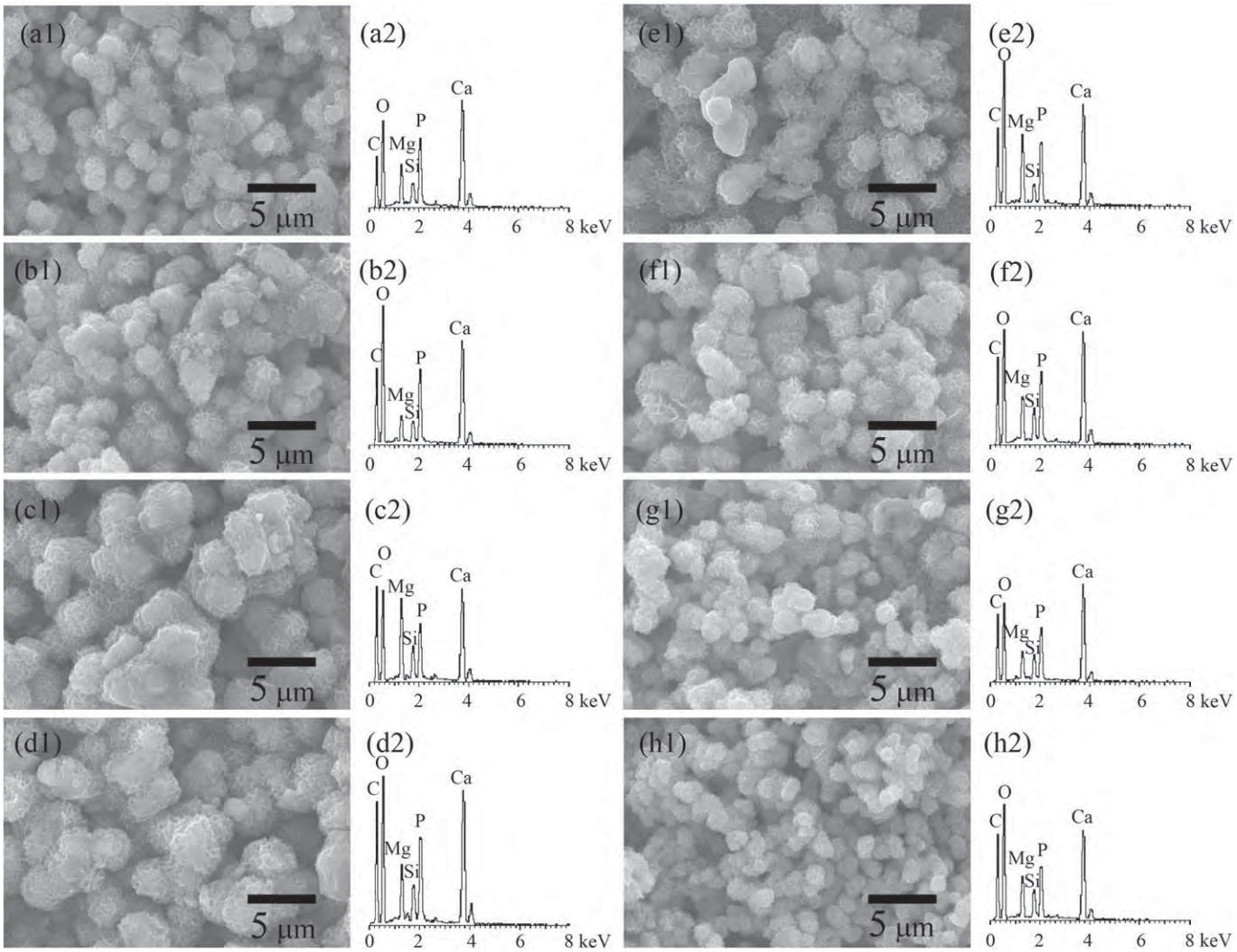

Fig. 8. SEM and EDX spectra of (a1, a2) WPC0$CaCl_2$, (b1, b2) WPC1$CaCl_2$, (c1, c2) WPC2$CaCl_2$, (d1, d2) WPC3$CaCl_2$, (e1, e2) WPC4$CaCl_2$, (f1, f2) WPC5$CaCl_2$, (g1,g2) WPC7$CaCl_2$, (h1, h2) WPC10$CaCl_2$ after immersion in SBF solution for 7 days.

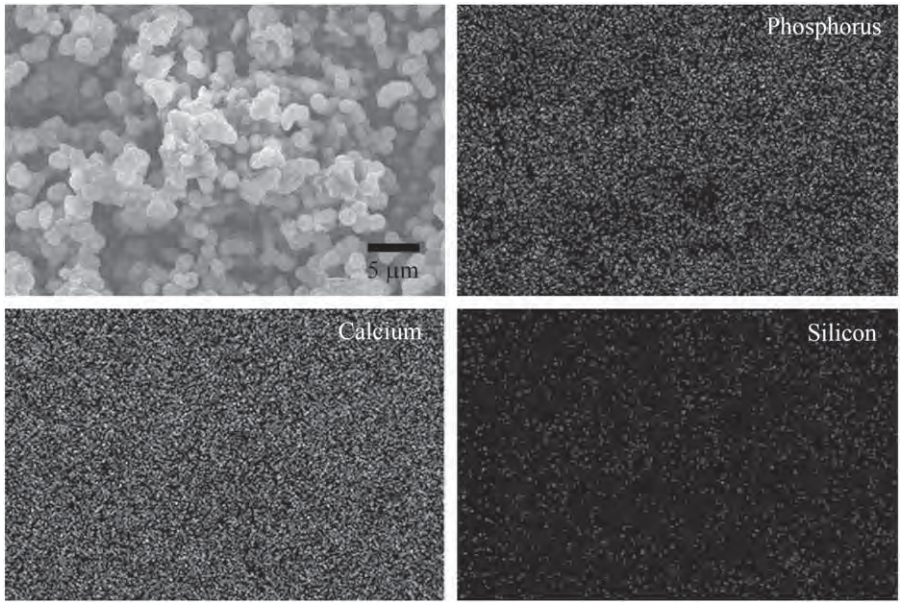

Fig. 9. The EDX mapping images of pure WPC0$CaCl_2$ after immersion in SBF solution for 7 days.

found to be significantly different from each other. In addition, it should be noted that WPC3$CaCl_2$ had the highest intensity peak of HA.

Fig. 8 shows SEM micrographs and EDX spectra of WPC pastes containing various amount of $CaCl_2$ following immersion in SBF for 7 days. These spectra provide information for establishing bioactivity by observing the physical appearances of the pastes. During SEM inspection of the surface, HA formation was observed on all WPC pastes with similar morphology, as reported with other bioactive materials [40–46]. The pastes were covered with circular flake-like agglomerated hydroxyapatite consisting of elongated crystallite within 7 days of immersion [46]. The presence of calcium (Ca) and phosphorus (P) in EDX spectra of the pastes is responsible for the formation of HA. Furthermore, EDX mapping images of elemental phosphorus provide evidence that grown crystals of HA cover the whole surface of WPC0$CaCl_2$ (Fig. 9) after immersion in SBF solution for 7 days.

It is generally accepted that Si–OH functional groups on a material's surface (such as calcium silicate glasses and ceramics) have been shown to act as nucleation sites for HA precipitation, i.e. the Si–OH group is effective for inducing hydroxyapatite [27, 45]. However, supersaturation of Si–OH is not in itself enough to promote the formation of hydroxyapatite crystals on the material in a SBF environment [47–49]. From the XRD pattern in Fig. 7, and based on the reported literature [47–49], the bioactivity of the materials is presumably dependent on the ratio of silica to calcium oxide. WPC (containing ≈20% SiO_2 and ≈70% CaO) exhibited the best bioactivity with the addition of 3% $CaCl_2$, where the highest intensity peak of HA was observed.

Despite increasing clinical interest in WPC with use $CaCl_2$ as an accelerator to improve setting property, their bioactivity and dissolution characteristics in SBF have not yet been reported. The present study confirms the well-established bioactivity of the WPC pastes and suggests that the optimum $CaCl_2$ addition of WPC for orthopedic application is at 3% $CaCl_2$. However, the acceleration of cement hydration by adding $CaCl_2$ will result in heat generation during hydration process which may affect to the living cell. Therefore, if WPC modified $CaCl_2$ is to be considered as a new cement for use in orthopedics application, the effect of heat generation from hydration process on the living cell (biological constituents such as cells, protein structure, etc.) should be investigated. Further work is needed to determine the effect of heat released during cement hydration process on the living cells and explain the exact mechanism as to why the trends of hydroxyapatite formation observed in this study are occurring.

4. Conclusions

The addition of calcium chloride could accelerate the hydration of white Portland cement, resulting in a decrease in setting time and an increase in early strength of the pastes. The optimization of calcium chloride addition to achieve the highest strength of white Portland cement paste was 8 wt.%. Furthermore, white Portland cement paste containing 3%$CaCl_2$ exhibited the best bioactivity as the highest amount of hydroxyapatite was observed after immersed in SBF solution. Therefore, it can be concluded from this finding that the addition of 3%$CaCl_2$ to white Portland cement is the optimal content for clinical application. In addition, hydroxyapatite formation in WPC2$CaCl_2$, WPC3$CaCl_2$ and WPC4$CaCl_2$ pastes was noticeably greater than that observed in WPC0$CaCl_2$ paste.

Acknowledgements

Financial support from the Thailand Research Fund through the Royal Golden Jubilee Ph.D. Program (Grant No. PHD/0281/2550) to Ms. Pincha Torkittikul and Assist. Prof. Dr. Arnon Chaipanich is gratefully acknowledged. The authors also appreciate useful comments and advice given by Dr. Guocheng Wang and Associate Prof. Dr. Hala Zreiqat of Biomaterials and Tissue Engineering Research Group, School of Aerospace, Mechanical & Mechatronic Engineering, The University of Sydney. The authors would also like to thank the Thailand Research Fund, the Office of the Higher Education Commission, Thailand, and Faculty of Science, Chiang Mai University for the TRF-CHE Research grant for Mid-career University Faculty awarded to Assist. Prof. Dr. Arnon Chaipanich. The Graduate School of Chiang Mai University is also acknowledged.

References

[1] R. Holland, V. de Souza, M.J. Nery, J.A.O. Filho, P.F.E. Bernabe, E. Dezan, J. Endod. 25 (1999) 728–730.
[2] D.R. Hachmeister, W.G. Schindler, W.A. Walker, D.D. Thomas, J. Endod. 28 (2002) 386–390.
[3] J. Saidon, J. He, Q. Zhu, K. Safavi, L.S.W. Spångberg, Oral Surg. Oral Med. Oral Pathol. 95 (2003) 483–489.
[4] C.R.A. Valois, E.D. Costa Jr., Oral Surg. Oral Med. Oral Pathol. 97 (2004) 108–111.
[5] R.L. Martin, F. Monticelli, W.W. Brackett, R.J. Loushine, R.A. Rockman, M. Ferrari, D.H. Pashley, F.R. Tay, J. Endod. 33 (2007) 272–275.

[6] C. Boutsioukis, G. Noula, T. Lambrianidis, J. Basic Res. Technol. 34 (2008) 1239–1242.
[7] M. Torabinejad, D.J. White, US Patent No. 5,769,638, May 1995.
[8] D.A. Ribeiro, M.A.H. Duarte, M.A. Matsumoto, M.E.A. Marques, D.M.F. Salvadori, J. Endod. 31 (2005) 605–607.
[9] J.F. Reyes-Carmona, M.S. Felippe, W.T. Felippe, J. Endod. 35 (2009) 731–736.
[10] S. Asgary, M.J. Eghbal, M. Parirokh, J. Ghoddusi, S. Kheirieh, F. Brink, J. Endod. 35 (2009) 243–250.
[11] S. Shahi, S. Rahimi, H.R. Yavari, H. Mokhtari, L. Roshangar, M.M. Abasi, S. Sattari, M. Abdolrahimi, J. Endod. 36 (2010) 899–903.
[12] K.B. Wiltbank, S.A. Schwartz, W.G. Schindler, J. Endod. 33 (2007) 1235–1238.
[13] S.T. Hong, K.S. Bae, S.H. Baek, K.Y. Kum, W.C. Lee, J. Endod. 34 (2008) 56–58.
[14] E.A. Bortoluzzi, N.J. Broon, C.M. Bramante, R.B. Garcia, I.G. de Moraes, N. Bernardineli, J. Endod. 32 (2006) 897–900.
[15] S. Shahi, S. Rahimi, M. Hasan, V. Shiezadeh, M. Abdolrahimi, J. Oral Sci. 51 (2009) 601–606.
[16] P. Taddei, A. Tinti, M.G. Gandolfi, P.L. Rossi, C. Prati, J. Mol. Struct. 924–926 (2009) 548–554.
[17] M. Torabinejad, C.U. Hong, F. McDonald, T.R.P. Ford, J. Endod. 21 (1995) 349–353.
[18] E.A. Bortoluzzi, N.J. Broon, C.M. Bramante, W.T. Felippe, M.T. Filho, R.M. Esberard, J. Endod. 35 (2009) 550–554.
[19] P.C. Hewlett, Lea's Chemistry of Cement and Concrete, fourth ed., Butterworth-Heinemann, Oxford, 2001, pp. 881–885.
[20] E.P. Nielsena, D. Herforta, M.R. Geikerb, Cem. Concr. Res. 35 (2005) 117–123.
[21] V.S. Ramachandran, R.F. Feldman, Cemento 3 (1978) 311–322.
[22] E.A. Bortoluzzi, N.J. Broon, M.A.H. Duarte, A.C.C. de Oliveira Demarchi, C.M. Bramante, J. Endod. 32 (2006) 1194–1197.
[23] M.G. Gandolfi, F. Perut, G. Ciapetti, R. Mongiorgi, C. Prati, J. Endod. 34 (2008) 39–44.
[24] B.S. Ber, J.F. Hatton, G.P. Stewart, J. Endod. 33 (2007) 1231–1234.
[25] P.P. Harrington, Post retention with mineral trioxide aggregate and accelerated Portland cement [dissertation]. West Virginia University, Morgantown, 2005.
[26] D. Abdullaha, T.R. Pitt Fordb, S. Papaioannouc, J. Nicholsond, F. McDonaldc, Biomaterials 23 (2002) 4001–4010.
[27] T. Kokubo, H. Takadama, Biomaterials 27 (2006) 2907–2915.
[28] W. Zhaoa, J. Wang, W. Zhai, Z. Wang, J. Chang, Biomaterials 26 (2005) 6113–6121.
[29] American Society for Testing and Materials ASTM C191-99, Easton, Standard test method for time and setting of hydraulic cement by Vicat needle, Vol 04.01, 2000.
[30] American Society for Testing and Materials ASTM C187-98, Easton, Standard test method for normal consistency of hydraulic cement, Vol 04.01, 2000.
[31] American Society for Testing and Materials ASTM C948-81, Easton, Standard test method for dry and wet bulk density, water absorption and apparent porosity of thin sections of glass-fiber reinforced concrete, Vol. 04.05, 1993.
[32] American Society for Testing and Materials ASTM C109-01, Easton, Standard test method for compressive strength of hydraulic cement mortars, Vol. 04.01, 2000.
[33] American Society for Testing and Materials ASTM C642-97, Easton, Standard test method for density, absorption, and voids in hardened concrete, vol. 04.02, 1997.
[34] D.C. Greenspan, J.P. Zhong, G.P. LaTorre, in: Ö.H. Andresson, A. Yli-Urpo (Eds.), Bioceramics, Vol. 7, 1994, pp. 55–60, Turku, Finland.
[35] P.W. Brown, C.L. Harner, E.J. Prosen, Cem. Concr. Res. 16 (1986) 17–22.
[36] X. Wang, H. Sun, J. Chang, Dent. Mater. 24 (2008) 74–82.
[37] M.C.G. Juenger, P.J.M. Monteirob, E.M. Gartnerc, G.P. Denbeauxd, Cem. Concr. Res. 35 (2005) 19.
[38] P. torkittikul, A. Chaipanich, Sci. Asia 35 (2009) 358–364.
[39] N.J. Coleman, J.W. Nicholson, K. Awosanya, Cem. Concr. Res. 37 (2007) 1518–1523.
[40] J. Ni, M. Wang, Mater. Sci. Eng., C 20 (2002) 101–109.
[41] K.R. Mohamed, A.A. Mostafa, Mater. Sci. Eng., C 28 (2008) 1087–1099.
[42] A.M. El-Kady, A.F. Ali, M.M. Farag, Mater. Sci. Eng., C 30 (2010) 120–131.
[43] P.P. Lopes, B.J.M. Leite Ferreira, N.A.F. Almeida, M.C. Fredel, M.H.V. Fernandes, R.N. Correia, Mater. Sci. Eng., C 28 (2008) 572–577.
[44] A. Saboori, M. Rabiee, F. Moztarzadeh, M. Sheikhi, M. Tahriri, M. Karimi, Mater. Sci. Eng., C 29 (2009) 335–340.
[45] W. Zhao, J. Wang, W. Zhai, Z. Wang, J. Chang, Biomaterials 26 (2005) 6113–6121.
[46] Z. Gou, J. Chang, J. Eur. Ceram. Soc. 24 (2004) 93–99.
[47] Y. Zhu, C. Wub, Y. Ramaswamy, E. Kockrick, P. Simon, S. Kaskel, H. Zreiqat, Microporous Mesoporous Mater. 112 (2008) 494–503.
[48] S. Radin, S. Falaize, M.H. Lee, P. Ducheyne, Biomaterials 23 (2002) 3113–3122.
[49] X. Yan, X. Huang, C. Yu, H. Deng, Y. Wang, Z. Zhang, S. Qiao, G. Lu, D. Zhao, Biomaterials 27 (2006) 3396–3403.

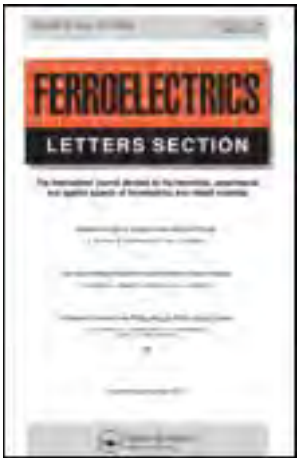

Ferroelectrics Letters Section
Publication details, including instructions for authors and subscription information:
http://www.tandfonline.com/loi/gfel20

Dielectric Properties of Lead-Free Composites from 0-3 Barium Zirconate Titanate-Portland Cement Composites

R. Potong [a] , R. Rianyoi [a] & A. Chaipanich [a]
[a] Department of Physics and Materials Science, Faculty of Science, Chiang Mai University, Chiang Mai, 50200, Thailand
Published online: 16 Jun 2011.

To cite this article: R. Potong , R. Rianyoi & A. Chaipanich (2011): Dielectric Properties of Lead-Free Composites from 0-3 Barium Zirconate Titanate-Portland Cement Composites, Ferroelectrics Letters Section, 38:1-3, 18-23

To link to this article: http://dx.doi.org/10.1080/07315171.2011.570176

Ferroelectrics Letters, 38:18–23, 2011

ISSN: 0731-5171 print / 1563-5228 online
DOI: 10.1080/07315171.2011.570176

Dielectric Properties of Lead-Free Composites from 0-3 Barium Zirconate Titanate-Portland Cement Composites

R. POTONG, R. RIANYOI, AND A. CHAIPANICH*

Department of Physics and Materials Science, Faculty of Science, Chiang Mai University, Chiang Mai, 50200, Thailand

Communicated by Dr. George W. Taylor
(*Received in final form December 20, 2010*)

The dielectric properties of lead-free composites from 0-3 barium zirconate titanate-Portland cement composites were investigated. 0-3 BZT-PC composites were produced using BZT content at 30–70% by volume. The dielectric properties at various frequencies with difference BZT content were investigated. Parallel, cube and series models were also compared to the dielectric measurement results. The results showed that the dielectric constant of BZT-PC composites increased with increasing BZT content where ε_r values at 1 kHz are 225 and 549 for composites with 30 and 70% by volume respectively. The dielectric properties of BZT-PC composites were also found to depend on the frequency tested.

Keywords BZT; Composites; Cement; Dielectric Properties

1. Introduction

The piezoelectric materials are widely used for capacitors and various application such as lead zirconate titanate (PZT) as it has excellent dielectric constant (ε_r) and piezoelectric coefficient (d_{33}) [1–4]. Cement based composites consisting of PZT have been developed for applications where the composites can be inserted into concrete structures to detect loading after they were fabricated. Lead based piezoelectric-cement composites have been investigated as promising materials for sensors application in civil engineering field [5–9]. However, because PZT contains lead which is toxic causing serious environment pollution, it is urgent to develop non-lead piezoelectric materials alternatives to replace PZT and lead based piezoelectric materials. Barium zirconate titanate (BZT) is non-lead piezoelectric material, exhibits high dielectric constant (ε_r) and is regarded as one of the promising compounds replacing the PZT materials. $Ba(Ti_{1-x}Zr_x)O_3$ ceramics at $x = 0.05$ mol showed high dielectric constant, remnant polarization and piezoelectric properties [10–12].

The dielectric constant has been measured for the purpose of fundamental understanding of cement-based materials. The dielectric properties of 0-3 cement based composites were found to depend on many factors, such as frequency, volume fraction of ceramic powder, method of fabrication. In this research, it is thus interesting to investigate the dielectric

*Corresponding author. Fax: 66 53 943445. E-mail: arnon@chiangmai.ac.th

properties of lead-free composites from 0-3 BZT-PC composites. BZT-PC composite was produced from barium zirconate titanate, $BaZr_{0.05}Ti_{0.95}O_3$ (BZT) with Portland cement of normal type (PC), commonly known as ordinary Portland cement to form 0-3 connectivity BZT-PC composites.

2. Experimental Procedure

Barium zirconate titanate, $BaZr_{0.05}Ti_{0.95}O_3$ (BZT) ceramic particles were produced using BZT powder sintered at 1,450 °C. Thereafter, the BZT ceramics were ground into particles of 425 μm in size. BZT ceramics of different BZT volume content of 30%, 40%, 50%, 60% and 70% were used. BZT ceramic particles were then mixed with normal Portland cement (The American Society for Testing and Materials Type I cement) to produce 0-3 connectivity BZT-PC composite using a hydraulic press to form disk samples of 15 mm diameter and 2 mm thickness. Thereafter, the composites were placed for curing at 60°C and 98% relative humidity for 3 days before measurements. For measurement of the dielectric properties, silver paste electrodes were formed at the two surfaces of disk-shaped specimens. An impedance meter (Hewlett Packard 4194A) was used to obtain the capacitance and the dielectric loss (*tanδ*) of the composites at room temperature and at vary frequency. The dielectric constant (ε_r) was calculated from the following equation:

$$\varepsilon_r = \frac{Ct}{\varepsilon_0 A} \tag{1}$$

Where C is the sample capacitance, t is the thickness, ε_0 is the permittivity of free space constant (8.854×10^{-12} Fm^{-1}) and A is the electrode area.

The dielectric constant was also compared with the composite models as follows;

- parallel model [13] $$\varepsilon_C = \nu_1\varepsilon_1 + \nu_2\varepsilon_2 \tag{2}$$
- series model [14] $$\frac{1}{\varepsilon_C} = \frac{\nu_1}{\varepsilon_1} + \frac{\nu_2}{\varepsilon_2} \tag{3}$$
- cube model [9] $$\varepsilon_C = \frac{\varepsilon_1 \cdot \varepsilon_2}{(\varepsilon_2 - \varepsilon_1) \cdot \nu_1^{-1/3} + \varepsilon_1 \cdot \nu_1^{2/3}} + \varepsilon_2 \cdot \left(1 - \nu_1^{2/3}\right) \tag{4}$$

3. Results and Discussion

At varying frequency, the effect of BZT-PC composites on the dielectric constant (ε_r) is shown against the frequency in Fig. 1. The dielectric constant of the composites can be seen to decrease with increasing frequency where 0.1 kHz and 100 kHz with dielectric constant = 1032 and 122 for 70% BZT composites. In addition, the dielectric loss (*tanδ*) was found to decrease with increasing frequency. This is mainly attributed to interface polarization of the composite and polarization in the cement matrix. It is well know that cement is a porous material with a complex microstructure and it is composed of an amorphous phase, crystallites in the micrometer range and bound water [15,16]. With an increasing frequency, some polarization, especially interfacial polarizations cannot follow

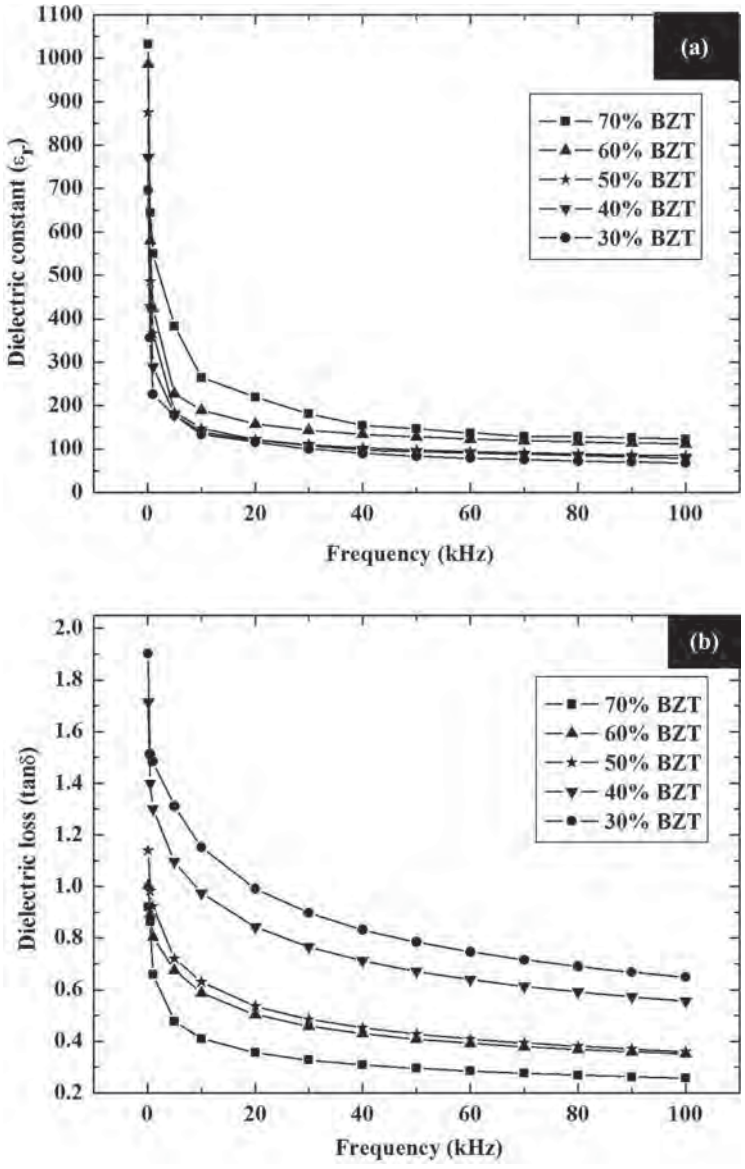

Figure 1. Effect of frequency on dielectric properties results of BZT-PC composites ((a) dielectric constant and (b) dielectric loss).

the change of the electric field due to lengthy time for the construction of space charge polarization. Therefore, dielectric constants are lower at high frequency [17,18].

The effect of BZT-PC composites on the dielectric constant (ε_r) is plotted against the BZT content. The dielectric constant of the composites can be seen to increase with increasing BZT contents and the dielectric constant is highest at 549 in 70% BZT composites at 1 kHz. The dielectric constant is lowest at 225 in 30% BZT composites at 1 kHz. Moreover, measured dielectric loss (*tanδ*) results of composites showing the effect of BZT

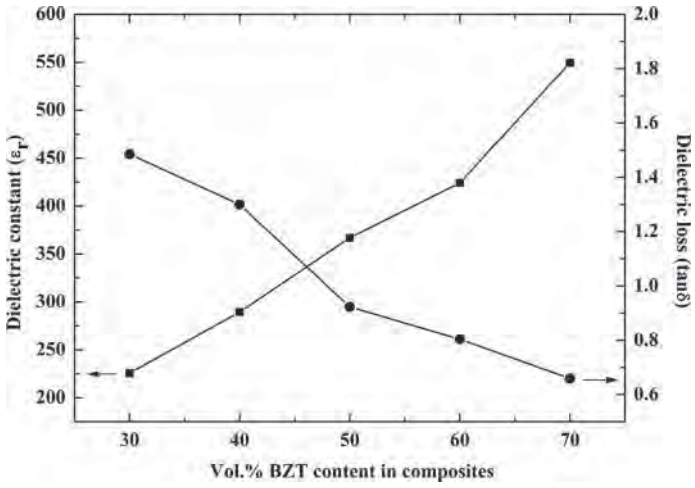

Figure 2. Effect of BZT on dielectric properties results of BZT-PC composites at 1 kHz.

content can be seen in Fig. 2. The dielectric loss is found to decrease with increasing BZT content and the *tan* δ value of 70% BZT composite is lowest at 0.65 ($f = 1$ kHz).

Furthermore, the parallel and series models were compared with the results taken from the measurements as shown in Fig. 3. It is clear that parallel model and series model are the upper limit and lower limits for relative dielectric constant, respectively. The dielectric results of 0-3 connectivity composites can be seen to fit closest to that of the cube model. For the cube model, it takes into account the anisotropic distribution of cubes in x, y, and z directions, which based on fundamental principal of the physical mixing and it is clear that the experimental results are close to the theoretical value of the cubes models, which means that the ceramic particles in the composites are well-dispersed [9, 19].

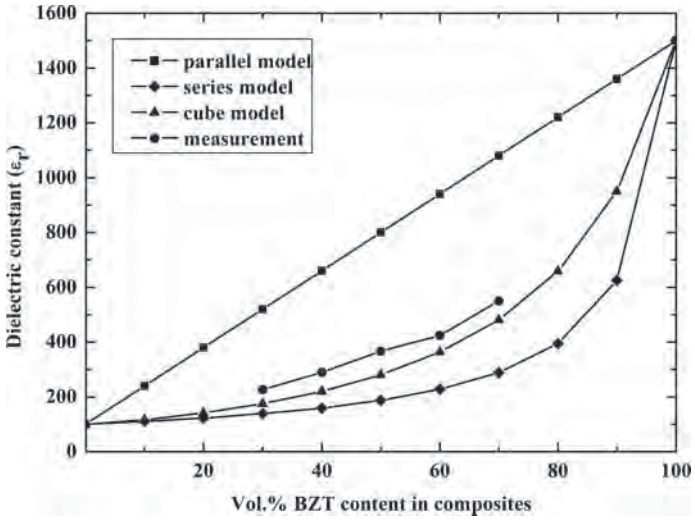

Figure 3. Comparison of models with the dielectric constant results of BZT-PC composites.

4. Conclusions

The results showed that the dielectric constant of 0-3 BZT-PC composites decrease with increasing frequency. Moreover, the dielectric constant was found to increase with increasing BZT Vol% content (for the range 30%-70% tested) and that the dielectric constant was highest at 549 for 70% BZT composites at 1 kHz. The dielectric loss was found to decrease with increasing BZT content. The dielectric results of 0-3 connectivity composites can be seen to fit closest to that of the cube model.

5. Acknowledgments

The authors are grateful to members of staff at the Electroceramics Research Laboratory, Faculty of science, and Chiang Mai University for the research facilities made possible for this research work. The authors would like to express their gratitude for financial support from the Thailand Research Fund (TRF) through the Royal Golden Jubilee Ph.D. Program (Grant No. PHD/0042/2552) to Ruamporn Potong and Assistant Prof. Dr. Arnon Chaipanich is acknowledged. The authors would also like to express their gratitude for TRF-CHE Research Grant for Mid-Career University Faculty awarded to Assistant Prof. Dr. Arnon Chaipanich by the Thailand Research Fund (TRF), Office of the Higher Education Commission (Thailand) and Chiang Mai University. The Graduate School of Chiang Mai University is also acknowledged.

References

R. E. Newnham, A. Amin, Smart systems: Microphones, fish farming, and beyond—Smart materials, acting as both sensors and actuators, can mimic biological behavior. *Chem Tech*. **29**, 38–47 (1999).

K. Uchino, Materials issues in design and performance of piezoelectric actuators: an overview. *Acta Mater.* **46**, 3745–3753 (1998).

R. Ranjan, R. Kumar, B. Behera, R. N. P. Choudhary, Effect of Sm on structural, Dielectric and conductivity properties of PZT ceramics. *Mater Chem Phys.* **115**, 473–477 (2009).

S. T. Lau, K. W. Kwok, H. L. W. Chan, C. L. Choy, Piezoelectric Composite Hydrophone Array. *Sens Actuators A.* **96**, 14–20 (2002).

Z. Li, D. Zhang, K. Wu, Cement-Based 0-3 piezoelectric composites. *J Am Ceram Soc.* **85**, 305–313 (2002).

H. Y. Gonga, Z. Li, Y. Zhang, R. H. Fan, Piezoelectric and dielectric behavior of 0-3 cement-based composites mixed with carbon black. *J Eur Ceram Soc.* **29**, 2013–2019 (2009).

A. Chaipanich, N. Jaitanong, R. Yimnirun, Effect of compressive stress on the ferroelectric hysteresis behavior in 0-3 PZT-cement composites. *Mater Lett.* **64**, 562–564 (2010).

A. Chaipanich, N. Jaitanong, R. Yimnirun, Ferroelectric hysteresis behavior in 0-3 pzt-cement composites: Effects of frequency and electric field. *Ferr Lett.* **36**, 59–66 (2009).

F. Xing, B. Dong, Z. Li, Dielectric, Piezoelectric, and elastic properties of cement-based piezoelectric ceramic composites. *J Am Ceram Soc.* **91**, 2886–2891 (2008).

Z. Yu, C. Ang, R. Guo, A. S. Bhalla, Piezoelectric and strain properties of $Ba(Ti_{1-x}Zr_x)O_3$ ceramics. *J Appl Phys.* **92**, 1489–1493 (2002).

Z. Yu, R. Guo, A. S. Bhalla, Dielectric behavior of $Ba(Ti_{1-x}Zr_x)O_3$ single crystals, *J Appl Phys.* **88**, 410–415 (2000).

N. Nanakorn, P. Jalupoom, N. Vaneesorn, A. Thanaboonsombut, Dielectric and ferroelectric properties of $Ba(Ti_{1-x}Zr_x)O_3$ ceramics. *Ceram Inter.* **34**, 779–782 (2008).

S. Mindess, J. F. Young, D. Darwin, *Concrete*. United States of America: Prentice-Hall, Pearson Education, Inc.; 2003.

D. H. Yoon, J. Zhang, B. I. Lee, Dielectric constant and mixing model of $BaTiO_3$ composite thick films. *Mater Res Bull.* **38**, 765–772 (2003).

N. Jaitanong, A. Chaipanich, Dielectric properties of 0-3 lead magnesium niobate titanate (PMT)-ordinary Portland Cement (PC) composites. *Key Eng Mater.* **421–422**, 407–410 (2010).

H. F. W. Taylor, *Cement Chemistry*. London: Thomas Telford Publishing; 1998.

R. Potong, R. Rianyoi, P. Jarupoom, K. Pengpat, A. Chaipanich, Effect of Particle Size on the Dielectric Properties of Sodium Potassium Niobate-Portland Cement Composites. *Ferr Lett.* **36**, 76–81 (2009).

C. Xin, S. Huang, C. Jun, L. Zongjin, Piezoelectric, dielectric, and ferroelectric properties of 0-3 ceramic/cement composite. *J Appl Phys.* **101**, 094110–094116 (2007).

B. Dong, Z. Li, Cement-based piezoelectric ceramic smart composites. *Comp Sci Technol.* **65**, 1363–1371 (2005).

Key Engineering Materials Vol. 484 (2011) pp 222-225
Online available since 2011/Jul/04 at www.scientific.net

doi:10.4028/www.scientific.net/KEM.484.222

Influence of Curing Age on Microstructure in Barium Titanate – Portland Cement Composites

R. Rianyoi[1,a], R. Potong[1,b], N. Jaitanong[1,c] and A. Chaipanich[1,d]

[1]Department of Physics and Materials Science, Faculty of Science,

Chiang Mai University, Chiang Mai 50200, Thailand

[a]r.rianyoi@gmail.com, [b]ja_rho@hotmail.com, [c] Jaitanong@hotmail.com, [d]arnon@chiangmai.ac.th

Keywords: Composites, Microstructure, Barium Titanate, Cement, Curing Age

Abstract. The objective of this study was to find out the influence of curing age on microstructure in barium titanate – Portland cement composites. Barium titanate, $BaTiO_3$ (BT) particles was mixed with Portland Cement (PC) and BT content of 50% by volume to produce the composites. All composites were cured in chamber of 60°C and 98% relative humidity for 1, 2, 3, and 7 days. Thereafter, scanning electron microscope (SEM) was used to examine the interfacial zone between cement and BT ceramics. SEM observation indicated that the BT-PC composite cured for 7 days clearly showed calcium silicate hydrate gel (an essential hydration product of Portland cement) surrounding the BT particles and has lower porosity. In BT-PC composite cured for 1 day, the gel can be seen but of less quantity and has higher porosity which clearly affected the interfacial zone.

Introduction

Recently, the development of the smart materials is gaining interests in the civil engineering applications. The cement-based piezoelectric functional composites incorporating lead based (such as lead zirconate titanate (PZT), lead niobium-magnesium zirconate titanate (P(MN)ZT), in cement matrix have been developed [1-6]. However, lead oxide from processing of lead-based piezoelectric materials is highly toxic and use of the lead-based materials has caused lead pollution and environmental problems. Therefore, lead-free piezoelectric materials received attention from environmental protection. In addition, barium titanate (BT) have long since attract attention because of high dielectric constant (ε_r=1000-2000) and low dielectric loss used for multilayer capacitors, heater, ferroelectric thin-film memories, etc. [7-8]. However, microstructure has a most pronounced influence on electrical properties of materials; Curie temperature, dielectric constant, piezoelectric coupling factor and piezoelectric strain constant are strongly dependent on microstructure [9-11]. In this study, BT ceramic particles were incorporated into Portland cement matrix at 50 vol % to form 0-3 composites. The scanning electron microscope was used to investigate the microstructure of hydration process in 0-3 barium titanate (BT) – Portland cement (PC) composites with cured for 1, 2, 3 and 7 days. In addition, porosity and the loss tangent of the composites were also measured.

Experimental procedure

The 0-3 barium titanate (BT) – Portland cement (PC) composites using BT ceramic of median particle size (≈ 187 μm) at 50% by volume were fabricated by a compressing technique to form disk samples of ≈ 15 mm in diameter and ≈ 2 mm in thickness. Thereafter, the composites were placed for curing at 60°C and 98 % relative humidity for periods of 1, 2, 3, 7 days. These composites were then immerged in acetone for 24 h to stop the hydration of cement and then dried at 105°C for 45

min. Microstructure and phase characterizations were carried out by means of scanning electron microscopy (SEM; JEOL JSM-5910LV). The composites were then fractured and a small piece of each sample was selected for scanning. The fracture surface was coated with a thin layer of gold, under vacuum prior to mounting for viewing. The dried composites were used for the porosity test. Porosity measurements were made using Archimedes' principle as described as described in Eq. 1:

$$P(porosity) = \frac{W_s - W_d}{W_s - W_{ss}} \quad (1)$$

where P is the percentage of porosity, W_s is the weight in the air of the composites saturated with water, W_d is the dry composites weight in air and W_{ss} is the weight of the composites saturated of water suspended in water.

For measurement of the loss tangent, an impedance meter (Hewlett Packard 4194A) was used.

Results and discussion

SEM micrographs of fracture surfaces of composites cured for 1, 2, 3 and 7 days in 98 % relative humidity at 60°C are shown in Figs. 1–4, respectively. The composites were prepared for viewing at a magnification of 3000×. In the figures, BT ceramic particles can be seen to be densely surrounded by the cement matrix. The hydration products found in composites primarily consist of calcium silicate hydrate gel (C-S-H) and accompanied by smaller amounts of ettringite. The fibrous-like morphology of the C-S-H phase and long needle-shaped of the ettringite phase are in agreement with previously reported works [12-14]. These hydration products are intermingled with pore spaces. At composite with cured for 1 day in Fig. 1, there is usually some big pores in the cement matrix. More over the interfaces between the cement matrix and BT ceramic particles are not perfect. With the increase of curing age, the porosity in the cement matrix remarkably decreases, accompanying with increases of hydration products at the same time, leading to a better combination between the BT ceramic particles and the cement matrix (Figs. 1–4). In addition, the results agree with the porosity measured where porosity of composite cured for 1 day is higher at 10.63% compared to the value of 8.49% for the composite with cured for 7 days (Table 1). Furthermore, energy-dispersive X-ray spectroscopy (EDX) analysis of the composites is shown to the right of the image in Figs. 1–4, where the barium titanate was detected (point A). EDX analysis of the area displayed the presence barium, titanium and oxygen were detected as the main elements. In point B is characteristic for calcium silicate hydrate; calcium, silicon and oxygen were detected as the main elements (hydrogen cannot be detected). In addition, the unlabeled peak to the right of 2.1 keV in the EDX spectrum corresponds to Au used for the sample preparation.

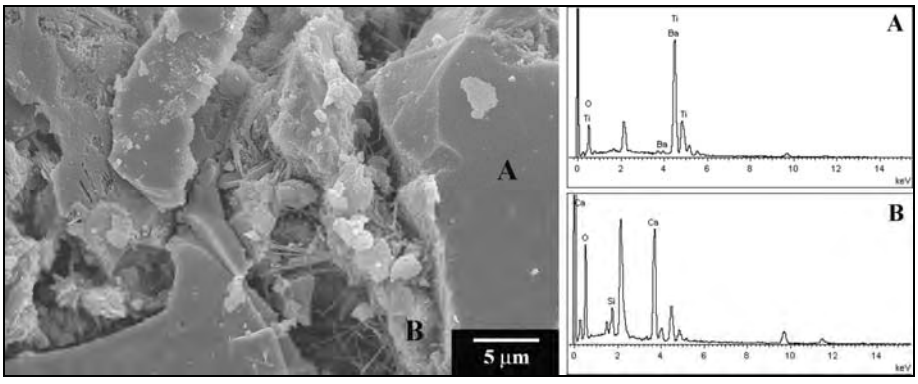

Figure 1 SEM micrograph with EDX of 0-3 BT-PC composite cured for 1 day.

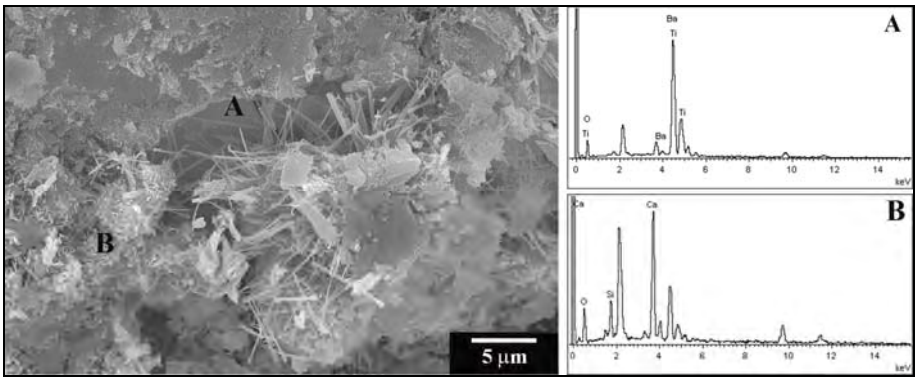

Figure 2 SEM micrograph with EDX of 0-3 BT-PC composite cured for 2 day.

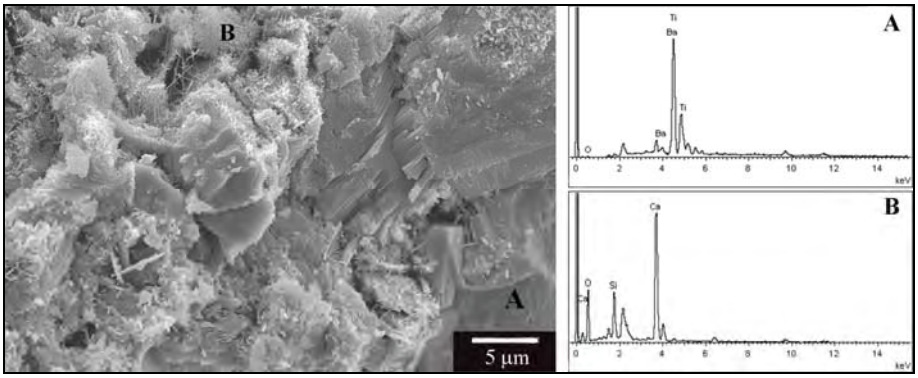

Figure 3 SEM micrograph with EDX of 0-3 BT-PC composite cured for 3 day.

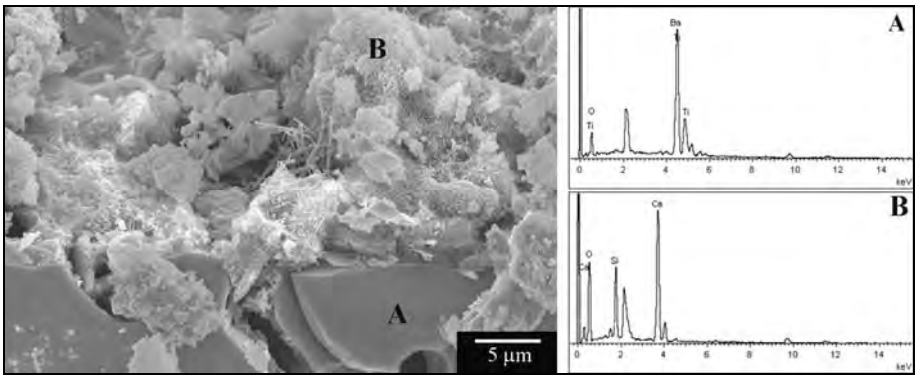

Figure 4 SEM micrograph with EDX of 0-3 BT-PC composite cured for 7 day.

Table 1 Porosity and the loss tangent results of 0-3 barium titanate (BT) – Portland cement (PC) composites

Curing age [days]	Porosity [%]	$tan\delta$
1	10.62	0.599
2	9.42	0.495
3	8.65	0.465
7	8.49	0.373

Table 1 show the effect of curing age on porosity and the loss tangent ($tan\delta$) of the composites. The loss tangent ($tan\delta$) of composites can be seen to reduce with increasing curing age which shows $tan\delta$ value reduces from 0.598 to 0.373 at curing age of 1 and 7 days, respectively. The hydration process in cement is the reaction between water and cement. The water and cement phases are the ones changing in volume during hydration, while the amount of ceramic phase does not change [15]. As the curing age increases, the amount of free water in the cement matrix decreases due to

the cement hydration. The water changes from a free to an adsorbed state, which reduces ionic polarization and also conductivity due to decrease in ion production. Also, the pore structure changes with curing age. The pore sizes become very small, thus making it difficult for the movement of the free ionized water remaining in cement matrix. Therefore, the dielectric loss would decrease with curing age.

Conclusions

The influence of curing age on microstructure in barium titanate – cement composites has been highlighted. SEM and EDX have been shown to be particularly effective in understanding the developing hydration produce, pore structure and interfaces between the cement matrix and BT ceramic particles in 0–3 barium titanate – cement composites. An appropriate of curing age with 3 days and 7 days have been the development of the microstructural features that are most beneficial in low porosity with small pores and more hydration products, which leading to a better combination between the BT ceramic particles and the cement matrix. In addition, the loss tangent would decrease with curing age, where $tan\ \delta$ value can be seen to decrease from 0.599 to 0.373 for curing age of 1 and 7 days, respectively.

Acknowledgments

Financial support from the Thailand Research Fund through the Royal Golden Jubilee Ph.D. Program (Grant No. PHD/0147/2551) to Miss Rattiyakorn Rianyoi and Asst. Prof. Dr. Arnon Chaipanich is gratefully acknowledged. The authors also wish to thank the staff members at the Electroceramics Research Laboratory, Faculty of Science, Chiang Mai University, for use of the research facilities which made this work possible. The authors would also like to express their gratitude to the Thailand Research Fund (TRF), Office of the Higher Education Commission (Thailand), Chiang Mai University and the graduate school of Chiang Mai University for additional financial support.

References

[1] Z. Li, D. Zhang and K. Wu: J. Am. Ceram. Soc. Vol. 85 (2002), p. 305
[2] Z. Li, B. Dong and D. Zhang: Cem. Concr. Compos. Vol. 27 (2005), p. 27
[3] B. Dong and Z. Li: Compos. Sci. Technol. Vol. 65 (2005), p. 1363
[4] A. Chaipanich, N. Jaitanong and T. Tunkasiri: Mater. Lett. Vol. 61 (2007), p. 5206
[5] X. Cheng, D. Xu, L. Lu, S. Huang and M. Jiang: Mater. Chem. Phys. Vol. 121 (2010), p. 63
[6] N. Jaitanong and A. Chaipanich: Key Eng. Mater. Vol. 421–422 (2010), p. 407
[7] J.-M. Hwu, W.-H. Yu, W.-C. Yang, Y.-W. Chen and Y.-Y. Chou: Mater. Res. Bull. Vol. 40 (2005), p. 1662
[8] M.T. Benlahrache, S.E. Barama, N. Benhamla and S. Achour: Mater Sci Semicond Process. Vol. 9 (2006) p. 1115
[9] H. S. Lee and T. Kimura: J. Am. Ceram. Soc. Vol. 81 (1998), p. 3228
[10] S. Diamond: Cem. Concr. Compos. Vol. 26 (2004), p. 919
[11] X. Cheng, S. Huang, J. Chang, R. Xu, F. Liu and L. Lu: J. Eur. Ceram. Soc. Vol. 25 (2005), p. 3223
[12] A. Chaipanich, T. Nochaiya, W. Wongkeo and P. Torkittikul: Mater. Sci. Eng. A. Vol. 527 (2010), p. 1063
[13] W. Wongkeo and A. Chaipanich: Mater. Sci. Eng. A. Vol. 527 (2010), p. 3676
[14] Otto Labahn, in: Cement Engineers' Handbook, edited by B. Kohlhaas, Wiesbaden, Berlin, Bauverlag (1983).
[15] A. van Beek and M.A. Hilhorst: HERON Vol. 44 (1999), ISN 0046-7316

Advanced Engineering Ceramics and Composites
doi:10.4028/www.scientific.net/KEM.484

Influence of Curing Age on Microstructure in Barium Titanate – Portland Cement Composites
doi:10.4028/www.scientific.net/KEM.484.222

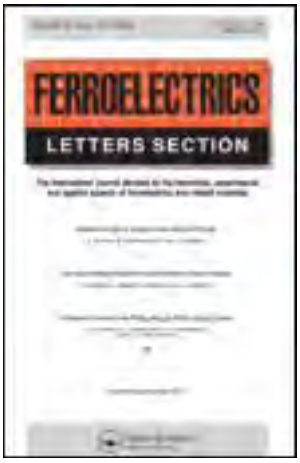

Ferroelectrics Letters Section
Publication details, including instructions for authors and subscription information:
http://www.tandfonline.com/loi/gfel20

Effect of Temperature on the Dielectric Properties of 0-3 PZT-Cement Composites

A. Chaipanich [a] , R. Rianyoi [a] , R. Potong [a] & N. Jaitanong [a]
[a] Department of Physics and Materials Science, Faculty of Science, Chiang Mai University, Chiang Mai, 50200, Thailand
Published online: 06 Jan 2011.

To cite this article: A. Chaipanich , R. Rianyoi , R. Potong & N. Jaitanong (2010): Effect of Temperature on the Dielectric Properties of 0-3 PZT-Cement Composites, Ferroelectrics Letters Section, 37:4, 76-81

To link to this article: http://dx.doi.org/10.1080/07315171.2010.527799

Ferroelectrics Letters, 37:76–81, 2010

ISSN: 0731-5171 print / 1563-5228 online
DOI: 10.1080/07315171.2010.527799

Effect of Temperature on the Dielectric Properties of 0-3 PZT-Cement Composites

A. CHAIPANICH,* R. RIANYOI, R. POTONG, AND N. JAITANONG

Department of Physics and Materials Science, Faculty of Science, Chiang Mai University, Chiang Mai 50200, Thailand

Communicated by Dr. George W. Taylor
(*Received July 20, 2010*)

In this work, 0-3 lead zirconate titanate (PZT) was mixed with normal Portland cement to produce 0-3 connectivity composites. The effect of temperature on the dielectric properties such as the dielectric constant and dielectric loss was determined. It was found that with increasing PZT content the T_c increases where the optimum dielectric constant was observed and that at the temperature up to 100°C there is a significant change in the dielectric properties in PZT-cement composites. This is due to the loss of water molecules at up to 100°C. At above 100°C, the dielectric properties of the composites were found to have a similar behavior to that of PZT ceramic with T_c being ≈420°C.

Keywords PZT; cement; composites; dielectric properties; temperature

1. Introduction

Recently, lead zirconate titanate, $Pb(Zr_{0.52}Ti_{0.48})O_3$ (PZT) ceramic has been used with a cement based material to produce new types of composite [1–12]. All previous reported works have been taken at room temperature. The dielectric properties, however, are known to change with temperature for ferroelectric material such as PZT changing from ferroelectric to paraelectric and the Curie temperature (T_c) can be determined from the change in the dielectric values with temperature. For example, T_c for PZT is known to be in the region of ≈400°C with the dielectric constant to be higher than 10,000 compared to around 1000–2000 at room temperature. The dielectric constants of cement paste at room temperature were reported to be in the region of 20–100 [4, 6, 9–11]. Moreover, due to the fact that the cement can be cast as powder by pressing or as paste (with water) to form any desirable shape, it is of an interest to investigate the effect of temperature since there have been no reports on the effect of temperature on the dielectric properties of these cement based piezoelectric composites. The dielectric properties such as dielectric constant and the dielectric loss of these cement based piezoelectric composites from room temperature up to 500°C are reported.

*Corresponding author. Fax: 66 53 357512; E-mail: arnon@chiangmai.ac.th

2. Experimental

Lead zirconate titanate, $Pb(Zr_{0.52}Ti_{0.48})O_3$, (PZT) ceramic particles of 30, 50, and 70% by volume were then mixed with Portland cement (PC) and pressed to produce PZT-cement composites [3]. The composites were then cured for 3 days to allow the cement to hydrate

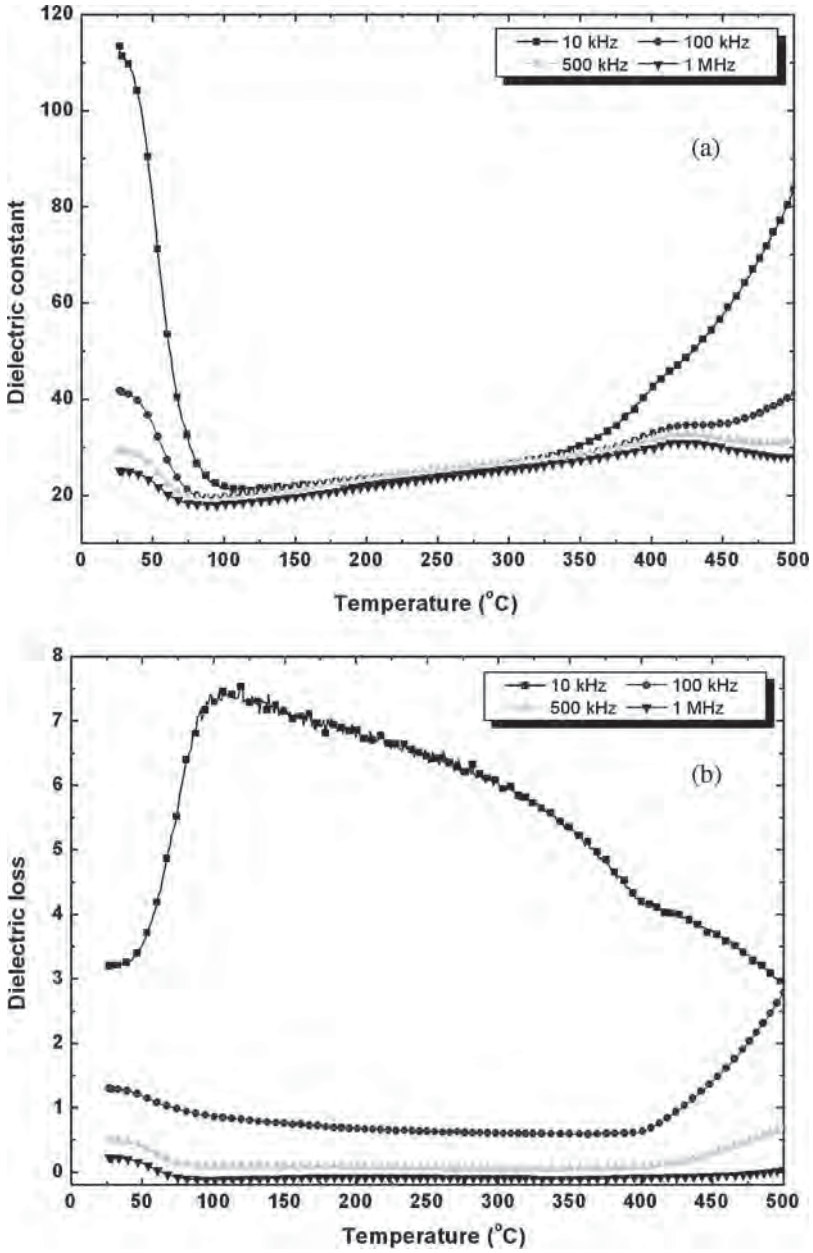

Figure 1. Effect of temperature on (a) the dielectric constant results and (b) the dielectric loss of PZT-Cement composites with 30% PZT at different frequency.

thus binding the composites together and gaining desirable strength to be easily handled. The capacitance and the dielectric loss of the composites were measured using an impedance meter (Hewlett Packard 4194A) from room temperature up to the temperature of 500°C at the frequency of 1 kHz. The permittivity or the relative dielectric constant (ε_r) was then

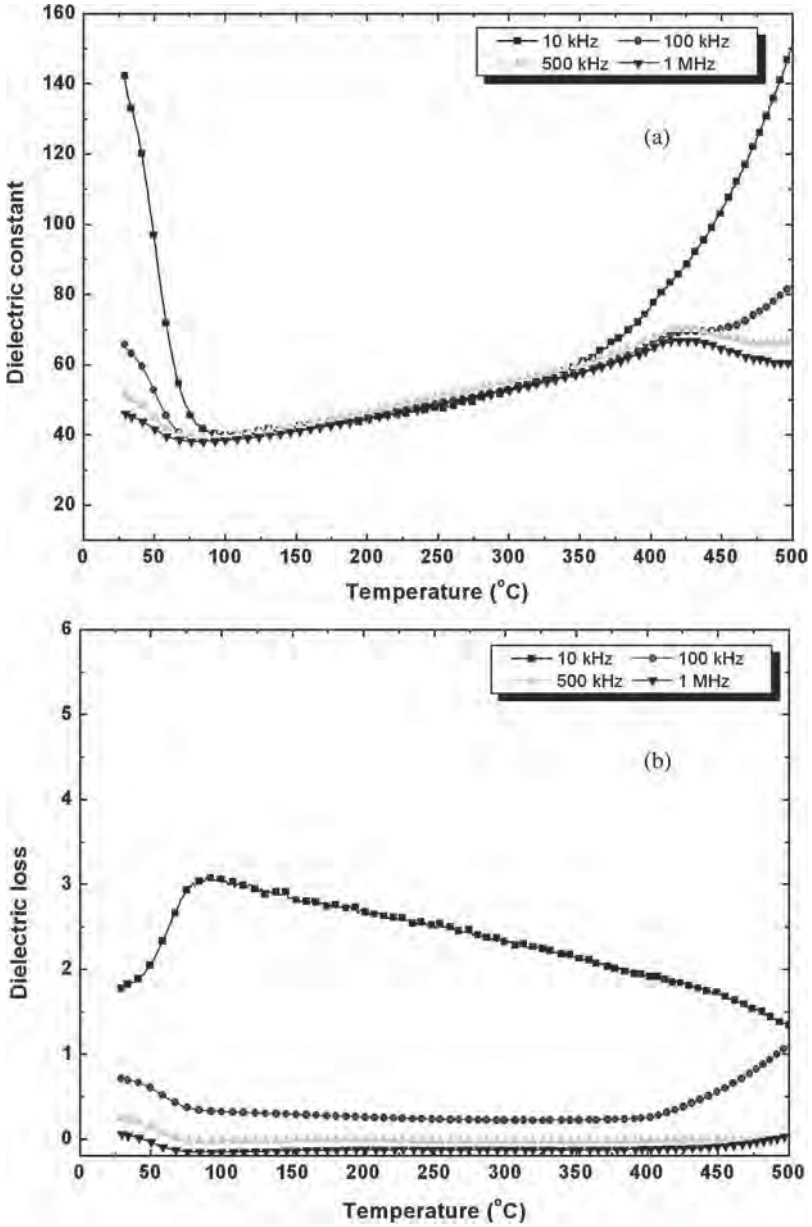

Figure 2. Effect of temperature on (a) the dielectric constant results and (b) the dielectric loss of PZT-Cement composites with 50% PZT at different frequency.

calculated from the equation;

$$\varepsilon_r = \frac{Ct}{\varepsilon_0 A}$$

where C is the sample capacitance, t is the thickness, ε_0 is the permittivity of free space constant (8.854×10^{-12} Farad per meter), and A is the electrode area.

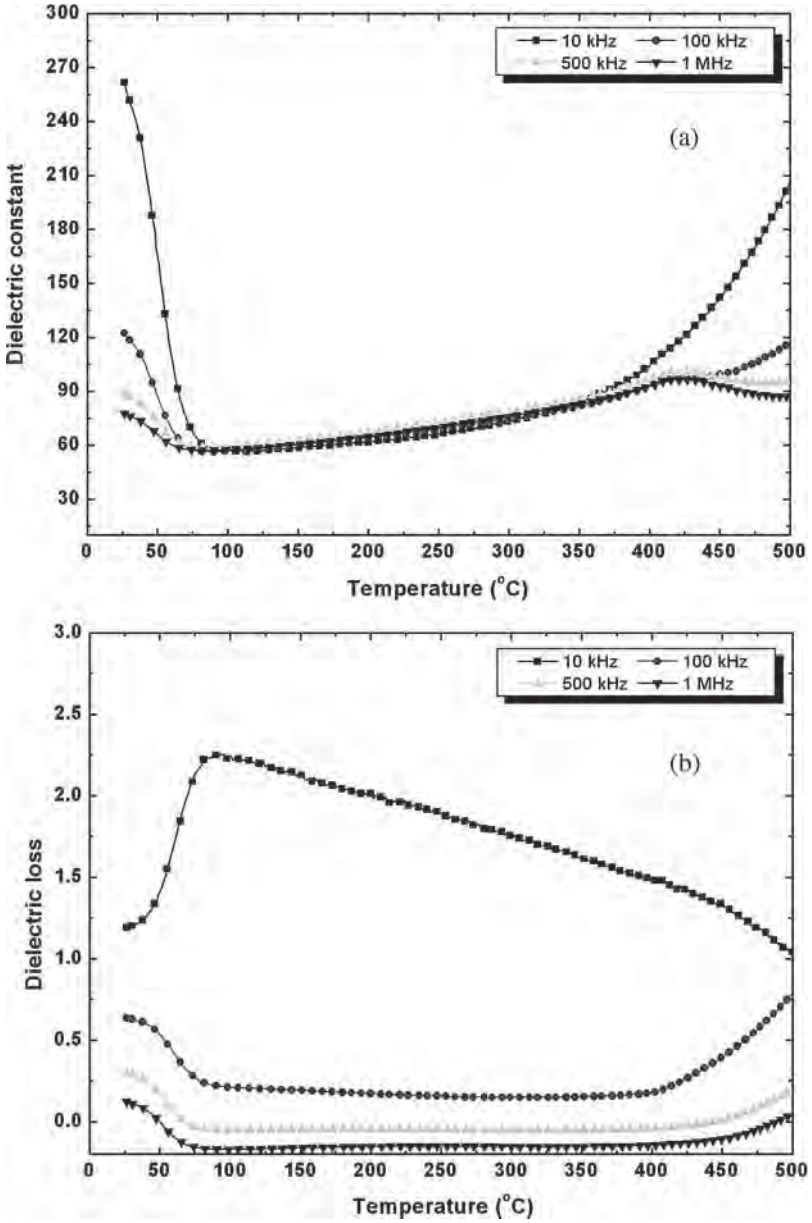

Figure 3. Effect of temperature on (a) the dielectric constant results and (b) the dielectric loss of PZT-Cement composites with 70% PZT at different frequency.

3. Results and Discussion

The dielectric constant and dielectric loss results of PZT-cement composites and PZT ceramic at room temperature up to the temperature of 500°C and at the frequency of 10 kHz to 1 MHz are shown in Figs. 1–3 with respect to the PZT Vol. content. It is seen that for PZT-cement composites, the dielectric constant is seen to decrease with increasing temperature as the temperature increased from room temperature to 100°C. At the room temperature the ε_r value for 50% PZT composite for example is 142 at 10 kHz. Further decrease is observed (at 10kHz) and at 50°C ($\varepsilon_r = 97$) and the lowest value of 40 was found at 100°C. At higher temperature from 100–500°C, an increase in the dielectric constant value was observed where the dominating factor at this range of temperature being from the PZT ceramic in the composite thus the T_c can be noticed to be at ≈420°C. Moreover, this trend can be noticed for all PZT-cement composites. Furthermore, the dielectric constant was also found to decrease with increasing frequency. For the composite of 50% vol. PZT, the ε_r value is 140 at 10 kHz and then a significant reduction was observed at 100 kHz ($\varepsilon_r = 65$). Further reduction is observed and the lowest value of 45 was found at 1 MHz. A similar trend was found in all PZT-cement composites.

It is interesting to note that the dielectric loss of the composites at 30, 50 and 70 vol.% PZT were all above 1 at 10 kHz and was found to further increase with increasing temperature. At 10kHz, the tanδ values of these composites were found to first increases as the temperature increases from room temperature to 100°C. The reason for this is not yet fully understood but is believed to be due to the water molecules being thermally active and thus may increase the conductivity of the samples leading to the greater loss recorded. The water molecules although likely to be relatively small but is a dominant factor. As the temperature increased to above the boiling point of water, the effect of the water become less since the water as moisture trapped inside the pores of the cement matrix would have escaped and thus would then exhibit a more similar behavior to that of PZT ceramic.

4. Conclusions

For the dielectric constant the results of PZT-Portland cement show that there are changes in the dielectric value with temperature. It was found that the dielectric constant decreases initially from room temperature to 100°C, thereafter at the temperature above 100°C there is a notable increases in the dielectric constant of PZT-cement composites. For composite with 50% Vol. PZT composite, ε_r value at the room temperature is 142 at 10 kHz and is lowest at 40 at 100°C. This is believed to be due to the loss of water molecules at up to 100°C. At above 100°C, the dielectric properties of the composites were found to have a similar behavior to that of PZT ceramic.

Acknowledgments

The authors are grateful to members of staff at the Electroceramics Research Laboratory for the research facilities made possible for this research work and also to the Thailand Research Fund (TRF) and the Commission on Higher Education (Thailand) for financial support.

References

1. A. Chaipanich and N. Jaitanong, Effect of poling time on piezoelectric properties of 0-3 PZT-Portland cement composite. *Ferr. Lett.* **35**, 73–78 (2008).
2. N. Jaitanong and A. Chaipanich, Effect of poling temperature on piezoelectric properties of 0-3 PZT-Portland cement composite. *Ferr. Lett.* **35**, 17–23 (2008).
3. A. Chaipanich and N. Jaitanong, Effect of PZT particle size on the electromechanical coupling coefficient of 0-3 PZT-cement composites. *Ferr. Lett.* **36**, 37–44 (2009).
4. Z. Li, D. Zhang, and K. Wu, Cement-based 0-3 piezoelectric composites. *J. Am. Ceram. Soc.* **85**, 305–313 (2002).
5. B. Dong and Z. Li, Cement-based piezoelectric ceramic smart composites. *Comp. Sci. Tech.* **65**, 1363–1371 (2005).
6. Z. Li, B. Dong, and D. Zhang, Influence of polarization on properties of 0-3 cement-based PZT composites. *Cem. Concr. Compos.* **27**, 27–32 (2005).
7. A. Chaipanich, N. Jaitanong, and T. Tunkasiri, Fabrication and properties of PZT-ordinary Portland cement composites. *Matls. Letts.* **61**, 5206–5208 (2007).
8. A. Chaipanich, G. Rujijanagul, and T. Tunkasiri, Properties of Sr and Sb doped PZT-Portland cement composites. *Appl. Phys. A.* **94**, 329–337 (2008).
9. A. Chaipanich, Effect of PZT particle size on dielectric and piezoelectric properties of PZT-cement composites. *Curr. Appl. Phys.* **7**, 574–577 (2007).
10. N. Jaitanong, A. Chaipanich, and T. Tunkasiri, Properties 0-3 PZT–Portland cement composites. *Ceram. Inter.* **34**, 793–795 (2008).
11. A. Chaipanich, Effect of PZT particle size on dielectric and piezoelectric properties of PZT-cement composites. *Curr. Appl. Phys.* **7**, 574–577 (2007).
12. A. Chaipanich, N. Jaitanong, and R. Yimnirun, Ferroelectric hysteresis behavior in 0-3 PZT-cement composites: Effects of frequency and electric field. *Ferr. Lett.* **36**, 59–66 (2009).

Ferroelectrics
Publication details, including instructions for authors and subscription information:
http://www.tandfonline.com/loi/gfer20

Fabrication and Electrical Properties of Lead Zirconate Titanate-Cement-Epoxy Composites

R. Rianyoi [a] , R. Potong [a] , N. Jaitanong [a] , R. Yimnirun [b] & A. Chaipanich [a]

[a] Department of Physics and Materials Science, Faculty of Science, Chiang Mai University, Chiang Mai, 50200, Thailand

[b] School of Physics, Institute of Science, Suranaree University of Technology, Nakhon Ratchasima, 30000, Thailand

Published online: 01 Dec 2010.

To cite this article: R. Rianyoi , R. Potong , N. Jaitanong , R. Yimnirun & A. Chaipanich (2010): Fabrication and Electrical Properties of Lead Zirconate Titanate-Cement-Epoxy Composites, Ferroelectrics, 405:1, 154-160

To link to this article: http://dx.doi.org/10.1080/00150193.2010.483194

Ferroelectrics, 405:154–160, 2010

ISSN: 0015-0193 print / 1563-5112 online
DOI: 10.1080/00150193.2010.483194

Fabrication and Electrical Properties of Lead Zirconate Titanate-Cement-Epoxy Composites

R. RIANYOI,[1] R. POTONG,[1] N. JAITANONG,[1] R. YIMNIRUN,[2] AND A. CHAIPANICH[1,*]

[1]Department of Physics and Materials Science, Faculty of Science, Chiang Mai University, Chiang Mai 50200, Thailand
[2]School of Physics, Institute of Science, Suranaree University of Technology, Nakhon Ratchasima 30000, Thailand

In this study, epoxy modified lead zirconate titanate-cement 0–3 and 1–3 composites were fabricated via two different techniques with epoxy added as the third phase. The 0–3 composites were fabricated by the normal paste mixing, while the 1–3 composites were fabricated using a dice-and-fill technique. The dielectric and ferroelectric properties of the composites were examined. The results showed that dielectric constant (ε_r) at frequency of 1 kHz of 1–3 composites was higher and dielectric loss was lower than those of the 0–3 composite. The ferroelectric hysteresis loops agree with the results showing reduction area in lossy characteristic and the loops become more apparent in 1–3 composites. The use of epoxy results in a lower P_{ir} value but a reduction in the lossy appearance of P-E loops is observed.

Keywords PZT; cement; composites; fabrication; electrical properties

1. Introduction

Recently, a number of cement-based piezoelectric has been developed to be used as sensors in concrete structure [1–11]. In civil engineering, concrete is the most popularly used structural material. But normal piezoelectric ceramics are not suitable for civil engineering application because of their distinct differences in the volume stability from concrete. For example, the single phase piezoelectric ceramic exhibit high acoustic impedance (21.2 MRayl) compared to that of concrete (9 MRayl) [3–5]. Previously reported experimental results showed that developed cement based piezoelectric composites are suitable for use in concrete structure as the acoustic impedance of ≈50% PZT is close to that of concrete [1–11]. The acoustic velocity and impedance are calculated according to the density and modulus of elasticity. The difference in acoustic impedance between PZT ceramics and concrete is large, which could degrade the coupling between the functional materials and the host structures [3]. Epoxy is a material with low acoustic impedance (3.2 MRayl) [21], which is often used to lower the acoustic impedance of other composite materials. By using epoxy resin as the third phase, it is possible to use higher volume of piezoelectric ceramic (PZT), while maintaining desired acoustic impedance (≈9–10 MRayl).

Received August 23, 2009; in final form October 1, 2009.
*Corresponding author. Fax: +66 53 357512. E-mail: arnon@chiangmai.ac.th

The density ρ_C of the composites can be expressed as [3]

$$\rho_C = \upsilon_1\rho_1 + \upsilon_2\rho_2 + \upsilon_3\rho_3 \tag{1}$$

where υ_1, υ_2 and υ_3 are the volume percentage of the ceramics phase, cement phase and epoxy phase, respectively, and ρ_1, ρ_2 and ρ_3 are the density of the ceramics phase, cement phase and epoxy phase respectively. The elastic modulus of the composites E_C can be written as Eq. (2) by using a series model [22].

$$E_C = \frac{1}{(\upsilon_1/E_1) + (\upsilon_2/E_2) + (\upsilon_3/E_3)} \tag{2}$$

where E_1, E_2 and E_3 are elastic moduli of the ceramics phase, cement phase and epoxy phase, respectively. The acoustic velocity V_C in the composite and acoustic impedance, I_C of the composite can be written as Eqs. (3) and (4), respectively.

$$V_C = \left(\frac{E_C}{\rho_C}\right)^{1/2} \tag{3}$$

$$I_C = \rho_C V_C = (\rho_C E_C)^{1/2} \tag{4}$$

It is clear that the composite's acoustic impedance can be tuned to have a compatible value with that of structure materials-concrete. From these equations, it is therefore possible to calculate the acoustic impedance I_C in accordance with the vol.% of PZT. For example, 70% vol. PZT and 30% vol. of cement results in $I_C \approx$13.3 MRayl and it is possible to add 5% epoxy with 70% PZT at 25% cement to obtain $I_C \approx$12.3 MRayl; a closer match to the acoustic impedance of concrete ($I_C \approx$9 MRayl).

There are eight different types of two phase piezoelectric composites have been studied: 0–3, 1–3, 2–2, 2–3, 3–0, 3–1, 3–2 and 3–3, where the first number in the notation denotes the physical connectivity of the active phase and the second number refers to the physical connectivity of the passive phase [19, 20]. Composites of 0–3 connectivity are relatively easier to fabricate than those of 1–3 connectivity at a low cost, although the latter composites possess higher electroactive responses than the former material [20].

In this paper, epoxy modified lead zirconate titanate-cement 0–3 and 1–3 composites were fabricated with epoxy as the third phase. The dielectric and ferroelectric properties of composites were then investigated.

2. Experimental Procedure

Lead zirconate titanate (PZT) powder was initially produced from the two-stage mixed oxide method by calcining lead zirconate and lead titanate at 800°C for 2 h. PZT ceramics were then produced by sintering PZT powder at 1,200°C for 2 h. These PZT ceramic particles were then mixed with normal Portland cement (also known as ordinary Portland cement or The American Society for Testing and Materials (ASTM) Type I or CEM I under the European standard: ENV197–1) to produce 0–3 connectivity epoxy modified PZT–Portland cement (PC) composites with PZT:PC:Epoxy of 70:30:0 and 70:25:5 by volume (disk samples of ≈15 mm diameter and ≈2 mm thickness). Thereafter, the composites were placed for curing at 60°C and 98% relative humidity for 3 days before measurements. For 1–3 connectivity epoxy modified PZT– Portland cement (PC) composites with PZT:PC:Epoxy of 70:30:0 and 70:25:5 by volume (disk samples of ≈12 mm diameter and

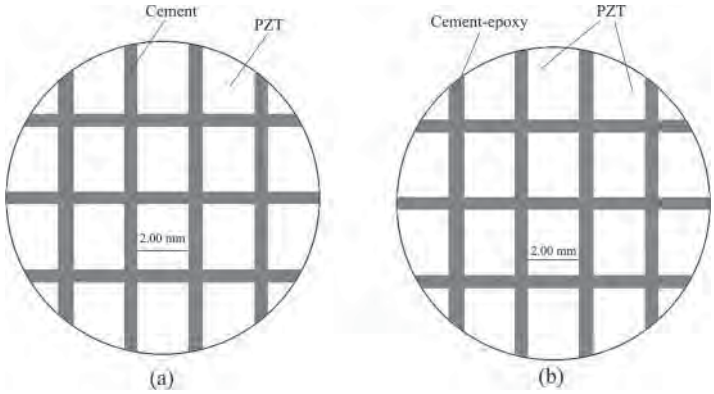

Figure 1. Illustrations of 1–3 composites with PZT:PC:Epoxy at (a) 70:30:0 (b) 70:25:5 by volume.

≈2 mm thickness) were fabricated using a dice-and-fill method [15, 16]. PZT ceramic disc was cut in one direction (y axial) using a diamond saw (Buehler ISOMET Low speed saw) with a ≈0.3 mm thick blade (giving a cut ≈0.5 mm). Cement paste (water: cement = 0.5) was used as the matrix phase of the composites. Thereafter, the samples were placed for curing at 60°C for five days under a condition of relatively high humidity and cut in second direction (x axial). Illustrations of 1–3 composites are shown in Fig. 1. After filling the second direction of cuts with cement paste and epoxy, the composite was curing at a temperature of 60°C and 98% relative humidity for five days before measurements. The dielectric properties of composites were measured using an impedance meter (Hewlett Packard 4194A) at room temperature. The dielectric constant (ε_r) was then calculated from the equation;

$$\varepsilon_r = \frac{Ct}{\varepsilon_0 A} \tag{5}$$

where C is the sample capacitance, t is the thickness, ε_0 is the permittivity of free space constant (8.854×10^{-12} Fm^{-1}), and A is the electrode area. The ferroelectric hyteresis (P-E) loop behaviors of the composites were measured by a computer controlled modified Sawyer-Tower circuit at room temperature. The electric field of 9 kV/cm was applied to a sample by a high-voltage ac amplifier with the input sinusoidal signal from a signal generator with the frequency of 90 Hz. The remnant polarization and coercive field can then be obtained from the ferroelectric hysteresis (P-E) loops.

3. Results and Discussion

The dielectric constant (ε_r) as plotted against frequency of epoxy modified PZT-PC composites are shown in Fig. 2. The dielectric constant of both 0–3 connectivity and 1–3 connectivity epoxy modified PZT– Portland cement (PC) composites can be seen to decrease with increasing frequency (from 0.1 kHz to 20 kHz). In addition, the dielectric constant (ε_r) at 1 kHz is plotted against epoxy content in composites in Fig. 3(a). The results show that with epoxy as the third phase, decrease in the dielectric constant was observed. The dielectric constant of 0–3 composites at 0% vol. of epoxy was found at 354 and the lower value of 100 was found with 5% vol. of epoxy. Similar trend in the results were found in 1–3 composites where a significant decrease was observed when the epoxy

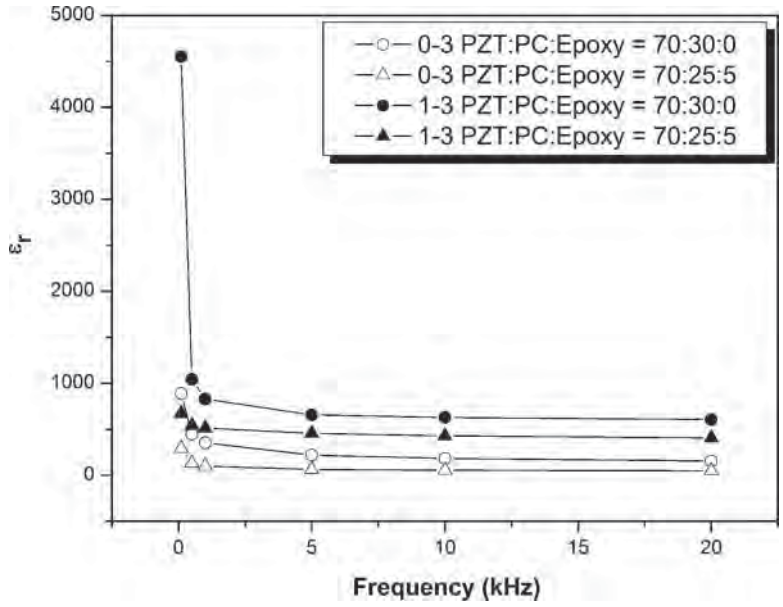

Figure 2. Effect of frequency on dielectric constant (ε_r) of epoxy modified lead zirconate titanate-cement 0–3 and 1–3 composites.

content was increased from 0% vol. to 5% vol. At 0% vol. of epoxy the ε_r value was 828 and a lower value of 512 was obtained when 5% vol. epoxy was added. This means that the dielectric constant of the PZT-PC composites is higher than that of the epoxy modified PZT-PC composites. In addition, it is clearly observed that dielectric constant (ε_r) in epoxy modified lead zirconate titanate-cement composites with 0–3 connectivity is lower than that of the composites with 1–3 connectivity. This is believed due to much more existing interface pores in 0–3 connectivity composite compared to 1–3 connectivity composite. As shown in Fig. 3(b), the dielectric loss (tanδ) of the composites with 0–3 connectivity is higher than that of composites with 1–3 connectivity. This is mainly because in 0–3

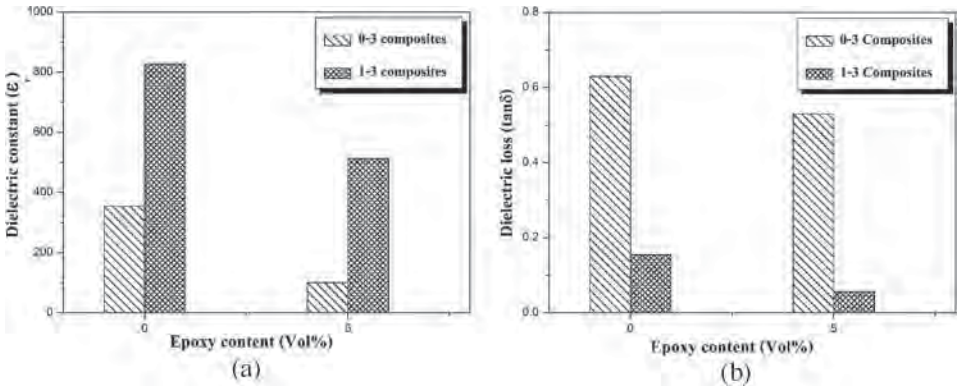

Figure 3. Dielectric properties results of epoxy modified lead zirconate Titanate-cement 0–3 and 1–3 composites (a) dielectric constant (b) dielectric loss at 1 kHz.

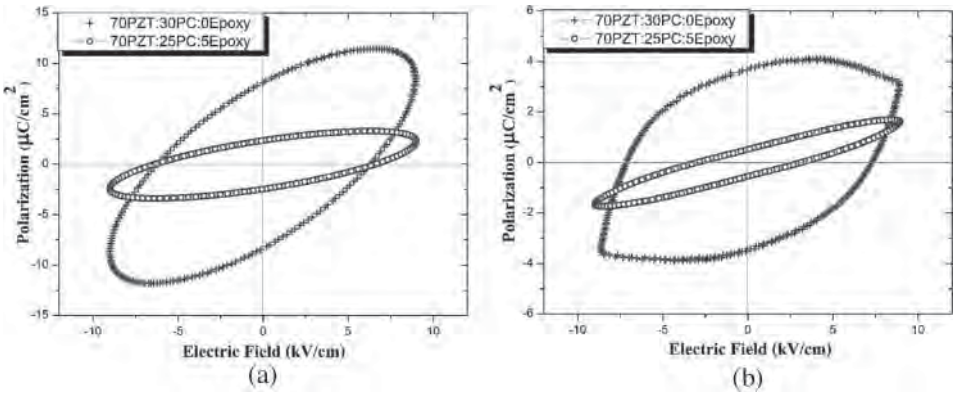

Figure 4. Hysteresis loops of (a) 0–3 composites and (b) 1–3 composites of epoxy modified lead zirconate titanate-cement composites.

composites the conducting ions would surround the interfaces of PZT, epoxy and cement matrix to a greater extent and more space charges available; thereby results in high loss.

The hysteresis loops of the composites under different epoxy contents with applied electric field of about 9 kV/cm are shown in Fig. 4(a) and (b). It must first be noted that all ferroelectric hysteresis loops of epoxy modified lead zirconate titanate-cement composites show lossy appearances with round tips as a result of both cement matrix and epoxy in the composite. In this paper, we can define the y-axis intercept is called the "instantaneous" remnant polarization ($P_{ir.}$) and the x-axis intercept as the "instantaneous" coercive field ($E_{ic.}$). From the results, it was found that the "instantaneous" remnant polarization (P_{ir}) of 0–3 composites is higher than that of 1–3 composites. However, the ferroelectric hysteresis loop of 1–3 composites showing reduction in lossy characteristic and ferroelectric hysteresis loop becomes more apparent. In addition, the hysteresis loop of the composites is far from saturation due to a presence of non piezoelectric cement layers between the PZT particles and epoxy [9]. For the 0–3 composites higher P_{ir} value ($P_{ir} \approx 8\ \mu C/cm^2$) was found in sample with no epoxy. When epoxy was added, the P_{ir} value reduced to $\approx 2\ \mu C/cm^2$ (Fig. 5(a)). However, it is noticed that less loss appearance is observed when epoxy was

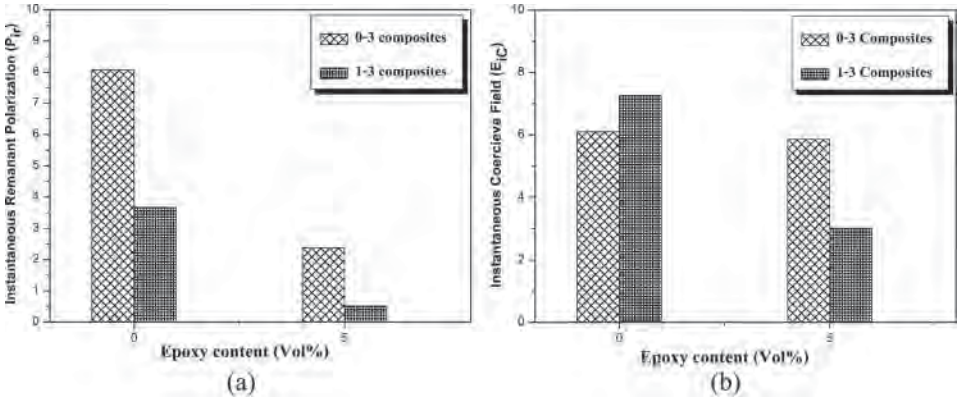

Figure 5. Ferroelectric properties results of epoxy modified lead zirconate titanate-cement 0–3 and 1–3 composites (a*) instantaneous* remnant polarization (P_{ir}) and (b) *instantaneous* coercive field (E_{ic}).

added. Similar results were observed in 1–3 connectivity where P_{ir} value of epoxy modified PZT-cement composite is lower then the composite with the epoxy and significantly less loss is observed when epoxy was added. For the "instantaneous" coercive field (*Eic*) of the composites of 0–3 and 1–3 composites were found to decrease with increasing the epoxy content from 0% vol. to 5% vol. (Fig. 5(b)). The "instantaneous" coercive field (*Eic*) of 0–3 composites at 0% vol. of epoxy was found at 6.1 kV/cm and a slightly lower value of 5.8 kV/cm was found with 5% vol. of epoxy. Similar trend in the results were found in 1–3 composites but a significant decrease was observed when the epoxy content was increased from 0% vol. to 5% vol. of epoxy was used. At 0% vol. of epoxy the E_{ic} value was 7.2 kV/cm and a lower value of 3.0 kV/cm was obtained when 5% vol. Nonetheless, one may consider that the 0–3 and 1–3 connectivity composites with added epoxy shows little or no hysteresis loop characteristics. This was suggested earlier by Fang *et al.* [23] that epoxy matrix composite can not find such hysteresis loops characteristic which was due to the fact that the strength of the relaxation property of the material is closely related to the dielectric relaxation time and these composites do not exhibit significant dielectric relation.

4. Conclusions

All epoxy modified PZT-PC 0–3 composites by the normal paste mixing and 1–3 composites by dice-and-fill technique were successfully fabricated. The result showed that the dielectric constant (ε_r) at frequency of 1 kHz of 1–3 composites was higher and dielectric loss (tanδ) was lower than 0–3 composites. In addition, the ferroelectric hysteresis loops agree with the results showing reduction area in lossy characteristic and ferroelectric hysteresis loop becomes more apparent in 1–3 composite. Furthermore, the use of epoxy results in a lower P_{ir} value but with a reduction in the lossy appearance.

Acknowledgments

The authors are thankful to members of staff at the Electroceramics Research Laboratory, Faculty of science, and Chiang Mai University for the research facilities made possible for this research work. The authors would also like to express their gratitude to Thailand Research Fund (TRF), the Commission on Higher Education (Thailand) and the graduate school of Chiang Mai University.

References

1. N. Jaitanong, R. Yimnirun, and A. Chaipanich, Effect of uniaxial stress on dielectric properties of 0–3 PZT-Portland cement composite. *Ferroelectrics* **384**, 174–181 (2009).
2. A. Chaipanich and N. Jaitanong, Effect of PZT particle size on the electromechanical coupling coefficient of 0–3 PZT-cement composites. *Ferr. Lett.* **36**, 37–44 (2009).
3. Z. Li, D. Zhang, and K. Wu, Cement-based 0–3 piezoelectric composites. *J. Am. Ceram. Soc.* **85**, 305–313 (2002).
4. Z. Li, B. Dong, and D. Zhang, Influence of polarization on properties of 0–3 cement-based PZT composites. *Cem. Coner. Compos.* **27**, 27–32 (2005).
5. B. Dong and Z. Li, Cement-based piezoelectric ceramic smart composites. *Compos. Sci. Technol.* **65**, 1363–1371 (2005).
6. S. Huang, J. Chang, R. Zu, F. Liu, L. Lu, Z. Ye, and Z. Cheng, Piezoelectric properties of 0–3 PZT/sulfoaluminate cement composites. *Smart Mater. Struct.* **13**, 270–274 (2004).
7. K. H. LAM and H. L. W. CHAN, Piezoelectric cement-based 1–3 composites. *Appl. Phys. A* **81**, 1451–1454 (2005).

8. C. Xin, S. Huang, C. Jun, Z. Ronghua, L. Futian, and L. lingchao, Piezoelectric and dielectric properties of piezoelectric ceramic-sulphoaluminate cement composites. *J. Eur. Ceram. Soc.* **25**, 3223–3228 (2005).
9. C. Xin, S. Huang, C. Jun, and L. Zongjin, Piezoelectric, dielectric, and ferroelectric propeties of 0–3 ceramic/cement composites. *J. App. Phys.* **101**, 094110 (2007).
10. A. Chaipanich, N. Jaitanong, and T. Tunkasiri, Fabrication and properties of PZT-ordinary Portland cement composites. *Mats. Letts.* **61**, 5206–5208 (2007).
11. A. Chaipanich and N. Jaitanong, Effect of polarization on the microstructure and piezoelectric properties of PZT-cement composites. *Adv. Mats. Res.* **55–57**, 381 (2008).
12. N. Jaitanong, K. Wongjinda, P. Tammakun, G. Fujijanagul, and A. Chaipanich, Effect of carbon addition on dielectric properties of 0–3 PZT-Portland cement composite. *Adv*. *Adv* **55–57**, 377 (2008).
13. N. Jaitanong, A. Chaipanich, and T. Tunkasiri, Properties 0–3 PZT-Portland cement composites. *Ceram. Inter.* **34**, 793–795 (2008).
14. A. Chaipanich and N. Jaitanong, Effect of poling time on piezoelectric properties of 0–3 PZT-Portland cement composites. *Ferr. Lett.* **35**, 73–78 (2008).
15. N. Jaitanong and A. Chaipanich, Effect of poling temperature on piezoelectric properties of 0–3 PZT-Portland cement composites. *Ferr. Lett.* **35**, 17–23 (2008).
16. A. Chaipanich, Dielectric and piezoelectric properties of PZT-cement composites. *Curr. App. Phys.* **7**, 537–539 (2007).
17. A. Chaipanich, Effect of PZT particle size on dielectric and piezoelectric properties of PZT-cement composites. *Curr. App. Phys.* **7**, 574–577 (2007).
18. A. Chaipanich, N. Jaitanong, and R. Yimnirun, Ferroelectric hysteresis Behavior in 0–3 PZT-cement composites: Effects of frequency and electric field. *Ferr. Lett.* **36**, 59–66 (2009).
19. R. E. Newham, D. P. Skinner, and Le Cross, Connectivity and piezoelectric-pyroelectric composites. *Mater. Res. Bull.* **13**, 535 (1978).
20. Y. Osada and D. E. DeRossi (Eds). *Polymer Sensors and Actuators*. New York: Springer (2000).
21. K. Nicolaides, L. Nortman, and J. Tapson, The effect of backing material on the transmitting response level and bandwidth of a wideband underwater transmitting transducer using 1–3 piezocomposite material. Paper#1111 Presented at the International Congress on Ultrasonics, Santiago, January 11–17, 2009, Session S27: Transducer technology.
22. S. Popovics, *Strength and Related Properties of Concrete*. New York: Wiley (1998).
23. D.-N. Fang, A. K. Soh, C.-Q. Li, and B. Jiang, Nonlinear behavior of 0–3 type ferroelectric composites with polymer matrices. *J. of Mater. Sci.* **36**, 5281–5288 (2001).

Available online at www.sciencedirect.com
ScienceDirect
Ceramics International 36 (2010) 1479–1483
CERAMICS INTERNATIONAL
www.elsevier.com/locate/ceramint

Short communication

Phase development and dielectric responses in PMN–BNT ceramics

N. Jaitanong, W.C. Vittayakorn, A. Chaipanich *

Department of Physics and Materials Science, Faculty of Science, Chiang Mai University, Chiang Mai, 50200, Thailand

Received 21 August 2009; received in revised form 4 November 2009; accepted 21 December 2009
Available online 28 January 2010

Abstract

$(1-x)Pb(Mg_{1/3}Nb_{2/3})O_3$–$x(Bi_{0.5}Na_{0.5})TiO_3$ ceramics were prepared by the conventional mixed-oxide method. All compositions show complete perovskite solid solutions and the structure to change from cubic to rhombohedral at $x = 0.5$. The dielectric constant and dielectric loss tangent were measured as a function of both temperature and frequency. The results indicated a relaxor ferroelectric behavior for all ceramics. The temperature at maximum of the dielectric constant of PMN–BNT ceramics were seen to increase with increasing BNT content. Moreover, the broadest dielectric peak occurs at $x = 0.9$, which leads to a morphotropic phase boundary in this system.

Keywords: C. Dielectric properties; Lead magnesium niobate (PMN); Bismuth sodium titanate (BNT); PMN–BNT

1. Introduction

Perovskite ferroelectric ceramics can be applied to several electronic devices such as transducers, actuators and sensors [1]. Among the many ferroelectric materials, lead magnesium niobate (PMN) and bismuth sodium titanate (BNT) are the most attractive because of their excellent electrical properties [2–7]. The compound $(Bi_{0.5}Na_{0.5})\ TiO_3$ (BNT) shows the perovskite structure with rhombohedral system at room temperature. Compared with the most widely used ferroelectric ceramics PZT, BNT based ceramics has been reported to possess a high anisotropic electro-mechanical coupling ($K_p \sim 16.5$–25.5%, $K_t \geq 48\%$) and a high frequency constant ($N_t \geq 2550$ Hz m) as demanded for ultrasonic applications [8]. However, the other electronic applications of pure BNT ceramics are limited by some of its shortcomings in electrical properties such as low dielectric constant (ε_r), narrow sintering temperature range and high conductivity at room temperature [2–3,9]. The $Pb(Mg_{1/3}Nb_{2/3})O_3$ (PMN) ceramic, a prototype relaxor ferroelectric with perovskite structure, demonstrates a quite high maximum dielectric constant around −10 °C with diffuse phase transition phenomena [5–6,10]. However, pure PMN perovskite is very difficult to obtain by solid-state reaction because of the unwanted pyrochlore phase. Thus, mixing PMN with BNT is expected to enhance the formation a more stabilized perovskite structure, purer perovskite with lower amount of undesirable pyrochlore phases. Moreover, it is expected that the dielectric constant may be enhanced in PMN–BNT ceramics.

Therefore, this study investigated the dielectric properties of $(1-x)$PMN–xBNT compositions prepared by solid-state reaction. The dielectric properties of the PMN–BNT system were determined as a function of temperature and frequency, and the Curie temperature (T_c) was engineered over a wide range of temperature by varying the compositions in the system. The phase development of the PMN–BNT system was investigated by XRD analysis. Finally, the relationships among these experimental results are discussed.

2. Experimental procedure

The following compositions of $(1-x)$PMN–xBNT ($x = 0.0$, 0.1, 0.25, 0.5, 0.75, 0.9 and 1.0) were prepared by a solid-state reaction method. The starting precursors, PMN and BNT, were first formed in order to avoid the unwanted pyrochlore phases. The PMN powder was synthesized through the columbite method, in which magnesium niobate ($MgNb_2O_6$) was first prepared and then used as precursor. Pure $MgNb_2O_6$ phase powder was formed by calcining $(MgCO_3)_4Mg(OH)_2{\cdot}5(H_2O)$ with Nb_2O_5 at 1150 °C for 2 h. $MgNb_2O_6$ powder was then mixed with PbO (99.0%) in ethanol and calcined at 800 °C to produce single phase PMN. For the preparation of BNT powder, Bi_2O_3,

* Corresponding author. Tel.: +66 53 943 367; fax: +66 53 943 445.
E-mail address: arnon@chiangmai.ac.th (A. Chaipanich).

0272-8842/$36.00
doi:10.1016/j.ceramint.2010.01.003

Na_2CO_3 and TiO_2 powders were homogeneously mixed via ball-milling for 24 h with zirconia media in ethanol. The well-mixed powder was calcined at 800 °C for 2 h. The $(1-x)$PMN–xBNT compositions were then formulated from PMN and BNT component by employing the similar mixed-oxide procedure and calcined at various temperatures between 1100 and 1250 °C for 2 h in order to obtain single phase $(1-x)$PMN–xBNT powders.

The calcined PMN–BNT powders were then pressed hydraulically to form disc-shaped pellets with a diameter of 15 mm and a thickness of 1.5 mm. The sintering was carried out for 2 h at 1150 °C with heating/cooling rates of 10 °C/min. X-ray diffraction (XRD), using CuK_α radiation, was employed to identify the phase formation. For the electrical measurement, silver paste was painted on both sides of the polished samples as electrodes. The dielectric properties of all sintered samples were measured with a HP4284A LCR meter in connection with a temperature chamber and a sample holder capable of high temperature measurement. The dielectric constant (ε_r) was then calculated using the geometric area and thickness of samples.

3. Results and discussion

The phase composition of the $(1-x)$PMN–xBNT ceramics, where $x = 0.0$, 0.1, 0.25, 0.5, 0.75, 0.9 and 1.0, is shown in Fig. 1. The XRD diffraction patterns of sintered ceramic with $x = 0.0$ match exactly with the perovskite $Pb(Mg_{1/3}Nb_{2/3})O_3$ (JCPDS file no. 81-0861), whereas that with $x = 1.0$ match exactly rhombohedral perovskite $(Bi_{0.5}Na_{0.5})TiO_3$ (JCPDS file no. 36-0340). In the ladder pattern, a series of continuous solid solutions PMN–BNT with perovskite structure normally forms. Previous works [11,12] reported that secondary or pyrochlore phases, such as $Pb_2Nb_2O_7$ and $Pb_3Nb_2O_{13}$, $Pb_3Nb_4O_{13}$ and $Pb_3Nb_2O_8$, always exist prior to perovskite formation in the conventional solid-state reaction as a result of interfacial reaction. However, in the work reported here, it is seen that the PMN–BNT system formed a pure perovskite phase without any trace of unwanted phases. With increasing BNT content, the diffraction peaks shifted towards higher angle. However, it was not possible to determine the correct symmetry for the structure of PMN–BNT ceramics by simply examining the appropriate diffraction patterns. These XRD patterns showed no evidence of any superlattice reflections. However, the strongest reflections were noticeably broader than others when x is increasing. It has been reported earlier that the transition is of the first order with considerable hysteresis [13]. In first-order transition,

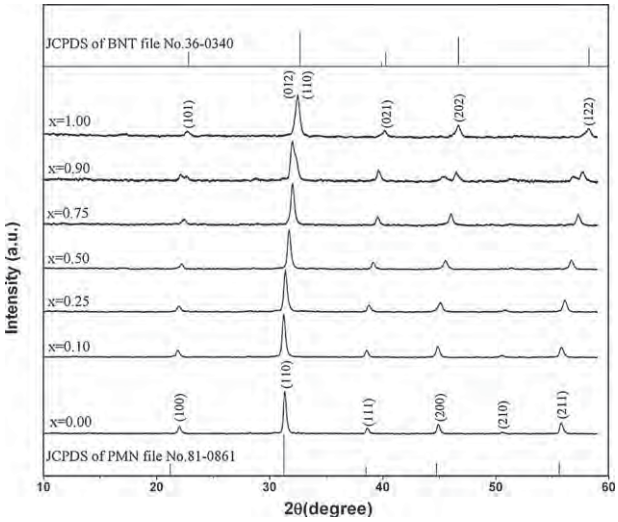

Fig. 1. XRD patterns of $(1-x)$PMN–xBNT ceramics.

coexistence of phases of two difficult structures is possible and this has been observed in a number of ABO_3 perovskites [14]. Moreover, it is believed that the broadening of the peaks in the diffraction patterns is due to a combination of effects including strain broadening and possibly a small shift in the position of the sample during processing [15]. This broadening meant that it was not possible to obtain high quality structural refinements in either space group, although reasonable estimates of the lattice parameters were possible. Examination of unit cell parameters and cell volume (shown in Table 1) suggests that the structure is still cubic at $x = 0.1$ and 0.25 and the transition to rhombohedral occurs at $x = 0.5$. The unit cell volume decreases as x increase. Moreover, XRD indicates that the use of high purity PMN and BNT precursors at the optimum firing temperatures can effectively enhance the yield of the perovskite phase.

The optimized sintering temperature, density and relative density of the sintered $(1-x)$PMN–xBNT ceramics are listed in Table 1. Higher firing temperatures were necessary for compositions containing a large fraction of PMN. The densities of PMN–BNT ceramics were therefore within the range of 5.91–7.94 g/cm^3. It should be noted here that the composition and densification of ceramic can influence the dielectric properties [16], but in the present work the relative density varies between 98.50 and 99.25%, as shown in Table 1, which should not play a significant role in the variation of dielectric properties. The temperature dependence of dielectric constant

Table 1
Characteristics of $(1-x)$PMN–xBNT ceramics with optimized processing condition.

Compositions	Structure	Sintering temperature (°C)	Density (g/cm^3)	Relative density (%)
$x = 0.00$	Cubic	1250	7.94	99.25
$x = 0.10$	Cubic	1200	7.6	97.43
$x = 0.25$	Cubic	1200	7.40	98.66
$x = 0.50$	Rhombohedral	1150	6.94	99.14
$x = 0.75$	Rhombohedral	1150	6.41	98.61
$x = 0.90$	Rhombohedral	1100	6.03	97.25
$x = 1.00$	Rhombohedral	1100	5.91	98.50

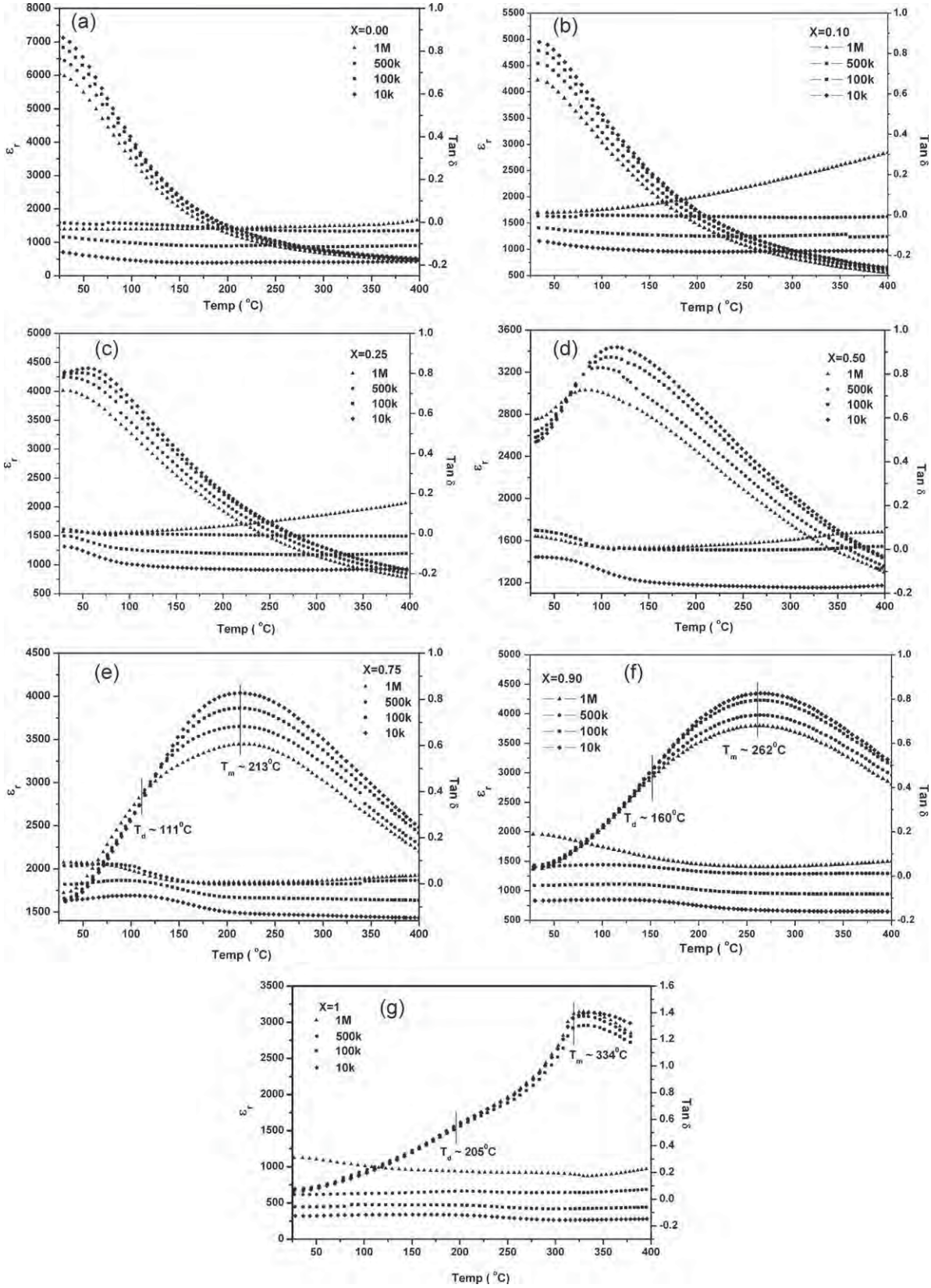

Fig. 2. Temperature dependence of dielectric constant and dielectric loss of $(1-x)$PMN–xBNT ceramics at different frequencies: (a) $x = 0.0$, (b) $x = 0.1$, (c) $x = 0.25$, (d) $x = 0.5$, (e) $x = 0.75$, (f) $x = 0.9$ and (g) $x = 1.0$.

(ε_r) and dielectric loss ($\tan\delta$) at various frequencies for compositions with $x = 0.0$, 0.1, 0.25, 0.5, 0.75, 0.9 and 1.0 is shown in Fig. 2. For pure PMN ($x = 0.0$) (Fig. 2a), the maximum temperatures (T_m) are not completely shown due to the limited range of the measuring set-up, though it is widely known to be close to $-10\,^{\circ}$C. However, from the dielectric curves it can be seen the typical relaxor behavior with the magnitude of dielectric constant decreases with increasing frequency. Relaxor ferroelectrics are characterized by diffuse phase transition, which has been interpreted as a result of short-range order [17]. For pure BNT ($x = 1.0$) (Fig. 2e), the phase transition temperature can be clearly seen to have a small frequency dependence. It is well known BNT has relaxor properties and has peculiar behavior of the diffused phase transition from the rhombohedral to nonpolar tetragonal phase [18]. Diffuse phase transitions of BNT can be described by a coexistence region between phases. In the present work, three phases of ferroelectric, anti-ferroelectric and paraelectric nature exist in the sample at different temperatures [19]. The depolarization temperature (T_d), referred to the transition temperature between the ferroelectric phase and the anti-ferroelectric phase, was increased to 205 °C and the maximum permittivity temperature (T_m) for this sample is about 334 °C. Two transition points (T_d and T_m at ~110 °C and 213 °C respectively) are still clearly seen in the ε–T plot for 0.25PMN–0.75BNT composition, as shown in Fig. 2e and T_d and T_m at ~160 °C and 264 °C respectively are still clearly seen in the ε–T plot for 0.1PMN–0.9BNT composition, as shown in Fig. 2f that gradually disappear after increasing of PMN amount or when $x \leq 0.50$.

The effect of BNT modification on the dielectric properties of PMN has then been investigated. When BNT is added to form the binary system with PMN, the maximum temperature is shifted towards that of BNT ceramic. The representative temperature dependence of the dielectric constant (ε_r) measured at 10 kHz for $(1-x)$PMN–xBNT samples with $x = 0.0$, 0.1, 0.25, 0.5, 0.75, 0.9 and 1.0 is shown in Fig. 3. With increasing BNT content, the maximum transition temperature (T_m) shifts monotonously to higher temperatures and the maximum dielectric constant (ε_m) significantly decreases with increasing BNT content up to 50 mol%. The ε_m value rises again after adding more BNT. The broadest dielectric peak is found at the 0.1PMN–0.9BNT composition which indicates diffused phase transition behavior. However, it is well know that PMN and BNT have relaxor characteristics and typical relaxor behavior is characterized by a diffused ferroelectric phase transition. This behavior is explained in terms of a coexistence region between phases [20], and in this case is dominated from one of both polar rhombohedral and nonpolar tetragonal phases of the BNT component [13]. To assess the diffuse phase transition of relaxor ferroelectric, the degree of broadening or diffuseness in the observed dielectric variation could be estimated with the diffusivity (γ) using the $\ln(1/\varepsilon_r - 1/\varepsilon_{max})$ versus $(T - T_{max})$. The following equation:

$$\frac{1}{\varepsilon} \approx (T - T_m)^2 \tag{1}$$

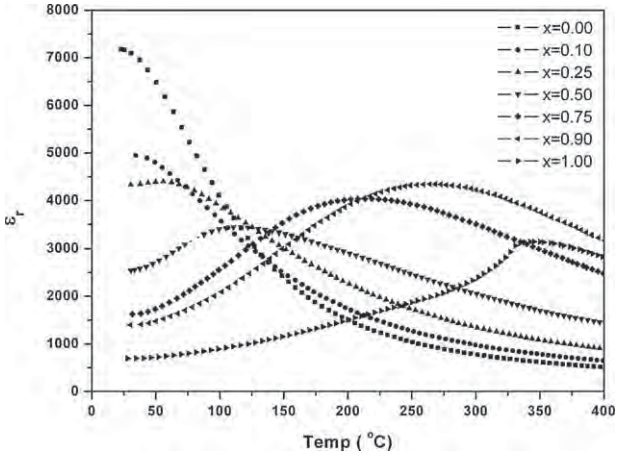

Fig. 3. Temperature dependence of dielectric constant (ε_r) of $(1-x)$PMN–xBNT ceramics at 10 kHz.

has been shown to be valid over a wide temperature range, where T_m is the temperature at which the dielectric constant is maximum [16]. If the local Curie temperature distribution is Gaussian, the reciprocal permittivity can be written in the form:

$$\frac{1}{\varepsilon} = \frac{1}{\varepsilon_m} + \frac{(T - T_m)^{\gamma}}{2\varepsilon_m \delta^2} \tag{2}$$

where ε_m is maximum dielectric constant, γ is diffusivity, and δ is diffuseness parameter. The γ and δ can be estimated from the slope and intercept of the dielectric data shown in Fig. 4, which should be a linear. The values of γ and δ are both material constants depending on the composition and structure [21]. In a composition with the diffused phase transition such as relaxor ferroelectric, the value of γ is expected to be 2 [20–21]. The plots of $\ln((1/\varepsilon) - (1/\varepsilon_m))$ as a function of $\ln(T - T_m)$ for all compositions are shown in Fig. 4. The value of γ reported in Table 2 varies between 1.77 and 1.99 which confirms relaxor behaviors. The diffusion factor for all composition fluctuates in the same range (1.7–1.9), however the results show the degree

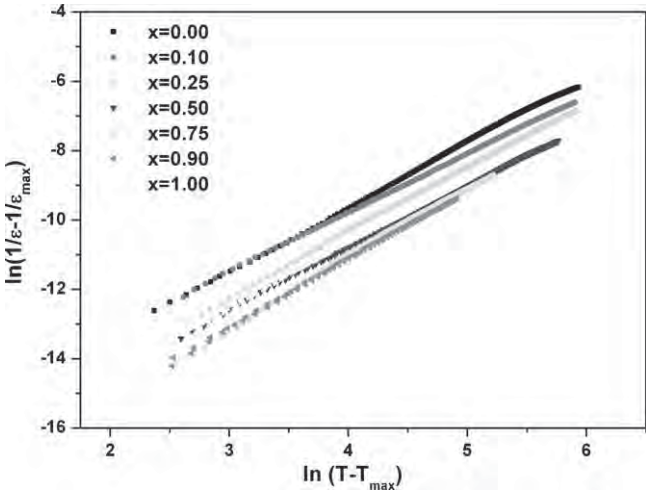

Fig. 4. Plot of $\ln(T - T_{max})$ versus $\ln((1/\varepsilon_r) - (1/\varepsilon_{max}))$ for $(1-x)$PMN–xBNT ceramics.

Table 2
Dielectric properties of $(1-x)$PMN–xBNT ceramics.

Compositions	T_d	T_m	ε_m	γ	δ
$x = 0.00$	–	–	>6030	–	–
$x = 0.10$		33	4948	1.68	−16.54
$x = 0.25$	–	31	4002	1.83	−17.68
$x = 0.50$	–	88	3044	1.77	−17.99
$x = 0.75$	111	213	3473	1.99	−19.03
$x = 0.90$	160	264	4347	1.99	−19.02
$x = 1.00$	205	334	3131	1.98	−18.52

of diffuseness of the phase transition to be highest at the 0.1PMN–0.9BNT composition, which lead to a morphotropic phase boundary (MPB) [22] in this system. In the MPB regions, enhanced dielectric constants are obtained. It was attributed to easily switching of the polarization vector between all allowed polarization orientations [23]. The relationship between phase formation and electrical properties is important and thus helps to improve the understanding on these compositions.

4. Conclusions

Phase formation characteristics of perovskite PMN–BNT ceramics have been investigated with XRD analysis. All compositions show complete solid solutions without any trace of unwanted phases. The crystal structure of PMN–BNT system gradually changes from cubic in PMN ceramic to rhombohedral with increasing BNT content. The dielectric studies indicated that all compositions in the PMN–BNT system exhibit a diffused phase transition and followed the Curie–Weiss law of relaxor ferroelectric behavior.

Acknowledgements

The authors are grateful to members of staff at the Electroceramics Research Laboratory, Faculty of science, and Chiang Mai University for the research facilities made possible for this research work. The authors would like to express their gratitude for financial support from the Thailand Research Fund (TRF), the Commission on Higher Education (Thailand) and the graduate school of Chiang Mai University.

References

[1] A.J. Moulson, J.M. Herbert, Electroceramics, Chapman and Hall, London, 1990.
[2] H.L.W. Chan, S.H. Choy, C.P. Chong, H.L. Li, P.C.K. Liu, Bismuth sodium titanate based lead-free ultrasonic transducer for microelectronics wirebonding applications, Ceramics International 34 (2008) 773–777.
[3] B.H. Kim, S.J. Han, J.H. Kim, J.H. Lee, B.K. Ahn, Q. Xu, Electrical properties of $(1-x)(Bi_{0.5}Na_{0.5})TiO_3$–$xBaTiO_3$ synthesized by emulsion method, Ceramics International 33 (2007) 447–452.
[4] L. Gao, Y. Huang, Yan Hu, H. Du, Dielectric and ferroelectric properties of $(1-x)BaTiO_3$–$xBi_{0.5}Na_{0.5}TiO_3$ ceramics, Ceramics International 33 (2007) 1041–1046.
[5] Z. Chen, J. Hu, Piezoelectric and dielectric properties of $(Bi_{0.5}Na_{0.5})_{0.94}$-$Ba_{0.06}TiO_3$–$Ba(Zr_{0.04}Ti_{0.96})O_3$ lead-free piezoelectric ceramics, Ceramics International 35 (2009) 111–115.
[6] Y.C. Liou, J.H. Chen, PMN ceramics produced by a simplified columbite route, Ceramics International 30 (2004) 17–22.
[7] Y.S. Kim, N.K. Kim, J. Ko, Processing and dielectric properties of $(Pb,Bi)(Mg,Nb,Ti)O_3$ ceramics, Ceramics International 33 (2007) 1083–1086.
[8] T.B. Wang, M. Gao, L.E. Wang, Y.K. Lu, D.P. Zhou, Study on piezoelectric ceramics without lead, Journal of Inorganic Materials 2 (1987) 223–232.
[9] Y. Qu, D. Shan, J. Song, Effect of A-site substitution on crystal component and dielectric properties in $Bi_{0.5}Na_{0.5}TiO_3$ ceramics, Materials Science and Engineering B 121 (2005) 148–151.
[10] P. Kumar, C. Prakash, O.P. Thakur, R. Chatterjee, T.C. Goel, Dielectric, ferroelectric and pyroelectric properties of PMNT ceramics, Physica B 371 (2006) 313–316.
[11] X. Chen, H. Fan, Y. Fu, L. Liu, J. Chen, Low-temperature fabrication and crystallization behavior of $Pb(Mg_{1/3}Nb_{2/3}O_3)$ crystallites by a hydrothermal process, Journal of Alloys and Compounds, in press.
[12] H. Bruncková, L. Medvecký, J. Mihalik, Effect of sintering conditions on the pyrochlore phase content in PMN–PFN ceramics prepared by sol–gel process, Journal of the European Ceramic Society 28 (2008) 123–131.
[13] T. Oh, M.H. Kim, Phase relation and dielectric properties in $(Bi_{1/2}Na_{1/2})_{1-x}Ba_xTiO_3TiO_3$ lead-free ceramics, Materials Science and Engineering B 132 (2006) 239–246.
[14] B.V.B. Saradhi, K. Srinivas, G. Prasad, S.V. Suryanarayana, T. Bhimasankaram, Impedance spectroscopic studies in ferroelectric $(Na_{1/2}Bi_{1/2})TiO_3$, Materials Science and Engineering B 98 (2003) 10–16.
[15] Y. Huang, L. Gao, Y. Hu, H. Du, Journal of Material Science: Materials in Electronics 18 (2007) 605–609.
[16] R. Yimnirun, S. Ananta, P. Laoratanakul, Effects of $Pb(Mg_{1/3}Nb_{2/3})O_3$ mixed-oxide modification on dielectric properties of $Pb(Zr_{0.52}Ti_{0.48})O_3$ ceramics, Materials Science & Engineering B 112 (2004) 79–86.
[17] H.Y. Tian, D.Y. Wang, D.M. Lin, J.T. Zeng, K.W. Kwok, H.L.W. Chan, Diffusion phase transition and dielectric characteristics of $Bi_{0.5}Na_{0.5}TiO_3$–$Ba(Hf, Ti)O_3$ lead-free ceramics, Solid State Communications 142 (2007) 10–14.
[18] Y. Hiruma, K. Yoshii, H. Nagata, T. Takenaka, Phase transition temperature and electrical properties of $(Bi_{1/2}Na_{1/2})TiO_3$–$(Bi_{1/2}A_{1/2})TiO_3$ (A = Li and K) lead-free ferroelectric ceramics, Journal of Applied Physics 103 (2008) 084121–84127.
[19] T. Takennake, K. Maruyama, S.K. Akata, $(Bi_{1/2}Na_{1/2})$ TiO_3-$BaTiO_3$ system for lead-free piezoelectric ceramic, Japanese Journal of Applied Physics 30 (1991) 2236–2239.
[20] C.J. Walsh, W.A. Schulze, Bond valence structure analysis of doped bismuth sodium titanate, IEEE international ultrasonics, Ferroelectrics (2004) 328–331.
[21] W. Chaisan, R. Yimnirun, S. Ananta, D.P. Cann, Dielectric and ferroelectric properties of lead zirconate titanate-barium titanate ceramics prepared by a modified mixed-oxide method, Materials Chemistry and Physics 104 (2007) 113–118.
[22] J.K. Lee, J.Y. Yi, K.S. Hong, Structural and electrical properties of $(1-x)$ $(Na_{1/2}Bi_{1/2})TiO_3$-$xPb(Mg_{1/3}Nb_{2/3})O_3$ solid solution, Journal of Solid State Chemistry 177 (2004) 2850–2854.
[23] C. Peng, J.F. Li, W. Gong, Preparation and properties of $(Bi_{1/2}Na_{1/2})TiO_3$–$Ba(Ti, Zr)O_3$ lead-free piezoelectric ceramics, Materials Letters 59 (2005) 1576–1580.

RESEARCH ARTICLE

ScienceAsia 35 (2009): **358**–**364**

doi: 10.2306/scienceasia1513-1874.2009.35.358

Investigation of the mechanical and in vitro biological properties of ordinary and white Portland cements

Pincha Torkittikul, Arnon Chaipanich*

Cement and Concrete Research Laboratory, Department of Physics and Material Science, Faculty of Science, Chiang Mai University, Chiang Mai 50200, Thailand

*Corresponding author, e-mail: arnon@chiangmai.ac.th

Received 20 Nov 2008
Accepted 13 Oct 2009

ABSTRACT: Biomaterials containing calcium silicate have been widely used in dental and bone repaired applications. This study investigated mechanical and in vitro biological properties of ordinary and white Portland cement both of which are composed mainly of calcium silicates. The time of setting was determined using a Vicat needle. Compressive strength was measured at the age of 1, 3, and 7 days. The 1 day set Portland cement pastes were soaked in a simulated body fluid to investigate the ability of the material to form a bond with living bone tissue. X-ray diffraction traces of samples following immersion in simulated body fluid demonstrated that both cement pastes form a hydroxyapatite layer within 7 days but white Portland cement shows a noticeably higher amount of apatite crystal than that of ordinary Portland cement. Scanning electron micrographs reveal a clear presence of hydroxyapatite on the surface of white, but not in ordinary Portland cement. In addition, white Portland cement can achieve a compressive strength of 30 MPa within 24 h after curing in distilled water at human temperature.

KEYWORDS: hydroxyapatite, bioactivity, setting time, compressive strength

INTRODUCTION

When the body exhibits disease or damage, defence mechanisms will stimulate the formation of a fibrous capsule around an artificial implant material in an attempt to isolate it from surrounding tissue. Glass and ceramic materials have been shown to form stable bonds with living bone tissue in vitro [1–4]. In 1969, the ability of material to form a bond with living bone tissue, referred to as bioactivity, was first observed [1]. Materials that exhibit bioactivity can therefore be used to repair damaged bone tissue.

Silicates have been shown to accelerate the formation of new bone tissue by inducing genetic activity of bone-regulating cells [2–7]. When a silicate is immersed in human plasma environment, a precipitation of ions forms. As human plasma is supersaturated with respect to hydroxyapatite, Si-OH functional groups on the material surface induce the nucleation of apatite crystals that grow spontaneously. The structure of the hydroxyapatite layer formation is similar to the mineral component of bone and provides a focus for the attachment and proliferation of new bone-forming cells [8–10].

Kokubo et al [10] developed a cellular simulated body fluid (SBF) which contains ion concentrations similar to those of human plasma in order to reproduce formation of apatite on bioactive materials in vitro. The hydroxyapatite layer formation on the material surface within 4 weeks of exposure to SBF in vitro gives an indication that the material is bioactive and will form a bond with living tissue.

A range of calcium silicate based materials are currently being investigated for their potential use in dental and bone-contact applications [11–14]. Previous research [15] has demonstrated the in vitro bioactivity of the calcium sulphate hemihydrate-tricalcium silicate composite bone cement. Huan and Chang [15] reported that silicate species could play an important role in forming hydroxyapatite in the simulated body environment and the formation of a homogeneous apatite layer on the material surface was dependent on the presence of tricalcium silicate.

For the past decade, mineral trioxide aggregate (MTA), consisting of 80% wt white Portland cement and 20% wt bismuth oxide, has been used as a root repair material in dentistry [16–22]. It was found that MTA shows bioactivity and clinical success in the sealing of connections between the root canal system and the surrounding tissues. In spite of the increasing potential clinical applications, the bioactivity of cement based material in SBF is barely known. Accordingly, the bioactivity of ordinary Portland cement and white Portland cement in vitro was carried out in SBF in

order to determine whether they form hydroxyapatite. The pH values of the SBF solutions containing both cements was also measured. In the addition, the setting and mechanical properties of both types of Portland cement were investigated.

MATERIALS AND METHODS

Preparation and characterization

Ordinary Portland cement (OPC) and white Portland cement (WPC) used in this investigation were produced by Siam Cement Public Company Limited. Cement paste samples were prepared in a polypropylene beaker with sterile distilled water at a water to cement ratio of 0.5 by mass. In each case, 50 g of cement was manually blended with 25 g of sterile distilled water using a polypropylene spatula. The specimens were then cast into a rubber mould (10 mm in diameter and 2 mm in height), sealed with plastic wrap, and cured at 23 ± 2 °C for 24 h. After curing, the sample were removed from the rubber moulds and their chemical compositions were determined at the Electron Microscopy Research and Service Centre of Chiang Mai University using low vacuum SEM with a JEOL JEM-5910LV microscope linked to an energy dispersive X-ray analyser (EDX).

Setting time of the OPC and WPC paste

The time of setting of Portland cement paste was determined using a Vicat needle according to ASTM C191-99[23]. The apparatus consisted of a movable rod (300 g, 10 mm in diameter) and a steel needle (1 mm diameter, 50 mm length). Portland cement powder (650 g) was mixed with the amount of distilled water required for normal consistency[24]. After mixing, a ring mould filled with the cement sample was placed on a base plate and the excess paste at the top of the mould was removed. A steel needle was plunged into the Portland cement paste every 10 min. The initial setting time is determined as the time necessary to achieve a penetration of 25 mm and the final setting time as the total time when the needle does not sink into the paste.

Compressive strength of the OPC and WPC paste

The compressive strength of the test materials was determined according to ASTM D695-91[25]. Portland cement powder was mixed with water using a constant water to cement ratio (W/C) of 0.5, and the mixture was cast in a cylindrical mould (6 mm diameter $\times$ 10 mm high). After setting for 24 h, the specimens were removed from the moulds and were cured in a water bath at 37 °C. The compressive strengths of the samples were measured at 1, 3, and 7 days using Hounsfield test equipment (H10KS-0407) at a loading rate of 0.5 mm/min. The reported results are the averages of five specimens.

Bioactivity in vitro and dissolution

Simulated body fluid (SBF) was prepared according to the procedure described by Kokubo[10]. The ion concentrations of the SBF solution are similar to those in human blood plasma. OPC and WPC paste disks at 1 day (10 mm in diameter and 2 mm in height) were immersed in the SBF solution in hermetically sealed polypropylene containers under sessile conditions at 37 °C for 7 days with a surface area-to-volume ratio of 0.1 cm^{-1} [26]. The pH values of SBF liquid were measured at 1, 3, and 7 days using an electrolyte-type pH meter (Ringer Ω Metrom 713 pH Meter). After 7 days, the disc specimens were removed from the SBF solution, gently rinsed with deionized water, and dried in air at room temperature. The surface morphologies and crystalline phase of the OPC and WPC paste discs after immersion in SBF were determined by SEM (JEOL JEM-5910LV) and X-ray diffraction (Philips PW-1729).

RESULTS

Characterisation of OPC and WPC before immersing in SBF

SEM characterization of the surface of OPC and WPC paste after setting for 1 day has demonstrated that the surfaces of the samples, taken as-cast from the mould before immersing in SBF, were smooth (Fig. 1). An EDX spectrum of OPC and WPC surface confirms the presence of the main elemental constituents which are calcium, silicon, aluminium, and oxygen (Fig. 2).

Setting time and compressive strength of Portland cement paste

It can be seen that the setting time of WPC was noticeably faster than that of OPC (Fig. 3). The results show that the initial and final setting times of OPC were 134 and 190 min respectively and that of WPC were 130 and 170 min respectively.

The compressive strength of WPC and OPC pastes after storage in a 100% humidity water bath at 37 °C for 1, 3, and 7 days is shown in Fig. 4. The result indicated that the compressive strength of Portland cement paste increased with increasing curing period and there was no significant difference between OPC and WPC paste specimens. In the addition, after 7 days of curing in distilled water at human body temperature, OPC and WPC paste specimens achieved

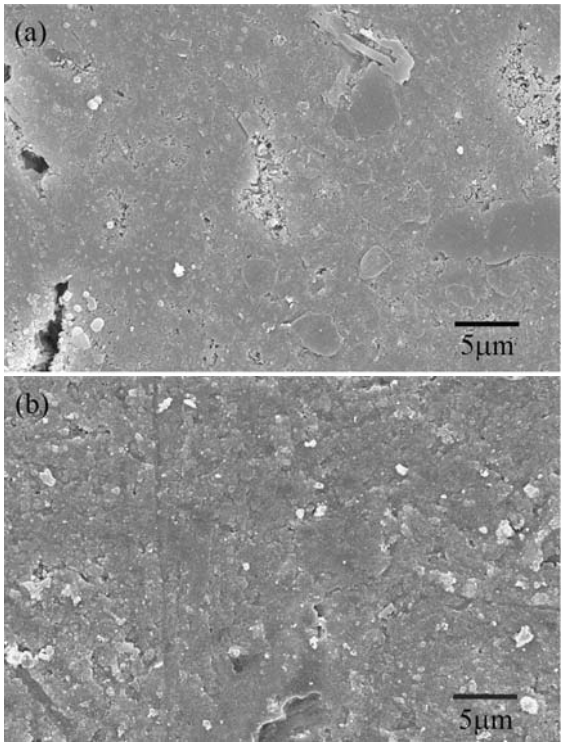

Fig. 1 SEM micrographs of the surface of (a) OPC paste disc and (b) WPC paste disc after setting for 1 day.

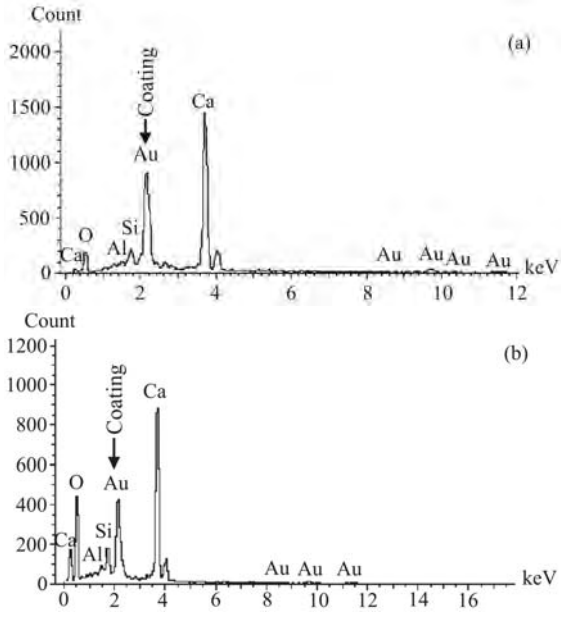

Fig. 2 EDX spectrum of (a) OPC paste disc surface (b) WPC paste disc surface after setting for 1 day.

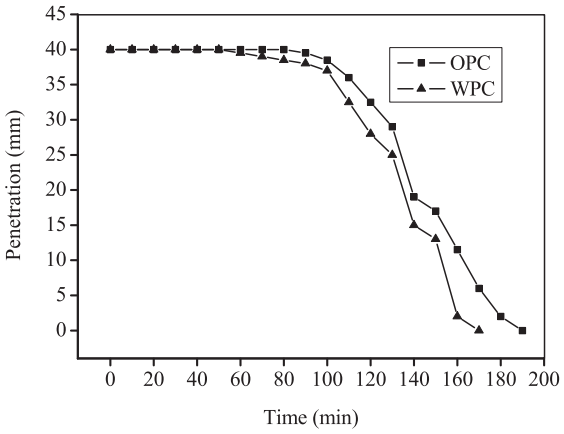

Fig. 3 The initial and final setting times of OPC and WPC paste samples.

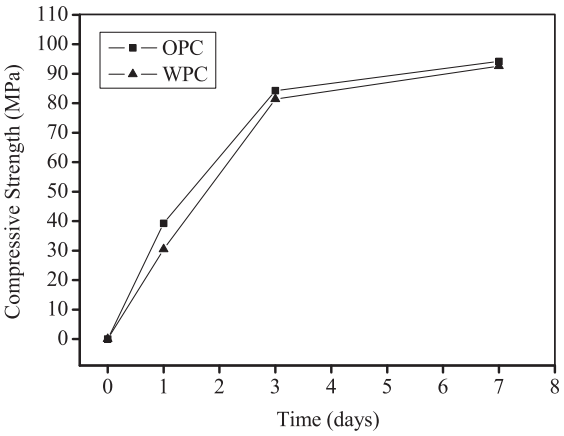

Fig. 4 The compressive strengths of OPC and WPC paste specimens at various times.

compressive strength of 94.2 MPa and 92.6 MPa respectively.

Dissolution characteristics

After 1 week of contact with an OPC paste disc with a surface area-to-volume ratio of 0.1 cm^{-1}, the pH of SBF increased from 7.25 to 9.25 (Fig. 5). In the case of WPC the pH of SBF increased to 9.06.

Bioactivity in vitro

The SEM analyses of the paste disc surfaces following immersion in SBF solution for 7 days are shown in Fig. 6. Formation of hydroxyapatite was only observed on the WPC surface. The surface of WPC after reaction with SBF is seen to support a particle deposit of similar morphology to the apatite layer reported to

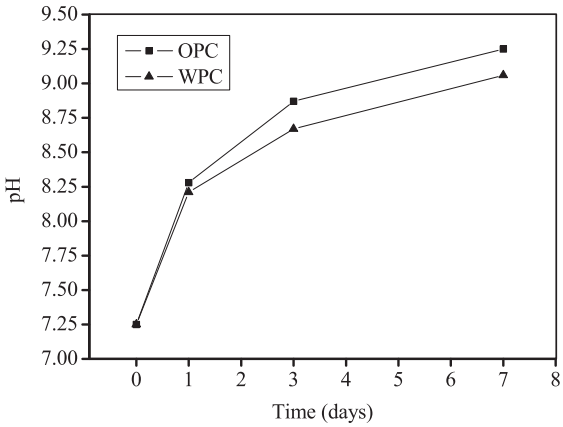

Fig. 5 pH of simulated body fluid after 7 days of exposure to OPC and WPC paste discs.

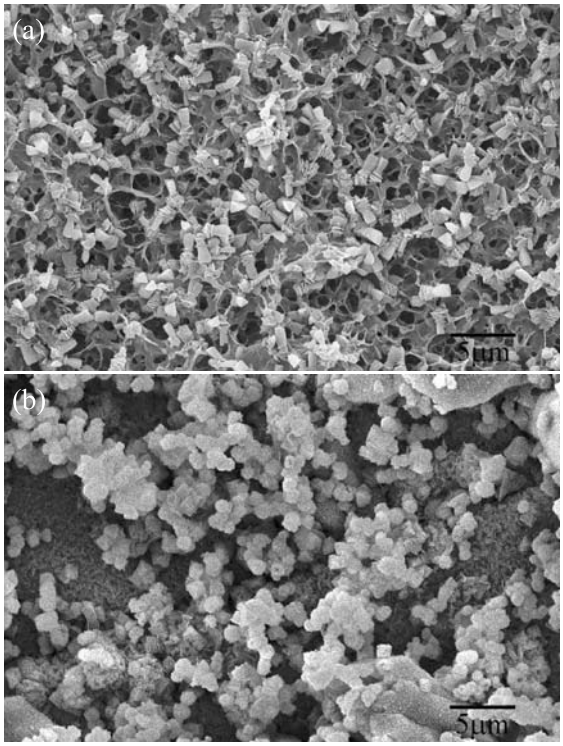

Fig. 6 SEM micrographs of the surface of (a) OPC paste disc and (b) WPC paste disc following immersion in SBF solution for 7 days.

form on bioactive material[27–29]. The higher magnification SEM micrograph shows that small particles of an apatite formed as agglomerates (Fig. 7). An EDX spectrum of the surface of OPC and WPC paste following a residence time of 7 days in SBF is shown in Fig. 8. The spectrum demonstrates that phosphorus

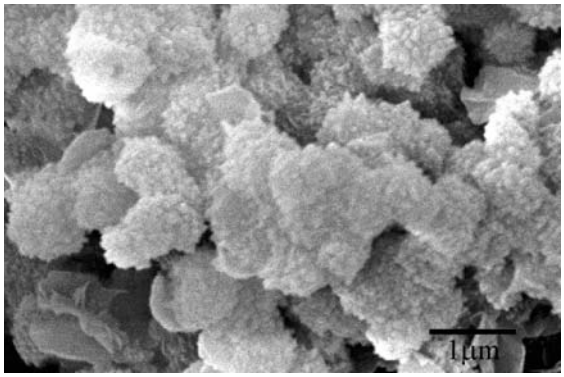

Fig. 7 High magnification SEM micrograph of hydroxyapatite on WPC paste surface.

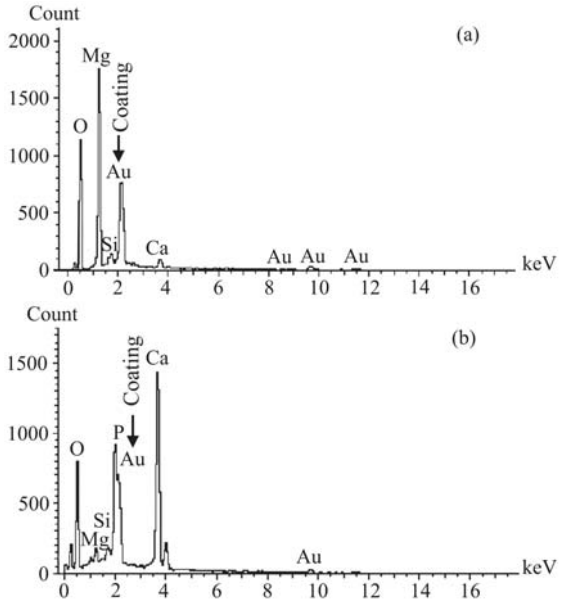

Fig. 8 EDX spectrum of (a) OPC (b) WPC paste disc surfaces following immersion in SBF solution for 7 days.

was present in the WPC paste after immersion but this was not observed for the OPC paste. Elemental mapping also shows that WPC surface had a high concentration of P (Fig. 9). These results confirm the formation of an apatite layer on the surface of WPC paste disc after immersion in SBF solution[30].

The X-ray diffraction (XRD) of the samples after immersion in SBF is shown in Fig. 10. The XRD pattern of OPC and WPC paste discs showed characteristic peaks of hydroxyapatite at $2\theta = 25.9$, 31.8, 32.9, and 34.1. On account of the larger peak for WPC at 31.8, it can be inferred that WPC induces a larger amount of apatite crystal.

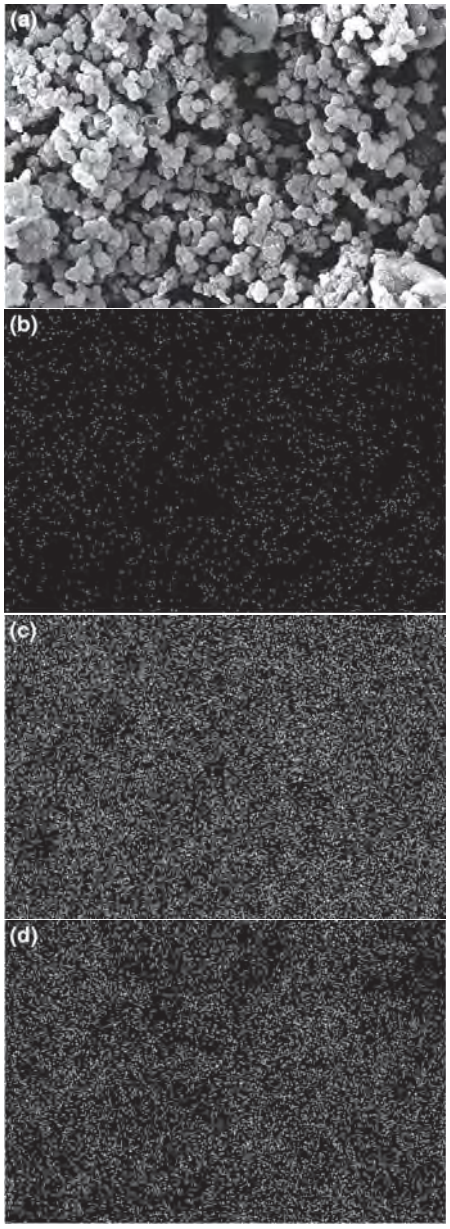

Fig. 9 (a) Hydroxyapatite crystals precipitated on WPC paste surface; distribution of (b) silicon (c) calcium (d) phosphorous.

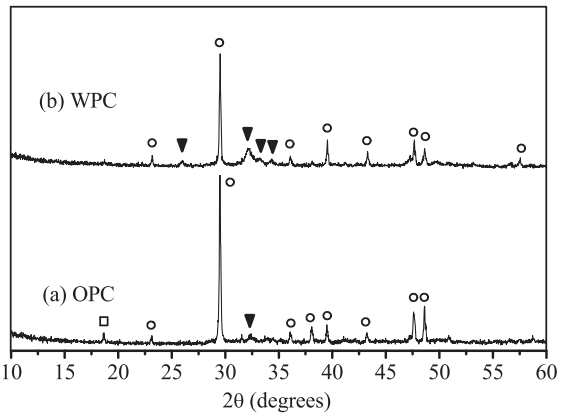

Fig. 10 XRD data for paste disc surface of (a) OPC (b) WPC after immersion in SBF for 7 days. □ calcium hydroxide; ○ calcium carbonate; ▼ hydroxyapatite.

DISCUSSION

Calcium phosphate cement has been successfully used in clinics as bone repair biomaterial for many years[31–36]. However, poor mechanical properties limit any further applications[37–39]. In this study, both OPC and WPC pastes can achieve a compressive strength more than 25 MPa within 24 h after curing in a water bath at 37 °C. With a high initial strength, OPC and WPC may be beneficial for clinical applications that require a certain high initial strength in the first stage of implantation. Portland cement mainly consists of tricalcium silicates, C_3S, and dicalcium silicates, C_2S, which react with water during the hydration[40].

On hydrating the cement, calcium silicate hydrate (CSH) and calcium hydroxide are produced. These provide strength and alkalinity to the material, respectively[40]. As time proceeds, the CSH phase formation increases giving a denser and more homogeneous cement matrix. This results in the formation of a solid network which affords a moderate increase in the mechanical strength and densification. The decrease in the initially high porosity is due to the formation of hydration products. In this study, when Portland paste disc was immersed in SBF solution, calcium hydroxide is leached from the Portland cement matrix. The released OH^- ions are partially buffered and cause a moderate increase in pH from 7.25 to approximately 9.

Bioactivity is shown by the formation of a hydroxyapatite layer on the surface of a material after immersion in SBF solution[3]. The Si-OH functional groups on the surface of silicate material, such as silicate glasses and ceramics, have been shown to act as nucleation centres for hydroxyapatite precipitation[3,41,42]. Recent research has shown that an increase in the super saturation of Ca^+ is not sufficient to promote the formation of new crystals of hydroxyapatite on the material surface in the SBF environment[43,44] and the formation of this homogeneous hydroxyapatite layer is dependent on the content of silicate material[15]. This explains why OPC shows lower intensity peak of

hydroxyapatite than WPC. When OPC is immersed in SBF, silicate ions are likely to concentrate around the CSH gel, and thus the formation of apatite crystal is limited in the CSH[15]. This may be due to the lower proportion of silicate species in OPC compared to WPC. Hence, it is thought that the deposition of hydroxyapatite layer onto the Portland cement paste surface is attributed to both the dissolution of calcium hydroxide and to the high proportion of preexisting Si-OH nucleation sites presented by the nanoporous calcium silicate hydrate gel structure. However, evidence of apatite formation on the OPC surface was not observed in the SEM micrograph. This may be because a very low amount of apatite cannot be detected by an SEM. Accordingly, the results of the XRD, SEM, and EDX analysis show that WPC paste, following immersion in SBF solution, can induce hydroxyapatite precipitation on the material surface within 7 days. This finding confirms the established bioactivity of the WPC paste.

Our study has indicated that the likely mechanism of bonding between WPC paste and viable bone tissue is the spontaneous formation of an intermediate layer of hydroxyapatite on contact with human plasma. However, as a material containing a large amount of calcium hydroxide, which is known to produce a pH of around 12.4 when in contact with water, the hydrated cement paste may induce cytotoxicity[45]. Such a result has been found in previous studies on biocompatibility and cytotoxicity of calcium hydroxide based root canal sealers[46,47]. Further research is now warranted to establish the biocompatibility and cytotoxicity properties to confirm the stimulatory effect of WPC for use in orthopaedic surgery.

Acknowledgements: Financial support from the Thailand Research Fund through the Royal Golden Jubilee PhD Program (Grant No. PHD/0281/2550) is acknowledged. The authors also gratefully acknowledged the Thailand Research Fund for Research Career Development Grant to the second author. The Graduate School of Chiang Mai University is acknowledged for additional support.

REFERENCES

1. Hench LL, Anderson Ö (1993) Bioactive glasses. In: Hench LL, Wilson J (eds) *An Introduction to Bioceramics*, World Scientific, Singapore, pp 41–6.
2. Hence LL, West JK (1996) Biological applications of bioactive glasses. *Life Chem Rep* **13**, 187–241.
3. Kokubo T (1992) Bioactivity of bioglasses and glass ceramics. In: Ducheyne P, Kokubo T, Blitterswijk CA (eds) *Bone-bonding Biomaterials*, Leidendorp, Reed Healthcare Communications, pp 31–46.
4. Hench LL (1997) Sol-gel materials for bioceramic application. *Curr Opin Solid State Mater Sci* **2**, 604–10.
5. Portera AE, Patela N, Skepperb JN, Besta SM, Bonfielda W (2003) Comparison of in vivo dissolution processes in hydroxyapatite and silicon-substituted hydroxyapatite bioceramics. *Biomaterials* **24**, 4609–20.
6. Cao W, Hench LL (1996) Bioactive Materials. *Ceram Int* **22**, 493–507.
7. Hench LL (1998) Biomaterials: a forecast for the future. *Biomaterials* **19**, 1419–23.
8. Kotani S, Fujita Y, Kitsugi T, Nakamura T, Yamamuro T (1991) Bone bonding mechanism of β-tricalcium phosphate. *J Biomed Mater Res* **25**, 1303–15.
9. Fujita Y, Yamamuro T, Nakamura T, Kotani S (1991) The bonding behaviour of calcite to bone. *J Biomed Mater Res* **25**, 991–1003.
10. Kokubo T, Takadama H (2006) How to useful is SBF in predicting in vivo bone bioactivity? *Biomaterials* **27**, 2907–15.
11. Ribeiro DA, Duarte MH, Matsumoto MA, Marques MA, Salvadori DF (2006) Biocompatibility In Vitro Tests of Mineral Trioxide Aggregate and Regular and White Portland Cements. *J Endod* **31**, 605–7.
12. Giovanna GM, Silvia F, David P, Gasparotto G, Carlo P (2008) Calcium silicate coating derived from Portland cement as treatment for hypersensitive dentine. *J Dent* **36**, 565–78.
13. Saidon J, He J, Zhu Q, Safavi K, Spångberg LSW (2003) Cell and tissue reactions to mineral trioxide aggregate and Portland cement. *Oral Surg Oral Med Oral Pathol Oral Radiol Endod* **95**, 483–9.
14. D, Abdullah Pitt Ford TR, Papaioannou S, J, Nicholson McOnald F (2002) An evaluation of accelerated Portland cement as a restorative material. *Biomaterials* **23**, 4001–10.
15. Huan Z, Chang J (2007) Self-setting properties and in vitro bioactivity of calcium sulfate hemihydrate-tricalcium silicate composite bone cements. *Acta Biomaterialia* **3**, 952–60.
16. Holland R, de Souza V, Nery MJ, Filho JAO, Bernabe PFE, Dezan E (1999) Reaction of dogs' teeth to root canal filling with mineral trioxide aggregate or a glass ionomer sealer. *J Endod* **25**, 728–30.
17. Hachmeister DR, Schindler WG, Walker WA, Thomas DD (2002) The sealing ability and retention characteristics of mineral trioxide aggregate in a model of apexification. *J Endod* **28**, 386–90.
18. Saidon J, He J, Zhu Q, Safavi K, Spångberg LSW (2003) Cell and tissue reactions to mineral trioxide aggregate and Portland cement. *Oral Surg Oral Med Oral Pathol Oral Radiol Endod* **95**, 483–9.
19. Valois CRA, Costa ED (2004) Influence of the thickness of mineral trioxide aggregate on sealing ability of root-end fillings in vitro. *Oral Surg Oral Med Oral Pathol Oral Radiol Endod* **97**, 108–11.
20. Martin RL, Monticelli F, Brackett WW, Loushine RJ, Rockman RA, Ferrari M, Pashley DH, Tay FR (2007)

Sealing properties of mineral trioxide aggregate orthograde apical plugs and root fillings in an in vitro apexification model. *J Endod* **33**, 272–5.
21. Boutsioukis C, Noula G, Lambrianidis T (2008) Ex vivo study of the efficiency of two techniques for the removal of mineral trioxide aggregate used as a root canal filling material. *J Endod* **34**, 1239–42.
22. Budig CG, Eleazer PD (2008) In vitro comparison of the setting of dry ProRoot MTA by moisture absorbed through the root. *J Endod* **34**, 712–4.
23. American Society for Testing Materials (2000) Standard test method for time and setting of hydraulic cement by Vicat needle, vol 04.01, Easton, USA, pp 179–81.
24. American Society for Testing Materials (2000) Standard test method for normal consistency of hydraulic cement, vol 04.01, Easton, USA, pp 175–6.
25. American Society for Testing Materials (1993) Standard test method for compressive properties of rigid plastics, vol 08.01, Easton, USA, pp 204–10.
26. Greenspan DC, Zhong JP, LaTorre GP (1994) Effect of surface area to volume ratio in vitro surface reactions of bioactive glass particulates. In: Andresson ŎH, Yli-Urpo A (eds) *Bioceramics* vol. 7, Turku, Finland, pp 55–60.
27. Zhao W, Wang J, Zhia W, Wang Z, Chang J (2005) The self-setting properties and in vitro bioactivity of tricalcium silicate. *Biomaterials* **26**, 6113–21.
28. Saboori A, Rabiee M, Moztarzadeh F, Sheikhi M, Tahriri M, Karimi M (2008) Synthesis, characterization and in vitro bioactivity of sol-gel-derived SiO_2–CaO–P_2O_5–MgO bioglass. *Mater Sci Eng C* **29**, 335–40.
29. Sun J, Li Y, Li L, Zhao W, Li L, Gao J, M, Ruan Shi J (2008) Functionalization and bioactivity in vitro of mesoporous bioactive glasses. *J Non Cryst Solids* **354**, 3799–805.
30. Salman SM, Salama SN, Darwish H, Abo-Mosallam HA (2008) In vitro bioactivity of glass–ceramics of the $CaMgSi_2O_6$–$CaSiO_3$–$Ca_5(PO_4)_3F$–Na_2SiO_3 system with TiO_2 or ZnO additives. *Ceram Int* **35**, 1083–93.
31. Ooms EM, Wolke JGC, van de Heuvel MT, Jeschke B, Jansen JA (2003) Histological evaluation of the bone response to calcium phosphate cement implanted in cortical bone. *Biomaterials* **24**, 989–1000.
32. Atsuro Y, Satoru Y, Takao KA, Takao KO, Masanori N (2002) Development of calcium phosphate cement using chitosan and citric acid for bone substitute materials. *Biomaterials* **23**, 1091–101.
33. Flautre B, Delecourt C, Blary MC, Van Landuyt P, Lemaître J, Hardouin P (1999) Volume effect on biological properties of a calcium phosphate hydraulic cement: experimental study in sheep. *Bone* **25**, 35S–9S.
34. Carey LE, Xu HHK, Simon CG, Takagi S, Chow LC (2005) Premixed rapid-setting calcium phosphate composites for bone repair. *Biomaterials* **26**, 5002–14.
35. Oreffo ROC, Driessens FCM, Planell JA, Triffitt JT (1998) Growth and differentiation of human bone marrow osteoprogenitors on novel calcium phosphate cements. *Biomaterials* **19**, 1845–54.
36. Gómez E, Martín M, Arias J, Carceller F (2005) Clinical applications of Norian SRS (calcium phosphate cement) in craniofacial reconstruction in children: Our experience at Hospital La Paz since 2001. *J Oral Maxillofac Surg* **63**, 8–14.
37. Gbureck U, Grolms O, Barraletb JE, Groverb LM, Thulla R (2003) Mechanical activation and cement formation of b-tricalcium phosphate. *Biomaterials* **24**, 4123–31.
38. Ratier A, Gibson IR, Best SM, Freche M, Lacout JL, Rodriguez F (2001) Setting characteristics and mechanical behaviour of a calcium phosphate bone cement containing tetracycline. *Biomaterials* **22**, 897–901.
39. Mariam Z, Anita L, Pierrette B, Jean G (2001) A self-setting single-component calcium phosphate cement. *Biomaterials* **22**, 1933–7.
40. Lea FM (1976) *The Chemistry of Cement and Concrete*, 3rd edn, Edward Arnold, London, pp 177–210.
41. Peitl O, Zanotto ED, Hench LL (2001) Highly bioactive P_2O_5-Na_2O-CaO-SiO_2 glass-ceramics. *J Non Cryst Solids* **292**, 115–26.
42. Jones JR, Ehrenfried LM, Hench LL (2006) Optimising bioactive glass scaffolds for bone tissue engineering. *Biomaterials* **27**, 964–73.
43. Nilsson M, Fernández E, Sarda S, Lidgren L, Planell JA (2002) Characterization of a novel calcium phosphate/sulfate bone cement. *J Biomed Mater Res* **61**, 600–7.
44. Cabañas MV, Rodríguez-Lorenzo LM, Vallet-Regí M (2002) Setting behavior and in vitro bioactivity of hydroxyapatite/calcium sulfate cements. *Chem Mater* **14**, 3550–5.
45. Gallego D, Higuita N, Garcia F, Ferrell N, Hansford DJ (2008) Bioactive coating on Portland cement substrate: Surface precipitation of apatite-like crystal. *Mater Sci Eng C* **28**, 347–52.
46. Leonardo RT, Consolaro A, Carlos IZ, Leonardo MR (2000) Evaluation of cell culture cytotoxicity of five root canal sealers. *J Endod* **26**, 328–30.
47. Al-Awadhi S, Spears R, Gutmann JL, Opperman LA (2004) Cultured primary osteoblast viability and apoptosis in the presence of root canal sealers. *J Endod* **30**, 527–33.

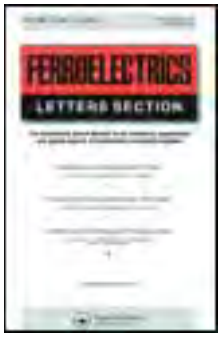

Ferroelectrics Letters Section
Publication details, including instructions for authors and subscription information:
http://www.tandfonline.com/loi/gfel20

Effect of Particle Size on the Dielectric Properties of Sodium Potassium Niobate -Portland Cement Composites

R. POTONG [a] , R. RIANYOI [a] , P. JARUPOOM [a] , K. PENGPAT [a] & A. CHAIPANICH [a]

[a] Department of Physics and Materials Science, Faculty of Science, Chiang Mai University, Chiang Mai, 50200, Thailand

Published online: 22 Sep 2009.

To cite this article: R. POTONG , R. RIANYOI , P. JARUPOOM , K. PENGPAT & A. CHAIPANICH (2009): Effect of Particle Size on the Dielectric Properties of Sodium Potassium Niobate -Portland Cement Composites, Ferroelectrics Letters Section, 36:3-4, 76-81

To link to this article: http://dx.doi.org/10.1080/07315170903152748

Ferroelectric Letters, 36:76–81, 2009

ISSN: 0731-5171 print / 1563-5228 online
DOI: 10.1080/07315170903152748

Effect of Particle Size on the Dielectric Properties of Sodium Potassium Niobate -Portland Cement Composites

R. POTONG, R. RIANYOI, P. JARUPOOM, K. PENGPAT, and A. CHAIPANICH*

Department of Physics and Materials Science, Faculty of Science, Chiang Mai University, Chiang Mai 50200, Thailand

Communicated by Dr. George W. Taylor

(Received April 1, 2009)

In this research, the effect of sodium potassium niobate, $(Na_{0.5}K_{0.5})NbO_3$ (NKN) particle size on the dielectric properties of 0-3 non lead based piezoelectric cement based composites were investigated. NKN of various particle sizes (75, 225 and 450 μm) were used at 50% by volume to produce the composites. Dielectric properties at various frequencies (0.1–20 kHz) were investigated. The results showed that the dielectric values of NKN-PC composites increased with increasing NKN particle size where ε_r at 1 kHz are 158.60 and 191.21 for composites with 75 μm and 450 μm NKN particle size respectively. The dielectric loss (tanδ) was found to reduce with increasing NKN particle size and the tan δ value was lowest at 0.39 for composite with 450 μm NKN particle size.

Keywords: NKN; Composites; Particle size; Dielectric Properties.

1. INTRODUCTION

Nowadays, the piezoelectric materials are widely used for capacitors and various application such as lead zirconate titanate (PZT) as it has excellent dielectric constant (ε_r) and piezoelectric coefficient (d_{33}) [1–4]. Cement based composites consisting of PZT have been developed for applications where the composites can be inserted into concrete structures to detect loading after they were fabricated [5–11]. Moreover, the use of such piezoelectric-cement

*Corresponding author. E-mail: arnon@chiangmai.ac.th

based composite would provide an advantage in the matching of structural concrete compared to other piezoelectric composites. However, lead oxide from processing of lead-based piezoelectric materials has high toxic and used of the lead-based materials has caused lead pollution and crucial environmental problems. Therefore, lead-free piezoelectric materials received attention from environmental protection. Recently, sodium potassium niobate, $NaKNbO_3$ (NKN) have begun to attract attention because of high piezoelectric coefficient (d_{33}) [12]. Dielectric measurements were first reported by Mathias and Remeika [13]. In addition, dielectric constant of $Na_{0.5}K_{0.5}NbO_3$ is 218.87 at 1 kHz and low dielectric loss by Kuldeep Singh et al. [14]. In this research, NKN-PC composite material was produced from sodium potassium niobate, $Na_{0.5}K_{0.5}NbO_3$ (NKN) with Portland cement of normal type (PC), commonly known as ordinary Portland cement to form 0-3 connectivity NKN-PC composites. The dielectric properties of the new composite material of lead-free piezoelectric materials, NKN, made with Portland cement were then investigated.

2. EXPERIMENTAL

$Na_{0.5}K_{0.5}NbO_3$ (NKN) ceramic of different median particle size (75 μm, 225 μm and 450 μm) were used. These NKN ceramic particles were then mixed with normal Portland cement (The American Society for Testing and Materials Type I cement) to produce 0-3 connectivity NKN-PC composite of 50:50 by volume using a hydraulic press to form disk samples of 15 mm diameter and 2 mm thickness. Thereafter, the composites were placed for curing at 60°C and 98 % relative humidity for 3 days before measurements. For measurement of the dielectric properties, silver paste electrodes were formed at the two surfaces of disk-shaped specimens. An impedance meter (Hewlett Packard 4194A) was use to obtain the capacitance and the dissipation factor ($\tan\delta$) of the composites at room temperature and at very frequency. The relative dielectric constant (ε_r) was the calculated from the following equation:

$$\varepsilon_r = \frac{Ct}{\varepsilon_0 A}$$

Where C is the sample capacitance, t is the thickness, ε_0 is the permittivity of free space constant (8.854×10^{12} Fm^{-1}), and A is the electron area.

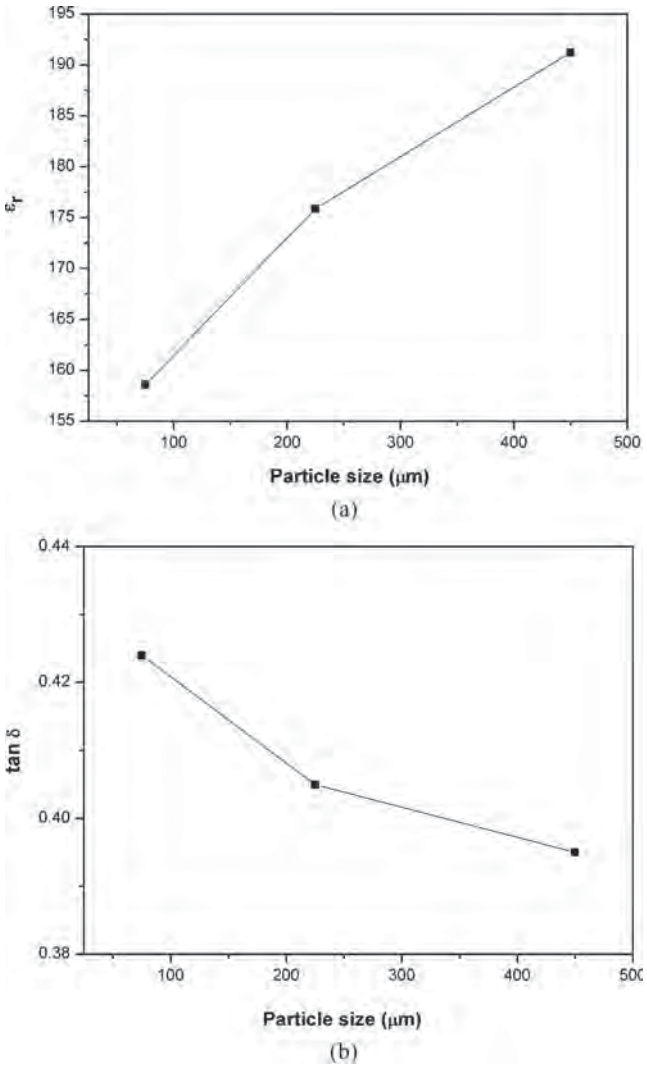

Figure 1. Effect of particle size on dielectric properties results of NKN-Portland cement composites (a) dielectric constant and (b) dielectric loss.

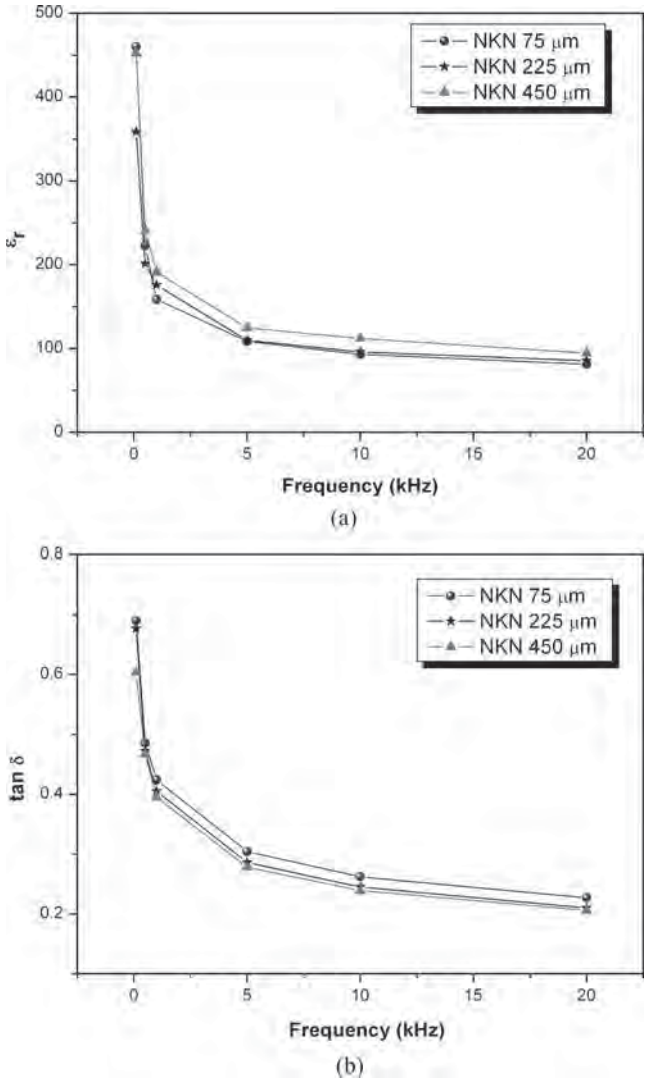

Figure 2. Effect of frequency on dielectric properties results of NKN-Portland cement (a) dielectric constant and (b) dielectric loss.

3. RESULTS AND DISCUSSION

The effect of NKN-PC composites on the dielectric constant (ε_r) is plotted against the NKN particle size in Fig. 1 (a) where the effect of NKN particle size on the dielectric constant can be seen. The dielectric constant of the composites can be seen to increase with increasing NKN particle size and that the dielectric constant was highest at 191.21 of 450 μm NKN particle size at 1 kHz.

Measured dielectric loss (tanδ) results of composites showing the effect of NKN particle size can be seen in Fig. 1 (b). The dielectric loss (tanδ) was found to reduce with increasing NKN particle size and the tan δ value at 1 kHz was lowest at 0.39 for composite at 450 μm NKN particle size.

At varying frequency, the effect of NKN-PC composites on the dielectric constant (ε_r) is shown against the frequency in Fig. 2 (a) where the effect of frequency on the dielectric constant can be seen. The dielectric constant of the composites can be seen to reduce with increasing frequency where 0.1 kHz and 20 kHz with dielectric constant = 452.31 and 94.24 for composites at 450 μm NKN particle size. In addition, the dielectric loss (tanδ) was found to reduce with increasing frequency where 0.1 kHz and 20 kHz with dielectric loss = 0.60 and 0.20 for composites at 450 μm NKN particle size. Moreover, the dielectric constant of the composites decrease sharply with increasing frequency and with an increasing frequency, some polarization, especially interfacial polarizations cannot follow the change of the electric field due to lengthy time for the construction of space charge polarization. The result, dielectric constants are lower at high frequency [15].

Furthermore, from the above results, high dielectric constant (ε_r) and low dielectric loss (tanδ) of 0-3 NKN-Portland cement composites were obtained with a particle size of NKN as large as 450 μm using the method described.

4. CONCLUSIONS

The results showed that the dielectric properties of 0-3 NKN-Portland cement composites reduced with increasing frequency. The dielectric constant (ε_r) was found to increase with increasing NKN particle size. Moreover, particle size of NKN ceramic as large as 450 μm can be produced and it gave the highest dielectric values (ε_r = 191.21). The dielectric loss (tanδ) was found to reduce with increasing NKN particle size and the tan δ value was lowest at 0.39 for composite at 450 μm NKN particle size. At varying

frequency, the dielectric constant and dielectric loss of the composites was found to reduce with increasing frequency.

ACKNOWLEDGMENTS

The authors are grateful to members of staff at the Electroceramics Research Laboratory for the research facilities made possible for this research work and also to the Thailand Research Fund (TRF)and the Commission on Higher Education (Thailand) for financial support.

REFERENCES

[1] S. T. Lau, K.W. Kwok, H. L. W. Chan, and C. L. Choy, Piezoelectric Composite Hydrophone Array. *Sens. Actuators A.*, **96**, 14–20 (2002).
[2] R. E. Newnham and A. Amin, Smart systems: Microphones, fish farming, and beyond—Smart materials, acting as both sensors and actuators, can mimic biological behavior. *Chem. Tech.* **29**, 38–47 (1999).
[3] R. Ranjan, R. Kumar, B. Behera, and R. N. P. Choudhary, Effect of Sm on structural, Dielectric and conductivity properties of PZT ceramics. *Mater Chem Phys.* **115**, 473–477 (2009).
[4] J. F. Tressler, S. Alkoy, and R. E. Newnham, *J. Electroceram: Piezoelectric Sensors and Sensor Materials*. **2**, 257–272 (1998).
[5] N. Jaitanong and A. Chaipanich, Effect of polling temperature on piezoelectric properties of 0-3 PZT-Portland cement composite. *Ferr. Lett.* **35**, 17–23 (2008).
[6] A. Chaipanich and N. Jaitanong, Effect of polling time on piezoelectric properties of 0-3 PZT-Portland cement composite. *Ferr. Lett.* **35**, 73–78 (2008).
[7] Z. Li, D. Zhang, and K. Wu, J. Am., Cement-Based 0-3 piezoelectric composites. *Ceram. Soc.* **85**, 305–313 (2002).
[8] S. Huang, J. Chang, R. Xu, F. Liu, L. Lu, Z. Ye, and X. Cheng, Piezoelectric properties of 0-3 PZT/sulfoaluminate cement composites. *Smart Mater. Struct.* **13**, 270–274 (2004).
[9] Z. Li, B. Dong, and D. Zhang, Influence of polarization on properties of 0–3 cement-based PZT composites. *Cem. Concr. Compos.* **27**, 27–32 (2005).
[10] B. Dong and Z. Li, Cement-based piezoelectric ceramic smart composites. *Compos. Sci. Technol.* **65**, 1363–1371 (2005).
[11] C. Xin, S. Huang, C. Jun, X. Ronghua, L. Futian, and L. Lingchao, Piezoelectric and dielectric properties of piezoelectric ceramic–sulphoaluminate cement composites. *J. Eur. Ceram. Soc.* **25**, 3223–3228 (2005).
[12] Y. Saito, H. Takao, T. Tani, T. Nonoyama, K. Takatori, T. Homma, T. Nagaya, and M. Nakamura, Lead-free piezoceramics, *Nature*, **43**, 84–87 (2004).
[13] B. T. Mathias and J. Remeika, Dielectric Properties of Sodium and Potassium Niobates. *Phys. Rev.* **82**, 727–729 (1951).
[14] K. Singh, V. Lingwal, S. C. Bhatt, N. S. Panwar, and B. S. Semwal, Dielectric properties of potassium sodium niobate mixed system. *Mater. Res. Bull.* **36**, 2365–2374 (2001).
[15] C. Xin, S. Huang, C. Jun, and L. Zongjin, Piezoelectric, dielectric, and ferroelectric properties of 0-3 ceramic/cement composite. *J. Appl. Phys.* 101 (2007)

Appl Phys A (2011) 104:661–666
DOI 10.1007/s00339-011-6307-2

Applied Physics A
Materials Science & Processing

Dielectric, ferroelectric and piezoelectric properties of 0-3 barium titanate–Portland cement composites

R. Rianyoi · R. Potong · N. Jaitanong · R. Yimnirun · A. Chaipanich

Received: 9 July 2010 / Accepted: 14 January 2011 / Published online: 5 February 2011

Abstract In this work, barium titanate (BT) and cement composites of 0-3 connectivity were produced with BT concentrations of 30%, 50% and 70% by volume using the mixing and pressing method. The dielectric constant (ε_r) and the dielectric loss ($\tan\delta$) at room temperature and at various frequencies (0.1–20 kHz) of the ferroelectric BT-Portland cement composites with different BT concentrations were investigated. The results show that the dielectric constant of BT-PC composites was found to increase as BT concentration increases, and that the highest value for ε_r—of 436—was obtained for a BT concentration of 70%. In addition, the dielectric loss tangent decreased with increasing BT concentration. Moreover, several mathematical models were used; the experimental values of the dielectric constants are closest to those calculated from the cube model. The 0-3 cement-based piezoelectric composites show typical ferroelectric hysteresis loops at room temperature. The *instantaneous* remnant polarization (P_{ir}), at an applied external electrical field (E_0) of 20 kV/cm (90 Hz) of 70% barium titanate composite, was found to have a value ≈3.42 μC/cm^2. Furthermore, the piezoelectric coefficient (d_{33}) was also found to increase as BT concentration increases, as expected. The highest value for d_{33} was 16 pC/N for 70% BT composite.

R. Rianyoi · R. Potong · N. Jaitanong · A. Chaipanich (✉)
Department of Physics and Materials Science, Faculty of Science, Chiang Mai University, Chiang Mai 50200, Thailand
e-mail: arnonchaipanich@gmail.com
Fax: +66-53-943445

R. Yimnirun
School of Physics, Institute of Science, Suranaree University of Technology, Nakhon Ratchasima 30000, Thailand

1 Introduction

In civil engineering, the cement-based material, concrete, is the most commonly used structural material. For many important engineering structures and infrastructure—such as high-rise buildings, large-span bridges, nuclear waste containment structures, etc.—severe vibration and significant internal damage may be caused by dynamic loading from different sources, such as strong winds or earthquakes [1]. This can pose a great threat to the safety of the structures. Therefore, structural health monitoring and active vibration control of structures have attracted much attention among civil engineers [2, 3].

Sensors and actuators are essential components for sensing and controlling. Among the techniques used in sensors and actuators, piezoelectricity has proved to be one of the most efficient mechanisms for application in smart structures [4–6]. Piezoelectric ceramics exhibit high dielectric constant and piezoelectric strain coefficient, and they can be used in a number of applications such as capacitors, transducers, sensors and actuators [7–9]. One of the most well-known and widely used piezoelectric ceramics is lead zirconate titanate (PZT). However, its relatively heavy density, high acoustic impedance, brittleness, and inconvenient machinability may render it undesirable for civil engineering purposes, due to the distinct differences in the properties between the smart materials and the concrete [10–12]. For example, single-phase piezoelectric ceramics exhibits high acoustic impedance (30 MRayl) compared to that of concrete (9 MRayl) [1]. To meet civil engineering structural requirements, lead-based electroceramic materials such as PZT have been used with cement in order to produce composites that can match the acoustic impedance of concrete structures [13–24]. However, lead-based electroceramic materials are highly toxic due to their lead oxide content, and

have caused concern because of pollution and environmental problems. Barium titanate $BaTiO_3$ (BT) was one of the first ferroelectric ceramics developed, and can be used in a variety of applications due to its excellent dielectric, ferroelectric and piezoelectric properties [25]. Barium titanate has a dielectric constant (ε_r) of ≈1000–2000, and low dielectric loss, and it has been used for multilayer capacitors, heaters, piezoelectric transducers, ferroelectric thin-film memories, etc. [26–29]. Furthermore it is a lead-free electroceramic material, and therefore still has attracted a great deal of attention [28, 30-32]. Rao et al. [30] recently worked on a polymer-ceramic composite, which consisted of a (85% by volume) barium titanate ceramic and epoxy matrix, where the composite had a dielectric constant value of 150. Liu et al. [31] also reported that when a polyimide/barium titanate composite with 50 vol% of $BaTiO_3$ was prepared via an in situ process, its dielectric constant reached 45 at 1 kHz. In addition, Kuo et al. [32] reported that a self-synthesized $BaTiO_3$/epoxy composite has the best dielectric property, with a dielectric constant of 44 at a ceramic composition of 40 vol%.

Therefore, barium titanate was chosen to develop lead-free piezoelectric cement-based composites because it exhibits high dielectric and piezoelectric properties, and is an environmentally friendly material. Barium titanate (BT) was mixed with Portland cement (PC) to form BT-PC composite material. Portland cement is chosen since it is the mostly used cement to produce concrete, and concrete is the most commonly used structural material. A preliminary investigation of the 0-3 connectivity properties—dielectric, ferroelectric hysteresis, and piezoelectric properties—of BT-PC composite materials is reported in this paper.

2 Experimental procedure

Barium titanate, $BaTiO_3$ (BT), powder was initially produced from the two-stage mixed oxide method using $BaCO_3$ and TiO_2. The starting powders were weighed and mixed (ball-milled) for 24 h using alumina balls in methanol alcohol as a grinding medium. BT ceramics were then produced by calcining the powder at 1,200°C and sintering at 1,400°C. BT ceramic particles were then mixed with normal Portland cement (American Society for Testing and Materials, type I cement) to produce 0-3 connectivity BT-PC composites using BT volume concentrations of 30%, 50% and 70%. This was performed under a hydraulic press at 80 MPa for 10 s to form disk samples of 15 mm diameter and 2 mm thickness. Thereafter, the composites were cured at 60°C and 98% relative humidity for 3 d before measurement. Density and porosity of the composites were measured using the Archimedes method. The densities of the composite samples were 3221 kg/m^3, 3833 kg/m^3 and 4403 kg/m^3 for composites with BT of 30%, 50% and 70% by volume, respectively; while the porosities of the composite samples were 8.52%, 9.22% and 9.30% for composites with BT of 30%, 50% and 70% by volume, respectively. These trends of porosity agree with the results reported for the case of 0-3 piezoelectric ceramic (P(LN)ZT)/sulphoaluminate cement composites by C. Xin et al. [1]. Phase characterizations were carried out by means of scanning electron microscopy (SEM; JEOL JSM-840A). For measurement of the dielectric properties, silver paste electrodes were painted onto the two surfaces of disk-shaped specimens. An impedance meter (Hewlett Packard 4194A) was used to obtain the capacitance and the dissipation factor ($\tan\delta$) of the composites at room temperature and at various frequencies (0.1–20 kHz). The relative dielectric constant (ε_r) was then calculated from the following equation:

$$\varepsilon_r = \frac{Ct}{\varepsilon_0 A} \tag{1}$$

where C is the sample capacitance, t is the thickness, ε_0 is the permittivity of the free space constant (8.854×10^{-12} F m^{-1}), and A is the electrode area.

A conventional Sawyer-Tower circuit was used to measure the room temperature ferroelectric hysteresis (P–E) loops at 90 Hz. The most important and difficult step for fabrication of piezoelectric materials is poling, especially for piezoelectric composites. A low voltage cannot fully activate the piezoelectricity of the materials, while a voltage that is too high can break down the sample. In our study, poling of the composites was carried out under a poling field of 1 kV/mm for 45 min in silicone oil at 80°C. The piezoelectric coefficient (d_{33}) was then measured using a piezometer PM25 d_{33} testing system (Take Control, Birmingham, UK) 24 h after poling.

3 Results and discussion

In Fig. 1, the scanning electronic microscopy (SEM) image of BT-PC composite (50% BT) shows a typical microstructure at the interfacial zone between the BT ceramic particles and the cement matrix where BT ceramic can be seen next to cement hydration products such as ettringite and calcium silicate hydrates. Grains of BT ceramics can be seen clearly surrounded by the cement matrix, suggesting good interaction between the two materials.

The dielectric constant results (ε_r) of the composites plotted against frequency are shown in Fig. 2, and the variation of the dielectric loss ($\tan\delta$) of the composites with frequency is shown in Fig. 3. It can be seen from Fig. 2 that the dielectric constant of the composites decreases with increasing frequency.

The calculated dielectric constant (ε_r) is shown against the BT volume concentration at a frequency of 1 kHz in

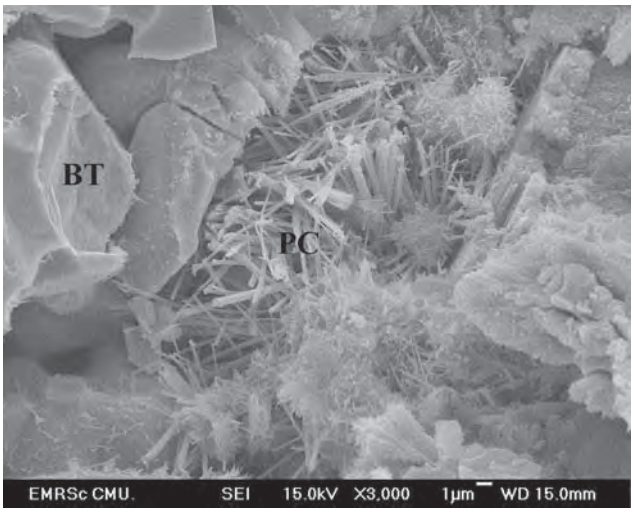

Fig. 1 SEM image of composite with 50% BT

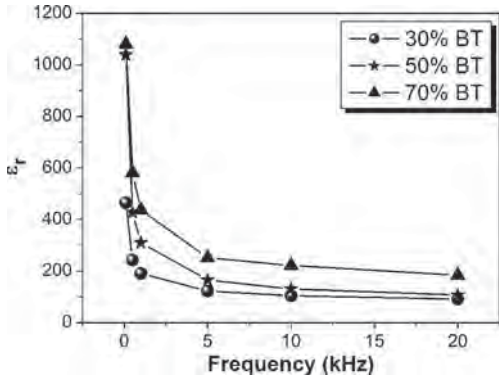

Fig. 2 Dielectric constant (ε_r) as a function of frequency of BT-Portland cement composites

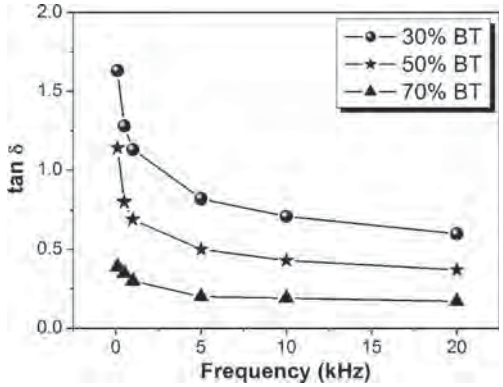

Fig. 3 Dielectric loss ($\tan\delta$) as a function of frequency of BT-Portland cement composites

Fig. 4, where the effect of BT can be observed. The dielectric constant can be seen to increase with increasing BT concentrations of 190 and 436 with composites of 30 and 70 vol%, respectively. On the other hand, the dielectric loss ($\tan\delta$) was found to be reduced with increasing BT concentration, in agreement with the dielectric constant results due to the direct influence of BT ceramic (Fig. 5). A noticeably lower $\tan\delta$ value was obtained for BT composite of 70% ($\tan\delta = 0.30$) when compared to a composite with higher cement content (BT = 30%).

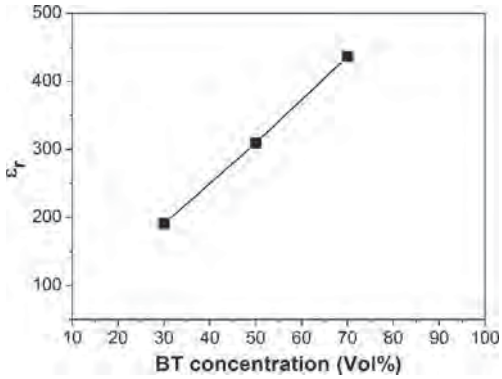

Fig. 4 Influence of BT concentration on the dielectric constant at a frequency of 1 kHz of BT-Portland cement composites

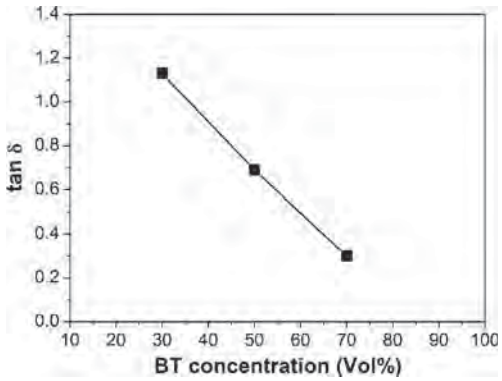

Fig. 5 Influence of BT concentration on the dielectric loss at a frequency of 1 kHz of BT-Portland cement composites

In comparison, it is interesting to note that the dielectric constant (ε_r) of BT-PC composites with 50 vol% of $BaTiO_3$ is 309 at 1 kHz, and that the value is higher than the dielectric constant of polyimide/barium titanate composite with 50 vol% of $BaTiO_3$ ($\varepsilon_r \approx 45$ at 1 kHz) [31]. The higher dielectric constant of BT-PC composites may be attributed to the effect of sum properties of two-phase [33]; this may be because of the high dielectric constant of BT ($\varepsilon_r = 936$). Furthermore, the dielectric constant and dielectric loss (at 1 kHz) for PC, BT and polyimide are shown in Table 2.

In the present work, three models—parallel (Voigt [35]), series (Reuss [36]) and cube (Banno [37])—were compared to evaluate the experimental results for the dielectric constants of the 0-3 BT Portland cement composites. The parallel and series mixing models represent extreme cases where the models are of alternating layers of each phase, perpendicular and parallel to an applied field, respectively. The cube mixing model characterizes a combined case of paral-

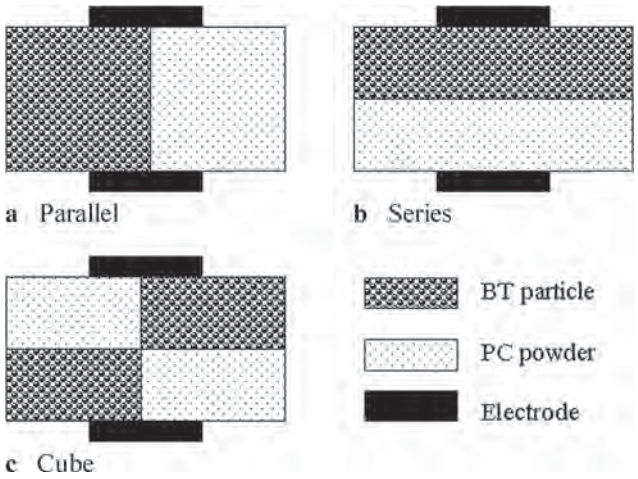

Fig. 6 Schematic configurations of parallel, series and cube models for BT-PC composites

lel and series mixing. The schematic configurations of parallel, series and cube models are represented in Fig. 6. The theoretical predictions according to different models are calculated from the following equations:

Voigt's model [35]

$$\varepsilon_C = \nu_1 \varepsilon_1 + \nu_2 \varepsilon_2 \tag{2}$$

Reuss's model [36]

$$\frac{1}{\varepsilon_C} = \frac{\nu_1}{\varepsilon_1} + \frac{\nu_2}{\varepsilon_2} \tag{3}$$

Banno's model [37]

$$\varepsilon_C = \frac{\varepsilon_1 \cdot \varepsilon_2}{(\varepsilon_2 - \varepsilon_1) \cdot \nu_1^{-1/3} + \varepsilon_1 \cdot \nu_1^{-2/3}} + \varepsilon_2 \cdot \left(1 - \nu_1^{2/3}\right) \tag{4}$$

where ε_1 and ε_2 are the dielectric constant values of the ceramics phase and the cement phase, respectively, and ν_1 and ν_2 are the volume percentages of the ceramics phase and the cement phase, respectively.

The dielectric constants of composites are shown plotted against BT concentration in Fig. 7. The theoretical predictions are also provided based on three different models, where measurements can be compared to the parallel, series and cube models. As one can see, the actual experimental data are somewhat far from the parallel model throughout the entire range. It is clear that the parallel model provides the upper limit, and that the series model gives the lower limit for relative dielectric constant. Moreover, the experimental results can be seen to most closely relate to the theoretical value of the cube model.

Hysteresis loops of composites with different BT volume fractions at various external electrical fields (E_0) from 10 to 20 kV/cm and at a fixed frequency of 90 Hz at room temperature are shown in Fig. 8(a–c). From the P–E loops, one can define two parameters based on the x- and y-axis intercepts.

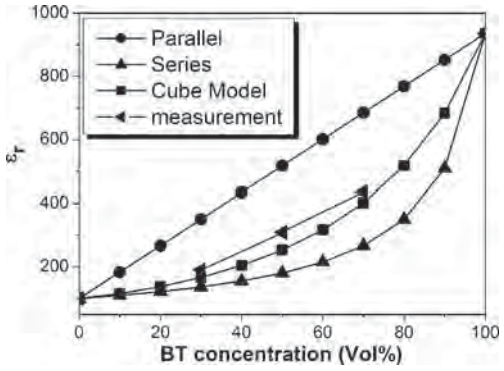

Fig. 7 Comparison between experimental and theoretical values for dielectric constants of composites with different vol% concentrations of BT particles. Theoretical values are based on parallel, series and cube models

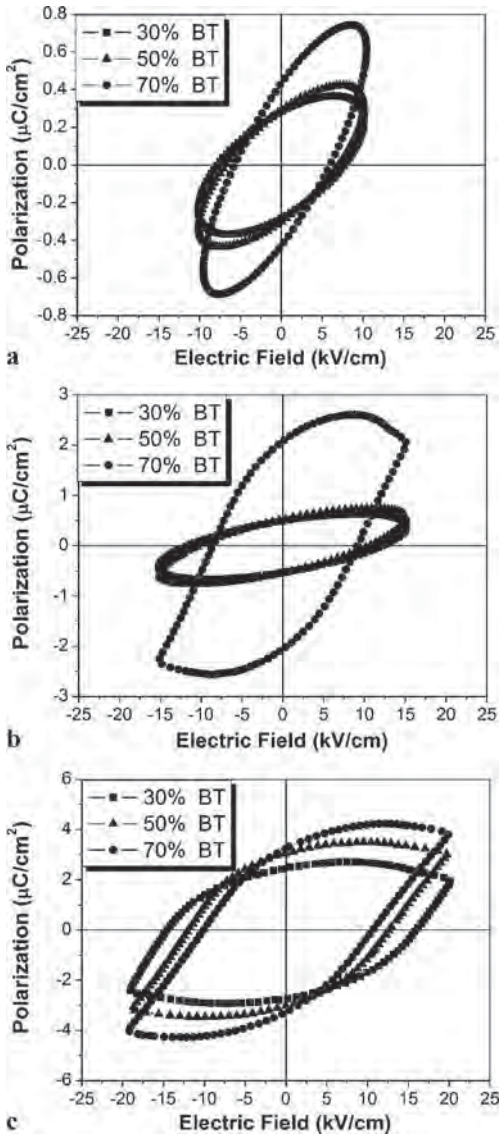

Fig. 8 Effects of BT concentration on the ferroelectric (P–E) hysteresis loops of BT-PC composites (with fixed f of 90 Hz) with external electric field amplitudes of (**a**) 10 kV/cm, (**b**) 15 kV/cm and (**c**) 20 kV/cm

Table 1 Properties of BT-PC composites

BT (vol%)	ε_r (1 kHz)	$\tan\delta$ (1 kHz)	P_{ir} at 20 kV/cm (μC/cm^2)	E_{ic} at 20 kV/cm (kV/cm)	d_{33} (pC/N)
30	190	1.13	2.59	16.52	–
50	309	0.69	3.21	13.28	10
70	436	0.3	3.42	11.14	16

With a lossy behavior, it is difficult to achieve fully saturated loops, hence the typical hysteresis parameters: i.e. the real remnant polarization (P_r) and the coercive field (E_c) cannot be extracted. For comparison, we define the y-axis intercept at a given applied field as the *instantaneous* remnant polarization (P_{ir}), while the x-axis intercept is the *instantaneous* coercive field (E_{ic}). From Fig. 8, it can be seen that the BT volume fraction has a significant influence on both P_{ir} and E_{ic}. With increasing BT volume fraction, P_{ir} increases while E_{ic} decreases at all applied external electrical fields (E_0). This can be explained based on the fact that BT is strongly piezoelectric and ferroelectric, so an increase in the BT concentration in the composites would yield higher P_{ir} [1]. Furthermore, the hysteresis loops of all composites at an applied voltage of 10 kV/cm were not saturated due to the non-piezoelectric layer of cement between the BT particles. Figure 9(a–c) shows the effects of BT concentration on P_{ir} and E_{ic} of BT-PC composites under various E_0 with fixed frequency of 90 Hz. It was found that when the BT volume fraction increased, P_{ir} increased at all E_0. As shown in Fig. 9(a–c), P_{ir} value was found to increase from 0.30 to 0.46 μC/cm^2 (at 10 kV/cm external electric field amplitude), 0.56 to 2.15 μC/cm^2 (at 15 kV/cm), and 2.59 to 3.42 μC/cm^2 (at 20 kV/cm) when the BT concentration increased from 30 to 70 vol%.

Moreover, E_{ic} value was found to be lower as BT concentration increased from 30 to 70 vol% for all external electrical fields tested (10 kV/cm to 20 kV/cm). After poling, the piezoelectric coefficients (d_{33}) of BT-PC composites were then measured. A summary of the results showing the dielectric, ferroelectric and piezoelectric properties of the composites is given in Table 1. The results show that d_{33} values of BT-PC composites increased with increasing BT volume. The d_{33} value was found to increase from 10 to 16 pC/N when the BT concentration increased from 50 to 70 vol%. Although the piezoelectric coefficient is not quite as high as for lead-based cement composites, the results are nonetheless promising—where a 70 vol% BT composite can have a d_{33} value comparatively close to that of 0-3 50 vol% PZT composites. In addition, this supports the trend toward the development and use of non-lead-based ceramics. However, it should be noted that it would become very difficult to pole samples with less than 50 vol% BT, because of the higher non-piezoelectric cement matrix volume fraction in the composite.

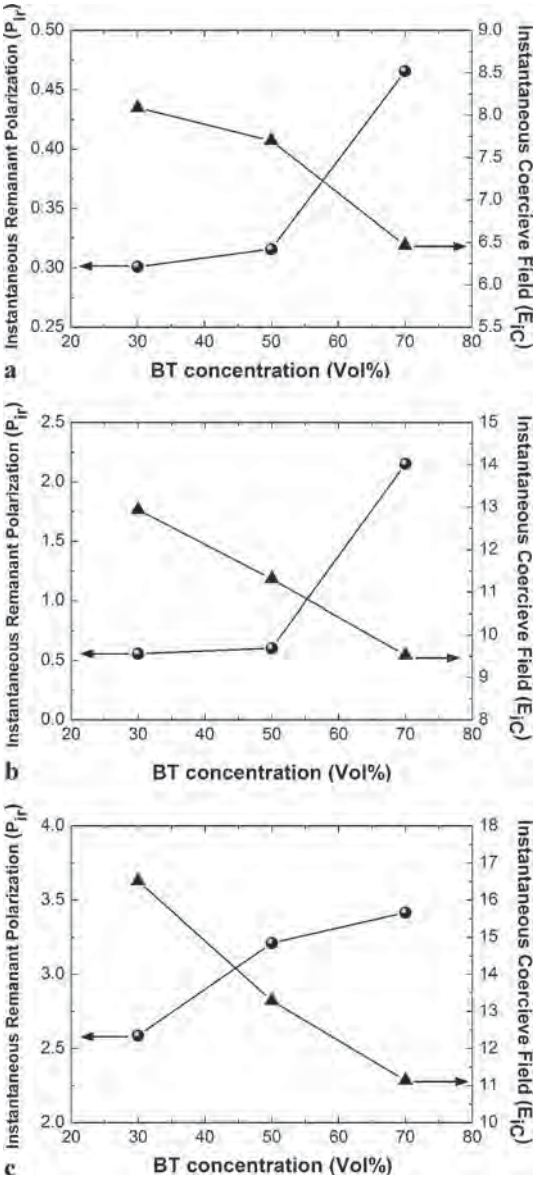

Fig. 9 Effects of BT concentration on *instantaneous* remnant polarization (P_{ir}) and *instantaneous* coercive field (E_{ic}) of BT-PC composites (with fixed f of 90 Hz) with external electric field amplitudes of (**a**) 10 kV/cm, (**b**) 15 kV/cm and (**c**) 20 kV/cm

4 Conclusions

The 0-3 barium titanate–Portland cement composites with various BT volume fractions were successfully fabricated

Table 2 Dielectric constant and dielectric loss (at 1 kHz) for PC, BT and polyimide

	ε_r	$\tan\delta$
PC[a]	100	1.45
BT[a]	936	0.063
Polyimide [34]	≈4	≈0.2

[a]Authors measurement

by a compressing technique. The results showed that the dielectric constant of the composites decreases with increasing frequency. Moreover, the dielectric loss of the composites decreases sharply with increasing frequency. In addition, the dielectric constant values of BT-PC composites increased when the volume percentage of BT was increased: in the case where ε_r values of the composites at 30 and 70 vol% are 190 and 436, respectively. Furthermore, dielectric loss results were found to decrease with increasing BT concentration, and a noticeably lower $\tan\delta$ value of 0.30 was obtained for 70% BT composite. The relative dielectric constants (ε_r) obtained from the experiment are close to the predictions of the cube model, indicating that the BT particles in the composites are uniformly dispersed. The 0-3 cement-based piezoelectric composites show typical ferroelectric hysteresis loops at room temperature. With an increase of the BT volume fraction, the *instantaneous* remnant polarization (P_{ir}) increased. The P_{ir} value of 70% BT composite was 3.42 μC/cm^2 at an applied external electrical field (E_0) of 20 kV/cm. On the other hand, the piezoelectric coefficient (d_{33}) was also found to increase as BT concentration increases, as expected. The d_{33} value was highest at 16 pC/N for 70% BT composite. Although the piezoelectric coefficient is not quite as high as for lead-based cement composites, the results are nonetheless promising—a 70 vol% BT composite can have a d_{33} value comparatively close to 0-3 50 vol% PZT composites. In addition, this will support the future concept of using non-leaded ceramics—thereby composites in development as a consequence will be comprised of non-lead-based ceramic.

Acknowledgements Financial support from the Thailand Research Fund through the Royal Golden Jubilee Ph.D. Program (Grant No. PHD/0147/2551) to Miss Rattiyakorn Rianyoi and Asst. Prof. Dr. Arnon Chaipanich is gratefully acknowledged. The authors wish to thank the staff members at the Electroceramics Research Laboratory, Faculty of Science, Chiang Mai University, for use of the research facilities which made this work possible. The authors would also like to express their gratitude to the Thailand Research Fund (TRF), Office of the Higher Education Commission (Thailand). The Graduate School of Chiang Mai University is also acknowledged for additional financial support.

References

1. C. Xin, S.F. Huang, C. Jun, Z.J. Li, J. Appl. Phys. **101**, 094110 (2007)
2. S. Aizawa, T. Kakizawa, M. Higasino, Smart Mater. Struct. **7**, 617 (1998)
3. F.-K. Chang (ed.), *Structural Health Monitoring* (Technomic Publishing, Basel, 2000)
4. H.T. Banks, R.C. Smith, Y. Wang, *Smart Material Structures: Modeling, Estimation and Control* (Wiley, New York, 1996)
5. E.P. George, R. Gotthardt, K. Otsuka, S. Trolier-McKinstry, M. Wun-Fogle, Mater. Res. Soc. Symp. Proc. **459**, 99 (1997)
6. B. Tao, *Smart/Intelligent Materials and Structures* (Defense Industry Press, Beijing, 1997) [in Chinese]
7. K. Uchino, *Piezoelectrics and Ultrasonic Applications* (Kluwer, Deventer, 1998)
8. S. Trolier-McKinstry, R.E. Newnham, Mater. Res. Bull. **18**, 27 (1993)
9. S. Schwarzer, A. Roosen, J. Eur. Ceram. Soc. **19**, 1007 (1999)
10. B. Dong, Z. Li, Compos. Sci. Technol. **65**, 1363 (2005)
11. Z. Dong, W. Keru, L. Zhongjin, J. Build. Mater. **5**, 141 (2002)
12. Z.J. Li, D. Zhang, K.R. Wu, Mater. Struct. **34**, 506 (2001)
13. A. Chaipanich, N. Jaitanong, Ferroelectr. Lett. **35**, 73 (2008)
14. A. Chaipanich, Curr. Appl. Phys. **7**, 537 (2007)
15. N. Jaitanong, A. Chaipanich, Ferroelectr. Lett. **35**, 17 (2008)
16. S.T. Lau, K.W. Kwok, H.L.W. Chan, C.L. Choy, Sens. Actuators A **96**, 14 (2002)
17. R.E. Newnham, A. Amin, Chem. Technol. **29**, 38 (1999)
18. A. Chaipanich, Curr. Appl. Phys. **7**, 574 (2007)
19. A. Chaipanich, G. Rujijanagul, T. Tunkasiri, Appl. Phys. A **94**, 329 (2009)
20. K.H. Lam, H.L.W. Chan, Appl. Phys. A **81**, 1451 (2005)
21. Z. Li, D. Zhang, K. Wu, J. Am. Ceram. Soc. **85**, 305 (2002)
22. N. Jaitanong, R. Rianyoi, R. Potong, R. Yimnirun, A. Chaipanich, Integr. Ferroelectr. **107**, 43 (2009)
23. A. Chaipanich, N. Jaitanong, Ferroelectr. Lett. **36**, 37 (2009)
24. A. Chaipanich, N. Jaitanong, R. Yimnirun, Ferroelectr. Lett. **36**, 59 (2009)
25. M.M. Vijatović, J.D. Bobić, B.D. Stojanović, Sci. Sinter. **40**, 235 (2008)
26. S.F. Wang, Y.R. Wang, K.C. Cheng, Y.P. Hsaio, Ceram. Int. **35**, 265 (2009)
27. J.M. Hwu, W.H. Yu, W.C. Yang, Y.W. Chen, Y.Y. Chou, Mater. Res. Bull. **40**, 1662 (2005)
28. X. Wang, R. Chen, H. Zhou, L. Li, Z. Gui, Ceram. Int. **30**, 1895 (2004)
29. M.T. Benlahrache, S.E. Barama, N. Benhamla, S. Achour, Mater. Sci. Semicond. Process. **9**, 1115 (2006)
30. Y. Rao, J. Yue, C.P. Wong, *Proc. 51st Electron. Compon. Technol. Conf.*, p. 1408 (2001)
31. W. Liu, B. Zhu, S. Xie, Z. Xu, Frontiers Chem. Eng. China **2**(4), 417 (2008)
32. D.-H. Kuo, C.-C. Chang, T.-Y. Su, W.-K. Wang, B.-Y. Lin, Mater. Chem. Phys. **85**, 201 (2004)
33. R.E. Newnham, Am. Rev. Mater. Sci. **16**, 47 (1986)
34. S.H. Xie, B.K. Zhu, X.Z. Wei, Z.K. Xu, Y.Y. Xu, Composites, Part A, Appl. Sci. Manuf. **36**, 1152 (2005)
35. S. Mindess, J.F. Young, D. Darwin, *Concrete* (Pearson Education, Upper Saddle River, 2003)
36. D.H. Yoon, J. Zhang, B.I. Lee, Mater. Res. Bull. **38**, 765 (2003)
37. F. Xing, B. Dong, Z. Li, J. Am. Ceram. Soc. **91**, 2886 (2008)

Applied Surface Science 257 (2011) 8385–8390

Contents lists available at ScienceDirect

Applied Surface Science

journal homepage: www.elsevier.com/locate/apsusc

Microstructure: Surface and cross-sectional studies of hydroxyapatite formation on the surface of white Portland cement paste in vitro

Arnon Chaipanich*, Pincha Torkittikul

Advanced cement-based materials research unit, Department of Physics and Materials Science, Faculty of Science, Chiang Mai University, Chiang Mai 50200, Thailand

ARTICLE INFO

Article history:
Received 6 July 2010
Received in revised form 7 April 2011
Accepted 7 April 2011
Available online 14 April 2011

Keywords:
Hydroxyapatite
Surface
Microstructure
Bioactivity
Cement

ABSTRACT

The formation of hydroxyapatite was investigated at the surface and at the cross-section of white Portland cement paste samples before and after immersion in simulated body fluid. Scanning electron microscope images showed that hydroxyapatite were found at the surface of white Portland cement after immersion in simulated body fluid. Hydroxyapatite grains of mostly ≈1 μm size with some grain size of ≈2–3 μm were seen after 4 days immersion period. More estabilshed hydroxyapatite grain size of ≈3 μm grains were observed at longer period of immersion at 7 and 10 days. The cross-section of the samples was investigated using line scanning technique and was used to determine the hydroxyapatite layer. A strong spectrum of phosphorus is detected up to 6–8 μm depth for samples after 4, 7 and 10 days immersion in simulated body fluid when compared to weak spectrum detected before immersion. The increase in the phosphorus spectrum corresponds to the hydroxyapatite formation on the surface of the samples after the samples were placed in simulated body fluid.

1. Introduction

The in vitro biological properties of calcium silicates and calcium silicates based materials such as white Portland cements have recently been investigated [1–6]. Hydroxyapatite was found to occur on the surfaces of these materials. Silicate materials have been shown to accelerate the formation of new bone-tissue by promoting the genetic activity of bone-regulating cells [6–10]. Si–OH functional group on the silicate material surface induces the nucleation of apatite crystals and which then continue to grow spontaneously. The structure of hydroxyapatite layer formation is similar to the mineral component of bone and provides a focus for the attachment and proliferation of new bone-forming cells [11–17]. Simulated body fluid (SBF) was developed by Kokubo and Takadama [18] containing ion concentrations similar to those of human plasma in order to reproduce formation of apatite on bioactive materials in vitro. Formation of hydroxyapatite layer on the material surface within 4 weeks of exposure to SBF in vitro gives an indication that the material is bioactive and will form a bond with living tissue. Calcium silicate based materials are currently being investigated with respect to their potential clinical use in dental and bone-contact applications [6,12,13,19–27]. Huan and Chang [20] has demonstrated that silicate species could play an important role in forming hydroxyapatite in the simulated body environment and the formation of a homogeneous apatite layer on the material surface was dependent on the content of tricalcium silicate.

White Portland cement of 80 wt.% and 20 wt.% bismuth oxide producing mineral trioxide aggregate (MTA), has also been used as a root repair material in dentistry [21,22,13,23–25]. Thus there has been an increasing interest in the investigation on cement based materials in the area of bio-medical application. However, the formation of hydroxyapatite on the surface, especially at the cross-section showing the hydroxyapatite layer on the sub-materials are not fully understood and have not been reported. In order to understand the formation of hydroxyapatite deposited on the surface of white Portland cement and between the deposit and the substrate materials, the surface and cross-section of the material was investigated and reported here in this paper.

White Portland cement was placed in the SBF to allow the formation of hydroxyapatite. The cement paste samples were placed for a period of 4, 7 and 10 days and compared to the control paste sample not being submerged in the SBF. The hydroxyapatite formation at the surface was investigated using scanning electron microscopy and energy dispersive spectrometry. The cross-section of the samples before and after immersion in the SBF was also examined to determine the formation and the thickness of HA and the results are reported.

2. Materials and methods

White Portland cement (WPC) produced by Siam cement Public Company Limited was used in this investigation. Cement paste samples were prepared in polypropylene beaker with sterile

* Corresponding author. Tel.: +66 5394 3367; fax: +66 5394 3445.
E-mail address: arnon@chiangmai.ac.th (A. Chaipanich).

0169-4332/$ – see front matter © 2011 Elsevier B.V. All rights reserved.
doi:10.1016/j.apsusc.2011.04.046

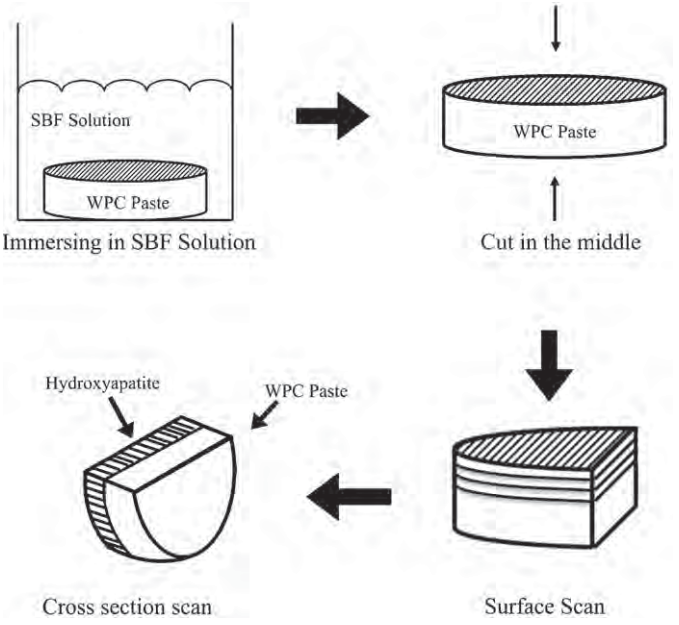

Fig. 1. Schematic diagram of the samples placed faced up for surface scan and preparations for line scan at cross-section.

distilled water at a water to cement ratio of 0.5 by mass. In each case, 50 g of cement was manually blended with 25 g of sterile distilled water using a polypropylene spatula. The specimens were then cast into rubber mould (10 mm in diameter and 2 mm in height) and sealed in moulds for 24 h before curing in water at 37 °C for 7 days.

Simulated body fluid was prepared according to the procedure described by Kokubo [18]. The ion concentrations of the SBF solution are similar to those in human blood plasma. WPC paste disks (as shown in Fig. 1) were immersed in the SBF solution in hermetically sealed polypropylene containers under sessile conditions at 37 °C for 4, 7 and 10 days with a surface area-to-volume ratio of 0.1 cm^{-1}. After reaching these specified periods, the disc specimens were removed from SBF solution, gently rinsed with de-ionized water and dried in air at room temperature. The disks were sliced cut in the middle and turned side way for cross-section scan (Fig. 1). The surface morphologies of both the surface and of the cross-section of the samples after immersion in SBF were characterized by scanning electron microscope (SEM) (JEOL JEM-5910LV) with the aid of energy dispersive spectrometry (EDS). Phase characterisations of the sample surface were also carried out by room temperature X-ray diffraction (XRD) using Ni-filtered Cu Kα radiation.

3. Results and discussion

SEM images of the sample surface can be observed at different ages of immersion in SBF as shown in Figs. 2–5. At the start (before submerging in the SBF as shown in Fig. 2), the paste is seen to be made up of mostly calcium silicate hydrate, the gel which provide the binding, as detected by EDS. Main peaks of Si and Ca as well as O, can be seen in the spectrum trace of the paste. When submerging in SBF, the surface texture and appearance can be seen to change completely. Crystals of hydroxyapatite occurred at the surface of the cement paste as the result of the nucleation of Ca from the cement and P in the solution. Therefore, a sharp increase in the P peak can be seen with the Si peak being minimized (after 4 days in SBF) since the cement paste would be acting as a substrate below the hydroxyapatite layer. The morphology of hyrodxyapatite forming at the surface of white Portland cement after the samples were submerged in SBF is seen to be similar to the apatite layer formed on previously reported bioactive materials [26,27]. Hydroxyapatite layer can form on the surface of a material after immersion in SBF solution as the result of bioactivity (the ability to form a chemical bond with living bone-tissue) taking placed [7]. Moreover,

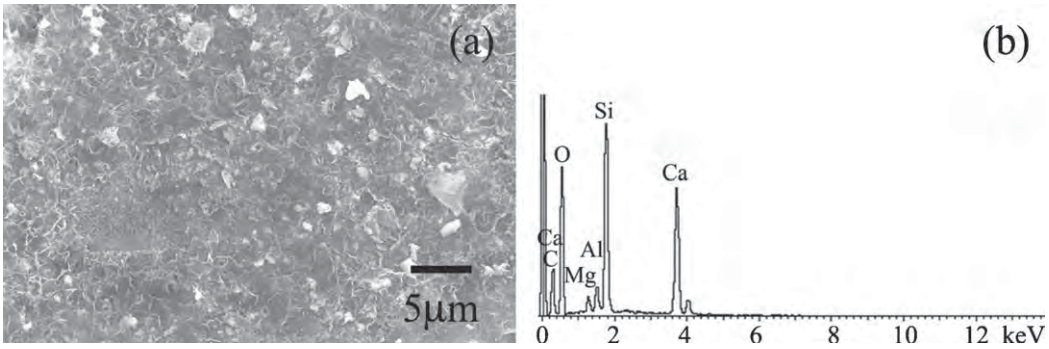

Fig. 2. (a) SEM micrograph and (b) EDX spectrum of the WPC paste disc surface before placing in SBF.

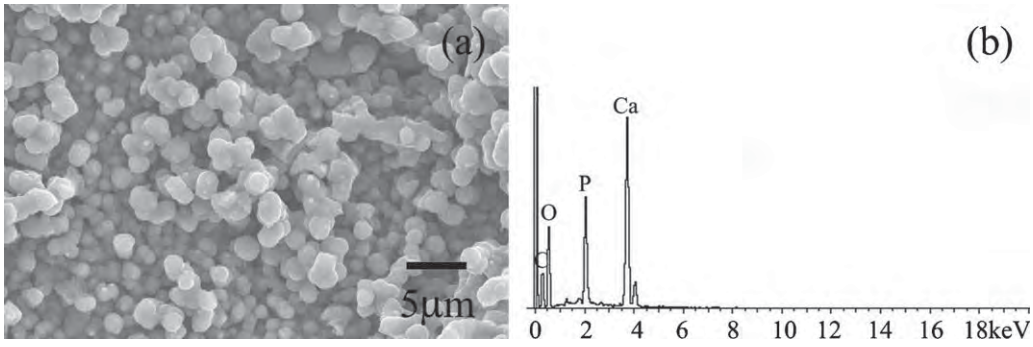

Fig. 3. (a) SEM micrograph and (b) EDX spectrum of the WPC paste disc surface after placing in SBF for 4 days.

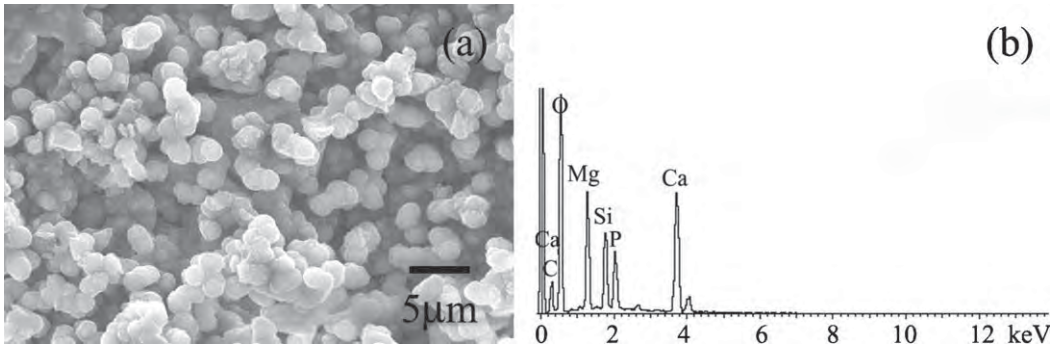

Fig. 4. (a) SEM micrograph and (b) spectrum of WPC paste disc surface after placing in SBF for 7 days.

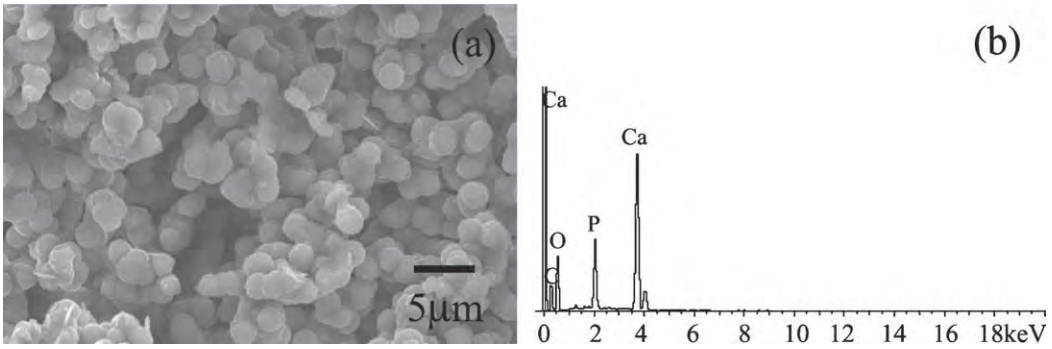

Fig. 5. (a) SEM micrograph and (b) spectrum of the surface of WPC paste disc after placing in SBF for 10 days.

minor peaks of C can be seen due to formation of calcium carbonate (calcite) due to the presence of HCO_3^- ions (4.2 mM) in SBF, which lead to the formation of calcite at the surface [28].

Furthermore, the size of hydroxyapatite grains appearing at 4 days is generally ≈1 μm with some grains of ≈2–3 μm observed. At 7 days and 10 days (Figs. 4 and 5, respectively), there are in general less of ≈1 μm grain size and more of the ≈2–3 μm grains. This is likely due to the increase in the age of immersion in SBF, which increase in the nucleation time for hydroxyapatite formation. Again, similar EDS spectrum with mainly Ca and P can be seen at 10 days with negligible trace of other elements. Nonetheless, it must be noted that for 7 day sample although the SEM image give a very clear presentation of the result, the elements shown detected comprises of Si and Ca as well. This is most likely due to penetrable pores in between the hydroxyapatite resulting in some Si and Ca being detected which is clearly not present in the SEM image but

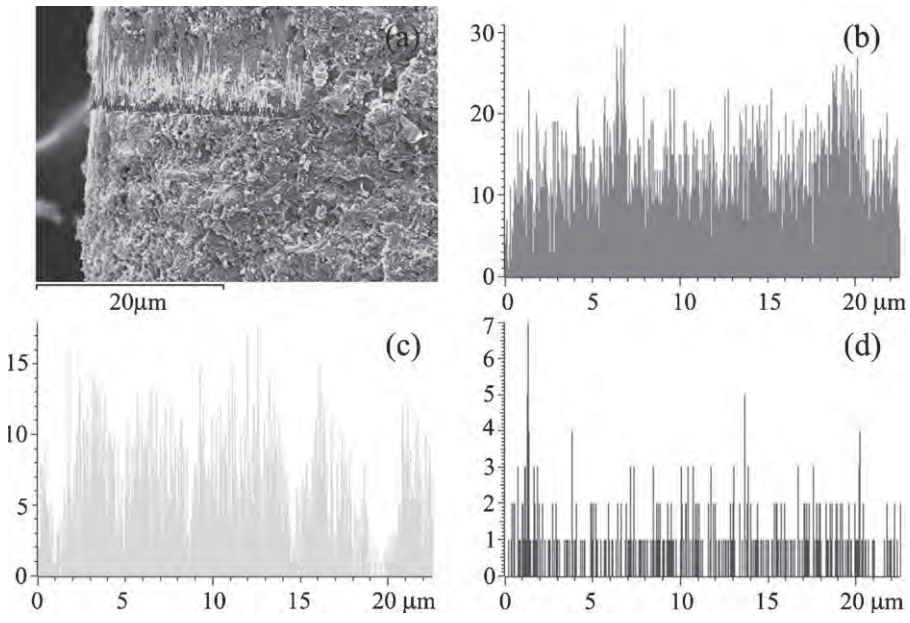

Fig. 6. (a) SEM micrographs showing the scanned line, (b) calcium spectrum, (c) silicon spectrum and (d) phosphorus spectrum of WPC paste disc cross-section before placing in SBF.

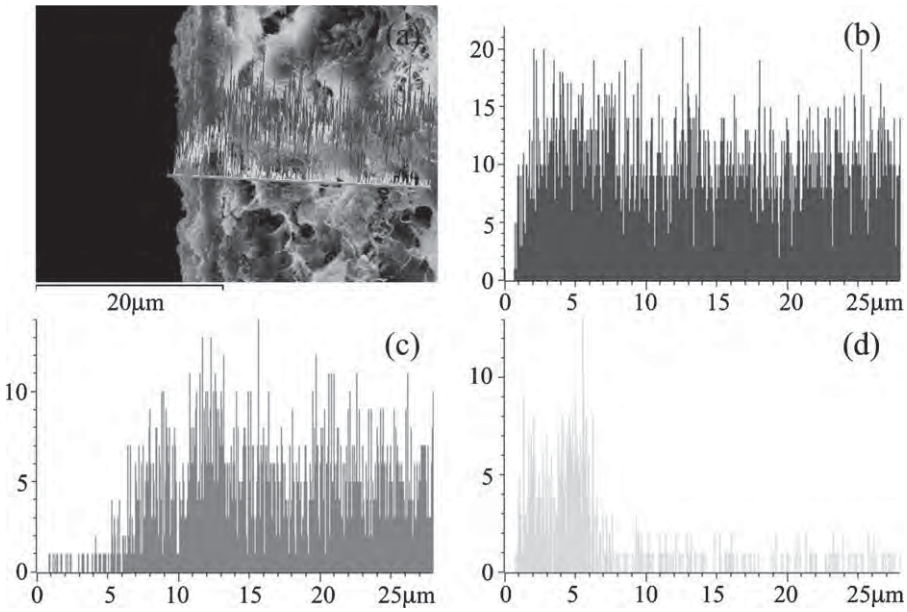

Fig. 7. (a) SEM micrographs showing the scanned line, (b) calcium spectrum, (c) silicon spectrum and (d) phosphorus spectrum of WPC paste disc cross-section after placing in SBF for 4 days.

can be detected as a result of pores those are not easily observed. It is therefore, ever more important to study the surface and transition area of the sample. This was done by viewing the sample's cross-section.

When white Portland cement is initially placed in SBF, calcium hydroxide is leached from the WPC matrix, which lead to a moderate increase in the pH [28]. This increase in the pH and Ca^{2+} ions is reported to enhance the supersaturation of SBF with respect to hydroxyapatite and promotes precipitation of hydroxyapatitie layer [28]. The Si–OH functional groups on the surface of silicate material, such as silicate glasses and ceramics, have been shown to act as nucleation centers for hydroxyapatite precipitation [7,28,29]. Moreover, recent reports indicate that the formation of these homogeneous hydroxyapatite layer was dependent on the content of silicate material [20] in addition to an increase in the super saturation of Ca^{2+} in promoting the formation of new crystals of hydroxyapatite on the material surface in the simulated body fluid environment. Hence, it is thought that the deposition of hydroxyapatite layer onto the Portland cement paste surface is attributed to both the dissolution of calcium hydroxide and to the high proportion of pre-existing Si–OH nucleation sites presented by the nanoporous calcium silicate hydrate gel structure [6].

In addition, line scanning technique was used starting from the edge of the sample scanning inwards (Figs. 6–9). Line scanned of samples before immersion in SBF can be seen in Fig. 6(a) and after

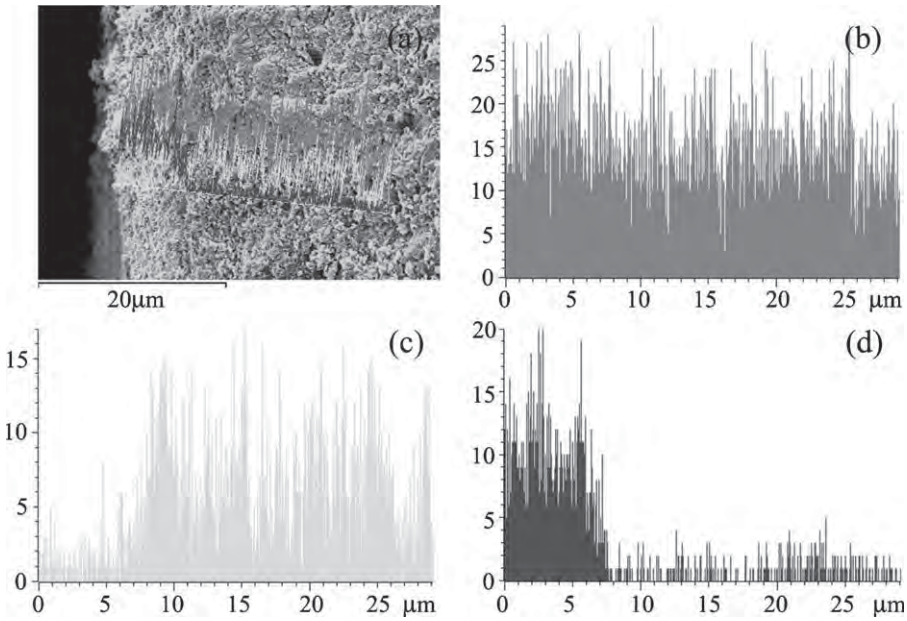

Fig. 8. (a) SEM micrographs showing the scanned line, (b) calcium spectrum, (c) silicon spectrum and (d) phosphorus spectrum of WPC paste disc cross-section after placing in SBF for 7 days.

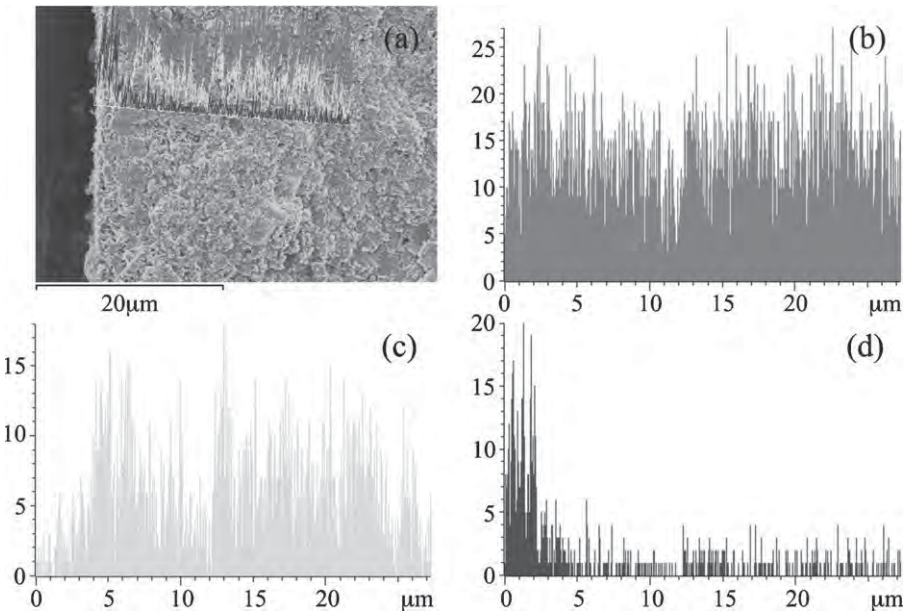

Fig. 9. (a) SEM micrographs showing the scanned line, (b) calcium spectrum, (c) silicon spectrum and (d) phosphorus spectrum of WPC paste disc cross-section after placing in SBF for 10 days.

placing in SBF for 4, 7 and 10 days can be seen in Figs. 7(a), 8(a) and 9(a), respectively. Calcium spectrums can be seen in Figs. 6(b), 7(b), 8(b) and 9(b). For silicon spectrum, Si, it is clear that there is negligible Si detected at the edge of the sample but is detected at ≈5–8 μm from the edge (Figs. 7(c), 8(c) and 9(c)). There is roughly similar intensity afterwards, although a drop in Si can be seen at intervals, which may be due to other cement hydration products that also known to exist other than calcium silicate hydrates (C–S–H) such as calcium hydroxide. This explanation agrees with the Ca spectrum which can be seen to be more steady than Si and therefore Ca would remain detected even at the intervals where Si being less in intensity. It is also important to study the Phosphorous (P) occurrence at the cross-section, which would concurrently be detected with Ca thus forming hydroxyapatite. Before immersion in SBF, there is very light trace of P detected (Fig. 6(d)) across the sample. When immersion in SBF (4 days), the P element intensity can be seen to grow showing a much stronger intensity (Figs. 7(d), 8(d) and 9(d)) when compared to the control paste sample, thus that confirming the hydroxyapatite formation at the surface. Moreover, P is mostly detected up to ≈6–8 μm from the edge of the sample hence being the thickness of hydroxyapatite. The sample at 7 day, P is detected until ≈6–8 μm from the sample edge. The sample at 10 day again showed P detection at upto ≈6 μm depth. Therefore, in general the evidence suggest that submerging the sample in SBF at 4, 7 and 10 days approximate thickness of hydroxyapatite formation is found to be 6–8 μm.

X-ray diffraction (XRD) patterns of the samples after immersion in SBF can be seen in Fig. 10. Crystallized peaks of calcium carbonate ($CaCO_3$) at 29.4°, 39.4°, 48.5° 2θ and hydroxyapatite (25.9°, 31.8°, 32.9°, 34.1° and 49.5° 2θ) can be observed for all samples. In general, the intensity of hydroxyapatite peaks of samples at 7 and 10 days immersion in SBF can be seen to be higher than the samples at 4 days period. The main peaks at 31.8° 2θ and 32.9° 2θ can be seen to be stronger with the peak at 25.9° 2θ can be seen to be clearly detected in both 7 and 10 days samples in comparison to the diffraction line of the samples at 4 days. Calcium carbonate was also detected due to the presence of HCO_3^- ions (4.2 mM) in the SBF [28]. These XRD results are, therefore, in line with that of the SEM micrographs and the line scanning

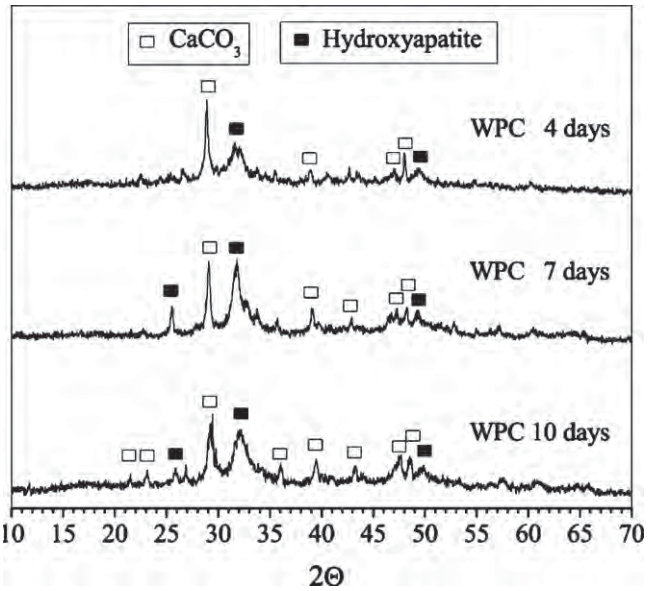

Fig. 10. (a) X-ray diffraction patterns of WPC paste surface after placing in SBF for 4, 7 and 10 days.

images at the surface and at the cross-section of the samples, which confirms there is hydroxyapatite formation and that the approximate thickness of the hydroxyapatite layer formed is in the region of 6–8 μm.

4. Conclusions

Hydroxyapatite formation on WPC was investigated at the surface and the cross-section of WPC before and after immersion in SBF. The results showed that formation of hydroxyapatite was seen just after 4 days where the grain size are mostly ≈1 μm with some grain size of ≈2–3 μm. At 7 and 10 days, in general ≈3 μm grains were observed. At the cross-sectional area of the samples, Phosphorus is detected at up to ≈6–8 μm for samples submerged in SBF for

4, 7 and 10 days when compared to the sample before immersion. Silicon, Si was found to reduce correspondingly at the same depth as the result of hydroxyapatite formation where only calcium and phosphorus were detected.

Acknowledgements

Financial support from the Thailand Research Fund through the Royal Golden Jubilee PhD Program (Grant No. PHD/0281/2550) is acknowledged. The authors would also like to express their gratitude for TRF-CHE Research Grant for Mid-Career University Faculty awarded to Assistant Prof. Dr. Arnon Chaipanich by the Thailand Research Fund (TRF), Office of the Higher Education Commission (Thailand) and Chiang Mai University. The authors would also like to thank Mr. Mongkol Kongtungmon at the Electron Microscopy Research and Service Center, Faculty of Science, Chiang Mai University for his assistance in using SEM.

References

[1] L.L. Hench, ö. Anderson, Bioactive glasses, in: L.L. Hench, J. Wilson (Eds.), An Introduction to Bioceramics, World Scientific, Singapore, 1993, pp. 41–46.
[2] L.L. Hence, J.K. West, Biological applications of bioactive glasses, Life Chem. Rep. 13 (1996) 187–241.
[3] R.K. Singh, G.P. Kothiyal, A. Srinivasan, In vitro evaluation of bioactivity of $CaO–SiO_2–P_2O_5–Na_2O–Fe_2O_3$ glasses, Appl. Surf. Sci. 255 (2009) 6827–6831.
[4] G. Li, D. Zhou, M. Xue, W. Yang, Q. Long, B. Cao, D. Feng, Study on the surface bioactivity of novel magnetic A–W glass ceramic in vitro, Appl. Surf. Sci. 255 (2008) 559–561.
[5] D.A. Ribeiro, M.H. Duarte, M.A. Matsumoto, M.A. Marques, D.F. Salvadori, Biocompatibility in vitro tests of mineral trioxide aggregate and regular and white Portland cements, J. Endod. 31 (2006) 605–607.
[6] P. Torkittikul, A. Chaipanich, Investigation of the mechanical and in vitro biological properties of ordinary and white Portland cements, J. Sci. Asia 35 (2009) 358–364.
[7] T. Kokubo, Bioactivity of bioglasses and glass ceramics, in: P. Ducheyne, T. Kokubo, C.A. Blitterswijk (Eds.), Bone-Bonding Biomaterials, Reed Healthcare Communications, Leidendorp, 1992, pp. 31–46.
[8] L.L. Hench, Sol–gel materials for bioceramic application, Curr. Opin. Solid State Mater. Sci. 2 (1997) 604–610.
[9] A.E. Portera, N. Patela, J.N. Skepperb, S.M. Besta, W. Bonfielda, Comparison of in vivo dissolution processes in hydroxyapatite and silicon-substituted hydroxyapatite bioceramics, Biomaterials 24 (2003) 4609–4620.
[10] W. Cao, L.L. Hench, Bioactive materials, Ceram. Inter. 22 (1996) 493–507.
[11] L.L. Hench, Biomaterials: a forecast for the future, Biomaterials 19 (1998) 1419–1423.
[12] G.M. Giovanna, F. Silvia, P. David, G. Gasparotto, P. Carlo, Calcium silicate coating derived from Portland cement as treatment for hypersensitive dentine, J. Dent. 36 (2008) 565–578.
[13] J. Saidon, J. He, Q. Zhu, K. Safavi, L.S.W. Spångberg, Cell and tissue reactions to mineral trioxide aggregate and Portland cement, Oral Surg. Oral Med. Oral Pathol. 95 (2003) 483–489.
[14] R.K. Singh, A. Srinivasan, Bioactivity of $SiO_2–CaO–P_2O_5–Na_2O$ glasses containing zinc–iron oxide, Appl. Surf. Sci. 256 (2010) 1725–1730.
[15] B. Cao, D. Zhou, M. Xue, G. Li, W. Yang, Q. Long, L. Ji, Study on surface modification of porous apatite–wollastonite bioactive glass ceramic scaffold, Appl. Surf. Sci. 255 (2008) 505–508.
[16] M. Wen, L. Zhou, W. Guan, Y. Li, J. Zhang, Formation and bioactivity of porous titania containing nanostructured Ag, Appl. Surf. Sci. 256 (2010) 4226–4230.
[17] E. Gyorgy, S. Grigorescu, G. Socol, I.N. Mihailescu, D. Janackovic, A. Dindune, Z. Kanepe, E. Palcevskis, E.L. Zdrentu, S.M. Petrescu, Bioactive glass and hydroxyapatite thin films obtained by pulsed laser deposition, Appl. Surf. Sci. 253 (2007) 7981–7986.
[18] T. Kokubo, H. Takadama, How useful is SBF in predicting in vivo bone bioactivity? Biomaterials 27 (2006) 2907–2915.
[19] D. Abdullah, T.R. Pitt Ford, S. Papaioannou, J. Nicholson, F. Mconald, An evaluation of accelerated Portland cement as a restorative material, Biomaterials 23 (2002) 4001–4010.
[20] Z. Huan, J. Chang, Self-setting properties and in vitro bioactivity of calcium sulfate hemihydrate–tricalcium silicate composite bone cements, Acta Biomater. 3 (2007) 952–960.
[21] R. Holland, V. de Souza, M.J. Nery, J.A.O. Filho, P.F.E. Bernabe, E. Dezan, Reaction of dogs' teeth to root canal filling with mineral trioxide aggregate or a glass ionomer sealer, J. Endod. 25 (1999) 728–730.
[22] D.R. Hachmeister, W.G. Schindler, W.A. Walker, D.D. Thomas, The sealing ability and retention characteristics of mineral trioxide aggregate in a model of apexification, J. Endod. 28 (2002) 386–390.
[23] C.R.A. Valois, E.D. Costa, Influence of the thickness of mineral trioxide aggregate on sealing ability of root-end fillings in vitro, Oral Surg. Oral Med. Oral Pathol. Oral Radiol. Endod. 97 (2004) 108–111.
[24] R.L. Martin, F. Monticelli, W.W. Brackett, R.J. Loushine, R.A. Rockman, M. Ferrari, D.H. Pashley, F.R. Tay, Sealing properties of mineral trioxide aggregate orthograde apical plugs and root fillings in an in vitro apexification model, J. Endod. 33 (2007) 272–275.
[25] C. Boutsioukis, G. Noula, T. Lambrianidis, Ex vivo study of the efficiency of two techniques for the removal of mineral trioxide aggregate used as a root canal filling material, J. Basic Res. Technol. 34 (2008) 1239–1242.
[26] W. Zhao, J. Wang, W. Zhia, Z. Wang, J. Chang, The self-setting properties and in vitro bioactivity of tricalcium silicate, Biomaterials 26 (2005) 6113–6121.
[27] D. Gallego, N. Higuita, F. Garcia, N. Ferrell, D.J. Hansford, Bioactive coating on Portland cement substrate: surface precipitation of apatite-like crystal, Mater. Sci. Eng. C 28 (2008) 347–352.
[28] N.J. Coleman, J.W. Nicholson, K. Awosanya, A preliminary investigation of the in vitro bioactivity of white Portland cement, Cem. Concr. Res. 37 (2007) 1518–1523.
[29] J.R. Jones, L.M. Ehrenfried, L.L. Hench, Optimising bioactive glass scaffolds for bone tissue engineering, Biomaterials 27 (2006) 964–973.

Current Applied Physics 11 (2011) S48–S51

Contents lists available at ScienceDirect

Current Applied Physics

journal homepage: www.elsevier.com/locate/cap

Dielectric and ferroelectric properties of 1-3 barium titanate–Portland cement composites

R. Rianyoi [a], R. Potong [a], N. Jaitanong [a], R. Yimnirun [b], A. Ngamjarurojana [a], A. Chaipanich [a,*]

[a] Department of Physics and Materials Science, Faculty of Science, Chiang Mai University, Chiang Mai 50200, Thailand
[b] School of Physics, Institute of Science, Suranaree University of Technology and Synchrotron Light Research Institute (Public Organization), Nakhon Ratchasima 30000, Thailand

ARTICLE INFO

Article history:
Received 23 June 2010
Received in revised form
26 October 2010
Accepted 7 March 2011
Available online 12 March 2011

Keywords:
$BaTiO_3$
Cement
Composites
Dielectric properties
Ferroelectric properties

ABSTRACT

In the current work, the dielectric and ferroelectric properties of 1-3 barium titanate (BT)–Portland cement (PC) composites have been studied as potential lead-free piezoelectric-cement-based composites. The 1-3 BT–PC composites were fabricated by a dice-and-fill technique with BT:PC ratios of 50:50, 60:40 and 70:30 by volume. The results indicate that the dielectric constant (ϵ_r) of the composite materials increases as the barium titanate volume fraction increases; this follows the parallel model. The room temperature ϵ_r at 1 kHz of 70% barium titanate composite was found to have values higher than 750. The loss tangent ($\tan\delta$) results were found to decrease with increasing barium titanate volume fraction. On the other hand, the ferroelectric hysteresis loops of composite materials indicate that the "instantaneous" remnant polarization (P_{ir}) increases as the barium titanate volume fraction increases. The P_{ir} at 15 kV/cm (90 Hz) of 70% barium titanate composite was found to have a value of ≈ 3 μC/cm^2.

1. Introduction

Cement-based piezoelectric composites have been widely studied for applications in civil engineering as sensors and actuators. Recently, cement-based piezoelectric composites incorporating lead zirconate titanate (PZT) in a cement matrix have been developed [1–10]. However, lead oxide, which is a component of PZT, is highly toxic; and its toxicity is further enhanced due to its volatilization at high temperature – particularly during calcination and sintering, causing environmental pollution [11,12]. Therefore, several kinds of materials have been studied in order to develop a lead-free piezoelectric ceramic. Barium titanate, $BaTiO_3$ (BT), is expected to be one of the superior candidates for lead-free piezoelectric ceramics due to its excellent dielectric, ferroelectric and piezoelectric properties [13].

In order to understand the poling mechanism of these piezoelectric-cement composites, ferroelectric hysteresis should also be studied. This is an important behavior of materials with ferroelectric properties [14]; it can be used to give an indication of the difficulty of the poling process in piezoelectric-cement composites. Thus, this study examines the ferroelectric hysteresis behavior of new, functional 1-3 lead-free piezoelectric-cement-based composites for smart structure applications. The 1-3 barium titanate–Portland cement composites with 50%–70% volume fractions of BT were prepared by a dice-and-fill method. The dielectric and ferroelectric properties were then investigated.

2. Experimental procedure

Barium titanate – $BaTiO_3$ (BT) – powder was initially produced via the two-stage mixed oxide method, by calcining the powder at 1200 °C and sintering at 1400 °C. The 1-3 barium titanate–Portland cement composites were fabricated by an improved dice-and-fill technique with BT:PC ratios of 50:50, 60:40 and 70:30 by volume (disk samples of ≈12 mm diameter and ≈2 mm thickness). First, each sintered BT disk was cut to make a set of grooves in the horizontal direction using a diamond saw with a ≈0.3-mm-thick blade; the grooves were then filled with cement paste (cement:water = 2:1). After the samples were cured at a temperature of 60 °C and 98% relatively humidity for five days, a second set of grooves was cut normal to the first direction. Fig. 1 shows specimens with BT ceramic volume fractions of 50%, 60% and 70%. For measurement of the dielectric properties, an impedance meter (Hewlett Packard 4194A) was used. The relative dielectric constant (ϵ_r) was then calculated from the following equation:

$$\epsilon_r = \frac{Ct}{\epsilon_0 A} \quad (1)$$

* Corresponding author. Tel.: +66 1 8858048; fax: +66 53 943445.
E-mail address: arnon@chiangmai.ac.th (A. Chaipanich).

1567-1739/$ – see front matter © 2011 Elsevier B.V. All rights reserved.
doi:10.1016/j.cap.2011.03.010

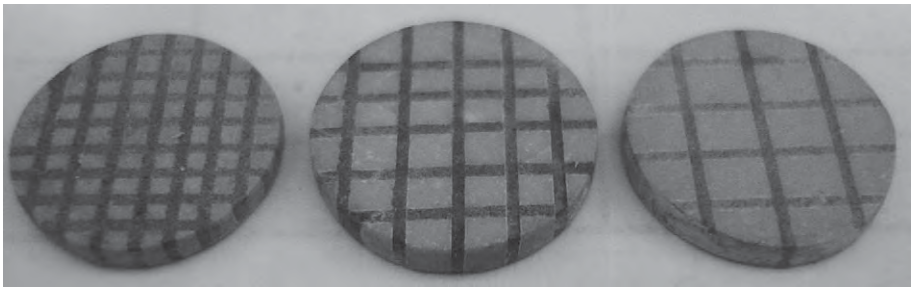

Fig. 1. 1-3 Barium titanate (BT)–Portland cement (PC) composites with different BT ceramic volume fractions of 50%, 60% and 70%.

where C is the sample capacitance, t is the thickness, ϵ_0 is the permittivity of free space constant (8.854×10^{-12} Fm^{-1}), and A is the electrode area.

The room temperature ferroelectric hysteresis (P-E) loops were characterized using a conventional Sawyer-Tower circuit.

3. Results and discussion

The calculated results of ϵ_r and tanδ of composites at a frequency of 1 kHz are shown in Fig. 2, where the effect of BT content can be observed. The results show that with increasing volume of BT content, ϵ_r value shows an increasing trend, while tanδ decreases. It can be seen that the higher the BT volume fraction is, the greater the contribution of the ion and electron polarization on the composites; thus the dielectric constant of the composites will also be higher. When BT content is 50 and 70 vol %, ϵ_r values are 527 and 787, respectively. However, the dielectric loss (tanδ) of the composites decreases with increasing BT ceramic volume fraction. On the other hand, a noticeably lower tanδ value was obtained for the composite with BT of 70% (tan$\delta = 0.26$) when compared to the composite with higher cement content (BT = 50%). These values agree with the results reported for the case of 1-3 P(MN)ZT–PC composites by Cheng et al. [15].

The parallel (Voigt [16]), series (Reuss [17]) and cube (Banno [18]) models were compared to evaluate the experimental results for the dielectric constants (ϵ_r) of the 1-3 BT–PC composites. The parallel and series mixing models represent the extreme cases where the model consists of alternating layers of each phase, perpendicular and parallel to the applied field, respectively. The cube mixing model characterizes the combined case of parallel and series mixing. The theoretical equations of parallel, series and cube models can be denoted as follows:

- Voigt's model [16]

$$\epsilon_C = \nu_1\epsilon_1 + \nu_2\epsilon_2 \tag{2}$$

- Reuss's model [17]

$$\frac{1}{\epsilon_C} = \frac{\nu_1}{\epsilon_1} + \frac{\nu_2}{\epsilon_2} \tag{3}$$

- Banno's model [18]

$$\epsilon_C = \frac{\epsilon_1 \cdot \epsilon_2}{(\epsilon_2 - \epsilon_1)\cdot \nu_1^{-1/3} + \epsilon_1 \cdot \nu_1^{-2/3}} + \epsilon_2 \cdot \left(1 - \nu_1^{2/3}\right) \tag{4}$$

where ϵ_1 and ϵ_2 are dielectric constant values of the ceramics phase and the cement phase, respectively, and ν_1 and ν_2 are the volume percentages of the ceramics phase and the cement phase, respectively.

In Fig. 3, the dielectric constant is plotted against BT content in the composites. The theoretical predictions according to different models are superimposed in the same figure. As one can see, the actual experimental data are far from the series model throughout the entire range, and differ from the cube model in the case of a high BT volume fraction. The experimental results are close to the theoretical value of the parallel model because the 1-3 connectivity is more closely related to the 2-2 parallel model.

The P-E loops of the studied composites at various external electrical fields (E_0) from 5 to 15 kV/cm and fixed frequency of 90 Hz at room temperature are shown in Fig. 4(a–c). From the P-E loops, one can define two parameters based on the x- and y-axes intercepts. With a lossy behavior, it is difficult to achieve fully saturated

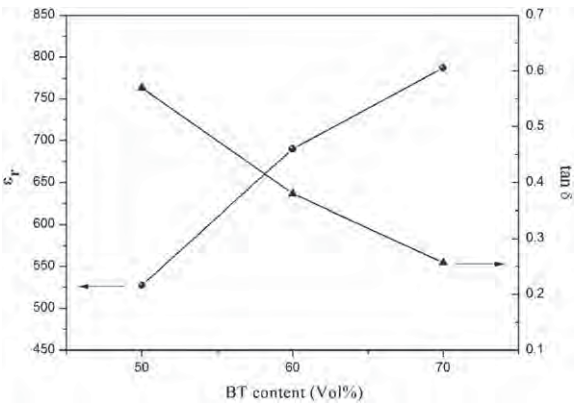

Fig. 2. Effect of BT content on the dielectric constant and dielectric loss (tanδ) of 1-3 BT–Portland cement composites.

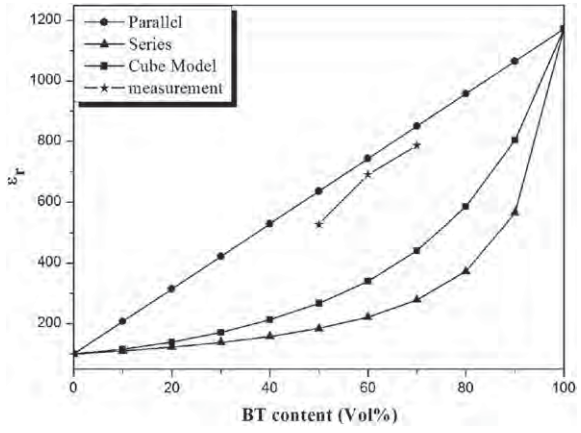

Fig. 3. Comparison between experimental and theoretical values for dielectric constants of composites with different vol % content of BT ceramic. Theoretical values are based on parallel, series and cube models.

loops – hence the typical hysteresis parameters: i.e. the real remnant polarization (P_r) and the coercive field (E_c) cannot be extracted. For comparison, we define the y-axis intercept at a given applied field as the "instantaneous" remnant polarization (P_{ir}), and the x-axis intercept as the "instantaneous" coercive field (E_{ic}) [10]. From Fig. 4 (a–c), it is observed that the BT volume fraction has a significant influence on P_{ir} and E_{ic}. With increasing BT volume fraction, P_{ir} increases while E_{ic} decreases at all applied E_0. As BT content increases from 50 to 70 vol %, the loop becomes too saturated because of the significant decrease in E_{ic}. In addition, with an increase in P_{ir} the loop becomes slightly slimmer. This behavior can be explained in two possible ways. One is that BT is strongly piezoelectric and ferroelectric, where an increase in the BT content

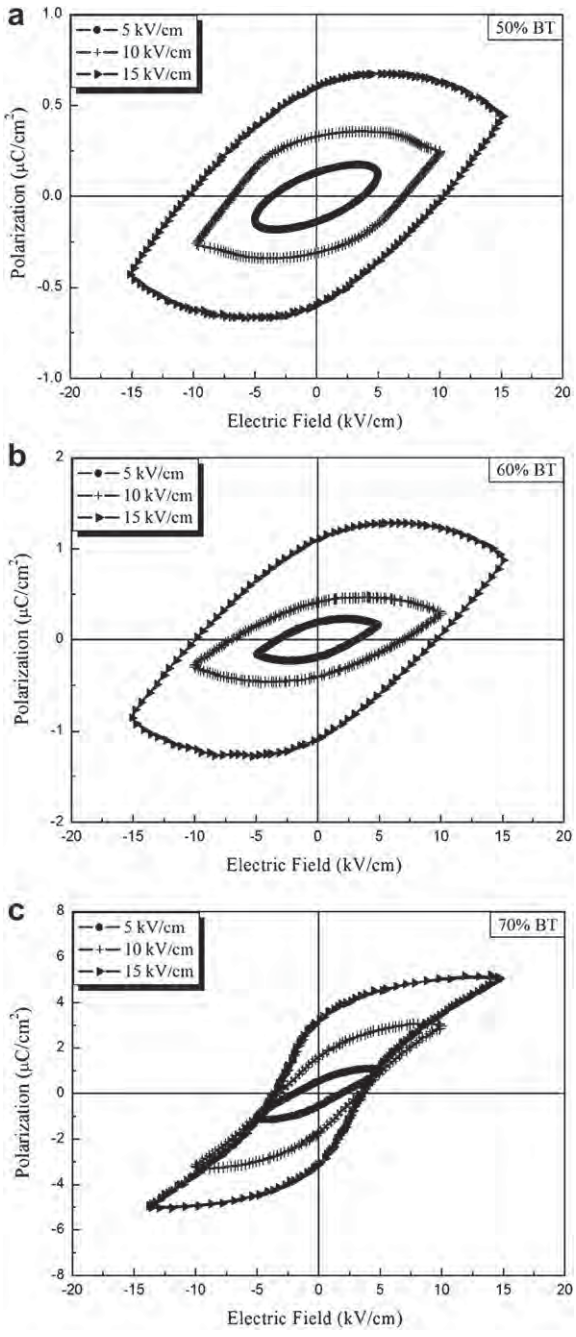

Fig. 4. *P-E* loops of 1-3 BT–PC composites at various external electrical fields (E_0) from 5 to 15 kV/cm (with fixed f of 90 Hz) with BT content of (a) 50 vol %, (b) 60 vol % and (c) 70 vol %.

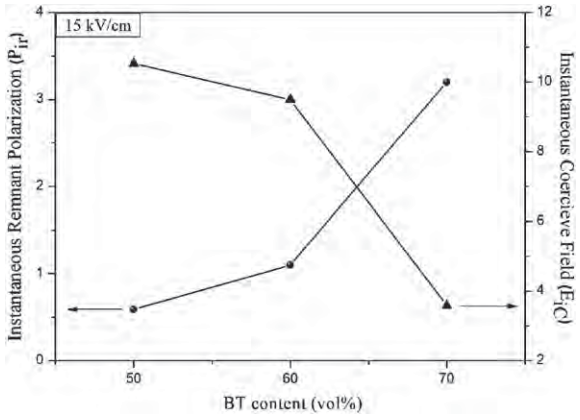

Fig. 5. Effects of BT content on P_{ir} and E_{ic} of 1-3 BT–PC composites at 15 kV/cm external electrical field amplitude.

in the composites would yield higher P_{ir} [19]. Another possibility is that this may be due to a lesser number of interfacial pores present in the composites. It is well-known that cement is a porous inorganic material with a complicated microstructure. An increase in cement content results in more pores in the composites, especially interfacial pores. When the external electric field acts on the composites, the weak conductive ions (such as OH^-, Ca^{2+}, SO_2^{4-} and Al^{3+}) in the cement will accumulate in interfacial pores. This generates a depolarization field, shielding the external electric field [9], which influences the carrying out of the total polarization and the area of the lossy characteristic of the composite. Therefore, the changes between 60% and 70% barium titanate composites are believed to be the transitions point where the benefit of lesser pores in cement and better piezoelectric properties can be noticed.

Moreover, as E_0 increases for each composite, an increase in the amplitude of E_0 makes the loop larger and increases its angle to the E axis of inclination for all composites. A consequent increase in P_{ir} is mainly due to an increase in E_0 caused by thermal excitation, leading to greater dipole alignment. The variations of P_{ir} and E_{ic} of composites with BT content under an electric field of 15 kV/cm are shown in Fig. 5. As the measured electric field increases to 15 kV/cm, a saturated and well-developed loop is observed. It can be seen that P_{ir} increases with increasing BT content, giving a maximum value of 3.20 μC/cm^2 with BT of 70 vol %, while the observed E_{ic} decreases from 10.53 kV/cm to 3.58 kV/cm as BT content increases from 50 to 70 vol %.

The plots of P_{ir} and E_{ic} against different E_0 of 70 vol % BT content can be seen in Fig. 6. It was found that when E_0 increases there is an increase in P_{ir} and E_{ic}. With applied E_0 at 5 kV/cm and 15 kV/cm, P_{ir}

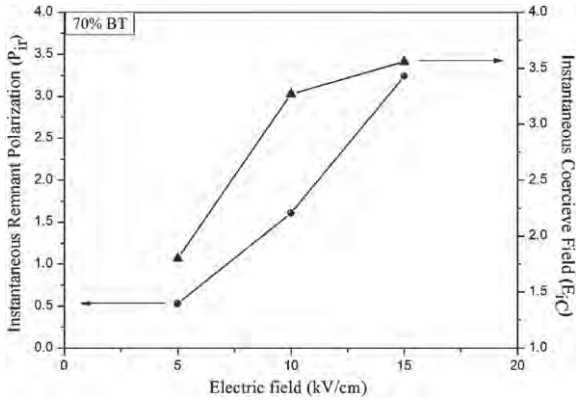

Fig. 6. Effects of external electrical field on P_{ir} and E_{ic} of 1-3 BT–PC composites (70 vol %).

values are 0.53 μC/cm^2 and 3.20 μC/cm^2, respectively, while the observed E_{ic} increases from 1.80 kV/cm to 3.58 kV/cm.

4. Conclusions

Several 1-3 BT–PC composites with various BT volume fractions have been fabricated successfully using the dice-and-fill technique. The ϵ_r values of BT–PC composites increased when the volume percentage of BT was increased. The dielectric constants of composites obtained from the experiment are close to the predictions of the parallel model, because the 1-3 connectivity is more closely related to the 2-2 parallel model. The ferroelectric hysteresis behavior of 1-3 cement-based piezoelectric composites shows that the BT volume fraction has an effect on the polarization-electric field loop. As BT volume fraction increases, P_{ir} increases while E_{ic} decreases at all applied E_0. In addition, it was found that both P_{ir} and E_{ic} increase when E_0 increases from 5 kV/cm to 15 kV/cm.

Acknowledgments

Financial support from theThailand Research Fund through the Royal Golden Jubilee Ph.D. Program (Grant No. PHD/0147/2551) to Miss Rattiyakorn Rianyoi and Asst. Prof. Dr. Arnon Chaipanich is gratefully acknowledged. The authors also wish to thank the staff members at the Electroceramics Research Laboratory, Faculty of Science, Chiang Mai University, for use of the research facilities which made this work possible. The authors would also like to express their gratitude to the Thailand Research Fund (TRF), Office of the Higher Education Commission (Thailand) and Chiang Mai University for Research Career Development Grant given to Asst. Prof. Dr. Arnon Chaipanich. The graduate school of Chiang Mai University is also acknowledged for additional support.

References

[1] Z. Li, D. Zhang, K. Wu, Cement-based 0–3 piezoelectric composites, J. Am. Ceram. Soc. 85 (2002) 305–313.
[2] S. Huang, J. Chang, R. Xu, F. Liu, L. Lu, Z. Ye, X. Cheng, Piezoelectric properties of 0-3 PZT/sulfoaluminate cement composites, Smart Mater. Struct. 13 (2004) 270–274.
[3] Z. Li, B. Dong, D. Zhang, Influence of polarization on properties of 0–3 cement-based PZT composites, Cem. Concr. Compos. 27 (2005) 27–32.
[4] B. Dong, Z. Li, Cement-based piezoelectric ceramic smart composites, Compos. Sci. Technol. 65 (2005) 1363–1371.
[5] X. Cheng, S. Huang, J. Chang, R. Xu, F. Liu, L. Lu, Piezoelectric and dielectric properties of piezoelectric ceramic–sulphoaluminate cement composites, J. Eur. Ceram. Soc. 25 (2005) 3223–3228.
[6] A. Chaipanich, N. Jaitanong, T. Tunkasiri, Fabrication and properties of PZT-ordinary Portland cement composites, Mater. Lett. 61 (2007) 5206–5208.
[7] A. Chaipanich, Dielectric and piezoelectric properties of PZT-cement composites, Curr. Appl. Phys. 7 (2007) 537–539.
[8] A. Chaipanich, Effect of PZT particle size on dielectric and piezoelectric properties of. PZT-cement composites, Curr. Appl. Phys. 7 (2007) 574–577.
[9] S. Huang, Z. Ye, Y. Hu, J. Chang, L. Lu, X. Cheng, Effect of forming pressures on electric properties of piezoelectric ceramic/sulphoaluminate cement composites, Comp. Sci. Tech. 67 (2007) 135–139.
[10] A. Chaipanich, N. Jaitanong, R. Yimnirun, Ferroelectric hysteresis behavior in 0-3 PZT-cement composites: effects of frequency and electric field, Ferr. Lett. 36 (2009) 59–66.
[11] Y. Wu, H. Zhang, Y. Zhang, J. Ma, D. Xie, Lead-free piezoelectric ceramics with composition of (0.97-x) Na1/2Bi1/2TiO_3-0.03$NaNbO_3$-x$BaTiO_3$, J. Mater. Sci. 38 (2003) 987–994.
[12] Y.M. Li, W. Chen, J. Zhou, Q. Xu, X.Y. Gu, R.H. Liao, Impedance spectroscopy and dielectric properties of $Na_{0.5}Bi_{0.5}TiO_3$-$NaNbO_3$, Physica B. 365 (2005) 76–81.
[13] M.M. Vijatović, J.D. Bobić, B.D. Stojanović, History and challenges of barium titanate: part II, Sci. Sintering 40 (2008) 235–244.
[14] J.-M. Liu, H.L.W. Chan, C.L. Choy, Y.Y. Zhu, S.N. Zhu, Z.G. Liu, N.B. Ming, Scaling on hysteresis dispersion in ferroelectric systems, Appl. Phys. Lett. 79 (2001) 236–238.
[15] X. Cheng, D. Xu, L. Lu, S. Huang, M. Jiang, Performance investigation of 1-3 p.ezoelectric ceramic-cement composite, Mater. Chem. Phys. 121 (2010) 63–69.
[16] S. Mindess, J.F. Young, D. Darwin, Concrete, second ed. Prentice Hall, Upper Saddle River NJ, 2003.
[17] D.H. Yoon, J. Zhang, B.I. Lee, Dielectric constant and mixing model of $BaTiO_3$ composite thick films, Mater. Res. Bull. 38 (2003) 765–772.
[18] F. Xing, B. Dong, Z. Li, Dielectric, piezoelectric, and elastic properties of cement-based piezoelectric ceramic composites, J. Am. Ceram. Soc. 91 (2008) 2886–2891.
[19] X. Cheng, S. Huang, J. Chang, Z. Li, Piezoelectric, dielectric, and ferroelectric properties of 0-3 ceramic/cement composites, J. Appl. Phys. 101 (2007) 094110–094116.

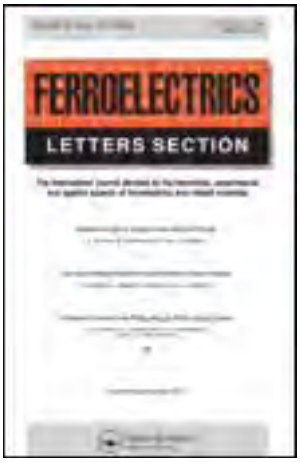

Ferroelectrics Letters Section
Publication details, including instructions for authors and subscription information:
http://www.tandfonline.com/loi/gfel20

Effect of Compressive Stress on the Ferroelectric Hysteresis Behavior in 0-3 PMN-PT/Cement Composites

N. Jaitanong [a] , R. Yimnirun [b] & A. Chaipanich [a]
[a] Department of Physics and Materials Science, Faculty of Science, Chiang Mai University, Chiang Mai 50200, Thailand
[b] School of Physics, Institute of Science, Suranaree University of Technology, and Synchrotron Light Research Institute, Nakhon Ratchasima 30000, Thailand
Published online: 16 Jun 2011.

To cite this article: N. Jaitanong , R. Yimnirun & A. Chaipanich (2011): Effect of Compressive Stress on the Ferroelectric Hysteresis Behavior in 0-3 PMN-PT/Cement Composites, Ferroelectrics Letters Section, 38:1-3, 11-17

To link to this article: http://dx.doi.org/10.1080/07315171.2011.570174

Ferroelectrics Letters, 38:11–17, 2011

ISSN: 0731-5171 print / 1563-5228 online
DOI: 10.1080/07315171.2011.570174

Effect of Compressive Stress on the Ferroelectric Hysteresis Behavior in 0-3 PMN-PT/Cement Composites

N. JAITANONG,[1] R. YIMNIRUN,[2] AND A. CHAIPANICH[1,*]

[1]Department of Physics and Materials Science, Faculty of Science, Chiang Mai University, Chiang Mai 50200, Thailand
[2]School of Physics, Institute of Science, Suranaree University of Technology, and Synchrotron Light Research Institute, Nakhon Ratchasima 30000, Thailand

Communicated by Dr. George W. Taylor
(*Received in final form October 9, 2010*)

Lead magnesium niobate titanate (PMN-PT)—Portland cement (PC) composites were produced. PMN- PT amount used in this work were 30, 50, and 70% by volume. The effects of PMN-PT content (using 30%, 50%, 70% PMN-PT) and stress on the ferroelectric polarization-electric field (P-E) hysteresis of the composites are reported in this present work. From the results, it was found that there was an increase in the instantaneous *remnant polarization* (P_{ir}) *when PMN- PT amount increased while* P_{ir} *was found to decrease when the stress was increased from 0 to 57 MPa.*

Keywords PMN-PT; cement; composite; ferroelectric hysteresis; Compressive Stress

Introduction

Recently, cement-based piezoelectric composites have been developed for structural health monitoring [1–9]. It not only has sensing function, but also actuating property, which is very suitable for application in civil engineering fields, such as high-rise buildings, long-span bridges and some buildings [1,2,10–13]. The benefit from the use of such piezoelectric-cement based composite is that these composites possess close matching to the host structure concrete than normal piezoelectric ceramic or other types of piezoelectric composites [14]. In recent years, lead magnesium niobate–lead titanate (PMN-PT) with high piezoelectric property has been widely studied as an alternative piezoelectric material for PZT [15,16]. It is the solid solution of a relaxor ferroelectric (lead magnesium niobate PMN) and a normal ferroelectric (lead titanate PT). PMN-PT with 33 mol% $PbTiO_3$ is near its morphotropic phase boundary (MPB) region (0.67PMN–0.33PT) [17], and the dielectric and piezoelectric properties are maximized because of the enhancement of polarizability between the energy states of rhombohedral and tetragonal structures [18]. Moreover, from the previous work reported that the (PMN-PT)-cement composite can be used more effectively than the PZT-cement composite with the same volume content [19].

*Corresponding author. Phone: +66 943367, Fax: +66 53 943445. E-mail: arnon@chiangmai.ac.th

In addition, the study on the ferroelectric hysteresis, which is an important behavior for materials with ferroelectric properties [20] that can be used to give indication of the difficulty of the poling process involved, of piezoleclectric-cement composites is limited. Furthermore, the study on the effect of stress on the ferroelectric hysteresis of these composites is very limited and there has been no work carry out on the study of 0–3 (PMN-PT)-cement composites. [21]. So, it is interesting to investigate the effect of stress and piezoelectric PMN-PT ceramic content on the ferroelectric polarization-electric field (*P-E*) hysteresis behavior of such piezoleclectric-cement composites.

Experimental

Cement based piezoelectric composites used in this investigation were prepared using two raw materials: normal Portland cement, PC (ordinary type: ASTM type I cement) and lead magnesium niobate titanate, PMN-PT (molar ratio of 0.67PMN—0.33PT). Solid solution of 33 mol% of lead titanate in PMN-PT system has been prepared by a columbite precursor method. Portland cement (PC) and PMN-PT ceramic particles of median size of 450 μm were mixed together and axially pressed into disks of 15 mm in diameter and about 1.75 mm in thickness to form (PMN-PT)-PC composites of 0–3 connectivity using PMN-PT volume content 30%, 50% and 70% respectively. Thereafter, the composites were cured at 98% relative humidity before taking electrical measurements. The room temperature ferroelectric hysteresis (*P–E*) loops were characterized using a computer controlled modified Sawyer-Tower circuit [22] under applied uniaxial stress of 0–57 MPa using a uniaxial compressometer at room temperature (25°C). The electric field was applied to a sample by a high-voltage ac amplifier with the input sinusoidal signal with a frequency of 50 Hz from a signal generator at the electrical field of 20kV/cm.

Results and Discussion

The (PMN-PT)-PC composites (various PMN-PT content as 30%, 50% and 70%) exhibit typical ferroelectric hysteresis (*P–E*) loops at fixed external electrical field (E_0) of 20 kV/cm and fixed frequency of 50Hz at room temperature as shown in Fig. 1(a). From Fig. 1(a), it was found that when the PMN-PT volume fraction increased, the *instantaneous* remnant polarization (P_{ir}) was increased. From Fig 1(b), the P_{ir} value was found to increase from 9.05 to 17.95 μC/cm^2 (from 30% to 70% PMN-PT content) and the value of *instantaneous* coercive field (E_{ic}) increased from 13.30 to 14.75 kV/cm (from 30% to 70% PMN-PT content). It can be explained that the PMN-PT has a strong ferroelectricity when increasing PMN-PT content in the composite, the higher *instantaneous* remnant polarization (P_{ir}) of the composite will be [6]. The *P-E* loops of the (PMN-PT)-cement composites show a "*lossy*" feature [12] for all PMN-PT content, as a result of cement matrix in the composites, in which possibly many weak conducting ions such as Ca^{2+}, OH^-, Si^{4+}, Al^{3+} begin to migrate besides the polarization of electron when an external electrical field acts on the cement matrix. These ions cause higher conducting loss in the composites; hence a lossy feature is observed in all the P-E loops obtained [8,10].

In addition, from Fig. 2(a, b and c), it can be seen that there are an decrease in the *instantaneous* remnant polarization (P_{ir}) when the stress increases from 0 to 57 MPa for PMN-PT content as 30%, 50% and 70% respectively. Furthermore, it is clearly seen that the stress has an effect on the hysteresis ferroelectric loop of these composites. In order to see the effect on P_{ir} and E_{ic} more clearly, the effect of stress on these values are plotted as

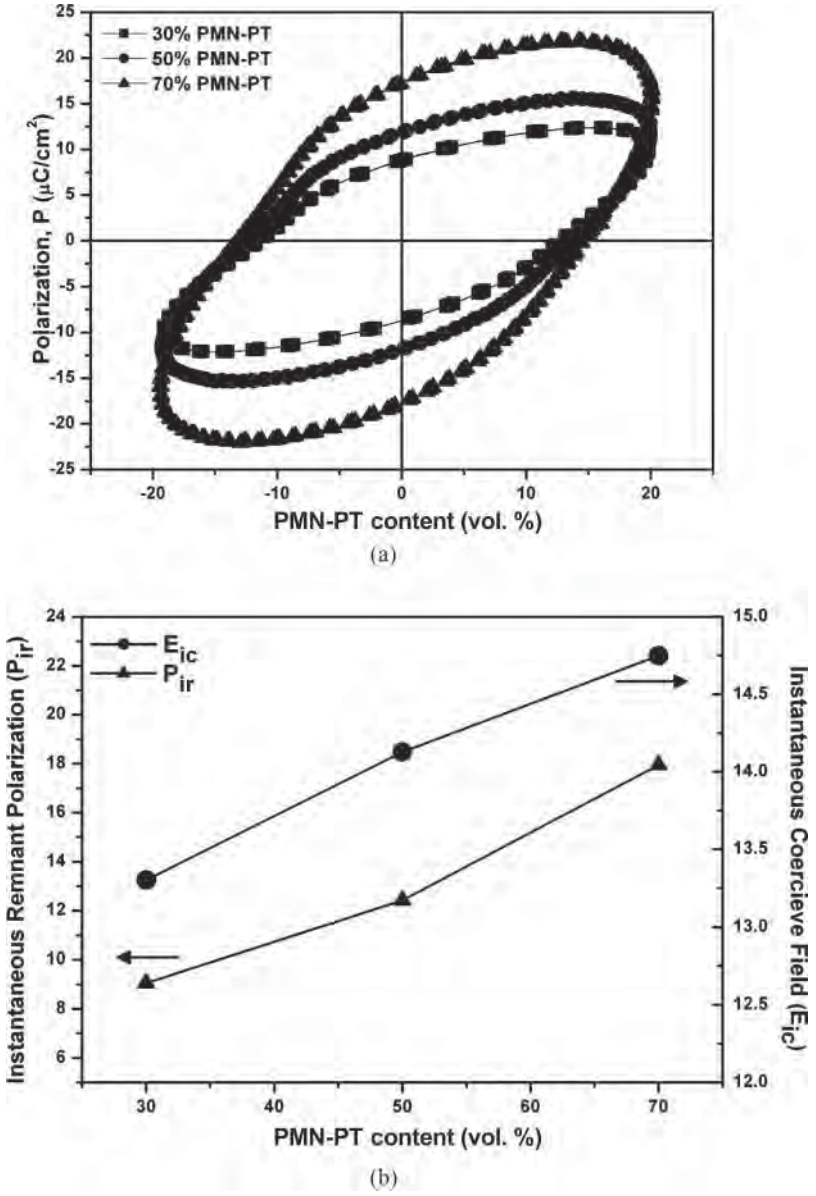

Figure 1. Effects of PMN-PT content on the ferroelectric (*P-E*) hysteresis loops (a), instantaneous remnant polarization (P_{ir}) and *instantaneous* coercive field (E_{ic}) (b), of (PMN-PT)-PC composites with fixed f of 50 Hz and fixed E_0 of 20 kV/cm.

shown in Fig. 3(a), (b) and (c) for PMN-PT content as 30%, 50% and 70% respectively. For the applied stress of 0 to 57 MPa the *instantaneous* remnant polarization (P_{ir}) was seen to decrease from 9.1 to 7.5 μC/cm^2 while the "*instantaneous*" coercive field (E_{ic}) values decrease from 13.6 to 12.9 kV/cm for PMN-PT content as 30% (Fig. 3(a)). Again, similar trends can be seen in these composites at higher PMN-PT content of 50% and 70% as shown in Fig. 3 (b) and (c), respectively.

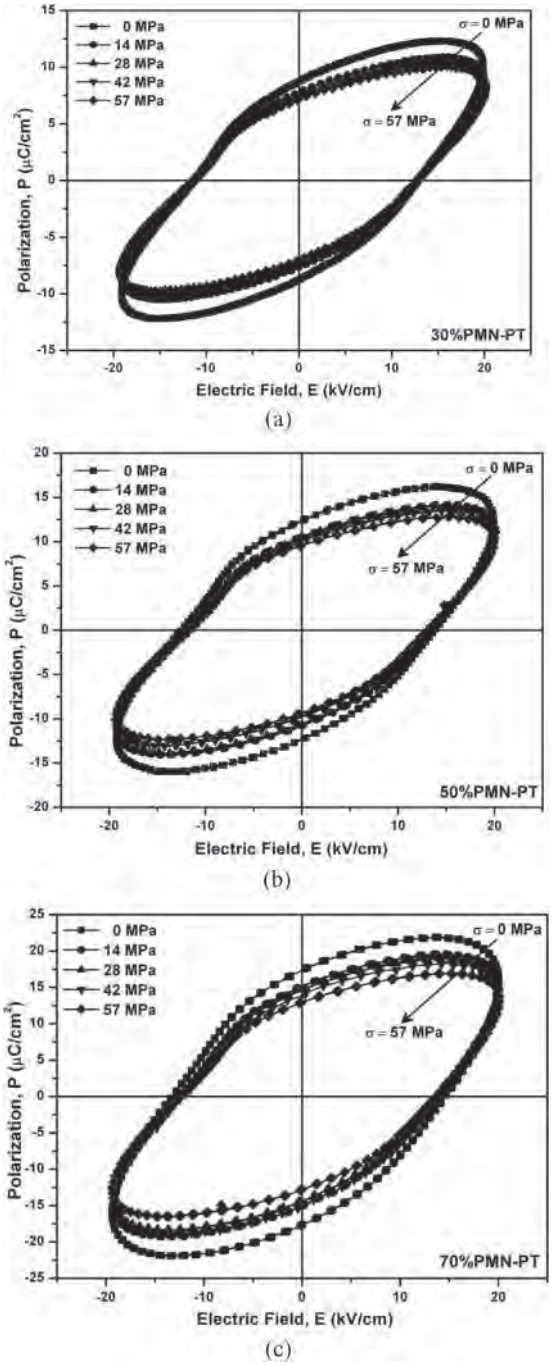

Figure 2. Effect of stress on the ferroelectric (*P-E*) hysteresis loops of (PMN-PT)-cement composites for 30% PMN-PT content (a), 50% PMN-PT content (b) and 70% PMN-PT content (c), with fixed f of 50 Hz and fixed E_0 of 20 kV/cm.

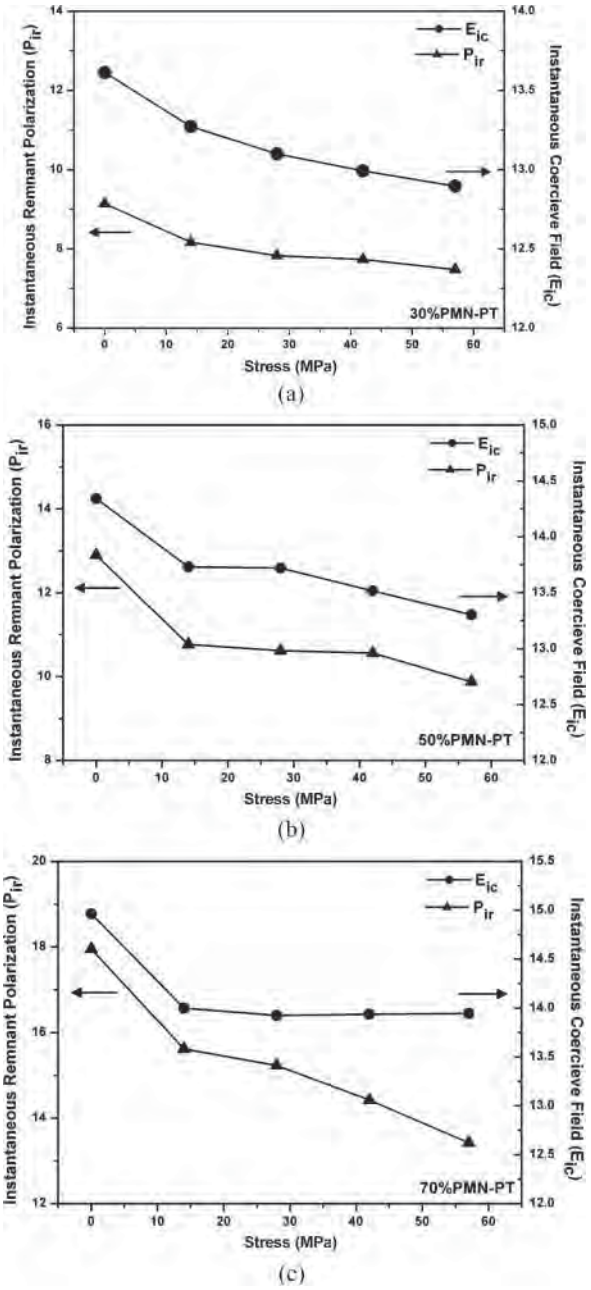

Figure 3. Effect of stress on the instantaneous remnant polarization (P_{ir}) and coercive field (E_{ic}) of of (PMN-PT)-cement composites for 30% PMN-PT content (a), 50% PMN-PT content (b) and 70% PMN-PT content (c), with fixed f of 50 Hz and fixed E_0 of 20 kV/cm.

At the PMN-PT content of 50%, with increasing the applied stress a reduction in the P_{ir} value is seen from 12.9 to 9.8 μC/cm^2 and the E_{ic} values decrease from 14.3 to 13.3 kV/cm. For the PMN-PT content of 70%, P_{ir} was seen to decrease from 17.9 to 13.4 μC/cm^2 and E_{ic} values decrease from 14.9 to 13.9 kV/cm. Furthermore, it is noted that

there is a greater effect of applied stress on the P_{ir} value of the composite at higher PMN-PT content. Therefore, the difference in the P_{ir} value between the applied stress of 57 MPa and 0 MPa at 30%PMN-PT content is $\approx 1.6 \mu C/cm^2$ and was found to be higher at 70%PMN-PT ($\approx 4.5\ \mu C/cm^2$).

Moreover, it is interesting to note that (PMN-PT)-cement based composite with the same volume content of 50% and at similar applied field conditions and stress (50Hz at 20kV/cm and 0–57MPa), P_{ir} for (PMN-PT)-cement composite is considerably higher than PZT-cement based composite previously reported [21]. This may suggests that the (PMN-PT)-cement composite can be used more effectively than the PZT-cement composite.

Conclusions

The 0–3 cement-based piezoelectric composites with various PMN-PT volume fractions and applied stress were fabricated by compressing technique. The results obtained from the experiments are summarized as follows: for the ferroelectric hysteresis properties, when the PMN-PT volume fraction increases from 30% to 70%, the *instantaneous* remnant polarization (P_{ir}) increases. Moreover, the stress is shown to have an effect on the ferroelectric hysteresis of (PMN-PT)-cement composites. While, P_{ir} is shown to reduce noticeably with an increase in applied stress.

Acknowledgments

Ms. Nittaya Jaitanong would like to thank the Office of the Higher Education Commission, Thailand supported by grant fund under the program Strategic Scholarships for Frontier Research Network for the Ph.D. Program Thai Doctoral degree for this research. Ms. Nittaya Jaitanong would also like to acknowledge the Graduate School of Chiang Mai University. The authors would also like to express their gratitude for TRF-CHE Research Grant for Mid-Career University Faculty awarded to Assistant Prof. Dr. Arnon Chaipanich by the Thailand Research Fund (TRF), Office of the Higher Education Commission (Thailand) and Chiang Mai University.

References

1. R. E. Newnham and A. Amin, Smart systems, Microphones, fish farming, and beyond—Smart materials, acting as both sensors and actuators, can mimic biological behavior. *Chem Tech.* **29**, 38–47 (1999).
2. H. Shifeng, Y. Zhengmao, H. Yali, C. Jun, L. Lingchao, and C. Xin, Effect of forming pressures on electric properties of piezoelectric ceramic/sulphoaluminate cement composites. *Comp Sci Tech.* **67**, 135–139 (2007).
3. A. Chaipanich, N. Jaitanong, and T. Tunkasiri, Fabrication and properties of PZT-ordinary Portland cement composites. *Mater Lett.* **61**, 5206–5208 (2007).
4. A. Chaipanich and N. Jaitanong, Effect of polarization on the microstructure and piezoelectric properties of PZT-Cement composites. *Adv Mater Res.* **55**, 381–384 (2008).
5. N. Jaitanong, K. Wongjinda, P. Tammakun, G. Rujijanagul, and A. Chaipanich, Effect of carbon addition on dielectric properties of 0–3 PZT-portland cement composite. *Adv Mats Res.* **55**, 377–380 (2008).
6. N. Jaitanong, A. Chaipanich, and T. Tunkasiri, Properties 0–3 PZT-Portland cement composites. *Ceram Inter.* **34**, 793–795 (2008).
7. N. Jaitanong and A. Chaipanich, Effect of poling temperature on piezoelectric properties of 0–3 PZT-Portland cement composites. *Ferr Lett.* **35**, 17–23 (2008).

8. A. Chaipanich, N. Jaitanong, and R. Yimnirun, Ferroelectric hysteresis behavior in 0–3 pzt-cement composites: Effects of frequency and electric field. *Ferr Lett.* **36**, 59–66 (2009).
9. A. Chaipanich and N. Jaitanong, Effect of PZT particle size on the electromechanical coupling coefficient of 0–3 PZT-cement composites. *Ferr Lett.* **36**, 37–44 (2009).
10. C. Xin, H. Shifeng, C. Jun, and Z. Li, Piezoelectric, dielectric, and ferroelectric properties of 0–3 ceramic/cement composites. *J App phys.* **101**, 094110–6 (2007).
11. A. Chaipanich and N. Jaitanong, Effect of poling time on piezoelectric properties of 0–3 PZT-Portland cement composites. *Ferr Lett.* **35**, 73–78 (2008).
12. N. Jaitanong, R. Yimnirun, and A. Chaipanich, Effect of uniaxial stress on dielectric properties of 0–3 PZT-Portland cement composite. *Ferroelectrics*. **384**, 174–181 (2009).
13. N. Jaitanong, R. Rianyoi, R. Potong, R. Yimnirun, and A. Chaipanich, Effects of PZT Content and Particle Size on Ferroelectric Hysteresis Behavior of 0–3 Lead Zirconate Titanate-Portland Cement Composites. *Int Ferro.* **107**, 43–52 (2009).
14. Z. Li, D. Zhang, and K. Wu, Cement-Based 0–3 piezoelectric composites. *J Am Cream Soc.* **85**, 305–313 (2002).
15. S. W. Choi, T. R. Shrout, S. J. Jang, and A. S. Bhalla, Morphotropic phase boundary in Pb ($Mg_{1/3}Nb_{2/3}$) O_3-$PbTiO_3$ system. *Mater Lett.* **8**, 253–255 (1989).
16. L. F. Brown, R. L. Carlson, J. M. Sempsrott, G. T. Stranford, and J. J. Fitzgerald, Investigation of the dielectric and piezoelectric properties of PMN and PMN-PT materials for ultrasonic transducer applications. *Ultra Sym Proceeding IEEE.* **1**, 561–564 (1997).
17. T. R. Shrout, Z. P. Chang, N. Kim, and S. Markgraf, Dielectric behaviour of single crystals near the (*1-x*) $Pb(Mg_{1/3}Nb_{2/3})O_3$-*x* $PbTiO_3$ morphotrophic phase boundary. *Ferr Lett.* **12**, 63–69 (1990).
18. K. H. Lam, H. L. W. Chan, H. S. Luo, Q. R. Yin, Z. W. Yin, and C. Choy, Dielectric properties of 65PMN–35PT/P(VDF–TrFE) 0–3 composites. *Microelectron Eng.* **66**, 792–797 (2003).
19. N. Jaitanong, W. C. Vittayakorn, R. Yimnirun, and A. Chaipanich, Ferroelectric hysteresis behavior of 0–3 PMNT-cement composites. *Ferr Lett.* **36**, 59–66 (2010).
20. J. M. Liu, H. L. W. Chan, C. L. Choy, Y. Y. Zhu, S. N. Zhu, Z. G. Liu, and N. B. Ming, Scaling on hysteresis dispersion in ferroelectric systems. *Appl Phys Lett.* **79**, 236–238 (2001).
21. A. Chaipanich, N. Jaitanong, and R. Yimnirun, Effect of compressive stress on the ferroelectric hysteresis behavior in 0–3 PZT-cement composites. *Mater Lett.* **64**, 562–564 (2010).
22. R. Yimnirun, S. Ananta, Y. Laosiritaworn, A. Ngamjarurojana, and S. Wongsaenmai, Scaling Behavior of dynamic ferroelectric hysteresis in soft PZT ceramic: Stress dependence. *Ferroelectrics.* **358**, 3–11 (2007).

www.amf-amec-2010.org

The 7th AMF-AMEC-2010

The 7th Asian Meeting on Ferroelectricity and the 7th Asian Meeting on ElectroCeramics

June 28 - July 1, 2010
Ramada Plaza Jeju Hotel, Jeju, Korea

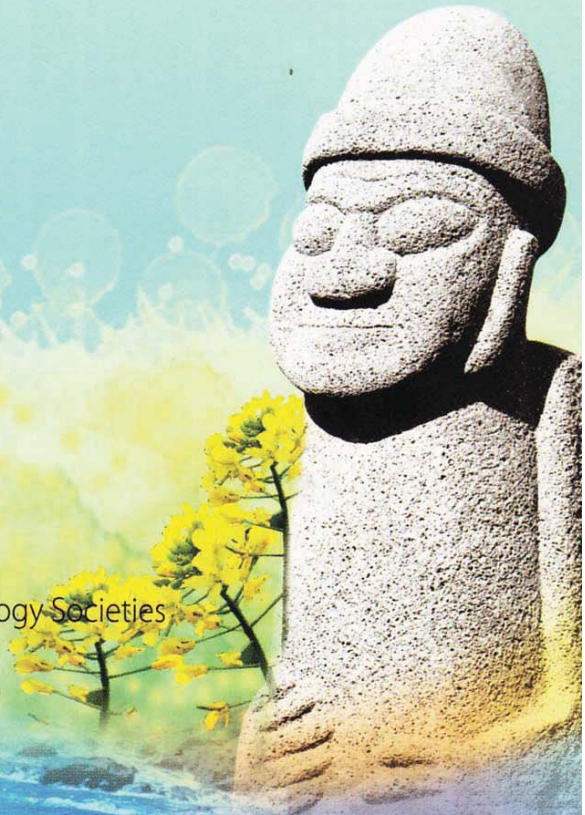

Organized by
The Korean Physical Society
The Korean Ceramic Society

Sponsored by
Korean Federation of Science and Technology Societies
National Research Foundation of Korea
IEEE-UFFC
Lotte Scholarship Foundation
Hynix Semiconductor Inc
Nextron Corporation
Park Systems
Seoul National University
BK 21 Materials Education and Research Division, Seoul National University
Kyonggi University
The Basic Science Research Institute, University of Ulsan
The Institute for Basic Science, Changwon National University
Jeju Special Self-Governing Province
Korea Tourism Organization

1-a-P118

Effects of Cr doping on ferroelectric properties of $K_{0.5}Bi_{4.5}Ti_4O_{15}$ thin films prepared by chemical solution deposition

Dalhyun Do[1], Jin Won Kim[1], Sang Su Kim[1], Won Jeong Kim[1], Tae Kwon Song[2], and Byung Chun Choi[3]*([1]Department of Physics, Changwon National University, Korea,[2]School of Nano and Advanced Materials Engineering, Changwon National University, Korea, [3]Department of Physics, Pukyong National University, Korea)*

1-a-P119

Effects of V-doping on electrical properties of $Na_{0.5}Bi_{4.5}Ti_4O_{15}$ thin films prepared by chemical solution deposition

Jin Won Kim[1], Dalhyun Do[1], Sang Su Kim[1], Won Jeong Kim[1], Tae Kwon Song[2], and Byung Chun Choi[3]*([1]Department of Physics, Changwon National University, Korea, [2]School of Nano and Advanced Materials Engineering, Changwon National University, Korea, [3]Department of Physics, Pukyong National University, Korea)*

1-a-P120

Improved Dielectric Properties of Grain Oriented $(Na_{0.51}K_{0.47}Li_{0.02})(Nb_{0.8}Ta_{0.2})O_3$ Thick Films Prepared by Electrophoretic Deposition

D. S. Lee[1,2], S. J. Jeong[1], M. S. Kim[1], J. S. Song[1] and K. H. Kim[2]*([1]Advanced Materials & Application Research Laboratory, Korea, Electrotechnology Research Institute, Korea,[2]National Core Research Center for Hybrid Materials Solution, Pusan National University, Korea)*

1-a-P121

Piezoelectric Effect in Composites of Polymer-Ferroactive Solid Solution with Deep Trapping Center at Interphase Boundary

M.A.Kurbanov, F.N.Tatardar, A.A.Bayramov, N.A.Safarov, A.A.Mextili, and I.S.Sultanaxmedova (Institute of Physics Azerbaijan National Academy of Sciences, Azerbaijan)

1-a-P122

Withdrwan

1-a-P123

Dielectric and Ferroelectric Properties of 1-3 Barium Titanate – Portland Cement Composites

R. Rianyoi[1], R. Potong[1], N. Jaitanong[1], R. Yimnirun[2], A. Ngamjarurojana[1] and A. Chaipanich[1] *([1]Department of Physics and Materials Science, Faculty of Science, Chiang Mai University, Thailand, [2]School of Physics, Institute of Science, Suranaree University of Technology, Thailand)*

1-a-P124

Ferroelectric Hysteresis Behavior and Dielectric properties of 1-3 Lead Zirconate Titanate –Cement Composites

R. Potong[1], R. Rianyoi[1], N. Jaitanong[1], R. Yimnirun[2], and A. Chaipanich[1] *([1]Department of Physics and Materials Science, Faculty of Science, Chiang Mai University, Thailand, [2]School of Physics, Institute of Science, Suranaree University of Technology, Thailand)*

1-a-P125

Investigations on Chemical Compositions of Lead Nickel Niobate Ceramics using X-ray

1-a-P123

Dielectric and Ferroelectric Properties of 1-3 Barium Titanate – Portland Cement Composites

R. Rianyoi[1*], R. Potong[1], N. Jaitanong[1], R. Yimnirun[2], A. Ngamjarurojana[1] and A. Chaipanich[1+]

[1] Department of Physics and Materials Science, Faculty of Science, Chiang Mai University, Chiang Mai, 50200, Thailand
[2] School of Physics, Institute of Science, Suranaree University of Technology, Nakhon Ratchasima, 30000, Thailand

*E-mail of the first author: r.rianyoi@gmail.com
+E-mail of the corresponding author: arnon@chiangmai.ac.th

In the current work, the dielectric and ferroelectric properties of 1-3 Barium titanate - Portland cement composites has been studied as a potential lead - free piezoelectric - cement - based composites. The 1-3 Barium titanate - Portland cement composites were fabricated by dice-and fill technique with Barium titanate : Portland cement ratios of 50:50, 60:40 and 70:30 by volume. The results indicate that the dielectric constant (ε_r) of the composite materials increases as the barium titanate volume fraction increases, which follows the parallel model. The room temperature dielectric constants (ε_r) at 1 kHz of 70% barium titanate composite was found to have values higher than 750. The loss tangent ($\tan\delta$) results were found to decrease with increasing barium titanate volume fraction. On the other hand, the ferroelectric hysteresis loops of composite materials indicate that the "instantaneous" remnant polarization (P_{ir}) increase as the barium titanate volume fraction increases. The "instantaneous" remnant polarization (P_{ir}) at 15 kV/cm (90 Hz) of 70% barium titanate composite was found to have value ≈ 3 $\mu C/cm^2$.

www.amf-amec-2010.org

The 7th AMF-AMEC-2010

The 7th Asian Meeting on Ferroelectricity and the 7th Asian Meeting on ElectroCeramics

June 28 - July 1, 2010
Ramada Plaza Jeju Hotel, Jeju, Korea

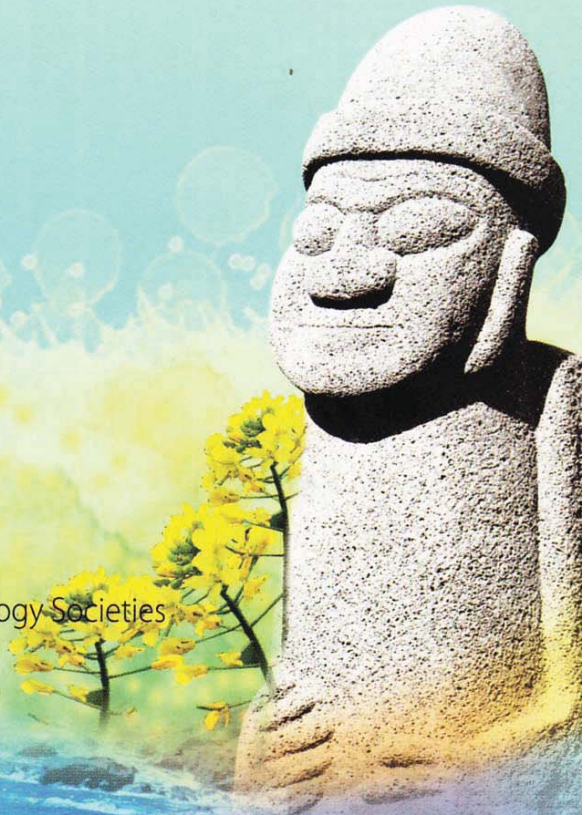

Organized by
The Korean Physical Society
The Korean Ceramic Society

Sponsored by
Korean Federation of Science and Technology Societies
National Research Foundation of Korea
IEEE-UFFC
Lotte Scholarship Foundation
Hynix Semiconductor Inc
Nextron Corporation
Park Systems
Seoul National University
BK 21 Materials Education and Research Division, Seoul National University
Kyonggi University
The Basic Science Research Institute, University of Ulsan
The Institute for Basic Science, Changwon National University
Jeju Special Self-Governing Province
Korea Tourism Organization

2-b-P41

Design and analysis of a piezoelectric film diaphragm used as a biosensor platform

Shaokang Li[1,2], Wei Ren[1], Xiaofeng Chen[1], Peng Shi[1], Xiaoqing Wu[1], and Xi Yao[1] *([1]Electronic Materials Research Laboratory , Key Laboratory of the Ministry of Education, Xi'an Jiaotong University, China, [2]School of Mechanical and Electronic Engineering , Xi'an Technological University, China)*

2-b-P42

A Characteristics of Piezoelectric thin films deposited on LTCC substrates

H. S. Hwang[1], W. S. Choi[2], and J. T. Song[3] *([1]Department of Elctronics, Seoil University, Korea, [2]Department of Electrical Engineering, Hanbat University, Korea, [3]School of Information and Communication Engineering, Sungkyunkwan University, Korea)*

2-d-PII Composites, Multiphase, and Nanostructured Ceramics

2-d-P01

Effect of Compressive Stress on the Ferroelectric Hysteresis Behavior in 0-3 (PMN-PT)-Cement Composites

N. Jaitanong[1], R. Yimnirun[2] and A. Chaipanich[1] *([1]Department of Physics and Materials Science, Faculty of Science, Chiang Mai University, Thailand, [2]School of Physics, Institute of Science, Suranaree University of Technology, Thailand)*

2-d-P02

Analyzing the Resonance Performance of the Square 1-3-2 Piezoelectric Composite Plate by ANSYS

Li Li[1], Wang Li-kun[2], Fan Tianbo[3], and Qin Lei[2] *([1]Department of Computer Science and Technology, Shenyang Institute of Chemical Technology, China, [2] Beijing key laboratory for sensor, Beijing Information Science & Technology University, China, [3]Department of Chemical Engineering, Shenyang Institute of Chemical Technology, China)*

2-d-P03

Dielectric and Ferroelectric Hysteresis Properties of 1-3 Lead Magnesium Niobate-Lead Titanate Ceramic/Portland Cement Composites

A. Chaipanich[1], R. Potong,[1] R. Rianyoi[1], L. Jareansuk [1], N. Jaitanong[1] , and R. Yimnirun[2] ([1] *Department of Physics and Materials Science, Faculty of Science, Chiang Mai University, Thailand,* [2] *School of Physics, Institute of Science, Suranaree University of Technology, Thailand)*

2-d-P04

Piezoelectric and dielectric properties of $(K_{0.44}Na_{0.52}Li_{0.04})(Nb_{0.86}Ta_{0.10}Sb_{0.04})O_3$ – PVDF composites

J.H. Seol[1], C.Y. Kim[1], J.S. Lee[2] and W.P. Tai[1] *([1] Ulsan Fine Chemical Industry Center, Ulsan Techno Park, Korea,* [2] *School of Materials Science and Engineering, University of Ulsan, Korea)*

2-d-P05

Zinc oxide nanowires fabricated by laser chemical vapor deposition using different metal catalyst

O. T. Tambunan[1,2], Hadiyawarman[1], C. U. Jung[1], B. W. Lee[1], C. Liu[1], J. W. Choi[3], H. J. Ji[3], and

2-d-P03

Dielectric and Ferroelectric Hysteresis Properties of 1-3 Lead Magnesium Niobate-Lead Titanate Ceramic/Portland Cement Composites

A. Chaipanich[1*+], R. Potong,[1] R. Rianyoi[1], L. Jareansuk [1], N. Jaitanong[1] and R. Yimnirun[2]

[1] Department of Physics and Materials Science, Faculty of Science, Chiang Mai University, Chiang Mai 50200, Thailand

[2] School of Physics, Institute of Science, Suranaree University of Technology, Nakhon Ratchasima 30000 Thailand

*E-mail of the first author: arnon@chiangmai.ac.th

+E-mail of the corresponding author: arnon@chiangmai.ac.th

In this work, lead magnesium niobate- lead titanate ceramic (PMN-PT) was used with Portland Cement (PC) to produce 1-3 connectivity PMN-PT/PC composites using the dice and fill method. Composites with PMN-PT ceramic volume content of 60 % were investigated. The room temperature dielectric constant (ε_r) at 1 kHz of the PMN-PT/PC composite was found to be ≈ 1500. At higher frequency (20 kHz), the dielectric constant reduced to the value of ≈ 1300. Ferroelectric polarization-electric field (*P*-*E*) hysteresis loops at 30-90 Hz and varying electric field were observed. The "instantaneous" remnant polarization (P_{ir}) measured at 50 Hz and at the electric field of 10 kV/cm of the PMN-PT/PC composite was found to be ≈ 10μC/cm^2.

www.amf-amec-2010.org

The 7th AMF-AMEC-2010

The 7th Asian Meeting on Ferroelectricity and the 7th Asian Meeting on ElectroCeramics

June 28 - July 1, 2010
Ramada Plaza Jeju Hotel, Jeju, Korea

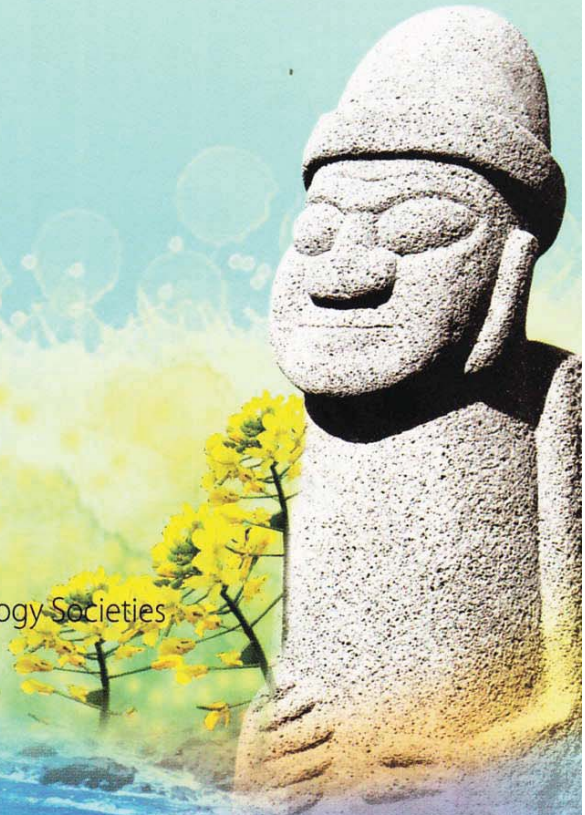

Organized by
The Korean Physical Society
The Korean Ceramic Society

Sponsored by
Korean Federation of Science and Technology Societies
National Research Foundation of Korea
IEEE-UFFC
Lotte Scholarship Foundation
Hynix Semiconductor Inc
Nextron Corporation
Park Systems
Seoul National University
BK 21 Materials Education and Research Division, Seoul National University
Kyonggi University
The Basic Science Research Institute, University of Ulsan
The Institute for Basic Science, Changwon National University
Jeju Special Self-Governing Province
Korea Tourism Organization

1-a-P118

Effects of Cr doping on ferroelectric properties of $K_{0.5}Bi_{4.5}Ti_4O_{15}$ thin films prepared by chemical solution deposition

Dalhyun Do[1], Jin Won Kim[1], Sang Su Kim[1], Won Jeong Kim[1], Tae Kwon Song[2], and Byung Chun Choi[3]*([1]Department of Physics, Changwon National University, Korea,[2]School of Nano and Advanced Materials Engineering, Changwon National University, Korea, [3]Department of Physics, Pukyong National University, Korea)*

1-a-P119

Effects of V-doping on electrical properties of $Na_{0.5}Bi_{4.5}Ti_4O_{15}$ thin films prepared by chemical solution deposition

Jin Won Kim[1], Dalhyun Do[1], Sang Su Kim[1], Won Jeong Kim[1], Tae Kwon Song[2], and Byung Chun Choi[3]*([1]Department of Physics, Changwon National University, Korea, [2]School of Nano and Advanced Materials Engineering, Changwon National University, Korea, [3]Department of Physics, Pukyong National University, Korea)*

1-a-P120

Improved Dielectric Properties of Grain Oriented $(Na_{0.51}K_{0.47}Li_{0.02})(Nb_{0.8}Ta_{0.2})O_3$ Thick Films Prepared by Electrophoretic Deposition

D. S. Lee[1,2], S. J. Jeong[1], M. S. Kim[1], J. S. Song[1] and K. H. Kim[2]*([1]Advanced Materials & Application Research Laboratory, Korea, Electrotechnology Research Institute, Korea,[2]National Core Research Center for Hybrid Materials Solution, Pusan National University, Korea)*

1-a-P121

Piezoelectric Effect in Composites of Polymer-Ferroactive Solid Solution with Deep Trapping Center at Interphase Boundary

M.A.Kurbanov, F.N.Tatardar, A.A.Bayramov, N.A.Safarov, A.A.Mextili, and I.S.Sultanaxmedova (Institute of Physics Azerbaijan National Academy of Sciences, Azerbaijan)

1-a-P122

Withdrwan

1-a-P123

Dielectric and Ferroelectric Properties of 1-3 Barium Titanate – Portland Cement Composites

R. Rianyoi[1], R. Potong[1], N. Jaitanong[1], R. Yimnirun[2], A. Ngamjarurojana[1] and A. Chaipanich[1] *([1]Department of Physics and Materials Science, Faculty of Science, Chiang Mai University, Thailand, [2]School of Physics, Institute of Science, Suranaree University of Technology, Thailand)*

1-a-P124

Ferroelectric Hysteresis Behavior and Dielectric properties of 1-3 Lead Zirconate Titanate –Cement Composites

R. Potong[1], R. Rianyoi[1], N. Jaitanong[1], R. Yimnirun[2], and A. Chaipanich[1] *([1]Department of Physics and Materials Science, Faculty of Science, Chiang Mai University, Thailand, [2]School of Physics, Institute of Science, Suranaree University of Technology, Thailand)*

1-a-P125

Investigations on Chemical Compositions of Lead Nickel Niobate Ceramics using X-ray

1-a-P124

Ferroelectric Hysteresis Behavior and Dielectric properties of 1-3 Lead Zirconate Titanate –Cement Composites

R. Potong[1*], R. Rianyoi[1], N. Jaitanong[1], R. Yimnirun[2], and A. Chaipanich[1+]

[1] Department of Physics and Materials Science, Faculty of Science, Chiang Mai University, Chiang Mai, 50200, Thailand

[2] School of Physics, Institute of Science, Suranaree University of Technology, Nakhon Ratchasima, 30000, Thailand

*E-mail of the first author: ja_rho@hotmail.com

+E-mail of the corresponding author: arnon@chiangmai.ac.th

The effect of 1-3 Lead Zirconate Titanate (PZT) – Portland cement (PC) Composites on the ferroelectric hysteresis behavior and dielectric properties were investigated. Lead zirconate titanate: Portland cement ratios used were 60:40, 70:30 and 80:20. PZT ceramic was mixed with Portland cement to form 1-3 connectivity PZT-PC composite by a dice-and-fill technique. The results showed that the dielectric constant of the composite materials increased with PZT content and the dielectric constant (ε_r) value was 781 for 80% PZT composite at 1 kHz. The dielectric loss tangent (tanδ) was found to decrease with increasing PZT content and the tanδ value of 80% PZT composite was 0.06. Parallel and series models were also compared to the dielectric measurement results. For the hysteresis measurements, the ferroelectric hysteresis loops can be seen for all composites. The "instantaneous" remnant polarization (P_{ir}) was found to increase with increasing PZT content from 3.20 to 4.28 μC/cm^2 at 90 Hz when PZT volume content used was 60% and 80% respectively.

Graduate School of Agriculture &
Center for Southeast Asian Studies

UNIVERSITY OF SHIZUOKA

UNIVERSITY OF
LIVERPOOL

The 1st *EnvironmentAsia* International Conference on

"Environmental Supporting in Food and Energy Security: Crisis and Opportunity"

22-25 March, 2011
Rama Garden Hotel, Bangkok, Thailand

ISBN 978-974-11-1446-7

สมาคมสถาบันอุดมศึกษาสิ่งแวดล้อมไทย

Thai Society of Higher Education Institutes on Environment

29 November 2010

Dear Rattiyakorn Rianyoi,

I am pleased to inform you that your abstract titled "Effect of BNT Content of 0-3 Bismuth Sodium Titanate-Portland Cement Composites on Dielectric Properties" have been accepted for a presentation at **The 1st *EnvironmentAsia* International Conference**, which will be held at the Rama Garden Hotel, from March 22 through March 25, 2011 in Bangkok, THAILAND.

As the abstract will be published in the book of abstract, I request you to kindly submit your well proofed abstract before **30 November 2010**, in case, if any corrections be needed, please have it done within the time stated. Full-paper to publish in Conference Proceedings or *EnvironmentAsia* International Journal must be submitted no later than **15 December 2010** via e-mail to enbrp@mahidol.ac.th and enljt@mahidol.ac.th.

Finally, I would like to remind you that the early-bird payment should be made no later than **30 December 2010**. Please find attached file here is registration form. Please choose your interest topics and your registration status (oral or poster presentation) in registration form.

I look forward to seeing you at The 1st *EnvironmentAsia* International Conference in Bangkok, Thailand.

Yours sincerely,

(Asst. Prof. Dr Sittipong Dilokwanich)
President of Thai Society of Higher Education Institutes on Environment

คณะสิ่งแวดล้อมและทรัพยากรศาสตร์ มหาวิทยาลัยมหิดล 999 ถนนพุทธมณฑลสาย ๔ ตำบลศาลายา อำเภอพุทธมณฑล จังหวัดนครปฐม 73170
โทรศัพท์ (662) 441 5000 ต่อ 212-214 โทรสาร (662) 441 9510 Website: www.en.mahidol.ac.th/tshepc

Faculty of Environment and Resource Studies, Mahidol University , 999 Phuttamonthon 4 Rd., Salaya, Puttamonthon, Nakhon Pathom 73170 Thailand
Tel. (662) 441 5000 ext 212-214 Fax. (662) 441 9510 Website: www.en.mahidol.ac.th/tshepc

Thai Society of Higher Education Institutes on Environment

The 1st EnvironmentAsia International Conference on
"Environmental Supporting in Food and Energy Security: Crisis and Opportunity"
22-25 March 2011, Bangkok, Thailand

Effect of BNT Content of 0-3 Bismuth Sodium Titanate–Portland Cement Composites on Dielectric Properties

Rattiyakorn Rianyoi*, Ruamporn Potong, Nittaya Jaitanong and Arnon Chaipanich
Department of Physics and Materials Science, Faculty of Science, Chiang Mai University, Chiang Mai 50200, Thailand. E-mail: r.rianyoi@gmail.com

Abstract

The use of lead-free piezoelectric materials such as bismuth sodium titanate (BNT) has recently become a very important concept in protection the earth environment. In this research, the effect of BNT content of 0-3 bismuth sodium titanate (BNT)- Portland cement (PC) composites on dielectric properties were studied as potential candidates as lead-free piezoelectric-cement-based composites. 0-3 BNT-PC composites were fabricated using 30%, 50% and 70% of BNT by volume. Dielectric constant (ε_r) and dielectric loss ($tan\delta$) at room temperature and at various frequencies (0.1-20 kHz) of the 0-3 BNT-PC composites with different BNT content were then investigated. The results indicate that the dielectric constant decreases with increasing frequency. The dielectric loss ($tan\delta$) also decreases with the increase of frequency and shows the variation similar to dielectric constant (ε_r). On the other hand, the dielectric constant (ε_r) of the composite materials increases as the BNT volume fraction increases. The room temperature ε_r at 1 kHz are 121 and 201 for composites with 30% and 70% bismuth sodium titanate composites respectively. The loss tangent ($tan\delta$) results were found to decrease with increasing bismuth sodium titanate volume fraction and the $tan\delta$ of 70% bismuth sodium titanate composite was found to have a lowest value of 0.41.

Keywords: BNT; cement; composites; dielectric properties

1. Introduction

Nowadays more attention has been paid to smart structures in civil engineering, the health monitoring of structures and active vibration control of structures. The structural health monitoring is helpful to assure the security of important structures such as high-rise buildings, large-span bridges, nuclear waste containment structures, etc [1-2]. In addition, piezoelectricity has been proved to be one of the most efficient mechanisms for most applications in smart structure. Therefore, piezoelectric materials have attracted grate attention. Recently, the development of 0-3 type cement-based piezoelectric ceramic composites, incorporating lead zirconate titanate (PZT) ceramic into cement matrix have been fabricated and studied [3-7]. Combining piezoelectric ceramics and cements, the composites appear to possess reasonable piezoactive properties as well as good compatibility with concrete. Its physical properties such as acoustic impedance and temperature coefficient are similar to that of concrete. However, lead oxide, which is a component of PZT, vaporization and contamination during processing and disposal cause a crucial environmental pollution. Therefore, it is desirable to use lead-free piezoelectric ceramics with similar properties to replace PZT in the near future. The search for alternative piezoelectric ceramic is now a very active research topic and a great deal of attention has been focused on bismuth sodium titanate $Bi_{0.5}Na_{0.5}TiO_3$ (BNT). BNT recently attracted attention as an environmentally friendly lead-free compound which exhibits attractive piezoelectric properties, high anisotropic electro-

mechanical coupling property (K_p = 16.5-25.5%, $K_t \geq$ 48%), high Curie temperature of 320 °C and a lower dielectric constant [8-10]. Therefore, it is interesting to study the 0-3 BNT-Portland cement composites for sensor application. However, as part of the preliminary investigation, 0-3 BNT-PC composite was first studied to investigate basic properties of new composite material. In this work, composites consist of Portland cement (PC) and bismuth sodium titanate (BNT) were prepared using the pressed method. Dielectric properties and the microstructure of the composites were then investigated.

2. Materials and Methods

Bismuth Sodium Titanate, $Bi_{1/2}Na_{1/2}TiO_3$ (BNT) powder was initially produced from the two-stage mixed oxide method using Bi_2O_3, Na_2CO_3 and TiO_2. The starting powders were weighed and mixed in ball-milled for 24 h using zirconia balls in ethanol alcohol as a grinding medium. BNT ceramic were then produced by calcining the powder at 800 °C and sintered at 1100 °C. BNT ceramic particles (425 μm) were then mixed with normal Portland cement (The American Society for Testing and Materials Type I cement) to produce 0-3 connectivity BNT-PC composite using BNT volume content of 30%, 50% and 70%. This was performed under a hydraulic press at 80 MPa for 10 s to form disk samples of 15 mm diameter and 2 mm thickness. Thereafter, the composites were cured at 60 °C and 98% relative humidity for 3 d before measurement. Phase characterizations were carried out by means of scanning electron microscopy (SEM; JEOL JSM-5910LV). For measurement of the dielectric properties, silver paste electrodes were painted onto the two surfaces of disk-shaped specimens. An impedance meter (Hewlett Packard 4194A) was used to obtain the capacitance and the dissipation factor ($tan\delta$) of the composites at room temperature and at various frequencies (0.1–20 kHz). The relative dielectric constant (ε_r) was then calculated from the following equation:

$$\varepsilon_r = \frac{Ct}{\varepsilon_0 A} \qquad (1)$$

where C is the sample capacitance, t is the thickness, ε_0 is the permittivity of the free space constant (8.854×10^{-12} Fm^{-1}), and A is the electrode area.

3. Results and Discussion

The dielectric constant (ε_r) results of the composites plotted against the frequency are shown in Fig. 1 and the variation of dielectric loss ($tan\delta$) of the composites with frequency is shown in Fig. 2. It can be seen from Fig. 1 that the dielectric constant of the composites decreases with increasing frequency. This means that the change of dielectric constants of the composites with an increasing frequency lead to some polarizations, especially interfacial polarizations cannot follow the change of the electric field due to lengthy time for the construction of space charge polarization. Thus, the dielectric constants of the composites are lower at high frequency [11]. Moreover, it can be clearly seen that in the range of about 0.1-20 kHz, the dielectric loss of the composites decrease sharply with increasing frequency.

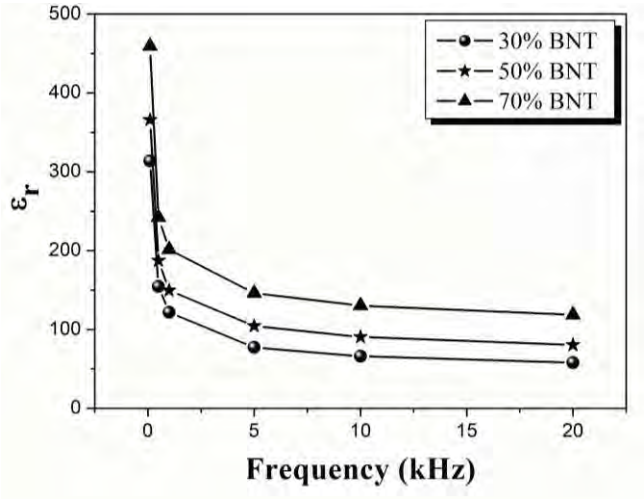

Fig. 1 Dielectric constant (ε_r) as a function of frequency of BNT-Portland cement composites

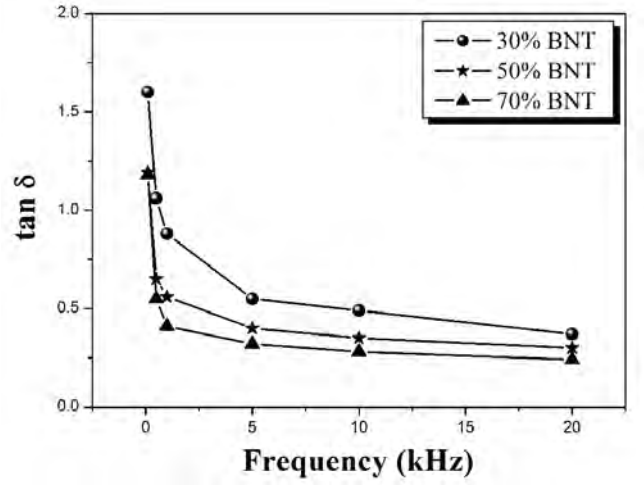

Fig. 2 Dielectric loss ($tan\delta$) as a function of frequency of BNT-Portland cement composites

The dielectric constant (ε_r) and dielectric loss ($tan\delta$) at frequency of 1 kHz is shown against the BNT volume content in Fig. 3 where the effect of BNT can be observed. The dielectric constant (ε_r) can be seen to increase with increasing BNT content with the composites at 30 and 70 vol.%, ε_r values are 121 and 201, respectively. On the other hand, the dielectric loss ($tan\delta$) was found to reduce with increasing BNT content agreeing with the dielectric constant results due to the direct influence of BNT ceramic. A reasonably low tanδ value was obtained for composite with BNT at 70% (tanδ = 0.41).

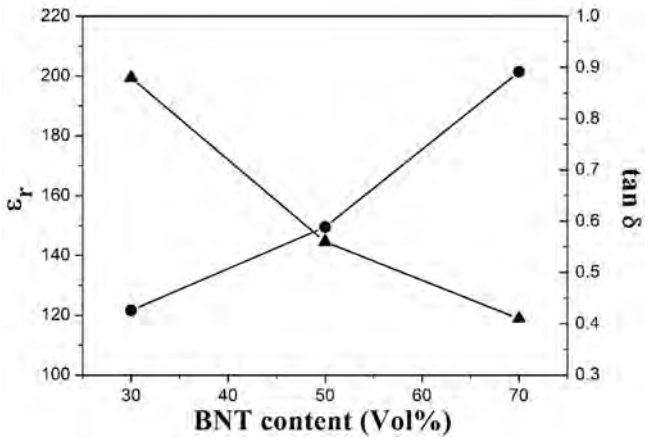

Fig. 3 Effect of BNT content on the dielectric constant and dielectric loss at a frequency of 1 kHz of BT-Portland cement composites

The scanning electron microscopy (SEM) image of fracture surfaces of BNT-PC composites (50% BNT) are shown in Fig. 4. In the figure, BNT ceramic particles can be seen to be densely surrounded by calcium silicate hydrate gel (an essential hydration product of Portland cement that provides the bonding and strength). Furthermore, energy-dispersive X-ray spectroscopy (EDX) analysis of the composites is shown to the right of the image in Figs. 4, where the calcium silicate hydrate and bismuth sodium titanate were detected. EDX analysis of the area displayed the presence bismuth, sodium, titanium and oxygen were detected as the main elements of bismuth sodium titanate. For calcium silicate hydrate; calcium, silicon and oxygen were detected as the main elements (hydrogen cannot be detected).

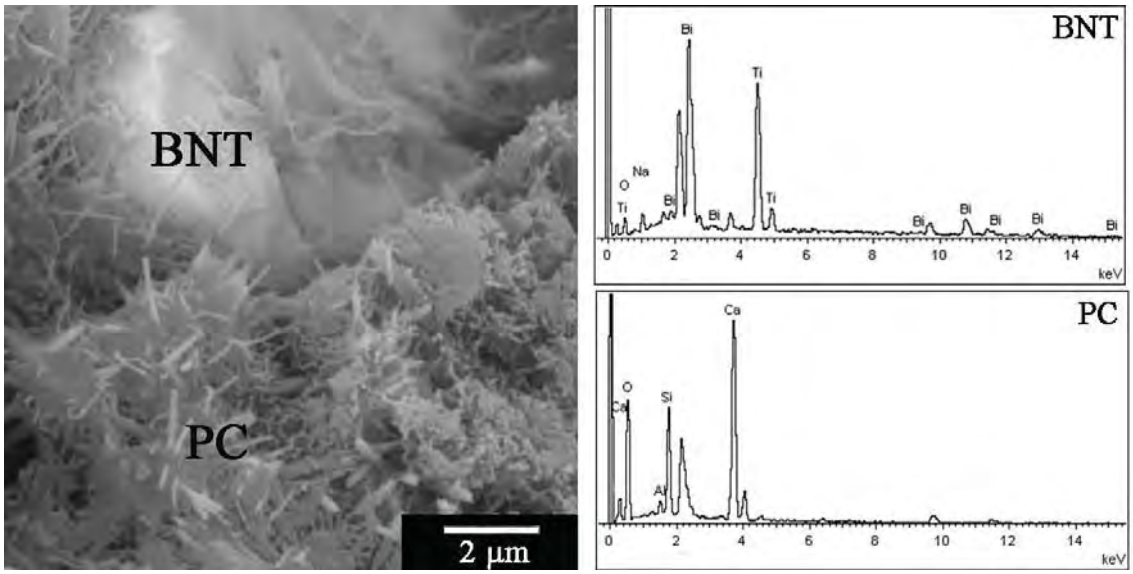

Fig. 1 SEM image of BNT-PC composites (50% BNT).

4. Conclusions

The dielectric constant of the composites was found to decrease with increasing frequency. Moreover, the dielectric loss of the composites decreases sharply with increasing frequency. In addition, the dielectric constant values of BNT-PC composites increased when

the volume percentage of BNT was increased, where ε_r values of the composites at 30 and 70 vol% are 121 and 201, respectively. Furthermore, dielectric loss results were found to decrease with increasing BNT concentration, and a noticeably lower $tan\delta$ value of 0.41 was obtained for 70% BNT composite.

5. Acknowledgements

Financial support from the Thailand Research Fund through the Royal Golden Jubilee Ph.D. Program (Grant No. PHD/0147/2551) to Miss Rattiyakorn Rianyoi and Asst. Prof. Dr. Arnon Chaipanich is gratefully acknowledged. The authors wish to thank the staff members at the Electroceramics Research Laboratory, Faculty of Science, Chiang Mai University, for use of the research facilities which made this work possible. The authors would also like to express their gratitude to the Thailand Research Fund (TRF), Office of the Higher Education Commission (Thailand), and Chiang Mai University. The Graduate School of Chiang Mai University is also acknowledged for additional financial support.

6. References

Aizawa S, Kakizawa T, Higasino M. Smart Mater. Struct. 1998; 7: 617-626.

Chang F-K. Structural Health Monitoring .Technomic Publishing, Basel, Switzerland, 2000.

Li Z, Zhang D, Wu K. Cement-based 0–3 piezoelectric composites. J. Am. Ceram. Soc. 2002; 85: 305–313.

Huang S, Chang J, Xu R, Liu F, Lu L, Ye Z, Cheng X. Piezoelectric properties of 0-3 PZT/sulfoaluminate cement composites. Smart Mater. Struct. 2004; 13: 270–274.

Dong B, Li Z. Cement-based piezoelectric ceramic smart composites. Compos. Sci. Technol. 2005; 65: 1363–1371.

Chaipanich A, Jaitanong N, Tunkasiri T. Fabrication and properties of PZT-ordinary Portland cement composites. Mater. Lett. 2007; 61: 5206–5208.

Chaipanich A. Dielectric and piezoelectric properties of PZT-cement composites Curr. Appl. Phys. 2007; 7: 537–539.

Roleder K, Franke I, Glazer AM, Thomas PA, Miga S, Suchanicz J. The piezoelectric effect in $Na_{0.5}Bi_{0.5}TiO_3$ ceramics. J. Phys.: Condens. Matter. 2002; 14; 5399.

Cho JH, Ma YJ, Lee YH, Chun MP, Kim BI. Piezoelectric ceramic powder synthesis of bismuth-sodium titanate by a hydrothermal process. J. Cer. Proc Res. 2006; 7: 91-94.

Thanaboonsombut A, Vaneesorn N. Effect of attrition milling on the piezoelectric properties of $Bi_{0.5}Na_{0.5}TiO_3$-based ceramics. J. Electroceram. 2008; 21: 414-417.

Xin C, Huang SF, Jun C, Li ZJ. piezoelectric, dielectric, and ferroelectric properties of 0-3 ceramic/cement composites. J. Appl. Phys. 2007; 101: 094110.

Graduate School of Agriculture &
Center for Southeast Asian Studies

UNIVERSITY OF SHIZUOKA

UNIVERSITY OF
LIVERPOOL

The 1st *EnvironmentAsia* International Conference on

"Environmental Supporting in Food and Energy Security: Crisis and Opportunity"

22-25 March, 2011
Rama Garden Hotel, Bangkok, Thailand

ISBN 978-974-11-1446-7

สมาคมสถาบันอุดมศึกษาสิ่งแวดล้อมไทย

Thai Society of Higher Education Institutes on Environment

15 February 2011

Dear Ruamporn Potong,

I am pleased to inform you that your full paper entitled “Effect of particle size on the dielectric properties of environmental friendly lead-free composites from 0-3 barium zirconate titanate-portland cement composites” by the authors Ruamporn Potong, Rattiyakorn Rianyoi and Arnon Chaipanich has been accepted for **a poster presentation** in the **Session VII. Environmental science and technology** at The 1st *EnvironmentAsia* International Conference, which will be held at the Rama Garden Hotel, from March 22 through March 25, 2011 in Bangkok, THAILAND.

Your full paper will be published in the **Proceedings of the 1st *EnvironmentAsia* International Conference**. Please find the guideline of presentation and detail of program in our website: http://www.tshe.org/EnvironmentAsia2011

I look forward to seeing you at The 1st *EnvironmentAsia* International Conference in Bangkok, Thailand.

Yours sincerely,

(Asst. Prof. Dr. Sittipong Dilockwanich)
President of Thai Society of Higher Education Institutes on Environment

Thai Society of Higher Education Institutes on Environment
The 1st EnvironmentAsia International Conference on
"Environmental Supporting in Food and Energy Security: Crisis and Opportunity"
22-25 March 2011, Bangkok, Thailand

Effect of particle size on the dielectric properties of environmental friendly lead-free composites from 0-3 barium zirconate titanate-portland cement composites

Ruamporn Potong, Rattiyakorn Rianyoi and Arnon Chaipanich*
Department of Physics and Materials Science, Faculty of Science, Chiang Mai University, Chiang Mai 50200, Thailand. E-mail: amon@chiangmai.ac.th

Abstract

Barium zirconate titanate-based materials are promising environmental friendly lead-free electroceramic because of their relatively high dielectric and piezoelectric properties. The purpose of this study was to find out the effect of particle size on the dielectric properties of environmental friendly lead-free composites from barium zirconate titanate-portland cement composites. Barium zirconate titanate, $BaZr_{0.05}Ti_{0.95}O_3$ (BZT), ceramics particles was mixed with Portland Cement (PC) using BZT of various particle sizes (75, 212 and 425 μm) content at 50% by weight to produce 0–3 $BaZr_{0.05}Ti_{0.95}O_3$-Portland cement BZT–PC composites. The 0–3 BZT–PC composites were then cured in 98%RH curing chamber for 3 days before measurements. The dielectric constant (ε_r) and dielectric loss ($tan\delta$) at room temperature and at various frequencies of 0–3 BZT–PC composites with difference BZT particle size were investigated. The results showed that the dielectric constant of BZT-PC composites increased with increasing BZT particle size where ε_r value at 1 kHz are 292 and 366 for composites with 75 μm and 425 μm BZT particle size respectively. The dielectric loss was found to decrease with increasing BZT particle size and the *tan δ* value was 0.92 for composite with 425 μm BZT particle size at 1 kHz.

Keywords: BZT; Composites; Particle size; Cement; Dielectric Properties

1. Introduction

In recent years, cement-based electroceramic composites have been exploited as promising materials for sensors and actuators in the field of civil engineering. Cement-based electroceramic composites have good compatibility with civil engineering's main structural material-concrete. Their performances show some advantages over traditional electroceramic materials, such as electroceramic and polymer-based electroceramic composites [1-4]. Previously the use of electroceramic such as lead zirconate titanate (PZT) has been used with cement to form cement-based electroceramic composites, but PZT ceramic is not environmental friendly due to lead oxide toxicity. For this reason, it is likable to find environmental friendly lead-free electroceramic with equivalent properties, which could be used as a replacement for lead-based ceramics such as PZT. Barium zirconium titanate (BZT) is environmental friendly lead-free electroceramic, exhibits high dielectric, piezoelectric properties and this material is of interest as a candidate to replace lead-based materials [5]. $Ba(Ti_{1-x}Zr_x)O_3$ ceramics at x = 0.05 mol showed high dielectric constant and piezoelectric properties [6-7].

A number of authors reported that the properties of the cement-based electroceramic composites depends on many factors such as method of preparation, properties of dispersed phase powder etc. [1–4, 8]. It was also found that the particle size of the ceramic powders played an important role in the properties of 0-3 composites. In addition, the dielectric

constant has been measured for the purpose of fundamental understanding of cement-based electroceramic composites. In this work, the effect of particle size on the dielectric properties of environmental friendly lead-free composites from 0-3 barium zirconate titanate-portland cement composites were investigated. Barium zirconate titanate (BZT) ceramics particles was mixed with Portland Cement (PC) using BZT of various particle sizes (75, 212 and 425 μm) content at 50% by weight to produce 0–3 BZT–Portland cement (BZT–PC) composites.

2. Materials and Methods

Barium zirconate titanate (BZT) ceramic particles of composition $BaZr_{0.05}Ti_{0.95}O_3$ were produced using BZT powder sintered at 1,450 °C. BZT ceramic of different median particle size (75μm, 212μm and 425μm) were used. These BZT ceramic particles were then mixed with normal Portland cement (The American Society for Testing and Materials Type I cement) to produce 0-3 connectivity BZT-PC composite of 50:50 by volume using a hydraulic press to form disk samples of 15 mm diameter and 2 mm thickness. Thereafter, the composites were placed for curing at 60 °C and 98 % relative humidity for 3 days before measurements. Density and particle size of BZT ceramic used in the investigation are given in Table 1. The dielectric constant (ε_r) and dielectric loss ($tan\delta$) at room temperature and at various frequencies (0.1-20 kHz) of 0–3 BZT–PC composites with difference BZT particle size were investigated. For measurement of the dielectric properties, silver paste electrodes were applied at the two surfaces of disk-shaped specimens. An impedance meter (Hewlett Packard 4194A) was used to obtain the capacitance and the dielectric loss of the composites. The dielectric constant was then calculated from a parallel-plate capacitor equation:

$$\varepsilon_r = \frac{Ct}{\varepsilon_0 A}$$

Where C is the sample capacitance, t is the thickness, ε_0 is the permittivity of free space constant (8.854×10^{-12} Fm^{-1})and A is the electrode area.

Table 1 Density and particle size of BZT-PC composites with different particle size BZT ceramic

Composites of various BZT particle size (μm)	Density (g/cm^3)
75	3.81
212	3.94
425	4.03

3. Results and Discussion

The effect of BZT-PC composites on the dielectric constant (ε_r) is shown against the frequency in Fig. 1 where the effect of frequency on the dielectric constant can be seen. The dielectric constant of the composites can be seen to decrease with increasing frequency where the dielectric constant at 0.1 kHz and 20 kHz = 874 and 121 respectively, for composites at 425 μm BZT particle size. The dielectric loss ($tan\delta$) was also found to decrease with

increasing frequency where the dielectric loss at 0.1 kHz and 20 kHz = 1.13 and 0.53 respectively (at 425 μm BZT particle size).

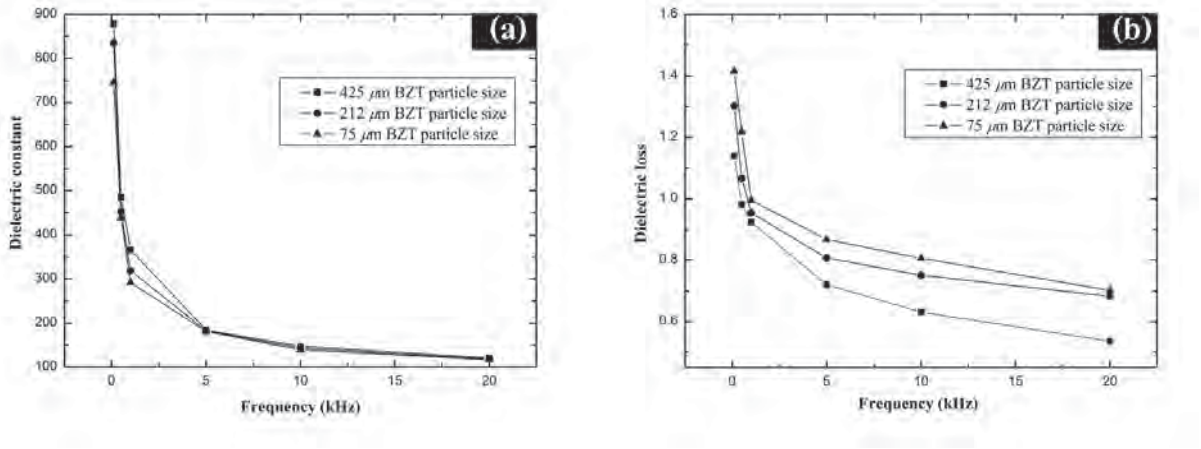

Fig. 1 Effect of frequency on dielectric properties results of BZT-Portland cement (a) dielectric constant and (b) dielectric loss.

Furthermore, the dielectric constant of the composites decrease sharply with increasing frequency and with an increasing frequency, some polarization, especially interfacial polarizations cannot follow the change of the electric field due to lengthy time for the construction of space charge polarization [8-10]. Moreover, this is mainly attributed to interface polarization of the composite and polarization in the cement matrix. Cement is a porous material and it is composed of an amorphous phase, crystallites in the micrometer range and bound water [9, 11]. Therefore, the dielectric constants of composites are higher at low frequency.

The effect of BZT-PC composites on the dielectric constant is plotted against the BZT particle size in Fig. 2. The dielectric constant of the composites can be seen to increase with increasing BZT particle size and that the dielectric constant was highest at 366 for composite with 425 μm BZT particle size at 1 kHz. The dielectric loss (*tanδ*) was found to decrease with increasing BZT particle size and the *tanδ* value at 1 kHz was lowest at 0.92 of 425 μm BZT particle size. The dielectric constant can be seen to increase with larger particle size of BZT used due to the fact that the contact surface areas between the cement matrix and the particles became smaller with increasing BZT particle size. These contact surface areas are greatest when BZT particle is smallest and became less when larger BZT ceramic particle was used at the same volume percentage thus brought out the optimum piezoelectricity in the 0–3 BZT-cement composites [4, 12-14].

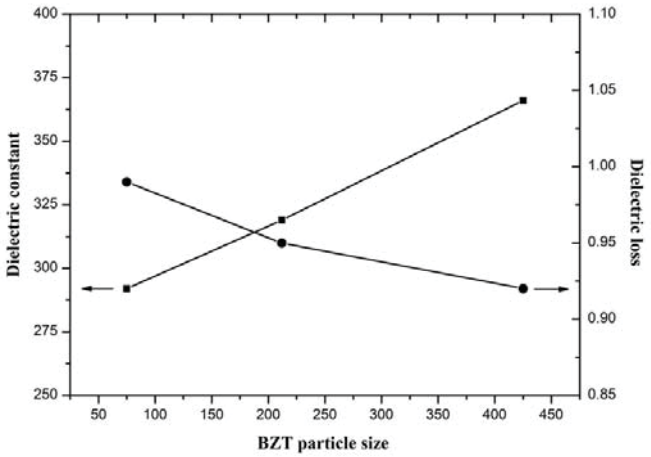

Fig. 2 Effect of particle size on dielectric properties results of BZT-Portland cement composites

4. Conclusions

All 0-3 connectivity cement-based composites with various BZT particle size were summarized as follows:

1. The result showed that the dielectric constant of 0-3 BZT-PC composites decrease sharply with increasing frequency. Furthermore, the dielectric loss was found to decrease with increasing frequency.

2. The enhancement in the dielectric properties was contributed to less contacting surface between the cement matrix and the BZT particle sizes. Furthermore, BZT ceramic of 425 μm particle size can be produced and it gave the highest dielectric constant (for the BZT particle size range tested).

5. Acknowledgements

The authors are thankful to members of staff at the Electroceramics Research Laboratory, Faculty of science, and Chiang Mai University for the research facilities made possible for this research work. The authors would like to express their gratitude for financial support from the Thailand Research Fund (TRF) through the Royal Golden Jubilee Ph.D. Program (Grant No. PHD/0042/2552) to Ruamporn Potong and Assistant Prof. Dr. Arnon Chaipanich is acknowledged. The authors would also like to express their gratitude for TRF-CHE Research Grant for Mid-Career University Faculty awarded to Assistant Prof. Dr. Arnon Chaipanich by the Thailand Research Fund (TRF), Office of the Higher Education Commission (Thailand) and Chiang Mai University. The Graduate School of Chiang Mai University is also acknowledged.

6. References

Chaipanich A. Effect of PZT particle size on dielectric and piezoelectric properties of PZT–cement composites. Current Applied Physics 2007; 7: 574–577.

Chaipanich A., Jaitanong N. Effect of PZT particle size on the electromechanical coupling coefficient of 0-3 PZT-cement composites. Ferroelectrics Letters Section 2009; 36: 37-44.

Gonga H.Y., Li Z., Zhang Y., Fan R.H. Piezoelectric and dielectric behavior of 0-3 cement-based composites mixed with carbon black. Journal of the European Ceramic Society 2009; 29: 2013-2019.

Jaitanong N., Chaipanich A. Dielectric properties of 0-3 lead magnesium niobate titanate (PMT)-ordinary Portland Cement (PC) composites. Key Engineering Materials 2010; 421-422: 407-410.

Jaitanong N., Rianyoi R., Potong R., Yimnirun R., Chaipanich A. Effects of PZT content and particle size on ferroelectric hysteresis behavior of 0-3 lead zirconate titanate - Portland cement composites. Integrated Ferroelectrics 2009; 107: 43-52.

Jarupoom P., Pengpat K., Rujijanagul G. Enhanced piezoelectric properties and lowered sintering temperature of $Ba(Zr_{0.07}Ti_{0.93})O_3$ by B_2O_3 addition. Current Applied Physics 2010; 10: 557–560.

Li Z., Gonga H.Y. Effects of particle size on the piezoelectric properties of 0-3 PZT/cement composites. AIP Conference Proceedings 2008; 973: 538–543.

Li Z., Zhang D., Wu K. Cement-Based 0-3 piezoelectric composites. Journal of the American Ceramic Society 2002; 85: 305-313.

Potong R., Rianyoi R., Jarupoom P., Pengpat K., Chaipanich A. Effect of particle size on the dielectric properties of sodium potassium niobate-portland cement composites. Ferroelectric Letters Section 2009; 36: 76–81.

Rujijanagul G., Jompruan S., Chaipanich A. Influence of graphite particle size on electrical properties of modified PZT–polymer composites. Current Applied Physics 2008; 8: 359–362.

Taylor HFW. Cement Chemistry. 2nd edition. London: Thomas Telford Publishing; 1997.

Xin C., Huang S, Jun C., Zongjin L. Piezoelectric, dielectric, and ferroelectric properties of 0-3 ceramic/cement composite. Journal of Applied Physics 2007; 101: 094110–094116.

Yu Z., Ang C., Guo R., Bhalla A. S. Piezoelectric and strain properties of $Ba(Ti_{1-x}Zr_x)O_3$ ceramics. Journal of Applied Physics 2002; 92: 1489–1493.

Yu Z., Guo R., Bhalla A.S. Dielectric behavior of $Ba(Ti_{1-x}Zr_x)O_3$ single crystals. Journal of Applied Physics 2000; 88: 410–415.

www.iffm2011.org

IFFM 2011 & AFM-2

2011 International Forum on Functional Materials
The 2nd Special Symposium on Advances in Functional Materials

July 28 – 31, 2011
Jeju Grand Hotel, Jeju, Korea

ABSTRACTS BOOK

Organized by

- The Korean Vacuum Society
- Research Institute of Advanced Nanomaterials at Sungkyunkwan University (SKKU)
- Pioneer Research Center for Nano-morphic Biological Energy Conversion and Storage at Gyeongsang National University (GNU)
- Plasma Bioscience Research Center (SRC) at Kwang Woon University
- Korean Battery Society

Supported by

- BK21 School of Chemical Materials Science, SKKU
- BK21 Physics Research Division, SKKU
- Center for Human Interface Nanotechnology (NCRC), SKKU
- Creative Research Initiative (CRI), Center for Smart Molecular Memory (SKKU)
- Global Leader Development Center for I-Cube Materials and Parts (BK21) at GNU
- Nano-convergence Core Technology for Human Interface, WCU Program, SKKU
- WCU Center for Next Generation Battery at GNU
- Solid State Chemistry Lab. (NRL), SKKU
- Fusion Nanostructured Solar Cell Lab. (NRL), SKKU
- Global Research Laboratory for RNAi Medicine (GRL), SKKU

NRF National Research Foundation of Korea

KOFST

Sponsored by

- National Research Foundation of Korea
- The Korean Federation of Science and Technology Societies
- Bosung Science
- ever Chem CO. LTD.
- H&A PharmaChem
- Korea Polytech CO. LTD.
- NEXCON Technology
- WON CHEMICAL CO. LTD.
- wonkangbio CO. LTD.

ong Convention Services Co., Ltd.

TEL: 2-783-3473/3474 / FAX: +82-2-783-3475 / E-Mail: sejong5@sejongconvention.com

Rm. 505 Taeyang Bldg. 44-2, Yeouido-dong, Youngdeungpo-gu, Seoul 150-890, Korea

P1-Fr-158 **Effect of various sintering aids on the piezoelectric and dielectric properties of NKN-LST ceramics**
Seung-Hwan Lee, Sung-Gap Lee[1], Young-Hie Lee*
Dept. of Electronic Materials Engineering, Kwangwoon University, Korea
[1] Dept. of Ceramic Engineering, Eng. Res. Insti., Gyeongsang National University, Jinju, Korea

P1-Fr-159 **Piezoelectric and dielectric properties of $0.98(Na_{0.5}K_{0.5})NbO_3$-$0.02Ba(Zr_{(1-X)}Ti_x)O_3$ ceramics.**
Seung-Hwan Lee, Sung-Gap Lee[1], Young-Hie Lee*
Dept. of Electronic Materials Engineering, Kwangwoon University, Korea
[1] Dept. of Ceramic Engineering, Eng. Res. Insti., Gyeongsang National University, Jinju, Korea

P1-Fr160 **Electrical properties of lead-free $0.98(Na_{0.5}K_{0.5})NbO_3$-$0.02Ba(Zr_{0.52}Ti_{0.48})O_3$ piezoelectric ceramics by optimizing sintering temperature**
Seung-Hwan Lee, Sung-Gap Lee [1], Sang-Chul Lee, Young-Hie Lee*
Dept. of Electronic Materials Engineering, Kwangwoon University, Korea
[1] Dept. of Ceramic Engineering, Eng. Res. Insti., Gyeongsang National University, Jinju, Korea

P1-Fr-161 **RAMAN AND N-14 NMR STUDY OF PEROVSKITE OXYNITRIDES $ATaO_2N$ (A = Ba, Sr, Ca)**
Young-Il Kim*[,a], Younkee Paik[b], and Charles S. Feigerle[c]
[a] Department of Chemistry, Yeungnam University, Gyeongsan, Korea
[b] Daegu Center, Korea Basic Science Institute, Daegu, Korea
[c] Department of Chemistry, University of Tennessee, Knoxville, Tennessee 37996, USA

P1-Fr-162 **STRUCTURE AND PIEZORESPONSE OF CSD $BiFeO_3$ THIN FILMS**
Chin-Chung Yu, Li-Wei Lin and Jiun-Yuan Liou
Department of Applied Physics, National University of Kaohsiung, Kaohsiung, Taiwan

P1-Fr-163 **Effect of Barium Titanate Particle Size on Electrical Properties of 0-3 BariumTitanate-Portland Cement Composites**
R. Rianyoi,[a]* R. Potong ,[a] R. Yimnirun,[b] A. Ngamjarurojana[a] and A. Chaipanich[a,*]
[a] Department of Physics and Materials Science, Faculty of Science, Chiang Mai University, Chiang Mai, Thailand
[b] School of Physics, Institute of Science, Suranaree University of Technology, and Synchrotron Light Research Institute (Public Organization), Nakhon Ratchasima, Thailand

P1-Fr-164 **Ferroelectric and Piezoelectric Properties of 0-3 Lead-Free Barium Zirconate Titanate-Portland Cement Composites**
R. Potong*, R. Rianyoi, A. Ngamjarurojana and A. Chaipanich*
Department of Physics and Materials Science, Faculty of Science, Chiang Mai University, Chiang Mai, Thailand.

P1-Fr-165 **Structural and Dielectric properties of $Sr[(Fe_{0.9}Al_{0.1})_{0.5}Nb_{0.5}]O_3$ ceramics**
T. Phatungthane* and G. Rujijanagul
Department of Physics and Materials Science, Faculty of Science, Chiang Mai University,

P1-Fr-166 **EFFECT OF PLASMA TREATMENT OF VERTICALLY GROWN CNT ANODES ON ELECTROCHEMICAL PROPERTIES OF LI ION BATTERIES**
Byeong-Joo Lee, Jin-Ju Kim, Yoon-Soo Park, Sung-Man Lee, and Goo-Hwan Jeong*
Department of Advanced Materials Science and Engineering, Kangwon National University, Chuncheon, Korea

P1-Fr-167 **IN-SITU ANNEALING EFFECTS ON $ZnO:Li/Al_2O_3$ THIN FILMS**
Byeong-Eog Jun[1], Seung In Shin[1], Yushin Kim[1], Choongmyoung Lee[1], Dongwon Jang[1], Jaeyoon Choi[1], Hyun Kyoung Yang[2], Byung Chun Choi[3]*, and Jung Hyun Jeong[3]
[1] Department of Physics and Earth Science, Korea Science Academy of KAIST, Busan, Korea
[2] Department of Physics, Dong-Eui University, Busan, Korea
[3] Department of Physics, Pukyong National University, Busan, Korea

Effect of Barium Titanate Particle Size on Electrical Properties of 0-3 BariumTitanate-Portland Cement Composites

R. Rianyoi,[a+] R. Potong,[a] R. Yimnirun,[b] A. Ngamjarurojana[a] and A. Chaipanich[a,]*

[a] Department of Physics and Materials Science, Faculty of Science, Chiang Mai University, Chiang Mai 50200, Thailand

[b] School of Physics, Institute of Science, Suranaree University of Technology, and Synchrotron Light Research Institute (Public Organization), Nakhon Ratchasima 30000, Thailand

[+]E-mail for presenting author: r.rianyoi@gmail.com

[*]E-mail for corresponding author: arnonchaipanich@gmail.com; Fax: +66 53 943445

ABSTRACT

In this paper, the effects of Barium Titanate (BT) particle size on the dielectric, ferroelectric and piezoelectric properties of BT–PC composites were investigated. BT of 75-425 μm were used at 50% by volume to produce the composites using the mixing and pressing method. The dielectric constant (ε_r) and the dielectric loss ($tan\delta$) at room temperature and at various frequencies of the ferroelectric BT-Portland cement composites with different BT particle size were investigated. The results show that the dielectric constant (ε_r) of BT-PC composite are found to be increased with increasing BT particle size and that the highest value for ε_r of 354 was obtained when BT of 425 μm size was used. In addition, the dielectric loss tangent ($tan\delta$) decreased with increasing particle size of BT ceramics. The ferroelectric hysteresis loops of composite materials indicate that the "apparent" remnent polarization (P_{ar}) of there composites increase as the BT particle size increases. Furthermore, the piezoelectric coefficient (d_{33}) was also found to increase as BT particle size increases, as expected.

References

[1] Z. Li, D. Zhang and K. Wu, J. Am. Ceram. Soc. 85 (2002) 305-313.
[2] S. Huang, J. Chang, R. Xu, F. Liu, L. Lu, Z. Ye, X. Cheng, Smart Mater. Struct. 13 (2004) 270-274.
[3] Z. Li, B. Dong, D. Zhang, Cem. Concr. Compos. 27 (2005) 27-32.
[4] B. Dong, Z. Li, Compos. Sci. Technol. 65 (2005) 1363-1371.
[5] A. Chaipanich, N. Jaitanong, T. Tunkasiri, Mater. Lett. 61 (2007) 5206-5208.
[6] A. Chaipanich, Curr. Appl. Phys. 7 (2007) 574-577.
[7] A. Chaipanich, Curr. Appl. Phys. 7 (2007) 537-539.
[8] N. Jaitanong, A. Chaipanich, T. Tunkasiri, Ceram. Inter. 34 (2008) 793-795.
[9] J. M. Hwu, W. H. Yu, W. C. Yang, Y. W. Chen, Y. Y. Chou, Mater. Res. Bull. 40 (2005) 1662-1679.
[10] H. Shifeng, Y. Zhengmao, H. Yali, C. Jun, L. Lingchao, C. Xin, Comp. Sci. Tech. 67 (2007) 135–139.
[11] A. Chaipanich, N. Jaitanong, Adv. Mats. Res. 55 (2008) 381–384.
[12] A. Chaipanich, N. Jaitanong, Ferr. Lett. 36 (2009) 37-44.
[13] A. Chaipanich, N. Jaitanong, R. Yimnirun, Ferr. Lett. 36 (2009) 59-66.
[14] R. Rianyoi, R. Potong, N. Jaitanong, R. Yimnirun, A. Chaipanich, Appl. Phys. A. DOI 10.1007/s00339-011-6307-2.

www.iffm2011.org

IFFM 2011 & AFM-2

2011 International Forum on Functional Materials
The 2nd Special Symposium on Advances in Functional Materials

July 28 – 31, 2011
Jeju Grand Hotel, Jeju, Korea

ABSTRACTS BOOK

Organized by

- The Korean Vacuum Society
- Research Institute of Advanced Nanomaterials at Sungkyunkwan University (SKKU)
- Pioneer Research Center for Nano-morphic Biological Energy Conversion and Storage at Gyeongsang National University (GNU)
- Plasma Bioscience Research Center (SRC) at Kwang Woon University
- Korean Battery Society

Supported by

- BK21 School of Chemical Materials Science, SKKU
- BK21 Physics Research Division, SKKU
- Center for Human Interface Nanotechnology (NCRC), SKKU
- Creative Research Initiative (CRI), Center for Smart Molecular Memory (SKKU)
- Global Leader Development Center for I-Cube Materials and Parts (BK21) at GNU
- Nano-convergence Core Technology for Human Interface, WCU Program, SKKU
- WCU Center for Next Generation Battery at GNU
- Solid State Chemistry Lab. (NRL), SKKU
- Fusion Nanostructured Solar Cell Lab. (NRL), SKKU
- Global Research Laboratory for RNAi Medicine (GRL), SKKU

NRF National Research Foundation of Korea

KOFST

Sponsored by

- National Research Foundation of Korea
- The Korean Federation of Science and Technology Societies
- Bosung Science
- ever Chem CO. LTD.
- H&A PharmaChem
- Korea Polytech CO. LTD.
- NEXCON Technology
- WON CHEMICAL CO. LTD.
- wonkangbio CO. LTD.

ong Convention Services Co., Ltd.

TEL: 2-783-3473/3474 / FAX: +82-2-783-3475 / E-Mail: sejong5@sejongconvention.com

Rm. 505 Taeyang Bldg. 44-2, Yeouido-dong, Youngdeungpo-gu, Seoul 150-890, Korea

P1-Fr-158 **Effect of various sintering aids on the piezoelectric and dielectric properties of NKN-LST ceramics**
Seung-Hwan Lee, Sung-Gap Lee[1], Young-Hie Lee*
Dept. of Electronic Materials Engineering, Kwangwoon University, Korea
[1] Dept. of Ceramic Engineering, Eng. Res. Insti., Gyeongsang National University, Jinju, Korea

P1-Fr-159 **Piezoelectric and dielectric properties of $0.98(Na_{0.5}K_{0.5})NbO_3$-$0.02Ba(Zr_{(1-X)}Ti_x)O_3$ ceramics.**
Seung-Hwan Lee, Sung-Gap Lee[1], Young-Hie Lee*
Dept. of Electronic Materials Engineering, Kwangwoon University, Korea
[1] Dept. of Ceramic Engineering, Eng. Res. Insti., Gyeongsang National University, Jinju, Korea

P1-Fr160 **Electrical properties of lead-free $0.98(Na_{0.5}K_{0.5})NbO_3$-$0.02Ba(Zr_{0.52}Ti_{0.48})O_3$ piezoelectric ceramics by optimizing sintering temperature**
Seung-Hwan Lee, Sung-Gap Lee [1], Sang-Chul Lee, Young-Hie Lee*
Dept. of Electronic Materials Engineering, Kwangwoon University, Korea
[1] Dept. of Ceramic Engineering, Eng. Res. Insti., Gyeongsang National University, Jinju, Korea

P1-Fr-161 **RAMAN AND N-14 NMR STUDY OF PEROVSKITE OXYNITRIDES $ATaO_2N$ (A = Ba, Sr, Ca)**
Young-Il Kim*[,a], Younkee Paik[b], and Charles S. Feigerle[c]
[a] Department of Chemistry, Yeungnam University, Gyeongsan, Korea
[b] Daegu Center, Korea Basic Science Institute, Daegu, Korea
[c] Department of Chemistry, University of Tennessee, Knoxville, Tennessee 37996, USA

P1-Fr-162 **STRUCTURE AND PIEZORESPONSE OF CSD $BiFeO_3$ THIN FILMS**
Chin-Chung Yu, Li-Wei Lin and Jiun-Yuan Liou
Department of Applied Physics, National University of Kaohsiung, Kaohsiung, Taiwan

P1-Fr-163 **Effect of Barium Titanate Particle Size on Electrical Properties of 0-3 BariumTitanate-Portland Cement Composites**
R. Rianyoi,[a*] R. Potong,[a] R. Yimnirun,[b] A. Ngamjarurojana[a] and A. Chaipanich[a,*]
[a] Department of Physics and Materials Science, Faculty of Science, Chiang Mai University, Chiang Mai, Thailand
[b] School of Physics, Institute of Science, Suranaree University of Technology, and Synchrotron Light Research Institute (Public Organization), Nakhon Ratchasima, Thailand

P1-Fr-164 **Ferroelectric and Piezoelectric Properties of 0-3 Lead-Free Barium Zirconate Titanate-Portland Cement Composites**
R. Potong*, R. Rianyoi, A. Ngamjarurojana and A. Chaipanich*
Department of Physics and Materials Science, Faculty of Science, Chiang Mai University, Chiang Mai, Thailand.

P1-Fr-165 **Structural and Dielectric properties of $Sr[(Fe_{0.9}Al_{0.1})_{0.5}Nb_{0.5}]O_3$ ceramics**
T. Phatungthane* and G. Rujijanagul
Department of Physics and Materials Science, Faculty of Science, Chiang Mai University,

P1-Fr-166 **EFFECT OF PLASMA TREATMENT OF VERTICALLY GROWN CNT ANODES ON ELECTROCHEMICAL PROPERTIES OF LI ION BATTERIES**
Byeong-Joo Lee, Jin-Ju Kim, Yoon-Soo Park, Sung-Man Lee, and Goo-Hwan Jeong*
Department of Advanced Materials Science and Engineering, Kangwon National University, Chuncheon, Korea

P1-Fr-167 **IN-SITU ANNEALING EFFECTS ON $ZnO:Li/Al_2O_3$ THIN FILMS**
Byeong-Eog Jun[1], Seung In Shin[1], Yushin Kim[1], Choongmyoung Lee[1], Dongwon Jang[1], Jaeyoon Choi[1], Hyun Kyoung Yang[2], Byung Chun Choi[3]*, and Jung Hyun Jeong[3]
[1] Department of Physics and Earth Science, Korea Science Academy of KAIST, Busan, Korea
[2] Department of Physics, Dong-Eui University, Busan, Korea
[3] Department of Physics, Pukyong National University, Busan, Korea

Ferroelectric and Piezoelectric Properties of 0-3 Lead-Free Barium Zirconate Titanate-Portland Cement Composites

*R. Potong[†], R. Rianyoi, A. Ngamjarurojana and A. Chaipanich**

Department of Physics and Materials Science, Faculty of Science, Chiang Mai University, Chiang Mai, 50200, Thailand.
[†]E-mail of the presenting author: ja_rho@hotmail.com
**E-mail of the corresponding author: arnonchaipanich@gmail.com; Fax: +66 53 943445*

ABSTRACT

Cement-based 0-3 type lead-free piezoelectric composites, made from barium zirconate titanate (BZT) ceramic particles and Portland cement (PC) are developed for smart or intelligent structure in civil engineering. Ferroelectric and piezoelectric properties of the composites with different BZT contents at 40-70% by volume were then investigated. The 0–3 BZT–PC composites were then cured in 98%RH curing chamber for 3 days before measurements. The results showed that the ferroelectric hysteresis loops can be seen for all composites. The "apparent" remnant polarization (P_{ar}) was found to increase with increasing BZT content. The "apparent" coercive field (E_{ac}) was found to decreases with increasing BZT content from 11.0 to 7.6 μC/cm^2 at 15 kV/cm when BZT volume content used was 40% and 70% respectively. Furthermore, the d_{33} values were also found to increase as BZT contents increases, as expected. The highest value for d_{33} was 43 pC/N for 70% BZT composite.

References

[1] Z. Li, D. Zhang, K. Wu, J. Am. Ceram. Soc. 85 (2002) 305-313.
[2] A. Chaipanich, N. Jaitanong, T. Tunkasiri, Mater. Lett. 61 (2007) 5206-5208.
[3] S. Huang, J. Chang, L. Lu, F. Liu, Z. Ye, X. Cheng, Mater. Res. Bull. 41 (2006) 291-297.
[4] A. Chaipanich, N. Jaitanong, R. Yimnirun, Ferro. Lett. 36 (2009) 59-66.
[5] A. Chaipanich, Curr. Appl. Phys. 7 (2007) 537-539.
[6] N. Jaitanong, A. Chaipanich, T. Tunkasiri, Ceram. Int. 34 (2008) 793-795.
[7] A. Chaipanich, N. Jaitanong, Ferro. Lett. 35 (2008) 73-78.
[8] N. Jaitanong, A. Chaipanich, Ferro. Lett. 35 (2008) 17-23.
[9] Z. Li, B. Dong, D. Zhang, Cem. Concr. Compos. 27 (2005) 27–32.
[10] H. Gong, Z. Li, Y. Zhang, R. Fan, J. Eur. Ceram. Soc. 29 (2009) 2013-2019.
[11] Z. Yu, C. Ang, R. Guo, A.S. Bhalla, J. Appl. Phys. 92 (2002) 1489-1493.
[12] Z. Yu, R. Guo, A.S. Bhalla, J. Appl. Phys. 88 (2000) 410-415.
[13] P. Kantha, K. Pengpat, P. Jarupoom, U. Intatha, G. Rujijanagul, T. Tunkasiri, Curr. Appl. Phys. 9 (2009) 460-466.
[14] F. Moura, A.Z. Simoes, B.D. Stojanovic, M.A. Zaghete, E. Longo, J.A. Varela, J. Alloys Compd. 462 (2008) 129-134.
[15] R. Rianyoi, R. Potong, N. Jaitanong, R. Yimnirun, A. Chaipanich, Appl. Phys. A. DOI 10.1007/s00339-011-6307-2.
[16] C. Xin, S. Huang, C. Jun, L. Zongjin, J. Appl. Phys. 101 (2007) 094110-094116.

www.icae.kr

ICAE 2011

International Conference on Advanced Electromaterials

November 7-10, 2011
Ramada Plaza Jeju Hotel, Jeju, Korea

Program Book

Organized by: KIEEME

Technically sponsored by: IEEE, DBS, KIST, ETRI, KERI, KIMS, KICET, KETI, KILT, KIEE, KCERS, The Korean Sensors Society, KIDS, OSK, LiFTRC, KLED

Supported by: Ministry of Education, Science and Technology, MKE Ministry of Knowledge Economy, KOFST, Jeju

Sponsored by: SAMSUNG, SAMSUNG ADVANCED INSTITUTE OF TECHNOLOGY, Signetics, LG Electronics

Effect of Barium Titanate Particle Size on Electromechanical Properties of Lead-Free Cement Based Piezoelectric Composites

R. Rianyoi[1], R. Potong[1] and A. Chaipanich[1]
[1] Department of Physics and Materials Science, Faculty of Science, Chiang Mai University, Chiang Mai, 50200, Thailand

Abstract

Lead-free cement based piezoelectric composites with 0-3 connectivity pattern were fabricated from barium titanate and Portland cement. In this study, the effect of barium titanate particle size on the electromechanical properties of 0-3 lead-free cement based piezoelectric composites was investigated. The 0-3 lead-free cement based piezoelectric composites were prepared by mixing and pressing the cement and barium titanate ceramic powder of 50% by volume with different average particle size raging from 75 μm to 425 μm. All composites were cured in chamber of 60°C and 98% relative humidity for 3 days before measurements. The results show that at the low frequency, the impedances of all composites decrease sharply with increasing the frequency, at the high frequency, the impedance of composites has little changes. In addition, the electromechanical coupling coefficient K_t increased with the increase of the barium titanate particle size where K_t values are found to be at 9.8% and 14% for composites with median particle size of 75μm and 425 μm respectively.

References

[1] Z. Li, D. Zhang, K. Wu, J. Am. Ceram. Soc. 85, 305 (2002)
[2] S. Huang, J. Chang, R. Xu, F. Liu, L. Lu, Z. Ye, X. Cheng, Smart Mater. Struct. 13, 270 (2004)
[3] Z. Li, B. Dong, D. Zhang, Cem. Concr. Compos. 27, 27 (2005)
[4] B. Dong, Z. Li, Compos. Sci. Technol. 65, 1363 (2005)
[5] A. Chaipanich, N. Jaitanong, T. Tunkasiri, Mater. Lett. 61, 5206 (2007)
[6] A. Chaipanich, Curr. Appl. Phys. 7, 574 (2007)
[7] A. Chaipanich, Curr. Appl. Phys. 7, 537 (2007)
[8] N. Jaitanong, A. Chaipanich, T. Tunkasiri, Ceram. Inter. 34, 793 (2008)
[9] J. M. Hwu, W. H. Yu, W. C. Yang, Y. W. Chen, Y. Y. Chou, Mater. Res. Bull. 40, 1662 (2005)
[10] H. Shifeng, Y. Zhengmao, H. Yali, C. Jun, L. Lingchao, C. Xin, Comp. Sci. Tech. 67, 135 (2007)
[11] A. Chaipanich, N. Jaitanong, Adv. Mats. Res. 55, 381 (2008)
[12] A. Chaipanich, N. Jaitanong, Ferr. Lett. 36, 37 (2009)
[13] A. Chaipanich, N. Jaitanong, R. Yimnirun, Ferr. Lett. 36, 59 (2009)
[14] R. Rianyoi, R. Potong, N. Jaitanong, R. Yimnirun, A. Chaipanich, Appl. Phys. A. (2011) doi: 10.1007/s00339-011-6307-2.
[15] S. Huang, L. Lu, J. Chang, D. Xu, F. Liu, X Cheng, Ferroelectrics. 332, 187 (2006)
[16] R. Potong, R. Rianyoi, L. Jareansuk, N. Jaitanong, R. Yimnirun, A. Chaipanich, Ferroelectrics. 405, 98 (2010)
[17] X. Cheng, S. Huang, J. Chang, R. Xu, F. Liu, L. Lu, J. Eur. Cer. Soc. 25, 3223 (2005)
[18] X. Cheng, S. Huang, J. Chang, R. Xu, F. Liu, L. Lu, J. Appl. Phys. 101, 094110 (2005)
[19] K. H. Lam and H. L. W. Chan, Journal of Electroceramics. 21, 724 (2008)

Corresponding author: Arnon Chaipanich, Department of Physics and Materials Science, Faculty of Science, Chiang Mai University, 239 Huay Kaew Road, Suthep, Muang District, Chiang Mai, Thailand, Fax: +66-53-943445, E-mail: arnonchaipanich@gmail.com

www.icae.kr

ICAE 2011

International Conference on Advanced Electromaterials

November 7-10, 2011
Ramada Plaza Jeju Hotel, Jeju, Korea

Program Book

Organized by: KIEEME

Technically sponsored by: IEEE, DBS, KIST, ETRI, KERI, KIMS, KICET, KETI, KILT, KIEE, KCERS, The Korean Sensors Society, KIDS, OSK, LiFTRC, KLED

Supported by: Ministry of Education, Science and Technology, MKE Ministry of Knowledge Economy, KOFST, Jeju

Sponsored by: SAMSUNG, SAMSUNG ADVANCED INSTITUTE OF TECHNOLOGY, Signetics, LG Electronics

Ferroelectric Hysteresis Behavior of 0-3 Sodium Potassium Niobate-Portland Cement Composites

A. Chaipanich[1], R. Potong[1], R. Rianyoi[1], P. Jarupoom[1], K. Pengpat[1] and R. Yimnirun[2]
[1]Department of Physics and Materials Science, Faculty of Science, Chiang Mai University, Chiang Mai, 50200, Thailand.
[2]School of Physics, Institute of Science, Suranaree University of Technology and Synchrotron Light Research Institute (Public Organization), Nakhon Ratchasima 30000, Thailand

Abstract

Alkaline based - sodium potassium niobate is a non lead piezoelectric material that has a potential for use in piezoelectric applications. Piezoelectric ferroelectric ceramic material can be combined with Portland cement to produce piezoelectric ceramic - cement composites those can be used for smart concrete structures. In this work, sodium potassium niobate was mixed with Portland cement composites to produce 0-3 connectivity using pressed and cured method. The ferroelectric hysteresis behavior of sodium potassium niobate - Portland cement composites at different temperatures (25-100 °C) and frequency (50-90 Hz) were investigated using 50% sodium potassium niobate by volume. At room temperature, a slim oval - shaped loop was observed. However, at higher temperature the results show a more typical ferroelectric hysteresis loop for sodium potassium niobate - Portland cement composites and that "apparent" remnant polarization ($P_{r'}$) and "apparent" coercive field ($E_{c'}$) results are found at 16.2 μC/cm^2 and 5.8 kV/cm respectively (at 100 °C).

Reference

[1] Z. Li, D. Zhang, K. Wu, J. Am. Ceram. Soc. 85, 305 (2002)
[2] A. Chaipanich, N. Jaitanong, T. Tunkasiri, Mater. Lett. 61, 5206 (2007)
[3] A. Chaipanich, N. Jaitanong, R. Yimnirun, Mater. Lett. 64, 562 (2010)
[4] A. Chaipanich, N. Jaitanong, R. Yimnirun, Ferr. Lett. 36, 59 (2009)
[5] N. Jaitanong, R. Yimnirun, A. Chaipanich, Ferroelectrics 384, 174 (2009)
[6] N. Jaitanong, R. Rianyoi, R. Potong, R. Yimnirun, A. Chaipanich, Integrated Ferroelectrics 107, 43 (2009)
[7] A. Chaipanich, N. Jaitanong, Ferr. Lett. 37, 44 (2009)
[8] A. Chaipanich, N. Jaitanong, Ferr. Lett. 35, 73 (2008)
[9] N. Jaitanong, A. Chaipanich, Ferr. Lett. 35, 17 (2008)
[10] A. Chaipanich, N. Jaitanong, Key Eng. Mater. 421-422, 428-431 (2010)
[11] P. Jarupoom, K. Pengpat, S. Eitssayeam, U. Intatha, G. Rujijanagul, T. Tunkasiri, Ferr. Lett. 35, 119 (2008)
[12] R. Potong, R. Rianyoi, P. Jarupoom, K. Pengpat, A. Chaipanich, Ferr. Lett. 36, 76 (2009)
[13] C. Xin, S. Huang, C. Jun, L. Zongjin, J. Appl. Phys. 101, 094110 (2007)
[14] R. Yimnirun, R. Wongmaneerung, S. Wongsaenmai, A. Ngamjarurojana, S. Ananta, Y. Laosiritaworn Appl. Phys. Lett. 90, 112906 (2007)

Corresponding author: A. Chaipanich, Department of Physics and Materials Science, Faculty of Science, Chiang Mai University, Chiang Mai, 50200, Thailand, Fax: 66 53 943445, E-mail: arnonchaipanich@gmail.com

www.icae.kr

ICAE 2011

International Conference on Advanced Electromaterials

November 7-10, 2011
Ramada Plaza Jeju Hotel, Jeju, Korea

Program Book

Organized by: KIEEME

Technically sponsored by: IEEE, DBS, KIST, ETRI, KERI, KIMS, KICET, KETI, KILT, KIEE, KCERS, The Korean Sensors Society, KIDS, OSK, LiFTRC, KLED

Supported by: Ministry of Education, Science and Technology, MKE Ministry of Knowledge Economy, KOFST, Jeju

Sponsored by: SAMSUNG, SAMSUNG ADVANCED INSTITUTE OF TECHNOLOGY, Signetics, LG Electronics

Electromechanical Properties of 0-3 Non Lead Barium Zirconate Titanate-Portland Cement Composites

R. Potong[1], R. Rianyoi[1] and A. Chaipanich[1]
[1]Department of Physics and Materials Science, Faculty of Science, Chiang Mai University, Chiang Mai, 50200, Thailand.

Abstract

0-3 Barium zirconate titanate - Portland cement composites new non lead environmentally friendly piezoelectric materials which are expected to find application in civil engineering. The influence of non lead piezoelectric ceramic contents on the electromechanical properties of 0-3 non lead barium zirconate titanate - Portland cement composites is reported in this present work. Barium zirconate titanate (BZT) - Portland cement (PC) of 0-3 connectivity were produced using 425 μm BZT particle size and different BZT contents at 40-70% by volume. The 0-3 BZT-PC composites were then cured in 98%RH curing chamber for 3 days before measurements. The results showed that the BZT content used to produce the composite has a noticeable effect on the electromechanical coupling factor (K_t). With a low poling field and low poling temperature, the K_t values was found to increase with increasing BZT content from 13% to 17% when BZT volume content used was 40% and 70% respectively.

Reference

[1] Z. Li, D. Zhang, K. Wu, J. Am. Ceram. Soc. 85, 305 (2002)
[2] A. Chaipanich, N. Jaitanong, T. Tunkasiri, Mater. Lett. 61, 5206 (2007)
[3] A. Chaipanich, Curr. Appl. Phys. 7, 537 (2007)
[4] Z. Li, B. Dong, D. Zhang, Cem. Concr. Compos. 27, 27 (2005)
[5] C. Xin, H. Gong, C. Jun, X. Ronghua, L. Futian, L. Lingchao, J. Eur. Ceram. Soc. 25, 2013 (2009)
[6] N. Jaitanong, A. Chaipanich, Ferro. Lett. 35, 17 (2008)
[7] N. Jaitanong, A. Chaipanich , T. Tunkasiri, Ceram. Int. 34, 793 (2008)
[8] I. Janotka T. Nürnbergerová, Nucl. Eng. Des. 235, 2019 (2005)
[9] S.K. Handoo, S. Agarwal, S.K. Agarwal, Cem. Con. Res. 32, 1009 (2002)
[10] N. Binhayeeniyi, P. Sukvisut, C. Thanachayanont, S. Muensit, Mater. Lett. 64, 305 (2010)
[11] K. H. Lam, H. L. W. Chan, J. Electroceram 21, 724 (2008)
[12] Z. Yu, C. Ang, R. Guo, A.S. Bhalla, J. Appl. Phys. 92, 1489 (2002)
[13] Z. Yu, R. Guo, A.S. Bhalla, J. Appl. Phys. 88, 410 (2000)
[14] P. Kantha, K. Pengpat, P. Jarupoom, U. Intatha, G. Rujijanagul, T. Tunkasiri, Curr. Appl. Phys. 9, 460 (2009)
[15] W. X. Cheng, A. L. Ding, X. Y. He, X. S. Zheng, P. S. Qiu, J. Electroceram 16, 523 (2006)
[16] A. Chaipanich, G. Rujijanagul, T. Tunkasiri, Appl. Phys. A 94, 329 (2009)
[17] R. Rianyoi, R. Potong, N. Jaitanong, R. Yimnirun, A. Chaipanich, Appl. Phys. A. (2011) doi: 10.1007/s00339-011-6307-2
[18] C. Xin, S. Huang, C. Jun, L. Zongjin, J. Appl. Phys. 101, 094110 (2007)

Corresponding author: A. Chaipanich, Department of Physics and Materials Science, Faculty of Science, Chiang Mai University, Chiang Mai, 50200, Thailand, Fax: 66 53 943445, E-mail: arnonchaipanich@gmail.com
E-mail of the presenting author: ja_rho@hotmail.com

Program and Abstracts Book

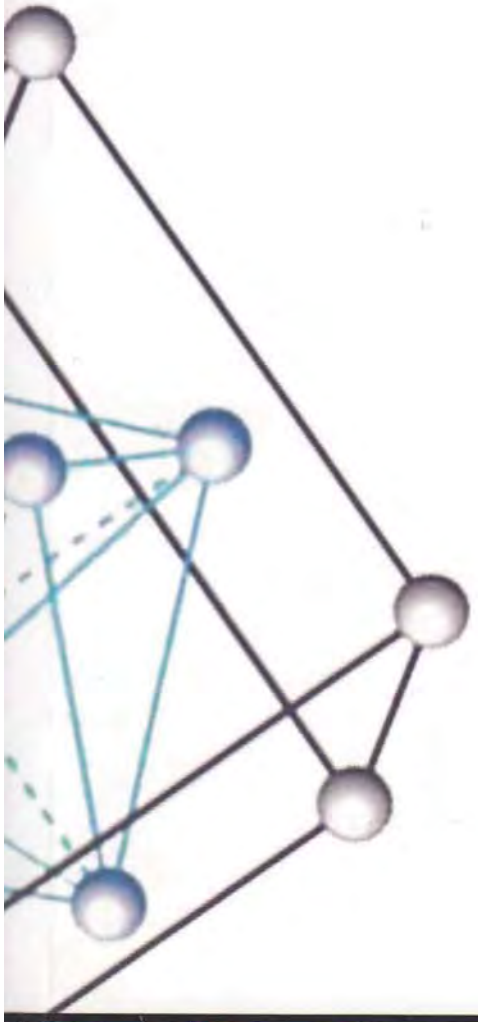

2012
1-5 July

8th Asian Meeting on Electroceramics

AMEC - 8

PENANG, MALAYSIA

Shangri-La's Rasa Sayang Resort and Spa, Penang, Malaysia.

Hosted by

USM

UNIVERSITI SAINS MALAYSIA

Influence of Barium Titanate Content and Particle Size on Electromechanical Coupling Coefficient of Lead-Free Piezoelectric Ceramic-Portland Cement Composites

R. Rianyoi, R. Potong and A. Chaipanich*

Department of Physics and Materials Science, Faculty of Science, Chiang Mai University, Chiang Mai 50200, Thailand

The 0-3 lead-free piezoelectric ceramic-Portland cement composites were prepared by mixing and pressing the Portland cement (PC) and barium titanate (BT) ceramic powder. The influences of BT particle size and BT content on the electromechanical coupling coefficient (K_t) of the composites were investigated. The results indicate that the particle size of BT used to produce the composite under the conditions of the same BT content (at 50% BT) and fabrication technique has influence on the K_t values. The electromechanical coupling coefficient was found to increase with the particle size of BT used where K_t values are found to be at 10.8% and 14.0% for composites with median particle size of 75 μm and 425 μm respectively. Furthermore, K_t of composites increase with increasing content of BT (at the same particle size of 425 μm) when the content of BT reaches 70%, K_t is 16.6%.

Keywords: composites, $BaTiO_3$, Portland cement

*** Corresponding author's e-mail:**
arnonchaipanich@gmail.com

Ferroelectric Relaxor Behavior and Impedance Spectroscopy of B^{3+}- doped $Ba(Ti_{0.9}Sn_{0.1})O_3$ Ceramics

K. Sutjarittangtham[1], N. Tawichai[2*], T. Tunkasiri[1], K. Pengpat[1], S. Eitssayeam[1] and G. Rujijanagul[1]

[1]Department of Physics and Materials Science, Chiang Mai University, 50200 Chiang Mai, Thailand
[2]School of Science, Mae Fah Luang University, 57100 Chiang Rai, Thailand

In this study, the B_2O_3 doped $Ba(Ti_{0.9}Sn_{0.1})O_3$ ceramics were prepared by using a solid state reaction method. The wide range of frequency (0.1 Hz - 1 MHz) and temperature (20 - 280 °C) dependence of the impedance relaxation were investigated. The impedance study indicates the presence of dielectric relaxation both bulk and grain boundary effects in the material. The relaxation times for grain and grain boundary estimated from Col-Cole plots varied with temperature according to the Arrhenius relation. The activation energy for grain and grain boundary were estimated to be 0.73 and 0.85 eV, respectively.

Keywords: ferroelectric, relaxor, impedance spectroscopy

*** Corresponding author's e-mail:**
n_tawichai@yahoo.com

Program and Abstracts Book

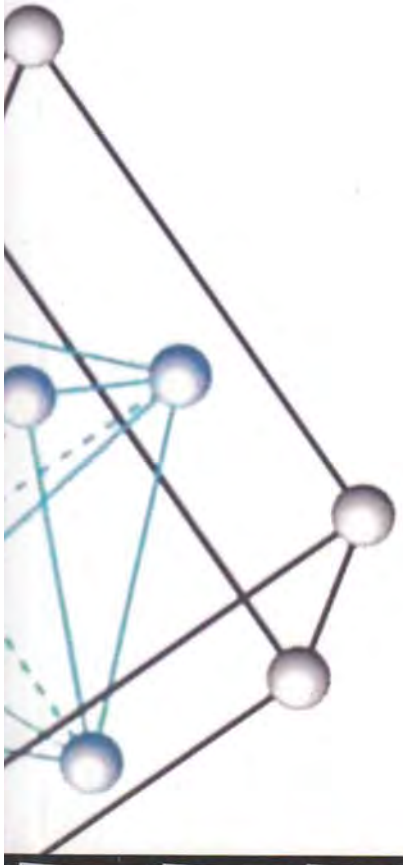

2012
1-5 July

8th Asian Meeting on Electroceramics

AMEC - 8

PENANG, MALAYSIA

Shangri-La's Rasa Sayang Resort and Spa, Penang, Malaysia.

Hosted by

USM

UNIVERSITI SAINS MALAYSIA

Influence of Ca Doping on Microstructure and Electrical Properties of $Ba(Zr,Ti)O_3$ Ceramics

N. Pisitpipathsin[1*], P. Kantha[1] and K. Pengpat[1,2]

[1]Department of Physics and Materials Science, Faculty of Science, Chiang Mai University, Chiang Mai 50200, Thailand
[2]Materials Science Research Center, Faculty of Science, Chiang Mai University, Chiang Mai 50200, Thailand

In the present work, lead-free $(Ba_{1-x}Ca_x)(Zr_{0.04}Ti_{0.96})O3$ (x = 0.0-0.12) ceramics were fabricated via a solid-state reaction. The microstructure and electrical properties of the ceramics were investigated. The microstructure of the BCZT ceramics showed a core shell structure at compositions of x = 0.03 and 0.06. The substitution of Ba^{2+} by Ca^{2+} for a small amount resulted in an improvement of the piezoelectric, dielectric and ferroelectric properties of the ceramics. The orthorhombic-tetragonal phase transition was found to depend on the Ca^{2+} concentration. Further the ferroelectric to paraelectric transition temperature shifted to room temperature with increasing Ca^{2+} concentration. The results suggested that Ca doping had strong effects on the properties of the ceramics.

Keywords: ferroelectric, core-shell, lead free

*** Corresponding author's email:**
bom_sep@hotmail.com

Dielectric and Piezoelectric Properties of 1-3 Non-lead Barium Zirconate Titanate-Portland Cement Composites

R. Potong, R. Rianyoi and A. Chaipanich[*]

Department of Physics and Materials Science, Faculty of Science, Chiang Mai University, Chiang Mai, 50200, Thailand

Non-lead barium zirconate titanate (BZT)-Portland cement (PC) composites have been seen as promising new non-lead composites. In this paper, we report a research work on the dielectric and piezoelectric properties of 1-3 non-lead barium zirconate titanate (BZT)-Portland cement (PC) composites. The 1-3 non-lead composites with different barium zirconate titanate contents at 40-70% by volume were fabricated by the dice-and-fill method. The results show that the dielectric constant (ε_r) of the 1-3 non-lead composite increases with increasing BZT content. The piezoelectric coefficient (d_{33}) of composite at 70% barium zirconate titanate was found to have values higher than 90 pC/N. The dielectric loss tangent ($tan\delta$) results were found to decrease with increasing barium zirconate titanate content.

Keywords: Dielectric properties, Piezoelectric properties, Composites

*** Corresponding author's email:**
arnonchaipanich@gmail.com